STABILITY LIMITS AND COMBUSTION MEASUREMENTS IN LOW CALORIFIC VALUE GAS FLAMES

by

Rooktabir Nandan SAUBA

Thesis submitted to the
Council for National Academic Awards
in partial fulfilment of the requirements
for the degree of Doctor of Philosophy.

The work was carried out at the Energy Centre
of Middlesex Polytechnic, Bounds Green Road,
London N11 2NQ

November 1987

To

my wife

INDEERA

ABSTRACT

A Hilton combustor was substantially modified to a suitable symmetrical configuration for research purposes. Provisions for swirl, preheat and injection of LCV gases were incorporated with appropriate burner management systems for safe operation. Instrumentation for temperature, velocity and concentration measurements was developed and fully automated by interfacing to a microprocessor for rapid data acquisition.

Flame stability limits were determined over a wide range of operating conditions by varying swirl, secondary air temperature and excess air levels while maintaining the burner momentum constant. Addition of swirl up to a limit of 0.69 generally improved stability. Preheating secondary air alone was beneficial only if the temperature was raised to at least 250°C. A combination of intermediate swirl and moderate preheat of the secondary air resulted in satisfactory flame stability over a wide range of calorific values of the fuel. Thus, existing concentric pipe burner systems may be easily modified at low cost to burn LCV gases of variable compositions.

With LCV gas flames the excess air factor (EAF) had a major influence on values of temperature, species concentration and velocity. Unburnt hydrocarbon (UHC) and CO not surprisingly increased in concentration close to the blow-off limits under the majority of operating conditions. This indicated incomplete combustion probably resulting from the lowered flame temperatures and partial flame lift-off. On the other hand, burnout efficiencies at the exhaust were reasonably high for most operating conditions involving LCV gases.

The combustion data were analysed to extract the characteristic mixing and chemical reaction times the ratio of which gave the parameter ε, originally proposed for unconfined flames. Close to the blow-off limit ε took the value 4.9 compared with 6.2 for fully stable flames. This finding showed that the criterion was also valid for confined flames, supporting the extinction mechanism proposed by Peters and Williams, and providing an important basis for predicting stability limits and burner design parameters.

ACKNOWLEDGEMENTS

It gives me great pleasure to express my gratitude to all those who provided me with assistance and guidance during my study.

First and foremost, I wish to acknowledge with gratitude the guidance, suggestions and encouragement provided by my supervisors, Dr. S.H. Ahmed and Dr. F.C. Lockwood, whose help greatly aided the progress and completion of this work.

Many thanks are due to Professor F.L. Tye who has maintained a keen interest in my work and without whose help and encouragement this project would have never got-off the ground. Special thanks are also due to Dr. W.C. Maskell who generously gave his time and knowledge for the completion of this work.

Thanks are due to Dr. A. White who helped in the design and manufacture of the parts required for the modification of the furnace. My appreciation and thanks are due to Mr. R. Foster, Mr. S. Barnard and Mr. P. Moye for their help with the gas analysing system.

The support of the technical staff was vital to the research programme. Thanks are due to Messrs. C. Ablett, R. Brick, H. Doiley, N. Salam, P. Burn, J. Cranston and J. Deakins. The precision and quality of their work is appreciated. I would also like to thank Dr. M.M.A. Hassan and Mr. G. Griffith for their help with the microprocessor system.

My thanks are offered to all my colleagues at the Energy Centre for sharing college life. In particular my thanks are due to Mr. J. Fitzpatrick, Mr. J.B. Soupart, Mr. D. Malpas, Mr. L. Vasanthakumar, Mr. H. Kochekali and Mr. A. Nowrouzi.

My thanks to Mrs. Pauline Hunt who had the patience to go through the typing details with great skill.

I wish to acknowledge Middlesex Polytechnic for the financial support of this work.

I would like to take this opportunity to thank my relatives for their help and encouragement during my studying career.

Finally, my appreciation and deepest gratitude are extended to my wife, Indeera, for her patience, support and ever-enhancing love which accompanied me throughout this effort.

CONTENTS

Page No.

CHAPTER 2 (Contd)

NOMENCLATURE

A	area, surface area
b(x)	axial burnout rate
C	volume concentration
c_i	mass concentration of species i
Cp	specific heat under constant pressure
CRZ	central recirculating zone
CV	calorific value of fuel
d, d_o	diameter, exit diameter of jet
D	internal diameter of combustor
D_q	diameter of quarl
EAF	excess air factor
EEA	equivalent excess air
f_{st}	stoichiometric fuel/air ratio
g	gravitational acceleration
G_x	axial momentum flux
G_ϕ	angular momentum flux
h	convection heat transfer coefficient
H	enthalpy
k	kinetic energy of turbulence, thermal conductivity
L_q	length of quarl
LCV	low calorific value
m	mass
$\dot{m}$	mass flow rate
M	molecular weight
Nu	Nusselt number
p	pressure
Pr	Prandtl number

PVC	precessing vortex core
$\dot{q}$	volume flow rate
$\dot{Q}$	heat transfer rate
r	radius of burner nozzle
R	radius, radial distance measured from combustor axis
Re	Reynolds number
R_j	Flame jet radius based on actual data
S	flame speed
Sw	swirl number $= G_\phi/G_x r$
t	time
T	temperature
u	axial velocity component
V	velocity
X	axial distance from furnace quarl exit

Greek Symbols

ε	blow-off parameter
μ	viscosity
ξ	measured angle of adjustment of swirl block generator
ρ	density
σ	Stefan-Boltzman constant
ν	kinematic viscosity
ϕ	equivalence ratio = (A/F) stoic./(A/F) actual

CHAPTER 1

INTRODUCTION

1.1 Preliminary Remarks

In the past few years there has been an increasing interest in combustible fuel gases having calorific values lower than that which would have been economically acceptable in more plentiful times. Such fuels may be natural gas deposits containing substantial quantities of nitrogen or by-products of steel plants such as blast-furnace, coke-oven and oxygen-blown-converter gases.

A good proportion of natural gas wells explored in the North Sea are found to contain a higher amount of nitrogen than is currently acceptable. There is also natural gas diluted with nitrogen present in oil wells which is just flared off thus wasting energy. The recovery costs per unit mass of naturally occurring fuel gases is roughly constant which obviously disfavours those of low energy content. Industrial waste gases are often produced in large quantities over short periods necessitating costly storage equipment if they are to be salvaged. Such cost disincentives are diminishing with time due to the limited amount of naturally occurring fuel gases available. Therefore acceptable ways of burning these low calorific value gases must be further explored in order to extend the lifespan of our indigenous supply of energy.

The main problem known is possible burner flame instability associated with combusting these gases. Variation in air and fuel input velocities, difference in calorific values and changes in operating conditions can all create severe burner problems. Such difficulties can be potentially dangerous as low calorific value gases are more prone to blow off if operating conditions are not favourable, a fact which highlights the flame stability problems on burner systems. There are various ways of conducting stability experiments owing to the numerous experimental parameters which can be altered; e.g. mass flow rates of fuel and air, temperature of secondary air, diameter of burner pipes, exit velocity of fuel and air, swirl number, excess air levels etc. The aims of the present study are: (i) to establish and develop a gas combustion facility which is relevant to industrial practices, (ii) to investigate the stability limits of low calorific value gases and (iii) to obtain combustion data on low calorific value gases under very carefully controlled conditions which can be used to understand burner instability problems and also to validate computer prediction codes.

Two types of flame can be identified: premixed where the fuel and oxidant are mixed before ignition or diffusion where the fuel and oxidant are injected separately. In premixed flames combustion is propagated by the interdiffusion of hot product molecules with those of unburnt reactants. While in diffusion flames combustion can only proceed after the fuel and oxidant have interdiffused at a molecular level and in the presence of hot product molecules. Turbulent diffusion flames are predominantly used in most industrial practices such as large furnaces, internal combustion engines, gas turbines, steam boilers, rotary cement kilns etc. For this reason it was decided to investigate turbulent diffusion flames.

1.2 Brief review of previous gaseous fuel and LCV gas flames experiments

This section gives a summary of the amount and type of work carried out on low calorific value (LCV) and other gas flames and provides the basic understanding behind the present study. The findings and conclusions reached by some of the investigators are presented in the next chapter. This section is divided into two parts; in subsection 1.2.1 work done on flame stability measurements is considered and inflame combustion measurements are dealt with in subsection 1.2.2.

1.2.1 Flame stability measurements

Beltagui and Maccallum (1986) carried out an experimental study of the stabilization of flames in premixed swirling jets using hubless vane-type swirlers. They considered both free, unconfined and enclosed, confined jets. Town gas and natural gas were both used as fuel and a range of fuel-air mixtures was covered including values close to the stability limit. A (Pt 5% Rh) - (Pt 20% Rh) thermocouple with a 0.25 mm bead diameter was used to measure temperatures and gas samples were removed via a water-cooled probe and analysed for carbon dioxide and unburnt combustibles.

Broadwell, Dahm and Mungal (1984) investigated the blow out of turbulent diffusion flames. They formulated a simple analysis to explain the mechanisms governing the stability of these flames. They used both pure and diluted gases to prove their analysis.

Chedaille, Leuckel and Chesters (1966) studied flame aerodynamics on behalf of the IFRF using pressure jet oil flames. The first part of

their work dealt with the flow patterns and mixing in double-concentric jets confined in long coaxial chambers. A boiler-type burner was qualitatively compared with a cement kiln burner resulting in the identification of four distinct flow zones. The main aerodynamic properties of jets with internal reverse flow together with their influence on turbulent diffusion flames were investigated separately in the second part of the work Two alternative means of producing internal reverse flow, swirl or the use of a bluff body, were also discussed with reference in particular to the size and stability of the zones of reverse flow and the length and combustion intensity of the resulting flames.

Eickhoff, Lenze and Leuckel (1984) carried out an experimental investigation on the stabilization mechanism of jet diffusion flames. Two different natural gas diffusion flames at exit velocities between flame detachment and blow-off were investigated.

Godoy et al. (1985) investigated the stability limits of pulverised coal burners. They defined a stable or "lit back" flame as one which is retained very near to the face, normally within a siwrl and/or quarl induced zone of recirculation. Ishizuka and Law (1982) carried out an experimental study on extinction and stability of stretched premixed flames. A counterflow burner and a stagnation flow burner with a water-cooled wall were used. They systematically investigated the effect of downstream heat loss on the extinction of a stretched premixed flame for lean and rich propane/air and methane/air mixtures. A variety of non-steady, non-planar flame configurations were observed and their response to concentration and flow field variations mapped. The possible controlling mechanisms were also discussed.

Jarosinski et al. (1982) experimentally studied the mechanisms of lean limit extinguishment of an upward and downward propagating flame. Their experiments were conducted in a vertical 51 mm square standard flamability tube, about 1.8 m long. Lean methane-air systems were studied; schlieren and direct light photography and temperature measurements were used to investigate the flames under transient loading. Kotani and Takeno (1982) conducted an experimental study on stability and combustion characteristics of an excess enthalpy flame burning mixtures of low heat content. A bundle of ceramic tubes was used as a combustion tube and four perforated ceramic plates were placed upstream and downstream of the tube to reduce the radiative heat loss from the heated tube. They used (Pt-Pt/13%Rh) thermocouples (0.3 mm wire dia.) to measure temperature profiles in their combustion tube.

Kalghatgi (1981) investigated the blow-out stability of gaseous jet diffusion flames in still air. A wide range of fuels were used. He found a universal non-dimensional formula that describes the blow-out stability limits experimentally. Its validity was established over a wide range of parameters that affected the blow-out limits. Negishi (1982) experimentally investigated lean premixture combustion on a coaxial burner in particular the interaction between internal and external coaxial flames. He worked on methane-air mixtures and measured the minimum equivalence ratio for complete combustion as a function of the flow rate by using a small pilot flame whose equivalence ratio was equal to unity or less.

Rawe and Kremer (1981) made an experimental study of flame stabilization in unconfined turbulent swirling natural gas flames using various

degrees of swirl. An IFRF moving block swirl burner was used and Slochteren (Dutch) natural gas was supplied through a central gas pipe. A multi-hole nozzle with radial gas injection was used as the burner which was surrounded by a small cylindrical quarl. A variety of these cylindrical quarls and gas nozzles both with different diameters were investigated. A 5-hole probe was used to measure velocity and static pressure; they also measured temperature and concentration of methane and oxygen in the flame. Syred et al. (1977) reviewed a number of recent developments in the field of burning low calorific value waste gases. Most of their work was done on cyclone combustors which successfully burnt gases of calorific value as low as 1.34 MJ/m^3. They also did some work on a small waste gas multi-fuel swirl burner for drying and other applications. Their cyclone combustors have low pressure drop, good turndown ratios of up to 5 or 6 : 1 but constructions were somewhat complicated.

The influence of burner rim aerodynamics on the behaviour of polyhedral flames of butane/air mixtures for different geometries was investigated by Sohrab and Law (1985). They identified regimes corresponding to stationary, rotating and unstable polyhedral flames with various number of sides by systematically varying the mixture concentration and velocity. Stabilization of laminar Bunsen flames was also studied and the critical flow velocity and concentration corresponding to flame flashback and blow-off for different burner rims were determined. Experimental studies of the structure and extinction of near-limit premixed flames in stagnation flow were performed by Tsuji and Yamaoka (1982). Near-limit rich and lean methane/air and propane/air flames were used in the experiment. The structure of the twin flames, the

flame temperature, the distance between the two flame zones, and the concentration of reactants on the stagnation surface were measured and the extinction mechanism was discussed.

Vanquikenborne and Van Tiggelen (1965) worked on the stabilization mechanism of lifted diffusion flames. They used a free jet of methane burning into an unconfined atmosphere to measure gas composition, gas flow velocity and Eulerian scale of turbulence. They also made a few inflame measurements with jets of methane diluted with nitrogen. Flame height, flame width and the limit of flame stability defined by the gas flow at which the flame was not maintained for longer than five seconds, were also measured. Yuasa (1986) made an experimental study of the effects of swirl on the stability of jet diffusion flames using a double-swirl burner. He used hydrogen and methane as fuel and measured the air stream velocity, the fuel injection velocity, the swirl intensity of the fuel jet and the swirl intensity of the air stream. The flames were studied through instantaneous (1 μs) schlieren photography and direct photography with a long exposure time of 10 s. He measured uncorrected radial temperature distributions in the swirling flames with a silica-coated Pt-Pt/13%Rh thermocouple of 0.33 mm wire diameter.

Schreier (1980-1983) carried out a number of trials at the IFRF. In the first study (1980) he investigated the combustion of variable quality lean gases found particularly in the iron and steel industry by using a new burner. He also studied the effects of other burner parameters like air distribution, flow velocities and burner load on

flame stability and shape for various lean gases. In a second trial (1981) he used five different types of burners burning a range of low calorific value gases to generate combustion data which could be used to improve the design of lean gas firing installations. The characteristics of these burners such as the maximum turndown ratio, the range of gases which could be fired and the change of heat transfer using different gases were also found. The trial was very extensive and was done on the IFRF No.2 furnace.

Fricker and Leuckel (1976) also did a series of tests at the IFRF. In part 3 of their work they investigated the effect of swirl and burner mouth geometry on industrial-scale natural gas flames. The experiments were performed on a 2 x 2 m square horizontal refractory-lined tunnel furnace. Slochteren natural gas which contains a high nitrogen concentration was burnt and artificial natural gases were also used to check the effect of gas composition on burner performance. Measurements were also made using different types of gas injectors.

1.2.2 Inflame combustion measurements

Ahmad, Andrews, Kowkabi and Sharif (1984) investigated centrifugal mixing forces in enclosed swirl flames. They used a flat bladed swirler and the downstream combustion was confined in a 76 mm diameter uncooled duct. A maximum swirl number of 0.7 was used which was sufficient to generate a central recirculation zone.

Beyler and Gouldin (1981) reported results of measurements of time-averaged chemiluminescent emissions from OH, CH and CO_2 and of Na tracer emissions in a cylindrical premixed, swirl-stabilized combustor.

Comparative study of Na emissions and chemiluminescent emissions was also made. The experiments were performed under two operating conditions, one with swirl in the two jets in the same direction (co-swirl) and one with swirl in opposite direction (counter-swirl). Beltagui and Maccallum (1976) investigated the aerodynamics of vane-swirled flames in furnaces. Measurements in isothermal and burning swirling flows were carried and in two furnaces. Both annular and hubless-vane swirlers were tested with furnace diameter/burner diameter ratios of 2.5 and 5.0. Flow with combustion gas was compared with isothermal flow : fuel/air ratios particularly when swirl was near the critical value for the creation of a recirculation zone were also investigated.

Claypole and Syred (1981) investigated the effect of swirl burner aerodynamics on NO_x formation. They measured mean temperature, local velocity and NO-NO_x concentrations for swirl numbers from 0.63 to 3.04. Natural gas at an approximate loading of 100 kW was injected axially to their combustor with the air supplied tangentially and 10% above the stoichiometric requirements. The instantaneous velocities were measured by dual beam laser anemometry. The flame was sampled with an aerodynamically quenching quartz probe and NO, NO_x concentrations were determined using a thermo-electron type chemiluminescent analyser. The local mean temperatures were obtained by time averaging the signals from a bare wire platinum/platinum rhodium thermocouple. Chigier and Dvorak (1975) made laser anemometer measurements in turbulent swirling jets under flame and no flame conditions. Time mean axial, radial and circumferential components of velocity and rms velocity fluctuations were measured.

Günther and Wittmer (1981) carried out a detailed study of the time mean and fluctuating properties in a concentric methane-air diffusion flame with 15 and 50 m/s exit velocities and slight oxygen stabilization. Data for time mean values and fluctuations of axial and radial velocity, of nozzle fluid concentration, ionization and temperature were obtained. Hassan et al. (1980) reported measurements of mean and fluctuating temperature, using the fine-wire thermocouple technique, and of mean concentrations of CO, CO_2 and O_2 in vertical turbulent free jet methane flames. They collected data for several Reynolds numbers and for varying amounts of nitrogen added to the fuel stream.

Hassan (1983) also collected temperature and concentration data in a 0.6 m diameter cylindrical gas fired furnace. Results were obtained for two excess air-levels and two swirl numbers. For species concentration of CO, CO_2 and O_2, comparative measurements were made using a quartz microprobe, a water-cooled probe and a direct water-quenched probe. Incident radiation fluxes to the walls were also measured with an ellipsoidal radiometer. The effects of preheating combustion air on flame properties in a furnace burning coke-oven gas were investigated by Hubbard (1957). Measurements for gas composition, radiation, flame temperature, velocity and carbon concentration were reported.

Lenze (1982) studied the influence of recirculation and excess air on enclosed turbulent diffusion flames. He made measurements in both cold systems and combusting conditions for different types of flames.

A diffusion flame of hydrogen in air was used by Kent and Bilger (1973) to obtain gas species concentration and temperature measurements. Further investigation by Bilger and Beck (1975) was carried out to

investigate the formation of nitric oxide in that same flame. The effects of probe size and construction on the concentration measurements were also considered. Lockwood et al. (1974) investigated turbulent mixing in a cylindrical furnace using town gas. Measurements of mixture fraction were obtained for four fuel/air ratios, two burner geometries, two Reynolds numbers and four different swirl levels imparted to the combustion air. Lockwood and Odidi (1975) reported measurements of mean, rms, probability density and spacial density of temperature and of positive ion concentration in unpremixed and premixed turbulent, round free-jet flames.

In a multi-part study Leuckel and Fricker (1976) and Wu and Fricker (1976) investigated the characteristics of swirl stablized natural gas flames. Part one dealt with different flame types and their relation to flow and mixing patterns. The main aim was to investigate flames produced when natural gas was injected directly into an internal reverse flow zone induced by strong rotation of the combustion air. In the second part, the behaviour of swirling jet flames in a narrow cylindrical furnace was investigated. They studied the influence of furnace shape and dimensions on swirling natural gas flames by comparing flow patterns in a narrow 0.9 m diameter cylindrical furnace with that of a large 2 x 2 m square sectioned one. Part three of the work was concerned with the effect of swirl and burner mouth geometry on the stability of industrial-scale natural gas flames. Data on blow-off characteristics, effects of swirl and quarl length, gas and air velocity at blow-off for different types of flames were reported.

Moneib (1980) reported data of the fluctuating temperature obtained in an inert heated round turbulent free jet and in round free jet diffusion

flames. Fine wire thermocouples compensated for the effects of thermal inertia were used for the measurements. Three types of turbulent diffusion flames were studied : (i) stabilized natural gas diffusion flames, (ii) lifted natural gas diffusion flames and (iii) stabilized natural gas/nitrogen diluted flames.

Rimai et al. (1982) performed an optical study of 2-D, stable, lean, laminar methane-air premixed flames and reported on the relation between temperature and flow-velocity fields. They used the Coherent Anti-Stokes Raman Spectroscopy (CARS) of N_2 to obtain temperature measurements and direct recording laser interferometric anemometry to obtain the 2-D vector velocity field. Rawe and Kremer (1981) measured temperature, concentration, velocity and flow direction under flame and no flame conditions near the stability limits in unconfined turbulent swirling natural gas flames using various degrees of swirl.

Starner and Bilger (1981) made simultaneous measurements of scattered light intensity and axial velocity in a turbulent hydrogen diffusion flame. They reported results on density, the mean and r.m.s. fluctuation of streamwise velocity component and its correlation with the mixture fraction and the density as well as other correlations and Favre or density weighted averages. Sadakata et al. (1981) investigated the effects of air preheating on the emissions of NO, HCN and NH_3 from single-stage and two-stage combustion. Their aim was to find a combustion method which could both save energy and reduce NO_x.

Steward et al. (1971) worked on the heat-transfer measurements in an oil-cooled, gas-fired cylindrical test furnace. They measured flow

patterns, gas-concentration profiles, temperature distributions and radiative and total heat flux distributions. Taylor and Whitelaw (1980) made comparative studies of measurements of velocity, temperature and noise characteristics between a premixed natural gas/air flame stabilized on a disc baffle and a corresponding isothermal flow. Yanagi and Mimura (1981) studied the velocity-temperature correlation in a turbulent premixed flame. Velocity and temperature data were obtained simultaneously with a laser Doppler anemometer and a compensated thermocouple; the cross-correlation was calculated on a micro computer.

Yoshida (1981) carried out an experimental study of wrinkled laminar flames. Detailed measurements of temperature and velocity were carried out using a fine-wire thermocouple and a laser Doppler velocimeter. Yoshida and Tsuji (1982) used an open turbulent flame burner to investigate the characteristic scale of wrinkles in turbulent premixed flames. Upstream turbulence was measured by a laser Doppler velocimeter and a hot wire anemometer. Temperature measurements using a fine-wire thermocouple were also used to determine the time scales of unburnt and burnt gas pockets in a lean propane-air turbulent flame.

As can be seen from the previous two subsections, with the exception of Schreier (1980-1983) and Syred et al. (1977), low calorific value gases have received very little attention. The work that has been done does not provide sufficient information for the better understanding of the stability limits and blow-off mechanism of these flames. Certainly there is a very little data published on the concentration of major species and nowhere has data on stability limits, temperature, concentration and velocity been collected under strictly controlled

conditions in confined low calorific value gas flames with various swirl intensities and excess air levels and with secondary air preheat.

1.3 Objectives and Scope of the Present Work

The main objectives of the present work were: 1) to collect data for the stability limits of natural gas flames under different furnace operating conditions and 2) to make inflame combustion measurements under these well-defined operating conditions prior to blow-off.

A Hilton combustion unit was modified into a symmetrical arrangement and a new burner system with a concentric pipe configuration and a movable block swirl generator added. The facility for providing preheated combustion air was also incorporated. A new fuel supply system with a mixing chamber was fitted to provide the facility for combusting low calorific value gases, obtained by premixing natural gas with various amounts of oxygen-free nitrogen. Instrumentation systems for measuring temperature, velocity and concentration were also set up.

Stability limits data were then obtained for various operating conditions. A combination of three excess air levels, four different secondary air preheat values and three swirl numbers were used to give a very wide range of operating conditions. To obtain a better understanding of the blow-off mechanism, inflame temperature, velocity and concentration measurements were carried out using pure natural gas as a reference, at some of the above operating conditions. The same measurements were then repeated under the same conditions but this time using low calorific value gases burning close to the blow-off limits.

1.4 Outline of the Thesis

The remainder of this thesis is contained in five additional chapters. Chapter 2 gives a more detailed account of previous work related to low calorific value gases. The effects and findings of investigations on excess air, swirl, secondary air preheat and nitrogen addition to flame aerodynamics are discussed. There is also a review of various flame types that are obtained under different operating conditions.

A detailed description of the furnace and its ancillary equipments is provided in chapter 3. The instrumentation systems used for temperature, velocity and concentration data collection are also outlined.

In chapter 4 the experimental conditions under which the stability limits data were obtained are described. Results of these measurements are presented and discussed in relation to how they are affected by the effects of secondary air temperature, swirl number and excess air levels.

Chapter 5 begins with the experimental conditions and procedures under which inflame combustion measurements were carried out. The measuring techniques used for temperature, velocity and concentration are outlined. The experimental results are then presented and discussed in the last section of the chapter.

A summary and the main conclusions of the present work are provided in chapter 6 together with recommendations for future work.

In addition to the six chapters, the thesis also contains two appendices. Appendix (A) outlines some of the basic theories behind the five hole pilot measurements of velocity. It also includes a calibration chart for the swirl generator. Appendix (B) gives some details of calculations used to obtain the burnout rate and blow-off criterion. There are also some additional concentration data presented in it.

CHAPTER 2

PREVIOUS WORK RELATED TO LCV AND NATURAL GAS FLAMES

2.1 Introduction

This chapter reports some of the findings on previous work related to low calorific value (LCV) and natural gas flames. Very little data is available on the study of stability limits and combustion measurements for confined turbulent flames burning low calorific value gases in an industrial type furnace.

Weinberg et al. (1975) have shown that by using massive heat recirculation, any substance that is capable of exothermic reaction can be used as a fuel. This was illustrated by their "Swiss roll" burner in which two metal alloy strips were wound together into a spiral. The majority of work on the subject of low calorific value gases was carried out by Syred et al. (1977) on cyclone combustors. These combustors have multiple air and gas inlets on the circumference and are complicated in construction. It was not until late 1970's that Michel and Payne (1979) initiated some work at the IFRF burning blast furnace gases as a fuel. This work was continued by Scheier in 1980 and he carried some major experimental investigations burning lean gases mostly found in the iron and steel industry.

Section (2.2) gives a brief review on flame aerodynamics while different types of flame is dealt with in Section (2.3). Section (2.4) deals with some of the findings and conclusion reached by other investigators working on LCV and natural gas flames. It is divided into two subsections, subsection (2.4.1) dealing mostly with stability studies and subsection (2.4.2) concentrated on combustion measurements. The last section points the main effects of swirl, excess air, preheat and nitrogen dilution on combustion.

2.2 Flame Aerodynamics

In turbulent diffusion flames such as those used in industrial furnace, the significant characteristics such as combustion length, angle of spread, stability, radiation from flames etc., depend largely upon the way in which fuel, oxidant and hot combustion products are mixed. This is because most of the chemical reactions in flames are very fast at elevated temperatures so that the time taken to complete the reaction after the reactants are mixed is negligible, Beér (1972). Therefore the rate at which combustion proceeds can very often be taken as the rate of mixing.

Swirl is known to improve flame stability by forming torroidal recirculation zones and to reduce combustion length resulting in high rate of entrainment and fast mixing particularly near the recirculating zones, see Fig. (2.2.). The axial pressure gradients in weak swirl are insufficiently large to cause internal recirculation. It mainly increases the rate of entrainment and the rate of velocity decay. When increasing the degree of swirl in a flow, the adverse pressure gradient along the jet axis cannot be further overcome by the kinetic energy of

the fluid particles flowing in the axial direction after a certain point. This results in the creation of a recirculating flow in the central portion of the jet. This internal recirculating zone plays an important role in flame stabilization due to the formation of a well mixed zone of combustion products, acting as a heat storage, and chemically active species located in the centre of the jet near the burner exit. The angle of spread of a jet is also increased with swirl. The transformation from weak to strong swirl occurs at a swirl number of approximately 0.6.

Considering a turbulent diffusion flame, below a critical exit velocity the flame remains attached to the burner lip. As this exit velocity is increased, the flame is lifted and combustion initiates a significant distance downstream of the burner exit. Further increase in the exit velocity will cause the flame to extinguish thus reaching a second critical velocity termed as the "blow-out" velocity. Two main theories exist on the concept of liftoff; Chakravarty et al. (1984) and Eickhoff et al. (1984) suggest that a lifted flame is stabilized in a zone where combustion is controlled by premixing. But Broadwell et al. (1984) and Peters and Williams (1982) believe that a collection of unsteady laminar diffusion flamelets is responsible for the stabilization of a lifted flame.

To get an idea of the complexity of the different types of flow present in a flame, Claypole and Syred (1981) have indicated these various zones and flow regions within a swirl combustor, see Fig. (2.1.).

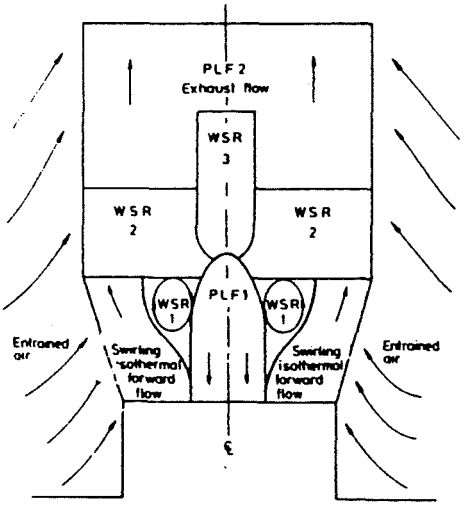

KEY:-

REGION	LOCATION
Mixing Region	Forward swirling isothermal jet
WSR1	Eye of Recirculation zone
WSR2	Breakdown region of swirling forward jet
WSR3	Downstream stagnation point of r.f.z.
PLF 1	Stable r.f.z.
PLF 2	Exhaust flow

Fig. (2.1) Flow regions within a Swirl Combustor

2.3 Flame Types

The two main categories of flame namely premixed and diffusion were outlined in chapter 1. This section will give a brief description of the three types of flame that are possible with turbulent diffusion jets. These flame types were designated mainly by investigators from the IFRF, in particular Fricker and Leuckel (1976) and Bortz (1983).

Fig. (2.2a) shows a very common type of industrial flame used and it is mainly a combination of type II and III flames. It is obtained by imparting a moderate amount of swirl to the combustion air and by injecting the fuel axially. This causes the fuel jet to penetrate the internal recirculation zone created. It also has an external recirculation zone as shown.

Type II flame is short and intense as shown in Fig. (2.2b). This type of flame is obtained by using a high degree of swirl together with radial or divergent fuel injection. The flame is stabilized very near to or inside the quarl with closed internal recirculation zone. Many industrial processes using wall fired boilers make use of this type of flame.

The absence of an internal recirculating zone characterizes type III flame, see Fig. (2.2c). It is long and more luminous and mostly used in cement kilns and corner fired boilers. This type of flame is produced by using axial fuel injection with zero swirl to the combustion air.

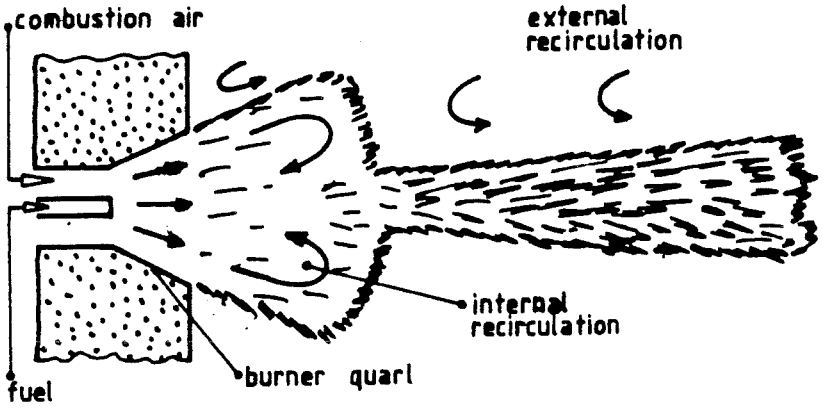

Fig.(2.2a) Type I Flame

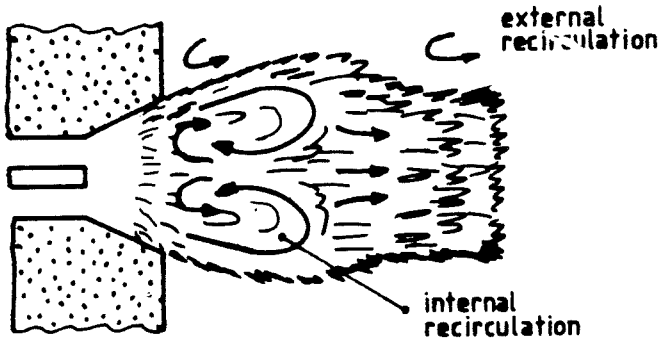

Fig. (2.2b) Type II Flame

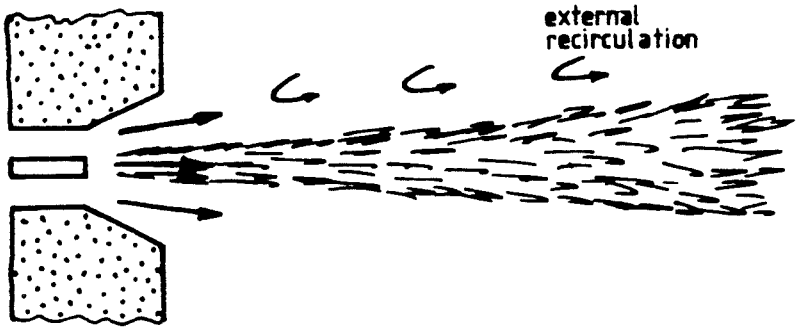

Fig. (2.2c) Type III Flame

2.4 Findings and Conclusions on Related Studies Using LCV and Natural Gas Flames

2.4.1 Stability Studies

Beltagui and Maccallum (1976) observed four different flow zones in their aerodynamic measurements of isothermal and burning swirling flames in two furnaces. They concluded that significant changes in the flow and combustion patterns can result from imparting swirl to the combustion air. A CRZ was created if the swirl was sufficiently strong and the critical swirl number for establishing this CRZ on their system was 0.11. They also found that the maximum diameter of a well established CRZ was a function of the furnace diameter and was only slightly changed by either further increase in swirl intensity or by the furnance to burner diameter ratio. From another experimental investigation based on free swirling premixed flames, Beltagui and Maccallum (1986) observation on weak extinction limits showed that there is a general relationship between the absolute velocity leaving the swirler and the effective fuel/air ratio at the anchoring region.

Beyer and Gouldin (1981) concluded from their work on premixed, swirl stabilized flames that the reaction zone is confined to a well defined flame region and is stabilized in front of the time-mean recirculation zone from where it propagates through the forward portions of the recirculation zone boundary layer and then into the inter-jet shear layer. They also noticed no fundamental differences in the flame structure under co-swirl and counter-swirl conditions at the point of flame stabilization or in the boundary layer of the recirculation zone; differences were noted in the flame thickness in the inter-jet shear layer.

Chedaille, Leuckel and Chesters (1966) found four flow zones along a furnace chamber after qualitatively comparing the aerodynamics downstream from a boiler-type burner with that of a cement kiln burner. They concluded that flow and turbulent mixing in the first two zones of a double-concentric confined jet are not noticeably influenced by the chamber walls. They also noticed that the difference between free and confined jets is limited to the fact that a free jet entrains stagnant air at its boundary, while a confined jet entrains recirculated gas from inside the enclosure and consisting, for an actual flame, of completely mixed and almost totally burnt products. The presence of internal reverse flow in turbulent diffusion flames tends to produce early ignition, faster mixing and increases the mean residence time of the fuel in the furnace, thus contributing to a shorter distance for complete combustion.

Claypole and Syred (1981) concluded that the flames produced by swirl stabilized combustion could be grouped into four types depending on the influence of the recirculation zone on flame stabilization. The types of flame were also dependent on the flow structure and were shown by their effects on the PVC. They found the most satisfactory type of flame as being one which produced well stirred combustion in the recirculation zone. This type of flame was obtained with a swirl number of 0.63, a quarl outlet with short parallel section and radial fuel injection.

Leuckel and Fricker (1976) found that when injecting natural gas on the axis of a swirled combustion air flow, the effects of burner parameters such as quarl shape and gas injection conditions were best considered by referring to two flow patterns and flame types resulting

from the situation. The best use of the quarl was assured by injecting the gas at the throat section for both types of flame. They found that the main effect of increasing swirl was to improve mixing of the fuel and air rather than to increase the reverse flow of hot burnt gases into the burner quarl. They also concluded that when the optimum fuel : air ratio for a burner approached the stoichiometric value, there was no further improvement by increasing the swirl intensity. This value of the swirl number was found to be under 1.0 for the cases they have investigated.

Measurements made by Godoy et al. (1985) showed that a small increase in the excess air level gave better flame stability due to the availability of more air for combustion in an otherwise rich recirculation zone. They also concluded that by lowering the inlet velocity thus giving a longer residence time and by improvement in mixing, flame stability is enhanced. Based on results of the concentration limits and flame separation distance at extinction, Ishizuka and Law (1982) have demonstrated that extinction by stretch alone was possible only when the deficient reactant was the one with less momentum. When it was the one with the higher momentum, downstream heat loss or incomplete reaction was also required to achieve extinction, the latter caused by insufficient residence time. They also concluded that flammability limits determined by counter-flow burner system agreed well with those determined by other techniques; thus raising the possibility that the controlling mechanisms of the flammability limits may be quite similar for apparently different flow situations.

Work done by Jarosinski et al. (1982) using a flammability tube concluded that the extinction mechanism for an upward propagating flame

is very different from that of a downward propagating one. The upward propagating flame is extinguished by a stretch mechanism in which the holding region is stretched to extinction and the extinction wave then washes down the skirt while the leading edge of the hot product gases still retains its constant upward speed. Heat transfer to the wall played no important part during this extinction process. Extinction of a downward propagating flame is triggered by heat loss to the wall and the flame is finally driven to extinction by differential buoyancy which forces cooler product gases ahead of the flame.

Working on an excess enthalpy flame, Kotani and Takeno (1982) found that the flame stabilized ahead of, in or behind the combustion tube, depending on flow rate and equivalence ratio. They also showed with the aid of temperature distributions that the heat recirculation through the perforated plates as well as the combustion tube played an important role on flame stabilization. Negishi (1982) concluded that a small amount of mixing played an important role in stabilizing the flame in a high speed flow of lean premixture. The minimum equivalence ratio for forming a conical flame in the test premixture is dependent upon the flow rate of the test premixture as well as the equivalence ratio of the coaxial pilot flame premixture.

From the evaluation of their data, Rawe and Kremer (1981) showed that the stability limits of swirling flames can be successfully correlated by means of dimensionless Peclet numbers. They concluded that flame stability depends on the location of the reaction zone within the flow field near to the burner exit. They found two main reasons for flame extinction which are firstly, a radial shift of the flame front in the regions of excessive local fluid velocities and secondly, lifting of the

flames by exceeding the maximum possible fuel concentration within the stabilization region.

During the first of a series of trials at the IFRF, Schreier (1980) confirmed that hydrogen was the most important species as far as flame stability was concerned. By testing a range of burners he found that using a fuel containing more than 4% hydrogen, all of them gave good flame stability results. Under the so-called worst conditions of cold combustion air, zero swirl and cold walls, only the Hoogovens G1 and twinair burners could stabilize a flame. A good turn-down ratio was also possible with the twinair burner. He concluded that CO-enrichment did not influence the flame stability but gave a higher flame temperature and caused a change in the amount of radiative and convective heat transfer. In a second trial using the twinair burner, he found that there were two different limitations for having a stable flame. One was that the flame speed could be too low to allow flame stabilization at the bluff body, which resulted in a blow-off. The second was that a minimum "ignition energy" must be available around the recirculation zone to guarantee ignition of the surrounding flow. He also found that combustion air preheat was beneficial only if it resulted in a higher air exit velocity. It had only minor effects if the cross-sectional areas were changed to keep the exit velocities constant.

Syred et al. (1977) concluded from their work on LCV gas flames that a combination of aerodynamics and re-radiation of heat to an annular flame front seemed to produce the most stable flame. Rough refractory walls increased the heat re-radiated thus increasing the flame stability.

They also noticed that the calorific value of a fuel seemed to be one of the most important factors in determining combustion limits and low NO_x formation was due to low flame front temperatures.

In a study of the influence of burner rim aerodynamics on flame stabilization, Sohrab and Law (1985) found that by reducing the fuel concentration, the polyhedral flame began a chaotic back and forth motion and the geometry of the flame became irregular. This chaotic mode of agitation was considered to be an unstable mode of a cellularly unstable flame. The transition from the stable to the unstable polyhedral flame was believed to be caused by the fact that as the fuel concentration was decreased from the rich side, the resulting increase in the flame propagation velocity reduced the flame stand off distance, which in turn increased the heat loss to the burner rim and thereby enhanced the tendency for flame front instability. When the flame was surrounded by a blanket of nitrogen they observed that the flame characteristics changed drastically in that the occurrance of polyhedral flames was greatly facilitated. They argued that the influence of nitrogen was due to heat loss and dilution. First, outer nitrogen enhanced downstream heat loss by partly removing the diffusion flame mantle. Secondly, in the presence of nitrogen, oxygen concentration in the atmospheric air was reduced, thereby allowing for more efficient mixture stratification by the preferential-diffusion mechanism. Thus, even though outside gases were entrained, the composition of the mixture was minimally modified insofar as only nitrogen rather than air was being entrained. They concluded that burner rim aerodynamics were found to influence flame stabilization substantially.

Tsuji and Yamaoka (1982) identified two distinct modes of extinction in their investigation on near-limit premixed flames. One was flame extinction which occured close to the stagnation surface due to incomplete combustion and the other was flame extinction which occured at a finite distance from the stagnation surface due to flame stretch. They also concluded that the extinction of a flame, in which the diffusion coefficient of the excess reactant was much larger than that of the deficient one, was not only dependent on the Lewis number of the deficient reactant but was also affected by dilution of the reaction zone by an excess of the reactant with the higher diffusion coefficient.

In an investigation on the stabilization mechanism of lifted diffusion flames carried out by Vanquikenborne and Van Tiggelen (1965), they found that the base of a lifted diffusion flame appeared to anchor in a region where a stoichiometric composition was attained. They also explained that the blow-off and flash-back of the flame were by interaction between aerodynamic flow patterns and burning velocity. Yuasa (1986) found that the stability of diffusion flames using a double-swirl burner depended on the co-swirl intensity of both the fuel jet and the air stream. This was explained in terms of the increase in turbulent burning velocity at the base of the lifted flame owing to the increase in turbulent intensities in the swirling jet.

2.4.2 Combustion Measurement Studies

Chigier and Dvorak (1975) detected substantial changes in flow patterns when comparing the flow fields in turbulent swirling jets under flame and no-flame conditions. The kinetic energy of turbulence per unit mass under flame conditions was higher than in the corresponding cold

conditions in almost all regions of the flame. They concluded that the big increases found in kinetic energy of turbulence and velocity fluctuations were direct consequences of combustion.

From their investigations, Claypole and Syred (1981) found good agreement between their NO_x concentration contours and those obtained by other investigators. They suggested that in a highly turbulent combustion system, NO_x was predominantly formed in the flame front. The highest concentration of NO_x resulted from a turbulent diffusion flame which stabilized in the wake of the recirculation zone.

Günther and Wittmer (1981) concluded from their study on premixed turbulent cool flames that the influence of the flame on the temperature spectra was exerted by two competing effects. On the one hand, the mean temperature increase accelerated the dissipation of the smaller eddies and increased the microscales. On the other hand, the specific effects due to chemical reaction shifted the dissipative region of the temperature spectrum towards smaller eddies and the microscalar fraction of temperature spectrum became more energetic and the dissipative microscales decreased. The relative intensities of these two effects finally determined the action of the flame on turbulence.

Hassan et al. (1980) observed that the location of maximum fluctuation intensity laid outside the region of most intense combustion. The location of maximum mean temperature corresponded roughly to that of maximum combined CO plus CO_2 concentrations. They also noticed a peculiar finite oxygen concentration upstream of the main flame region ($X/d < 80$). They suggested partial extinction due to very rapid mixing in the strongly sheared flow in the burner region, finite intermittency

on the jet axis, turbulent diffusion of oxygen "packets" into the axis, oxygen penetration between ring vortices shed from the burner and extinction due to an excess of a limiting equivalence ratio as being some of the possible reasons.

From the work carried out by Hassan (1983), the following conclusions were reached on his results obtained from a cylindrical furnace. Comparative concentration measurements indicated that the discrepancy in results obtained from three different types of probe (quartz, water-cooled and water-quenched) was not excessive. Considering the results of concentration measurements, obtained using a water-cooled probe, and temperature profiles, two regions were identified in the early stages of the flame. One was a central core containing the reaction zone and the other was an outer wall recirculation zone. He also concluded that by imparting swirl to the secondary air, the radiation fluxes in the burner zone increased and the reaction zone became more compact. Changing the excess air level from 5 to 10% only had slight effects on the incident radiation fluxes.

Lockwood and Odidi (1975) found their data on unpremixed turbulent, free-jet flames agreeing well with data of other workers. Their measurements of temperature and of positive ion current in unpremixed flames suggested the combination of a Gaussian type distribution and a Dirac delta function, the latter showing the effects of jet intermittency.

From measurements made in stabilized nitrogen-diluted flames, Moneib (1980) found that a small increase in the percentage of nitrogen dilution (with the same Reynolds number input) shortened the flame and

caused a progressive reduction in both the maximum level of the rms value of temperature fluctuations $(\overline{T'^2})^{1/2}$ and the relative turbulence intensity, $\{(\overline{T'^2})^{1/2}/\overline{T}\}$, but the maximum mean temperature attained by the flame remained nearly constant. He pointed out the two main zones forming the basic structure of lifted flames. One was an upstream zone which exhibited an initial steep rise in temperature due to the burning of premixed mixture and the other was a diffusion zone in which the flame behaviour was similar to that of the stabilized flame case.

Working on a turbulent diffusion flame, Starner and Bilger (1981) concluded that the streamwise velocity was found to have a substantial correlation with both density and mixture fraction. They also suggested that Favre-averaging or other means of accounting for the density-velocity correlation should be used to conserve axial momentum flux. By comparing measurements obtained in single and two-stage combustion, Sadakata et al. (1981) found that by preheating air up to 300°C, the emission of NO from ordinary single-stage combustion was increased by a factor of three but there was no significant increase in the case of two-stage combustion for both thermal and fuel NO. They also concluded that air preheating of up to 300°C caused a 50% decrease in hydrocarbon concentration at the primary stage of two-stage combustion.

Gas concentration profiles obtained by Stewart et al. (1971) showed the unburnt fuel concentration having a maximum at the centre of the jet, the oxygen concentration decreasing rapidly from its ambient value near the edge of the jet. The carbon dioxide concentration showed a maximum at the edge of the jet and a significant amount of carbon monoxide was found within the jet boundary. These measurements were obtained from a test furnace burning commercial grade propane with 20% excess air.

Taylor and Whitelaw (1980) concluded from their work on an axisymmetric combustor with a premixed natural gas/air flame that combustion-induced oscillations became increasingly important as the equivalence ratio approached unity. There was only a small range of equivalence ratio for which stable combustion could be achieved. The velocity variance was twice as much in the recirculating region compared with what it was in other parts of the combusting flow. Uniform mean temperature distribution was obtained which was consistent with a well-stirred reactor assumption. They also found that significant changes in the length of the recirculation region and to local flow properties resulted from small changes in the equivalence ratio.

Wu and Fricker (1976) found that firing a swirling jet flame into a narrow cylindrical furnace influenced the jet flow pattern and flame shape. The flow pattern differed from that in a large furnace with a swirled flame of good ignition and stabilization characteristics. They encountered severe oscillations and vibrations with the risk of loss of ignition stability when operating at low swirl numbers, in the range of 0.2-0.5, on that particular furnace. They also showed that a wide range of heat flux distribution was possible in a cylindrical furnace by using a combination of different swirl intensity and burner quarl configuration. Their twin-air burner system, with swirl imparted to the inner section, gave a more uniform heat distribution and good ignition stability.

In a study of cross-correlation between velocity and temperature in a turbulent premixed flame, Yanagi and Mimura (1981) found that the temperature fluctuations were induced by the velocity fluctuations.

They also pointed out that the bimodal nature of the PDF at the flame front suggested that the flame front structure was approximated by the wrinkled flame model; so the fluctuation of heat generation at the measuring point could not be neglected in modelling of the combustion process.

Yoshida (1981) found the characteristics of the temperature fluctuation in the turbulent premixed flame zone to be very close to those predicted by the wrinkled laminar flame model. The mean radial velocity appeared at the position where the mean temperature began to rise and increased with the mean temperature attaining a maximum outside the flame zone. There was also no visible sign of the flame generated turbulence or the Reynolds shear stress in the wrinkled laminar flame structure. By comparing his results with previous measurements he concluded that there must be a structure other than the wrinkled laminar flame.

Yoshida and Tsuji (1982) found the length scale of wrinkles in an open turbulent, premixed flame to be around 5 mm and almost independent of the upstream turbulence or the unburnt gas velocity. They also measured the periodicity of temperature signals which indicated that the wrinkles which appeared upstream were transported downstream along the flame front. The wavelength derived from the length scale grew longer along the flame front with a similar growth rate as that of the laminar burning velocity.

2.5 Main Effects of Operating Conditions on Combustion

2.5.1 Effects of Swirl on Combustion

The advantages of using a swirling jet as a mean of controlling flames in combustion was realized a long time ago by many investigators. It

was only recently that a concerted effort was made to understand how and why rotating flow has such an important influence on the stability and combustion intensity of flames. The majority of large scale investigations on swirling combustion has been carried out at the IFRF. Beltagui and Maccallum (1976) reported that the maximum diameter of the CRZ was uninfluenced by further increases in swirl once the CRZ was well established. They found the peak temperatures at a plane to lie just inside the CRZ which differed from observations in corresponding open flames where the peak temperatures were just outside the CRZ. They explained this difference by pointing out that the open flames entrained ambient air which lowered the temperatures, whereas confined flames entrained combustion gases from the peripheral recirculation zone which are comparatively hot.

Chedaille et al. (1966) put forward three main effects of swirl on turbulent diffusion flames. First, ignition could be stabilized very close to the burner exit due to back-flux of hot combustion products. They pointed out that the role of the internal recirculation zone was more effective than the external one because the gases recirculated from the internal zone were much hotter since they came from the hottest part of the flame, so the heating effect on the fuel was almost immediate. Secondly the internal reverse flow caused an acceleration of the mixing of fuel and air in the first part of the jet because the annular layer of combustion air in which this mixing took place was thin and also because of the intense turbulent exchange across this layer as well as between it and the vortex region due to the high shear velocity gradient present. The third main effect of an internal reverse flow was the increase in residence time of combustion matter for a given furnace

length. This third effect is more important in pulverized coal flames where more time in the hot reverse flow zone yield a greater amount of volatiles from the coal particles. They showed all three of the above effects from measurements made in their furnace and noticed that a much shorter distance was required for complete combustion when compared to flames without swirl.

Leuckel and Fricker (1976) also noticed similar effects of swirl on flames as Beltagui and Maccallum (1976). Once sufficient swirl was imparted to the combustion air so that an internal recirculation zone was formed which caused the ignition to stabilize inside the burner quarl, further increase in the swirl intensity had very little effect on either the flow pattern, flame length or flame temperatures. This was backed by large amounts of measurements made on IFRF furnaces burning natural gas. They also pointed out that two different types of stable flame can be achieved by using swirl stabilization; one giving a relatively long flame and the other a short intense flame. In the third part of the study they also concluded that the main effect of swirl was that of promoting the mixing of fuel and air rather than the increase of reverse flow of hot burnt gases back into the burner quarl. The same effects were observed by Hassan (1983); additionally he also found an increase in radiation fluxes near the burner zone as a consequence of swirl being imparted to the combustion air.

2.5.2 Effects of Excess Air on Combustion

Beltagui and Maccallum (1976) found that an increase in excess air levels for their confined swirled flame caused a central recirculation zone (CRZ) to be formed. The maximum reverse mass flow in the CRZ was

less than 10% of the burner mass flow. Although the CRZ disappeared with a reduction in excess air, troughs remained in the axial velocity around the axis near the burner.

Fricker and Leuckel (1976) have shown that at high excess air there was a deterioration in the burner performance helped by the use of swirl which has a tendency to shift the fuel-lean combustion limit towards higher equivalence ratios. They have also pointed out that with a flame with a CRZ (type II), there was no influence of gas injection velocity on ignition stability both with low and high excess air levels and at all swirl intensities. They argued that there was an advantage in reducing swirl to the mimimum required for obtaining an internal reverse flow, thus avoiding over-dilution of the fuel with excess combustion air upstream of the ignition zone, when working with burners operating with an excess air level of 100% or more.

Hassan (1983) observed that an increase in excess air from 5% to 10% had only a slight effect on the incident radiation flux. He also reported very little change in the radial temperature and concentration profiles. This is to be expected because the excess air level was not that high so as to cause major changes in the flame structure. Syred et al. (1977) found that by adding 10 to 20% excess air to their combustion process, the carbon monoxide formed in the flue gas, when burning waste gas near the stoichiometric mixture ratios, disappeared.

Schreier (1981) reported an improvement in flame stability by using 50% excess air on a baseline burner using low calorific value gases. It was also possible to increase the burner loading but further increase in the excess air level to 100% caused a reduction in the maximum load possible.

2.5.3 Effects of Preheating on the Combustion Air

Very little work has been done on the effects of preheating the combustion air supplied to flames. In general, it is recognized that by raising the temperature of the combustion air, faster mixing takes place due to the increased kinetic energy of the air molecules which results in a higher diffusion rate between the fuel and air molecules.

Using a twinair burner, Schreier showed that by preheating the combustion air to about 250°C a stable flame could be achieved in cases where without preheating it was impossible to sustain any type of flame. He also indicated that preheating shortened the length of the flame significantly. Sadakata et al. (1981) investigated the effects of air preheating on the emissions of NO, HCN and NH_3 from single and two-stage combustion. They found that by preheating the combustion air to 300°C, a three fold increase of NO resulted from the single stage combustion whereas no significant increase in emissions of both thermal and fuel NO was noticed from two stage combustion. There was also a 50% decrease of hydrocarbon and HCN at the primary stage by preheating the combustion air to 300°C for two stage combustion.

2.5.4 Effects of Nitrogen Dilution on Combustion

The main effect of adding nitrogen to a gaseous fuel is to bring its calorific value down. So for a required furnace output, a larger amount of fuel is necessary which can give rise to stability problems at the burner exit.

Hassan et al. (1980) showed a shortening of the flame length on work carried out using a free jet diffusion flame. They also found the maximum mean temperature attained by the flame remaining nearly constant over the range of nitrogen dilution investigated. From concentration measurements made on the same flame, under the same conditions, Hassan (1983) showed that the increase in the percentage of nitrogen caused a reduction in the level of unburnt hydrocarbon and the maximum levels of both carbon dioxide and carbon monoxide.

2.6 Closure

Despite the vast amount of work outlined above, it can be seen that there are many conflicting ideas about the structure of the flame under different prescribed conditions. There is still a great shortage of work on turbulent diffusion flames as used in industrial furnaces and in particular using low calorific value gases.

The present work will provide a better understanding of flame stability based on confined, turbulent diffusion flames burning low calorific value gases. The effects of swirl, combustion air preheat, excess air levels and nitrogen dilution on the stability limits and combustion will also be considered.

CHAPTER 3

FURNACE & INSTRUMENTATION

3.1 Introduction

Stability tests and combustion measurements were carried out in a substantially modified Hilton Combustion Demonstration Unit. In their original form many of these units are used by undergraduate and postgraduate students to carry out combustion experiments. The main research limitations of the unmodified furnace concerned the burner system, which was not respresentative of the majority of industrial burners, and the asymmetry of the furnace, a consequence of the exhaust duct being offset with respect to the burner axis. A symmetrical furnace allows the combustion measurements to be halved because full traverse across the furnace is then unnecessary.

Modifications to the burner system and the exhaust end of the furnace in order to correct the above-mentioned defects were therefore carried out. A concentric pipes system with radial injection of natural gas or natural gas/nitrogen mixture was utilized as the burner, Fig.(3.4), and a new back plate constructed with the exhaust duct placed in the centre, Fig. (3.2). A movable block swirl generator similar to the design of Beér and Chigier (1972), Fig. (3.5), was incorporated to impart swirl to the secondary air. Calibrated rotameters were employed to measure the mass flow rates of secondary air, natural gas and cooling water entering the furnace.

Inflame temperature measurements were made using a fine wire thermocouple system comprising of 40 μm platinum/platinum 13% rhodium wires. Velocity measurements were carried out with a 5-hole pitot tube connected to a micromanometer via a 10-way selection box. A water-cooled sampling probe was made to collect combustion gases in the furnace for concentration measurements through a multi-system combustion gas analyser. The temperature, velocity and concentration data were processed via an Apple IIe microprocessor system. A traversing mechanism was made to carry and move the various probes inside the combustion chamber and a motorized unit controlled by the Apple IIe was incorporated in the system to permit automatic data collection.

3.2 Furnace Arrangement

The furnace, Fig.(3.1), consisted of a horizontally orientated water-cooled combustion chamber with a front plate carrying a quarl and the burner with its swirl generator, see Panel (3.1). The back plate of the combustion chamber was refractory lined and contained the exhaust duct, an explosion vent, an observation port and a water-cooled mounting to connect the ultra-violet flame scanner, see Fig. (3.2).

Combustion air was supplied to the furnace by a rotary air compressor (BVC Eng. Ltd : Model Y3) and was measured by a calibrated rotameter (KDG Flowmeter : Model 47XE). A small preheater (Secomak Ltd : Model 25 BNY) was used to preheat the air to 50°C in order to satisfy the calibration requirements of the rotameter. The temperature of the air entering the rotameter was monitored by a Cr/Al thermocouple. The air was then fed to the main heater (Secomak Ltd : Model 441/2) where its temperature was raised to the preheated value required before being

delivered to the swirl generator through a lagged manifold. Each heater had its own potentiometer (Variac) to control the heating power required. Cr/Al thermocouples were used to measure the temperature of the air leaving the main heater and that of the flue gases in the exhaust duct.

3.2.1 Combustion Chamber

The combustion chamber was cylindrical and horizontally orientated with a length of 900 mm. Its internal diameter was 457 mm and it was of double skin construction permitting the entire section to be water-cooled; see Fig. (3.3). Three pairs of observation windows were located along the length of the combustion chamber; they also served as sampling ports. The windows were placed at distances of 203, 457 and 711 mm from the exit plane of the quarl. A factory fitted Cr/Al thermocouple was employed to monitor the cooling water temperature leaving the combustion chamber. The thermocouple signal was also connected to the safety management system of the furnace which shuts the gas supply off in the event of the cooling water temperature rising above a set value. To resist corrosive attacks, stainless steel was used for the combustion chamber body.

3.2.2 Burner System

Fig. (3.4) shows a schematic of the burner system used. Its design is similar to many existing types of industrial burner utilized in gas furnaces. A concentric pipe system was employed, with radial injection of the fuel. Many investigators have shown the benefits of improved stability by injecting the fuel radially, (Leuckel and Fricker (1976),

Hassan (1983) and Rawe & Kremer (1981). The air pipe had an internal diameter of 42 mm and an outer diameter of 45 mm. The inner and outer diameters of the gas pipe were 15 mm and 20 mm respectively. Eight holes of 3.0 mm diameter each were drilled on the circumference of the nozzle for the fuel to exit.

Swirl was imparted to the secondary air by means of a movable block swirl generator similar to the design of Beer and Chigier (1972); see Fig. (3.5). The swirl generator was calibrated by means of a swirl meter (Hassan 1983) and the results are shown in Appendix (A). A refractory quarl with a half angle of 9.7° was used to stabilize the flame; the burner exit was located at the throat of the quarl.

3.2.3 Igniter and Flame Failure System

A small igniter torch (Industrial Automated Systems Ltd : Model (CA 115)) with its own gas and air supplies was employed to ignite the main burner. After successful ignition of the furnace, the gas and air supplies to the igniter torch were cut-off by means of solenoid valves controlled by signals from the flame scanner.

In order to prevent an explosion, a good flame failure detector system was necessary. A protector relay (Honeywell : Model RA 890 G) in conjunction with a minipeeper ultraviolet flame detector (Honeywell : Model C 7027 A) were used. In the event of the main flame going out, no signal would reach the flame detector and the system would close the main solenoid valve (Alcon : Model GБóB) thus prohibitting the flow of fuel to the furnace. The protector relay also responded to abnormal exit temperatures of the cooling water and the absence of secondary air in the main preheater. After a blow-off, the system could not be restarted unless the furnace was purged for at least 2 minutes.

3.2.4 Gas Mixing System

Fig (3.6) shows a schematic of the gas mixing system. Natural gas from the main supply was monitored through a calibrated rotameter (KDG Flowmeters : Model 18 XE) and supplied to a cylindrical mixing chamber Fig. (3.7) via a pipe manifold system. Oxygen-free Nitrogen (BOC) was used to dilute the natural gas. After being measured by means of a calibrated rotameter (KDG Flowmeters : Model 14 XE), the nitrogen was fed to the mixing chamber via a nitrogen distributor. Eight pipes alternately feeding natural gas and nitrogen to the mixing chamber were chosen to improve mixing of the two gases. An emergency fuel shut-off valve (manual) and a Class I fuel solenoid valve were installed, as part of the safety features, on the fuel line connected to the burner. The temperature of the mixture in the mixing chamber was monitored by means of a Cr/Al thermocouple.

3.3 Instrumentation

The instrumentation system employed to obtain inflame temperature, velocity and concentration data is outlined in Fig. (3.8). A central data processing unit consisting of an Apple IIe microprocessor coupled with a 16-Channel, 12 bit analogue to digital (A to D) converter (Interactive Structures Inc.: Model AI13) was used in the system. After each of the above-mentioned data were converted into an appropriate voltage signal by their dedicated system, the A to D converter changed the signal into a form (digital) that was acceptable by the microprocessor. The signal was then processed and the output was displayed on the monitor as temperature, velocity or concentration, depending on what was being measured. At the end of a traverse, a

hard-copy of all the data collected was printed on a line printer (Epson : Model MX-100 Type III). Figure (3.9) shows a flow chart depicting the stages of the programs used for temperature, velocity and concentration measurements as well as controlling the traversing mechanism used for automatic data logging.

3.3.1 Temperature Measuring System

The time averaged inflame temperature was measured by a system similar to that used by many investigators (Hassan (1983), Hirji (1986), Monieb (1980)). The schematic of Fig. (3.10b) outlines the system employed. Details about the heat transfer characteristics and radiation and conduction corrections are well documented elsewhere; (Hassan (1983), Monieb (1980)). However a brief description of the probe and the system is given below.

A 40 μm platinum/platinum 13% rhodium thermocouple was used to measure the temperature. The appropriate wires were welded on a capacitor discharge welding unit (Spembly Ltd : Model WPL4). Several thermocouples were made and only those having a bead size diameter between 70 and 80 μm were selected. The thermocouple was then attached to the appropriate supporting wires which were 0.5 mm in diameter. A twin-bore alumina tube which was encased in a stainless steel sheath to give protection and strength was used to carry the length of supporting wires, see Fig. (3.10a). The ends of the supporting wires were connected to suitable socket terminals (Labfacility Ltd). Screened compensating leads (Labfacility Ltd) were used to carry the signal to a differential amplifier (RS : OP-27) where it was amplified by a factor of 100. It was then simultaneously fed to an oscilloscope (Solartron :

Model CX 144) and the data acquisition system (Interactive Structures Inc : Model AI13) where it was digitized before being manipulated by the microprocessor. The purpose of the oscilloscope was to assess the quality of the signal and the presence of an open circuit caused by breakage of the thermocouple.

A temperature measurement program then converted the signals into temperatures which were stored in the computer's memory for future use. A subroutine in the main program took care of the radiation corrections of the thermocouple. After two traverses across the furnace, a list of temperatures measured at intervals of 10 mm (up to the centre line) was printed together with the operating conditions of the furnace. At the end of four more runs, under two different conditions, a list printing the average temperatures for each of the three conditions was produced. A graph of mean tempeature ($\bar{T}^{o}C$) against radial distance traversed (R mm) was then plotted on the attached cylindrical plotter (Strobe 100). At each measuring point the average of 1000 readings was taken spanning over a period of 40 seconds, see Table (A1) of Appendix (A) for samples.

3.3.2 Velocity Measuring System

A five-hole water cooled pitot probe was employed to measure the velocity inside the combustor. Prior to its use on the furnace, the probe was calibrated on a small wind tunnel and the results of the calibration test are given in Appendix (A). Figure (3.11) shows details of the probe.

The pressure tappings on the probe head was connected to a digital micromanometer (Furness Controls Ltd : Model FCO 12/2) via a 10-pair selection box (Furness Controls Ltd : Model FCO 19). The layout of the velocity measuring system is given in Fig. (3.12). In order to select the different pressure tappings automatically, a special circuit was designed and made as shown in Fig. (3.13). This enabled the computer to select a particular pressure tapping as and when required by the program.

An output socket at the back of the micromanometer provided a voltage representing the reading on the display; see Table (A4) in Appenix (A). This voltage was then fed to the microprocessor via the data acquisition system where it was digitized. A special program was written to process these pressure measurements and convert them into velocity measurements. To account for the swirling flows, special subroutines were included to give the conical and dihedral angles.

Again an average of 1500 readings were sampled but this time spanning over a period of 5 minutes. Two traverses were performed at each operating condition and the results printed as shown in Table (A2) of Appendix (A). The velocity represents the magnitude of the mean value in the direction given by the conical and dihedral angles. Details of the method employed is outlined in Appendix (A).

3.3.3 Concentration Measuring System

Inflame species concentration were measured for UHC, NO_x, O_2, CO and CO_2 with the help of a water-cooled sampling probe, Fig (3.14). Sample gases were sucked continuously and delivered to an analysis system for

combustion monitoring via a 5 m length of heated sample line. The analysis system was made of a sampling unit and five analysers measuring unburnt total hydrocarbon (UHC), nitric oxide + nitrogen dioxide (NO_x), Oxygen (O_2), carbon monoxide (CO) and carbon dioxide (CO_2); see Panel (3.2). Specific concentration of span gases were available for calibration of the instruments. All the analysers had analogue voltage outputs which could be used to dirv chart recorders or data logging systems; see Fig. (3.15). Table (A3) of Appendix (A) shows some sample results.

Sampling Unit

Fig. (3.16) shows a line diagram of the sampling unit. Gas samples were pumped into the unit by means of a twin head vacuum pump (ADI : Model 193231). A filter assembly containing a microfibre filter element (Balston Ltd : Model 050-11-BQ) disposed of any particulate matter present in the sample prior to entering the pump. The sample was then distributed in two separate lines; one line was fed into a permeation dryer which in turn supplied dry sample gases to the oxygen, carbon monoxide and carbon dioxide analysers. The other line was further subdivided into two, one feeding the total hydrocarbon analyser and the other the NO_x unit. The flow and pressures of these two units were controlled by preset needle valves.

A mini vacuum pump (ADI : Model 19312N) was employed to supply purge gas for the permeation dryer. The sample pump, preset needle valves, part of the permeation dryer and the filter assembly were located in an insulated heated enclosure which was maintained at a temperature of 110°C. Thermocouples (Cr/Al) and temperature controllers were employed to keep the temperatures of the heated enclosure, external heated

sampling line and the internal heated total hydrocarbon unit connecting line at their designated values. All the flow bypasses and gases that have been analysed by the units were piped into one common vent which was connected to the laboratory exhaust system for safe disposal.

Unburnt Total Hydrocarbon Analyser

The unburnt total hydrocarbon analyser (AAL : Model 523) was an advanced design high temperature instrument utilising the flame ionisation detector (FID) technique. A small, continuous flow of sample gas was burnt in a polarised hydrogen flame. During the combustion process compounds containing carbon-hydrogen bonds formed ions; a potential was applied between the flame and a collector electrode causing migration of the ions to the electrode. The resulting ion current was related to the concentration of hydrocarbon in the sample. This signal was amplified and displayed by the electronics modules of the analyser.

NOx Analyser

The NO_x analyser (AAL : Model 443) used the principle of chemiluminescence to measure the nitric oxide (NO) present within a system. It was also capable of measuring the total level of nitrogen dioxide (NO_2) and nitric oxide (NO) present. This measurement is termed 'NO_x'. The unit contained its own heated sample module.

The instrument detected and measured nitric oxide using its chemiluminescent reaction with ozone (O_3). The ozone was generated within the instrument and after the reaction any residual ozone was catalytically destroyed.

The sample gas and ozone are mixed within the reaction chamber in front of the photomultiplier tube. Nitric oxide reacts with ozone to produce nitrogen dioxide; some molecules of which are in the ground state and some in an excited state. The reaction processes are shown below. A molecule of electronically excited nitrogen dioxide decays to the ground state either by loss of a photon of energy or by energy transfer to other species (M) by collison. M can either be the walls of the chamber, or other molecules of gas in the sample flow.

$NO + O_3 \longrightarrow NO_2 + O_2$	Production of nitrogen dioxide
$NO + O_3 \longrightarrow NO_2^* + O_2$	Production of electronically excited nitrogen dioxide
$NO_2^* + h^\circ \longrightarrow NO_2 + h\nu$	Chemiluminescence
$NO_2^* + M \longrightarrow NO_2$	Collisional Deactivation

where

h° = hole

h = Planck's constant

$h\nu$ = Energy of light (photon energy).

It is found to a good approximation that the intensity of the emitted light (I) is given by the equation

$$I = \frac{Io\{NO\}\ \{O_3\}}{\{M\}}$$

where Io = a constant, NO = concentration of nitric oxide, M = concentration of deactivating species and O_3 = concentration of ozone.

If the concentration of ozone is sufficiently high to ensure its concentration does not change before and after the reaction, then the intensity of emitted light is linear with respect to the nitric oxide concentration. This intensity was monitored by the photomultiplier tube within the detector assembly.

The chemiluminescence process is specific to nitric oxide. Using a catalyst contained within the analyser NO_2 can be converted to NO prior to entering the detector chamber, thus allowing the determination of NO_x. Readings thus obtained from the analyser were the sum of the concentrations of nitrogen dioxide and nitric oxide. The instrument could be operated as an NO_x or NO analyser by switching the converter in or out of stream.

CO/CO_2 Analysers

Both of these instruments were housed in one unit and worked on the principles of non-dispersive infrared (NDIR) gas analysis. The measurements were accomplished by measuring the infrared absorbtion of the selected component in the gas mixture.

Infrared absorbtion in gas mixtures is a characteristic of the type and arrangement of the constituent atoms of the gas molecules. The infrared radiant energy interacts with the molecules of the gas mixture. The degree of interaction is a function of the spectral regions or spectral bands for the different gas components. These spectral bands are different for different gases and therefore lend themselves to NDIR analysis.

Basically each analyser consisted of an optical unit, signal processor and meters. The optical unit assembly was the heart of the analyser system. It was conceived on the dual beam spectrometer principle to attain the superior stability characteristics associated with this configuration. The optical unit contained the infrared energy source, an optical chopper, sample and reference tubes, optical filters and detectors.

Oxygen Analyser

This analyser utilizes a Micro-fuel cell to measure the concentration of oxygen in a gas stream. The analysis is specific for oxygen; i.e. the measuring cell will not generate an output current unless oxygen is present in the sample gas. Oxygen is consumed by the cell from the gas around it, and a proportionate micro-ampere current is generated. The low level signal is then amplified by a solid state, integrated circuit amplifier, and the resulting D.C signal is suitable for driving a high impedence recording device, a temperature compensation circuit for the cell and an integral 0-100 microampere meter.

3.3.4 Data Logging System

To facilitate and speed up the data collection process an automatic data logging system was designed and produced. The system was controlled by the Apple IIe microprocessor. A traversing mechanism to carry the probes in and out of the furnace was also made, see Fig. (3.17) and Panel (3.3). A special lead screw with a 2 mm pitch was utilized to transport a saddle on which the probe was mounted at a prescribed distance. Two polished steel struts running through brass bushings were employed to stabilise the saddle movement.

The lead screw was driven by a digital stepping motors (SIGMA, Model 20-2235 D 200 F 3.7B) in an open loop configuration. Two hundred steps were required for one complete revolution of the motor and by using it with the 2 mm pitch lead screw, a resolution of 10 μm could be achieved. To operate the stepping motor a bipolar stepper drive (DIGIPLAN, Model SD2) was employed; power was obtained by a 36V 2A transformer (DIGIPLAN, Model TO 119). The pulses required to control the system were provided by the Apple IIe microprocessor boosted by a 12V power supply (R.S. Model 591 310) and a transistor circuit. A special assembly language subroutine was written to deliver the pulses at the desired rate. A block diagram of the system is shown in Fig. (3.18).

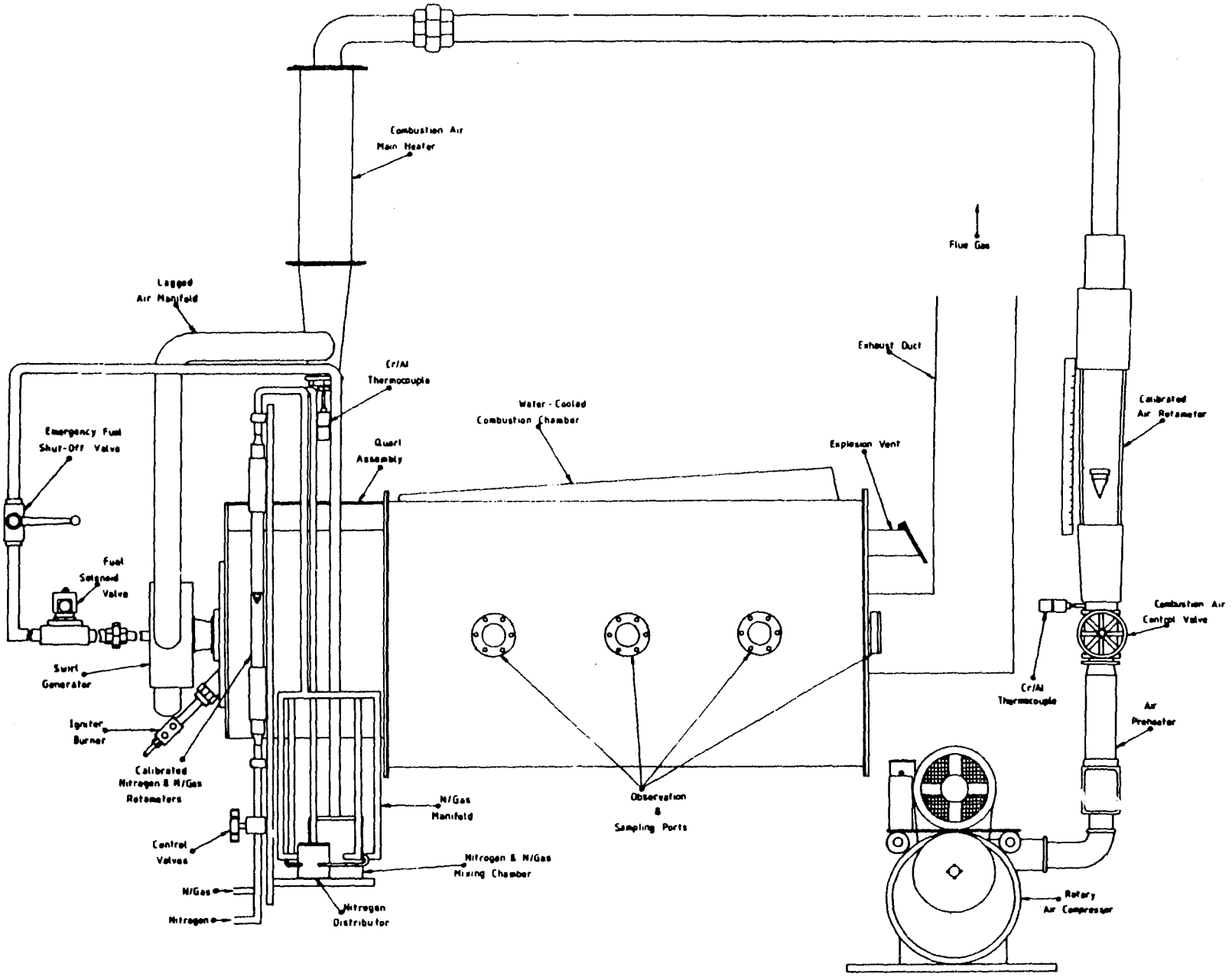

Fig (3.1) Furnace Arrangements

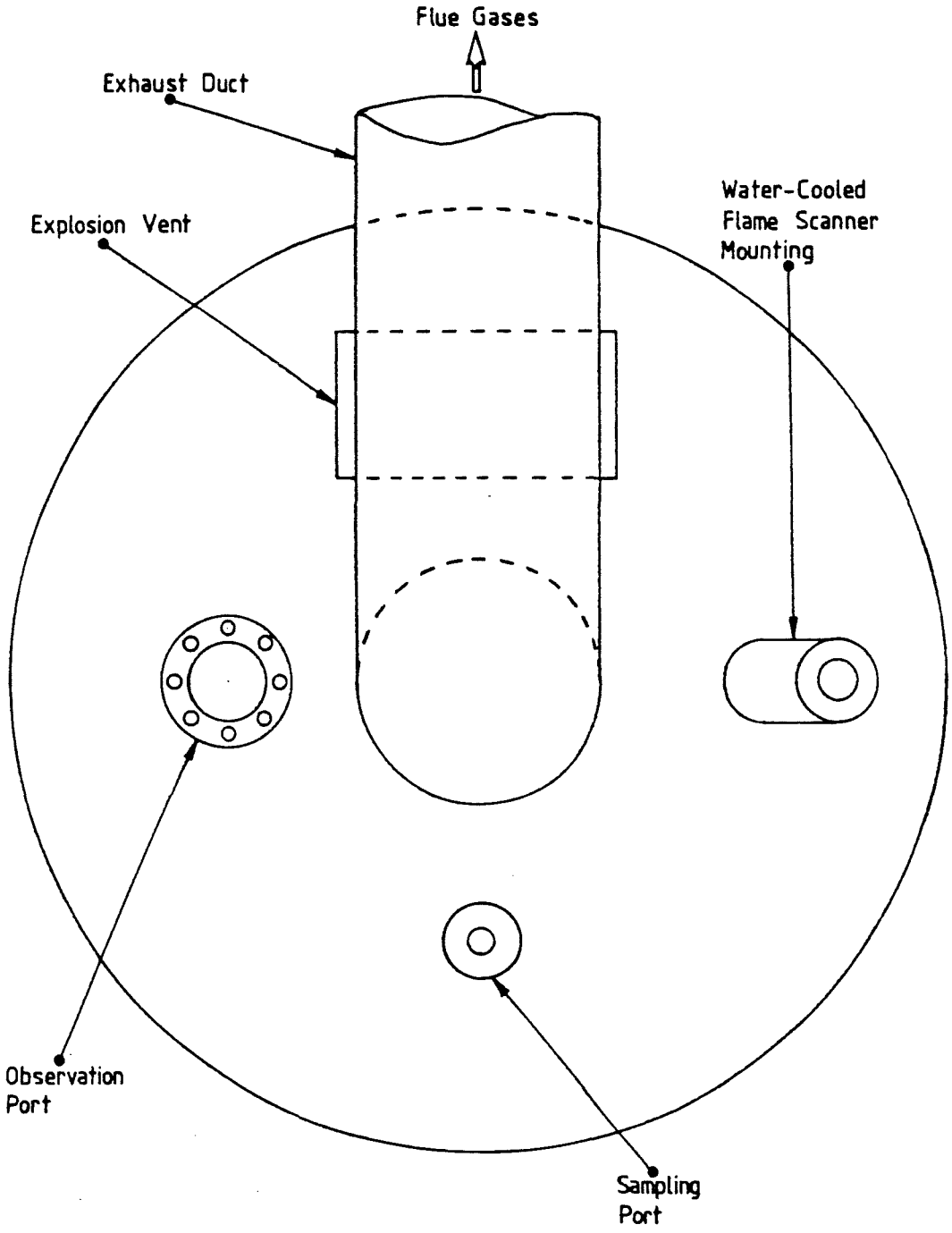

Fig (3.2) Details of exhaust end of furnace

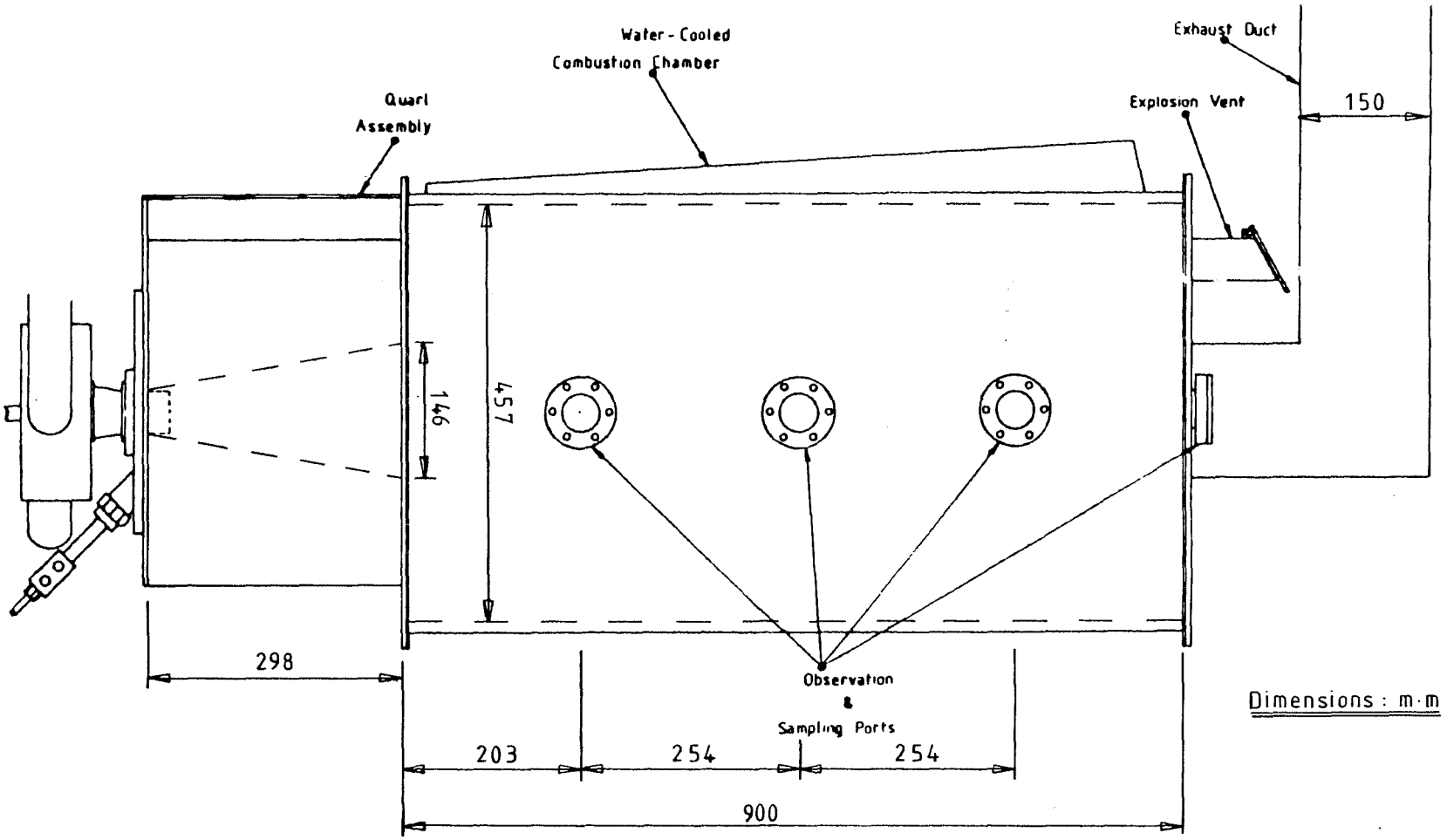

Fig (3.3) Details of combustion chamber.

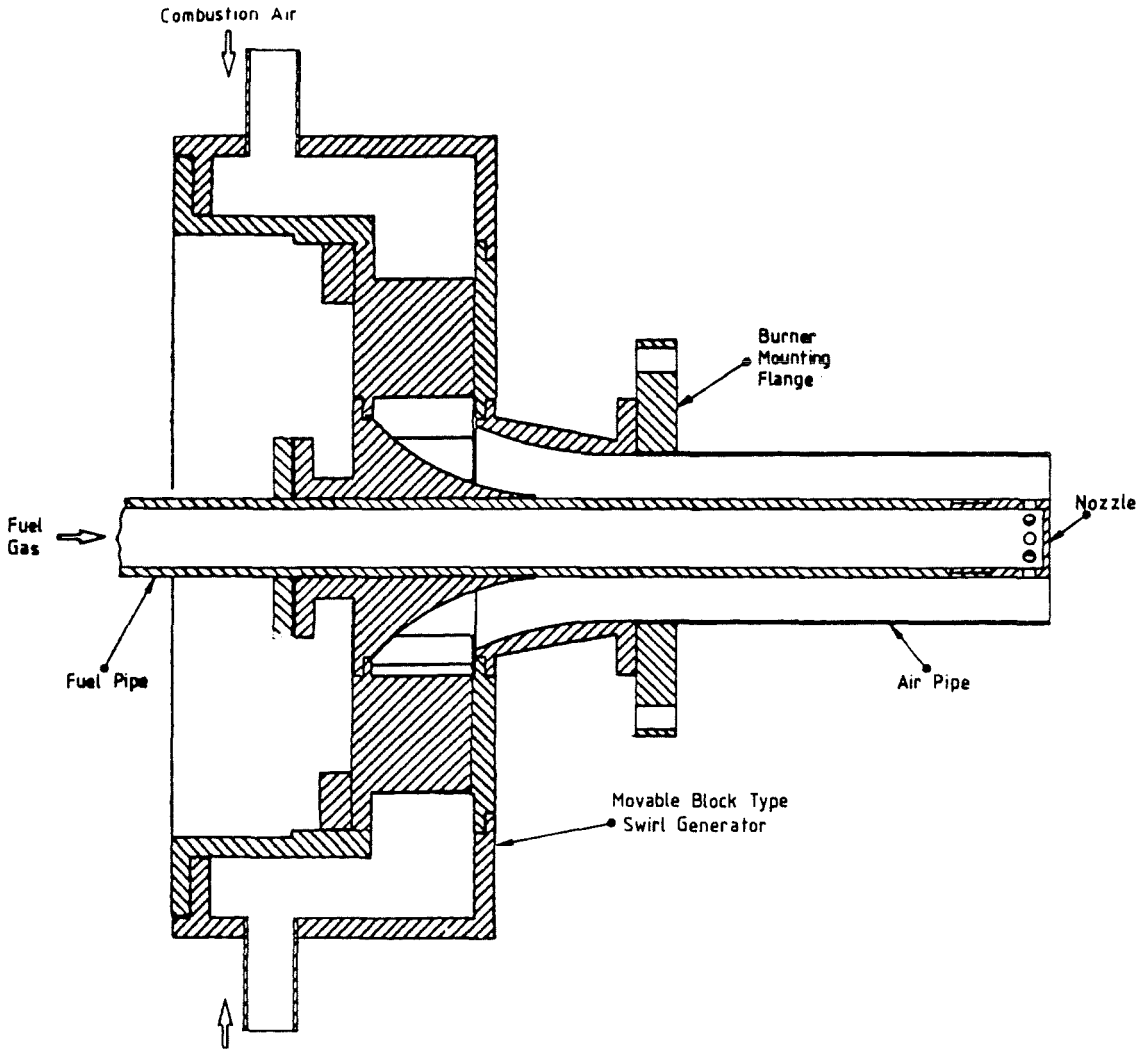

Fig (3.4) Schematic of Burner System

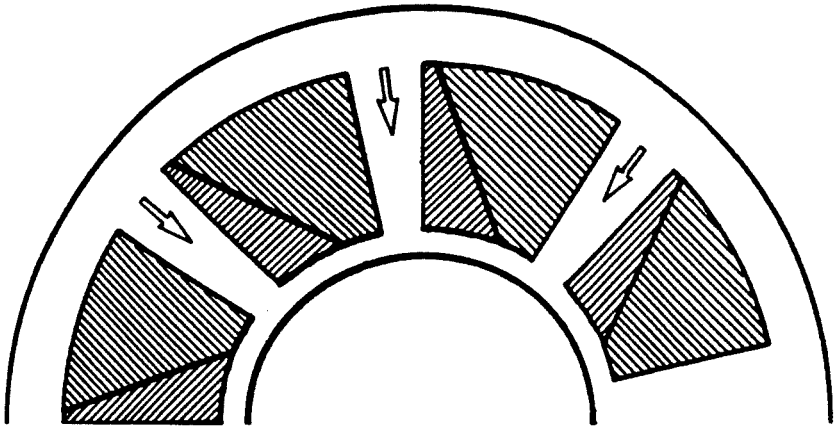

Zero Swirl

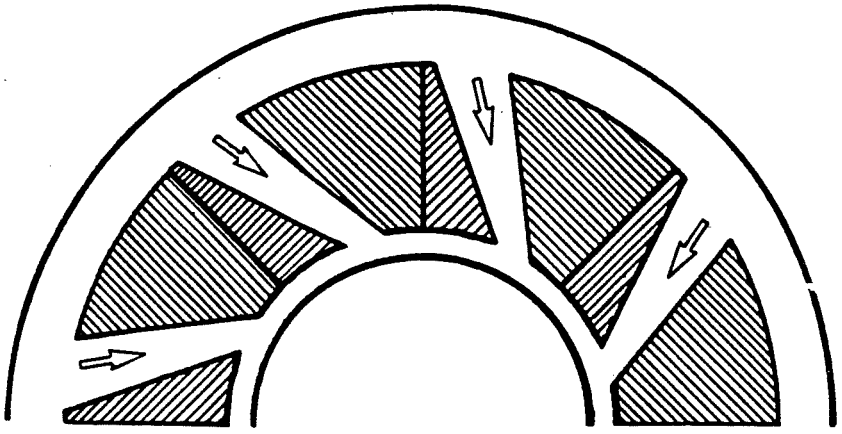

Maximum Swirl

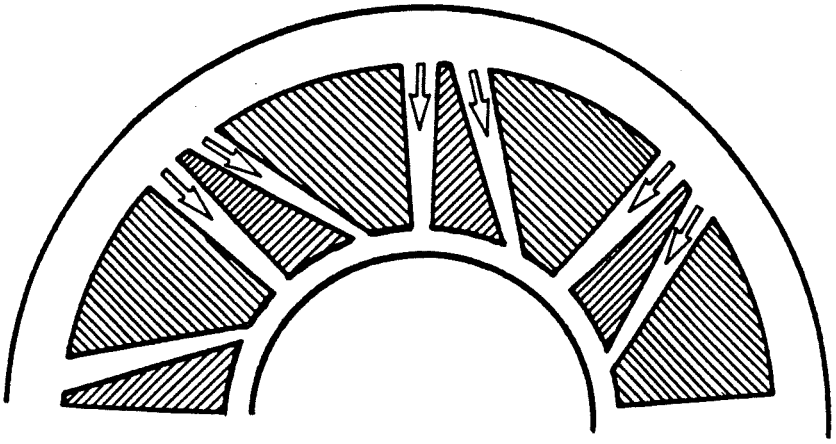

Intermediate Swirl

Fig (3.5) Details of moving block swirl generator.

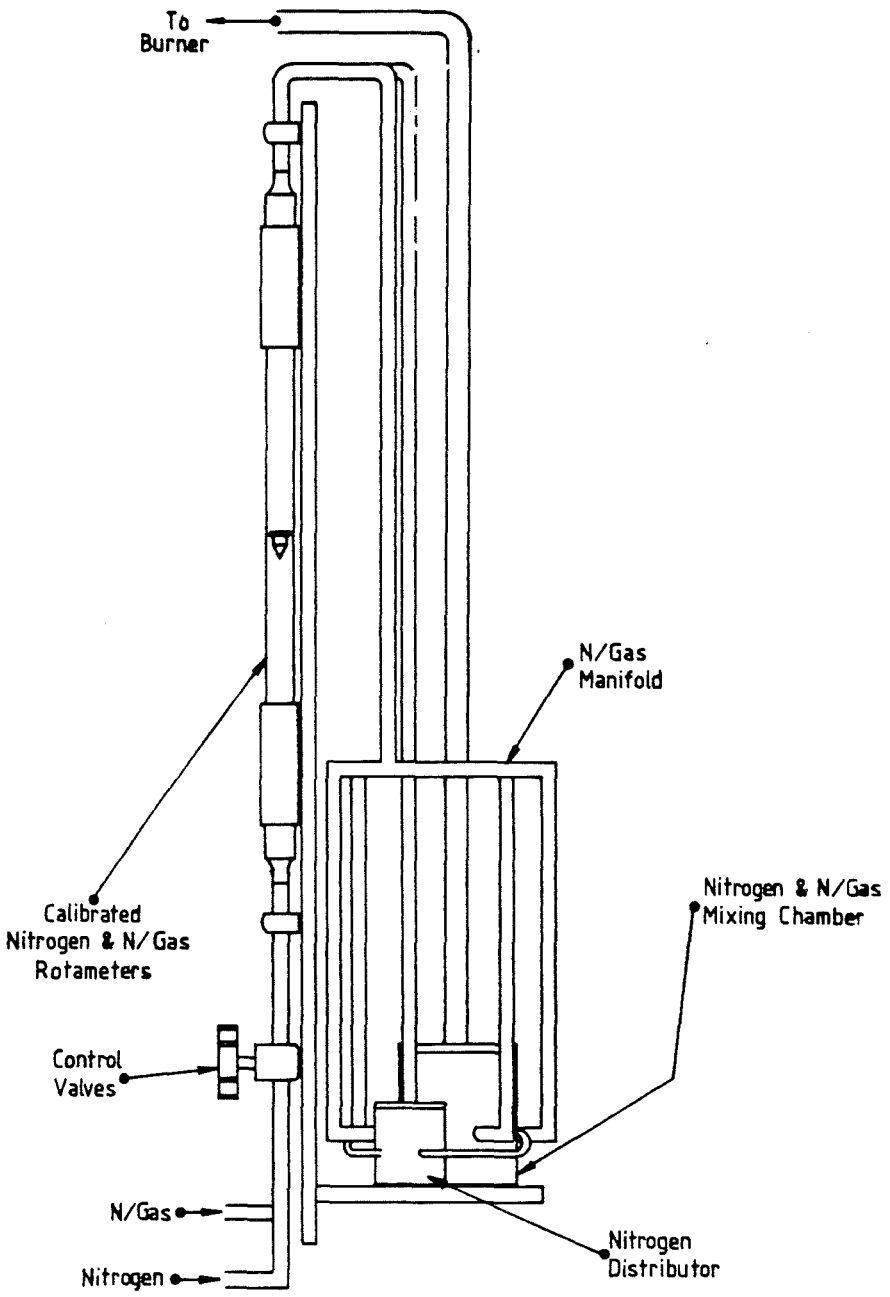

Fig (3.6) Details of gas mixing system

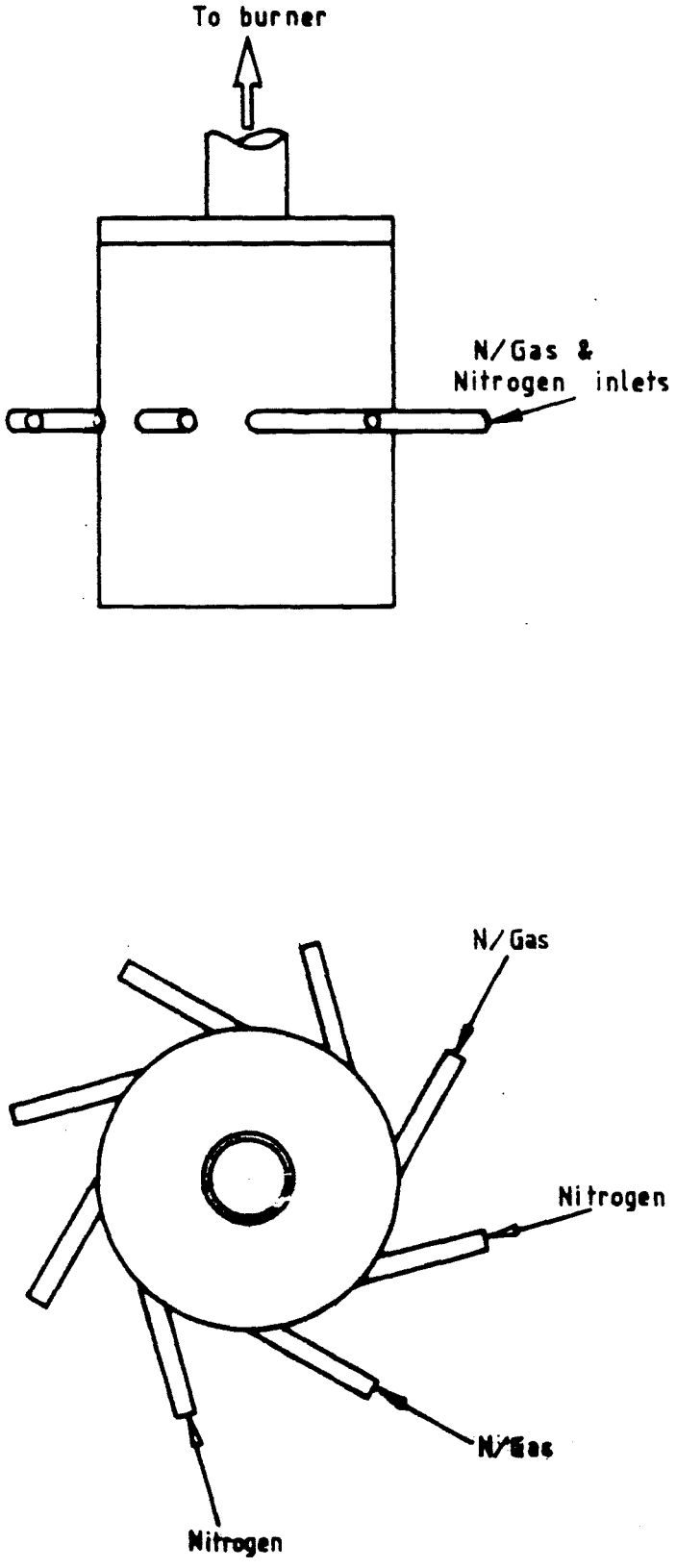

Fig (3.7) Details of cylindrical mixing chamber.

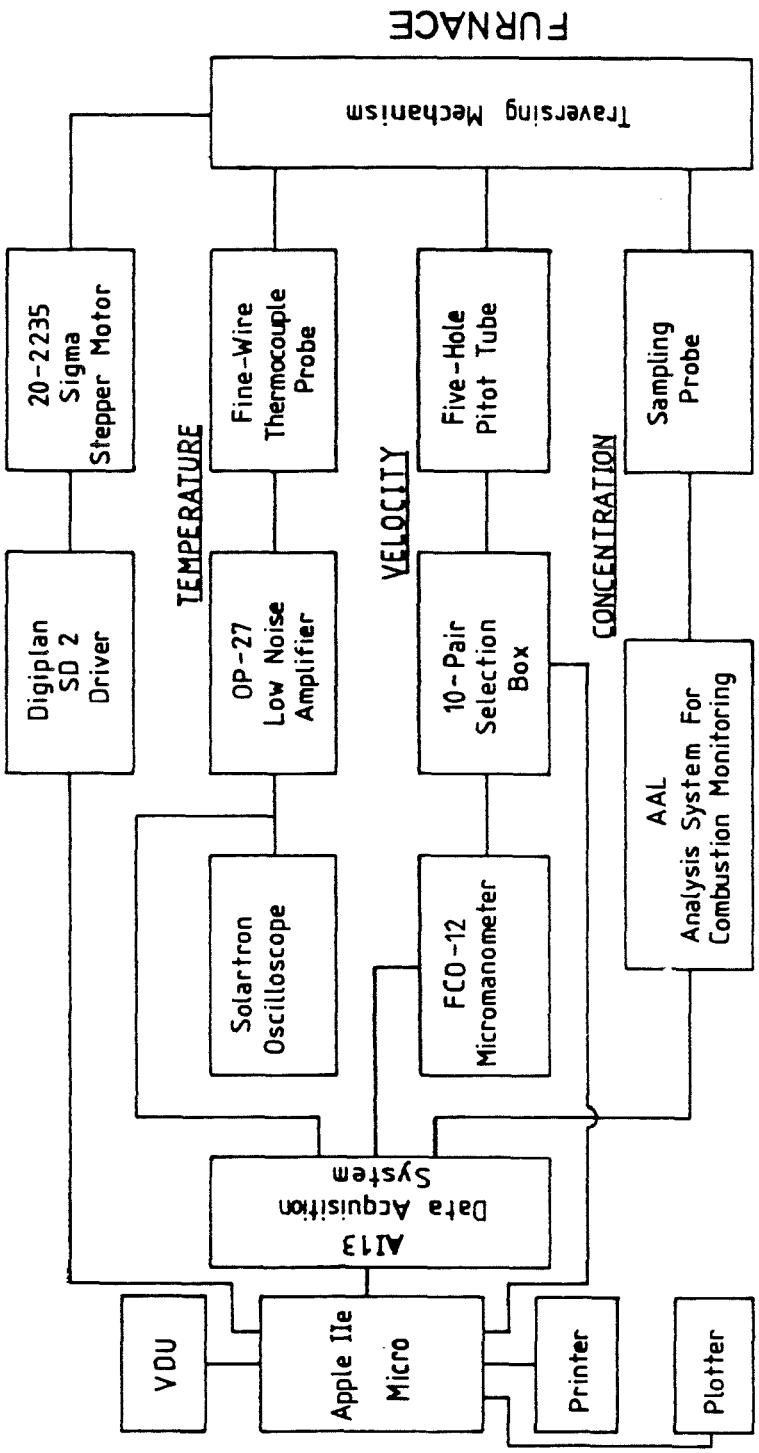

Fig (3.8) Instrumentation system.

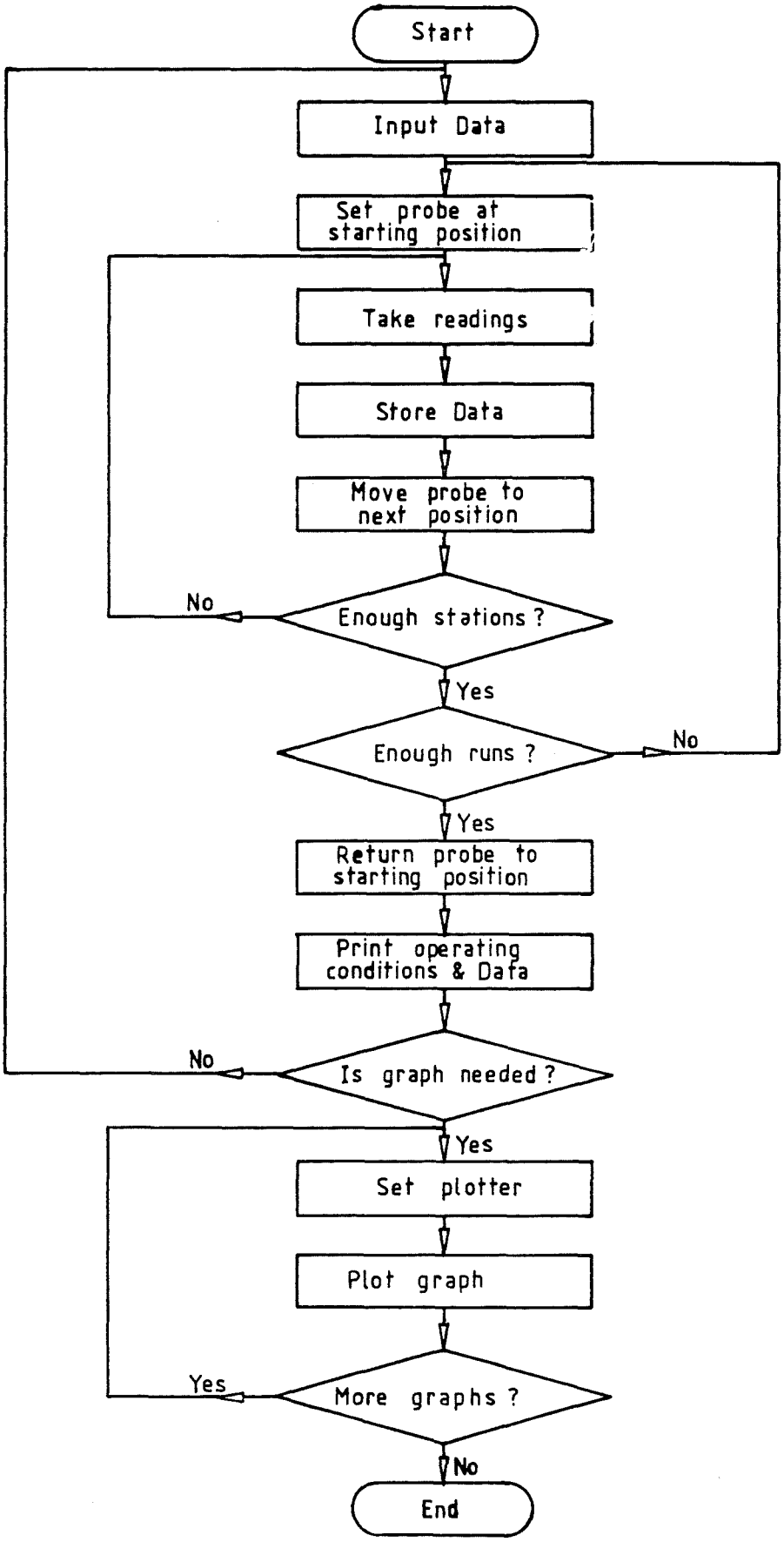

Fig (3.9) Flowchart of Data Collection program

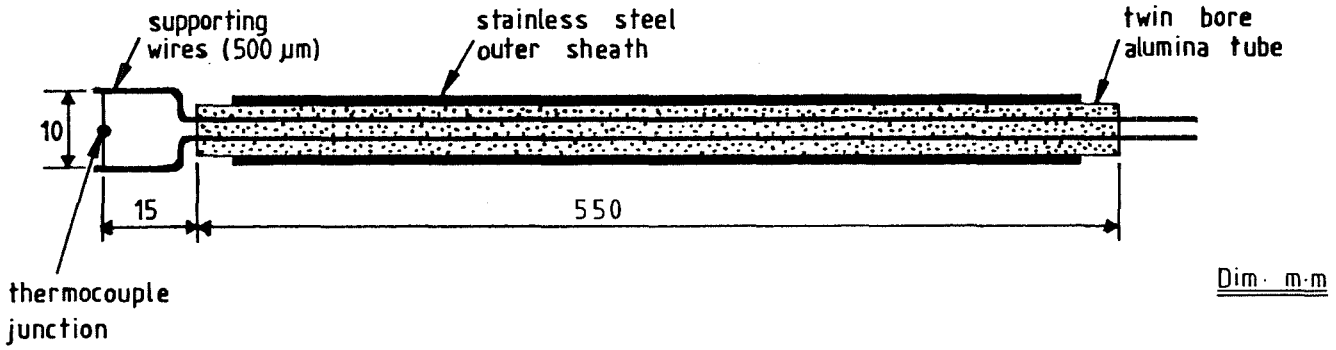

Fig(3.10a) Details of Thermocouple probe

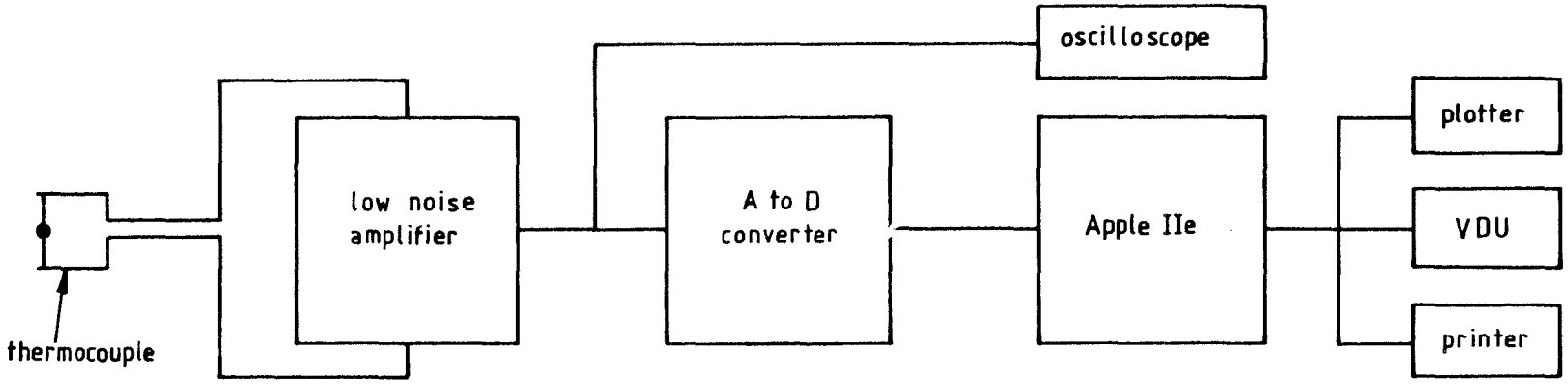

Fig (3.10b) Temperature measurement system

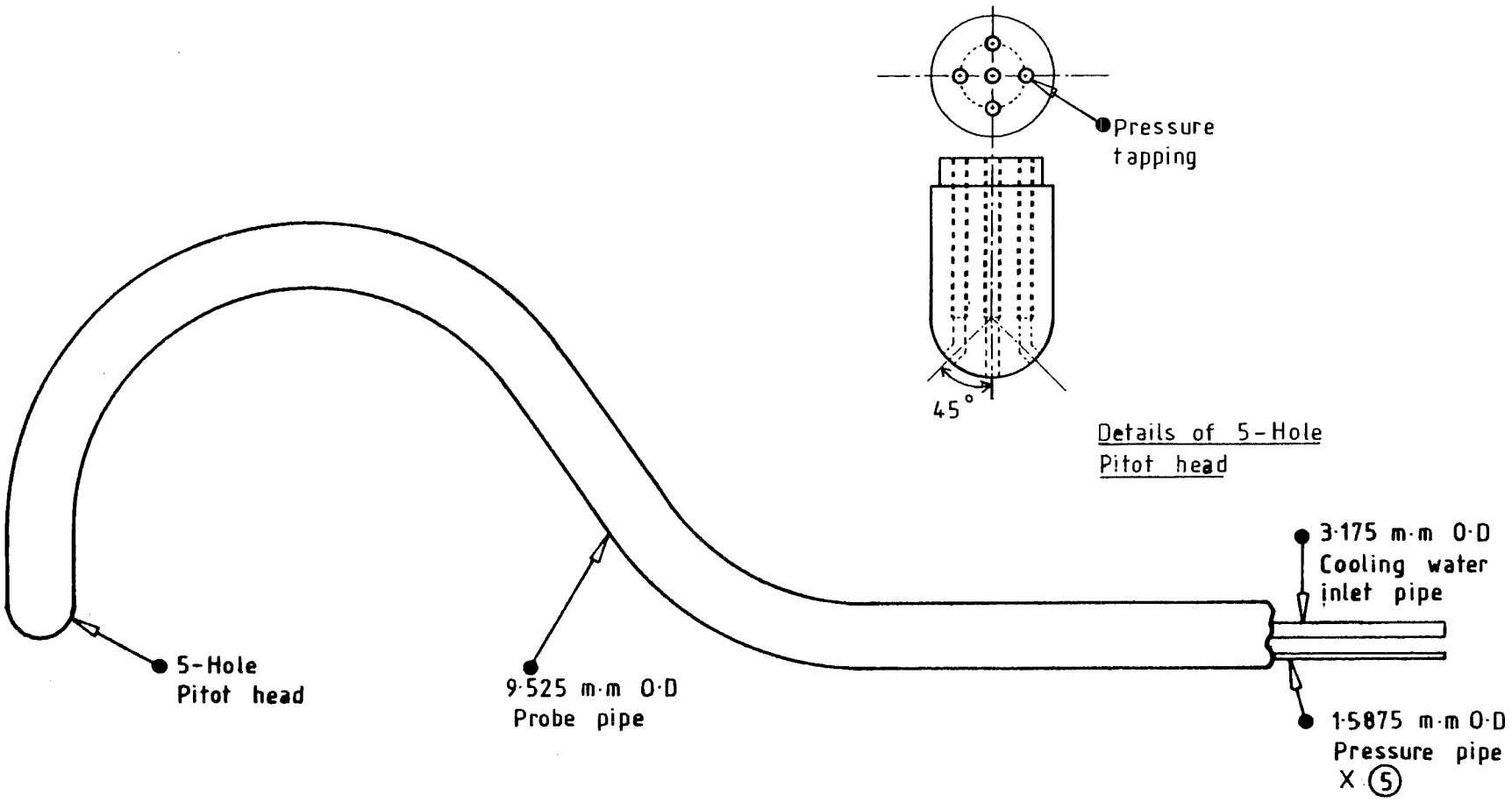

Fig. (3.11) Details of 5-Hole Pitot probe

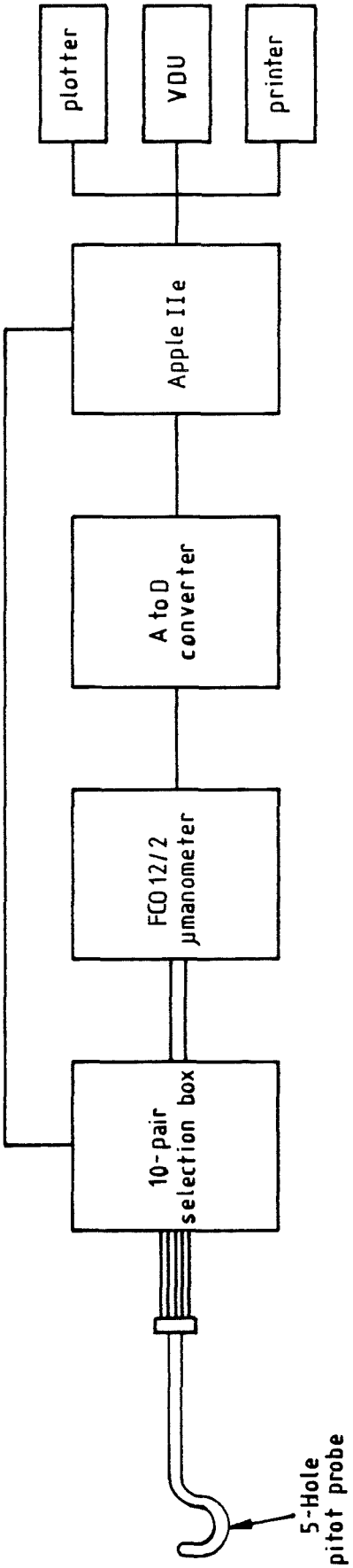

Fig (3.12) Layout of velocity measuring system

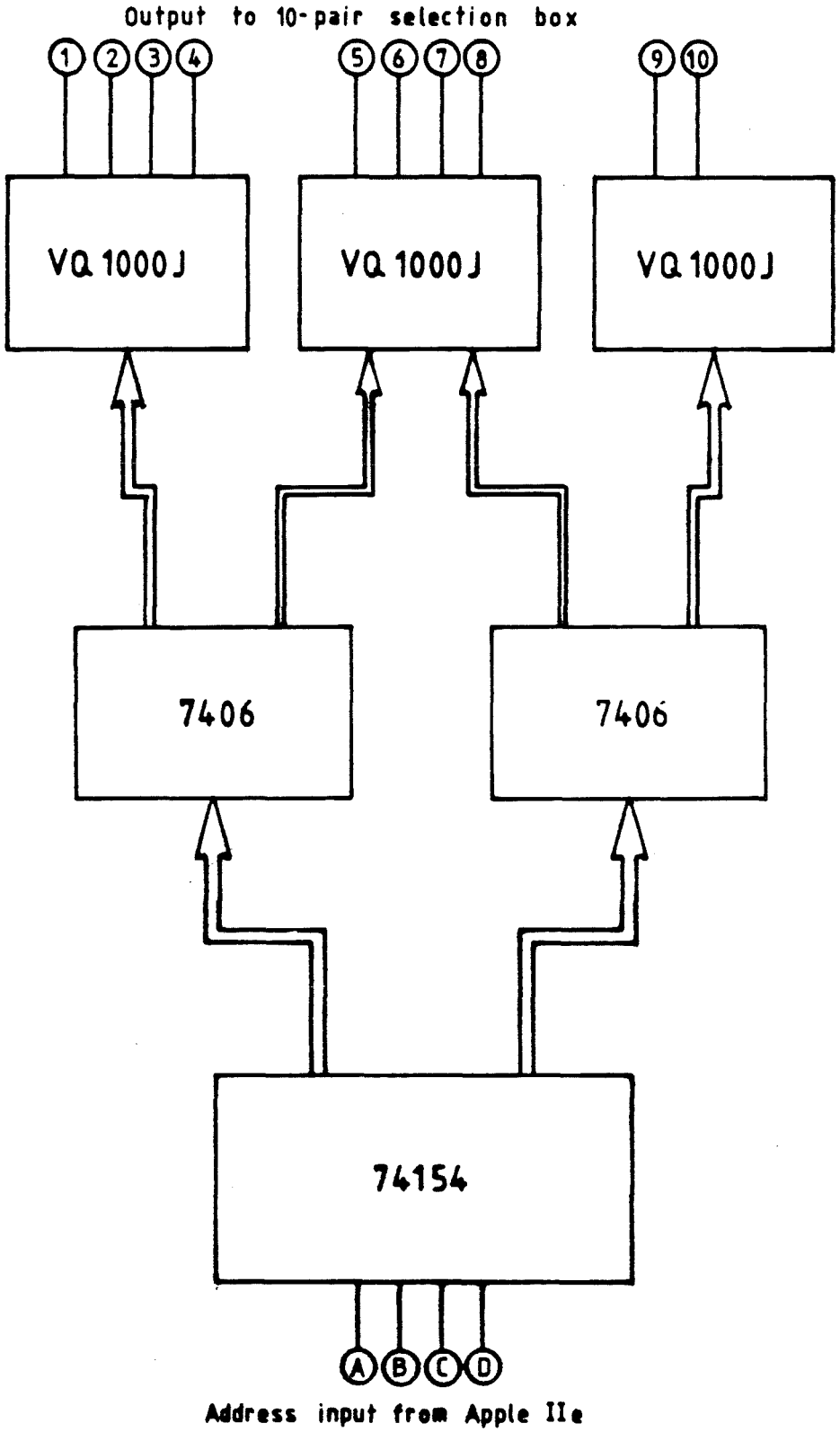

Fig (3.13) Circuit diagram of selection box automation

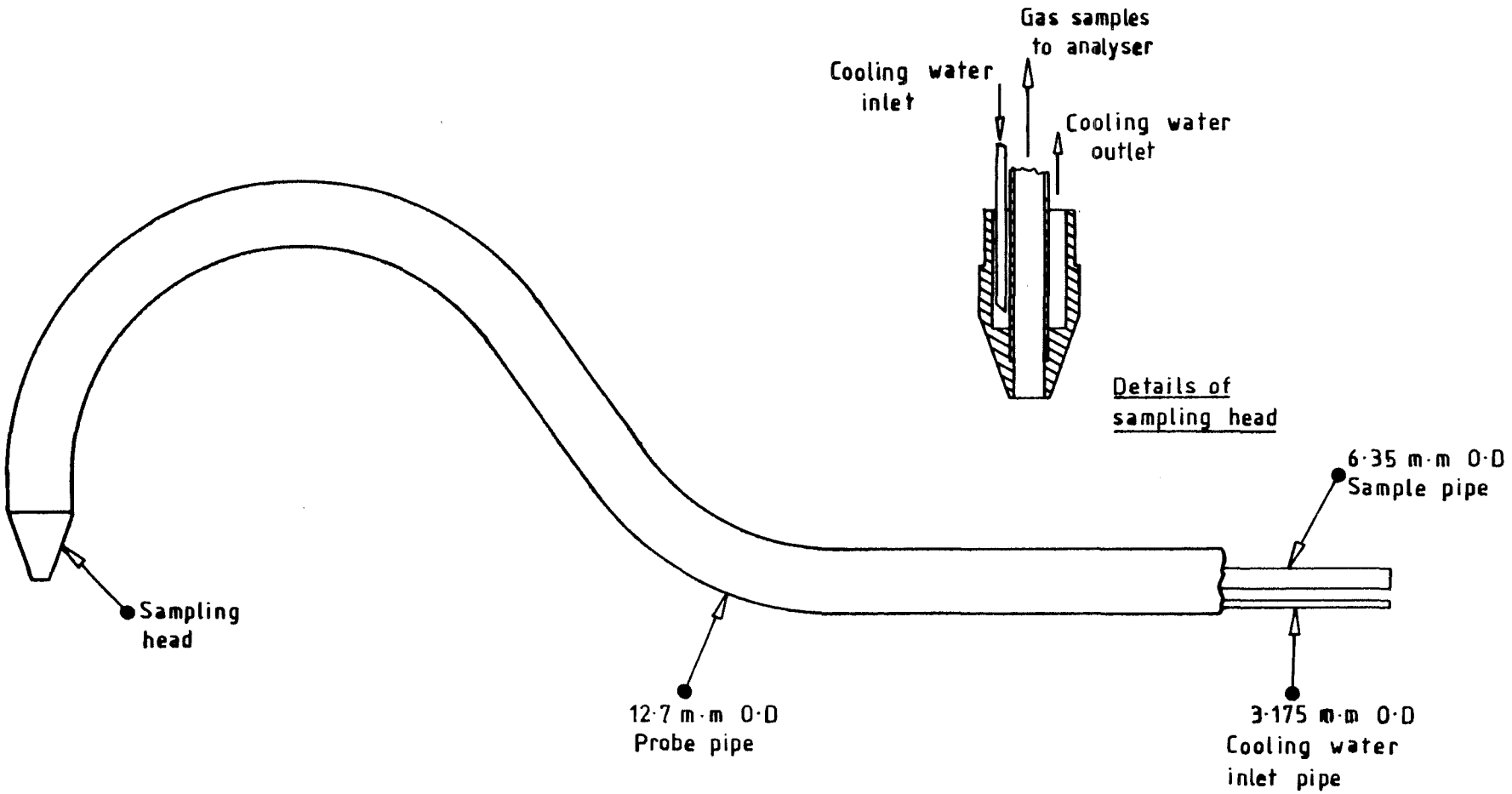

Fig (3.14) Water cooled sampling probe

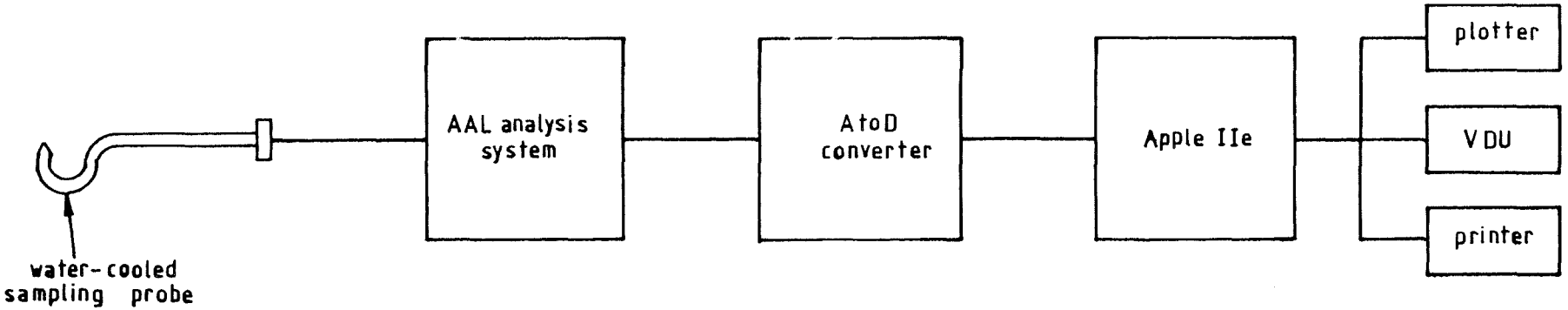

Fig (3.15) Layout of concentration measuring system

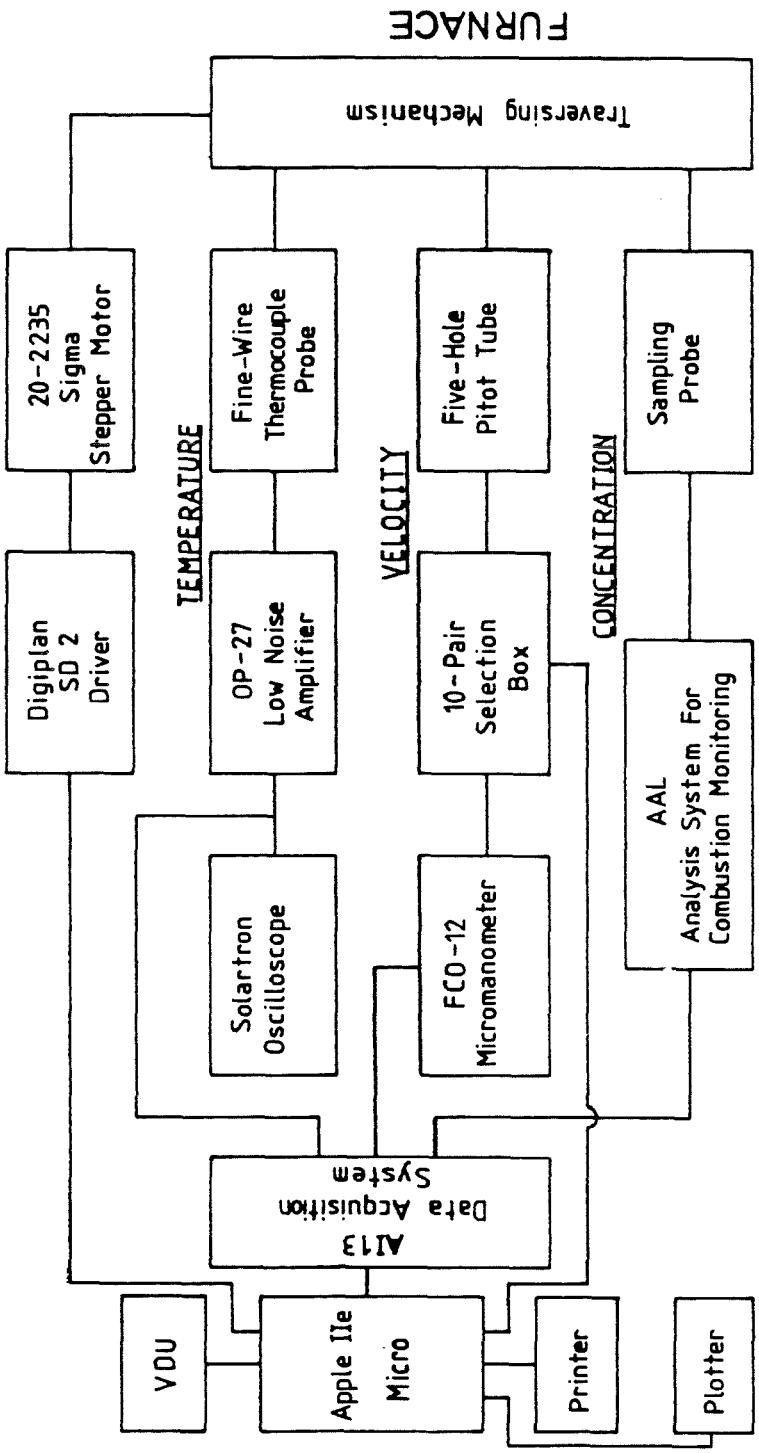

Fig (3.8) Instrumentation system.

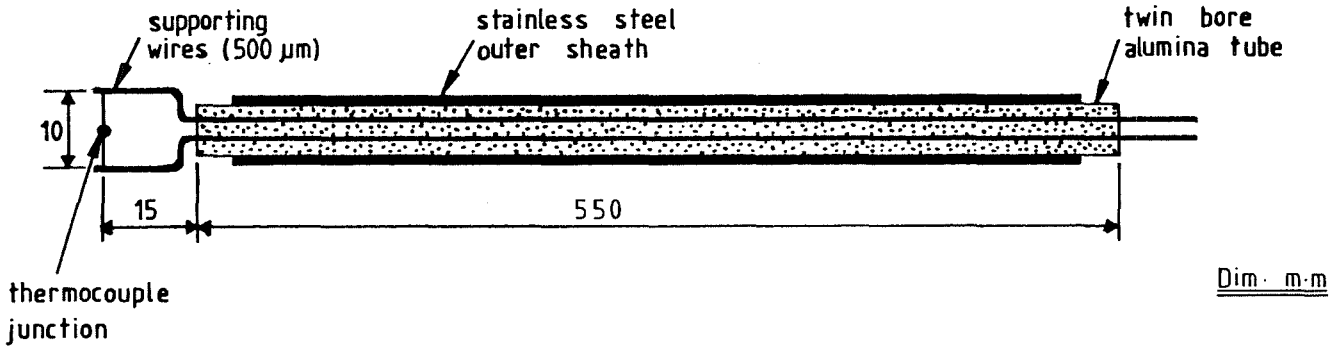

Fig(3.10a) Details of Thermocouple probe

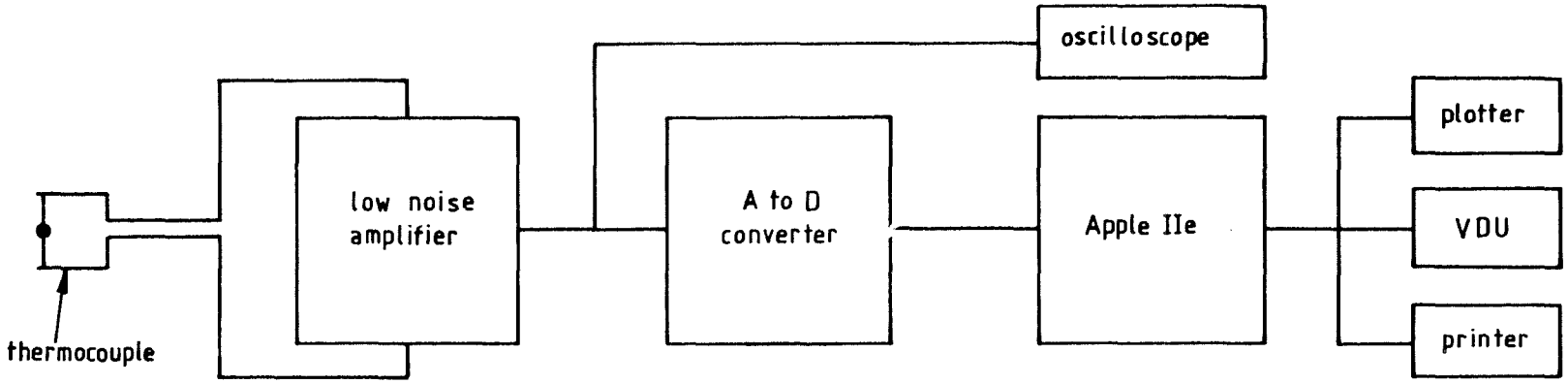

Fig (3.10b) Temperature measurement system

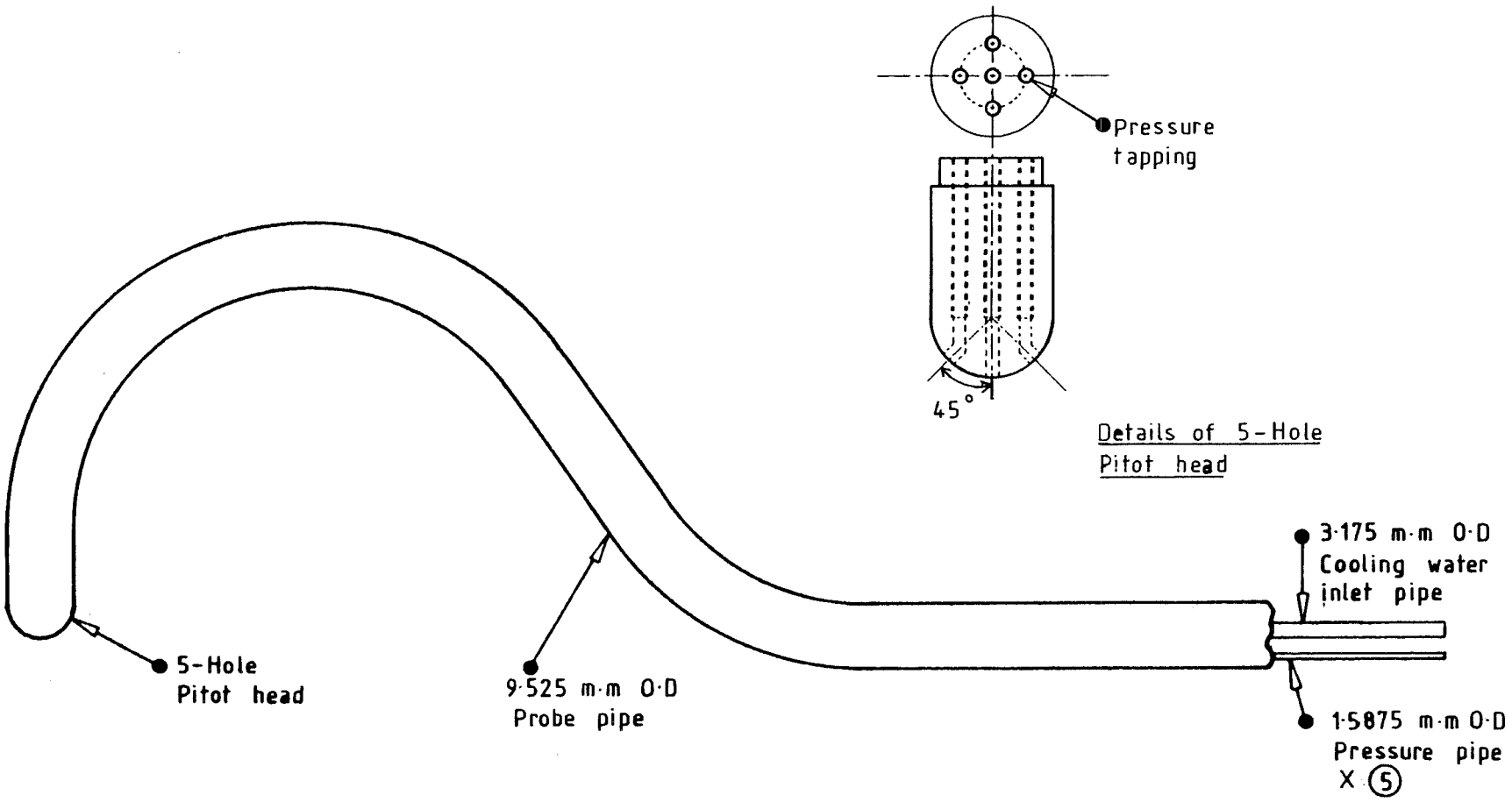

Fig. (3.11) Details of 5-Hole Pitot probe

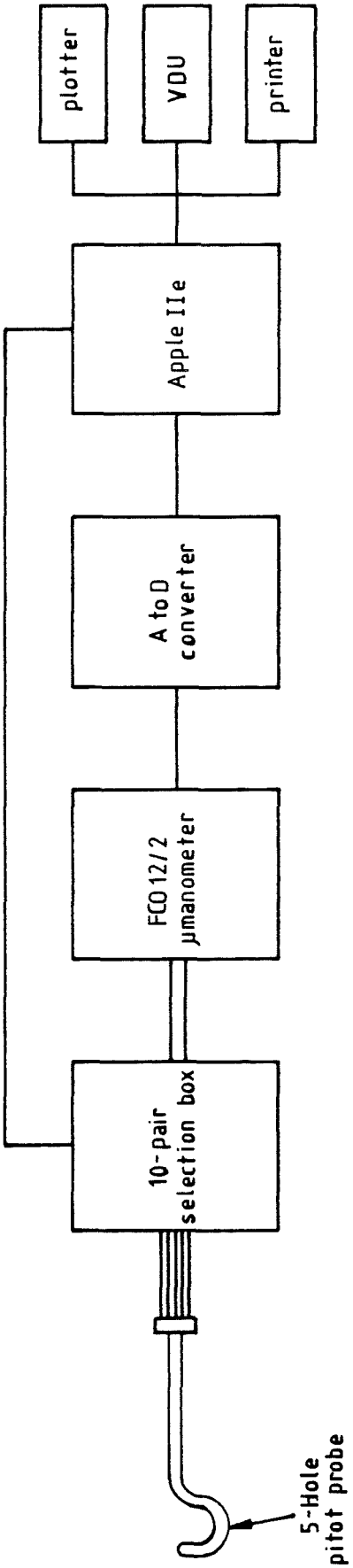

Fig (3.12) Layout of velocity measuring system

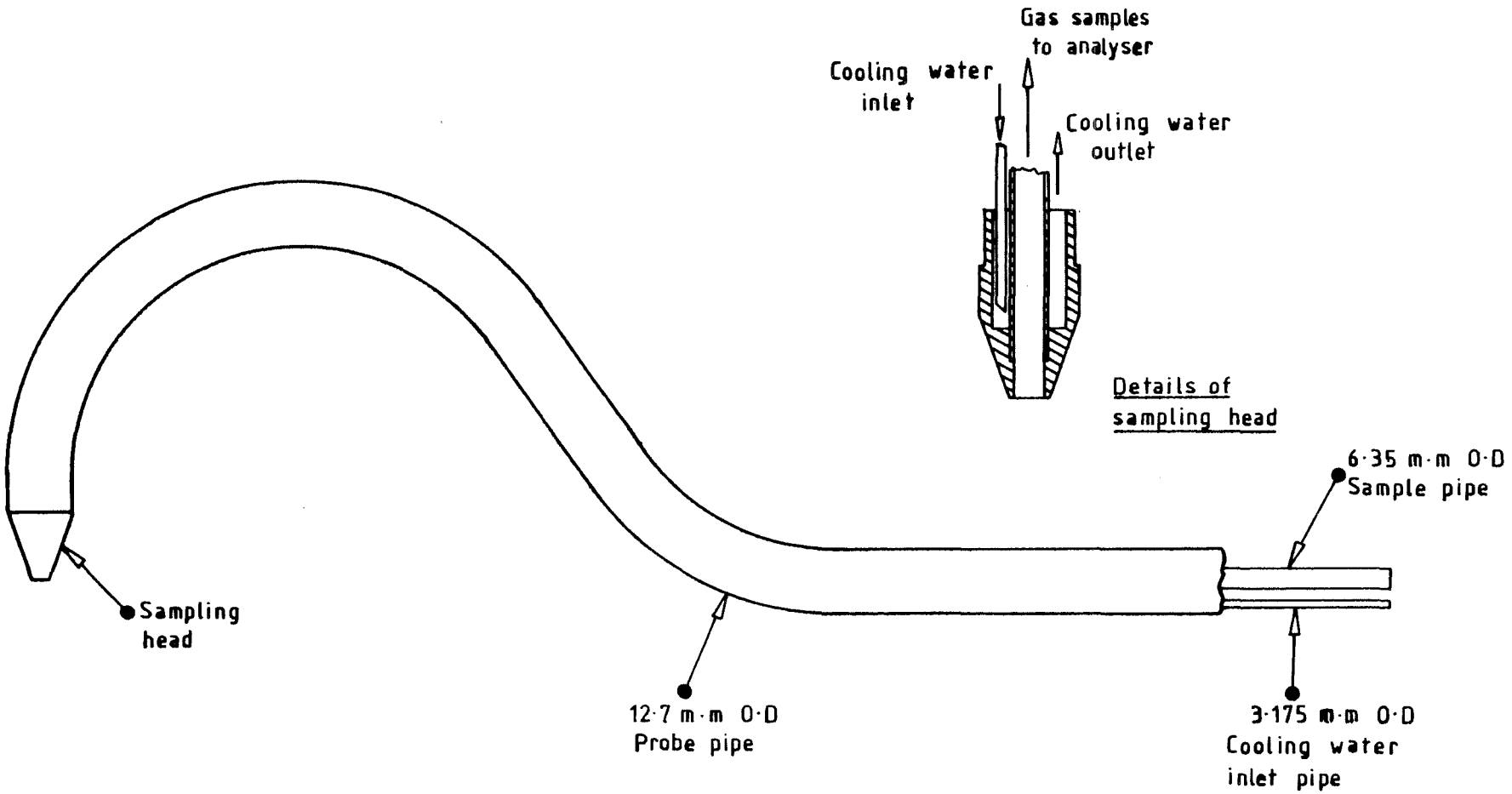

Fig (3.14) Water cooled sampling probe

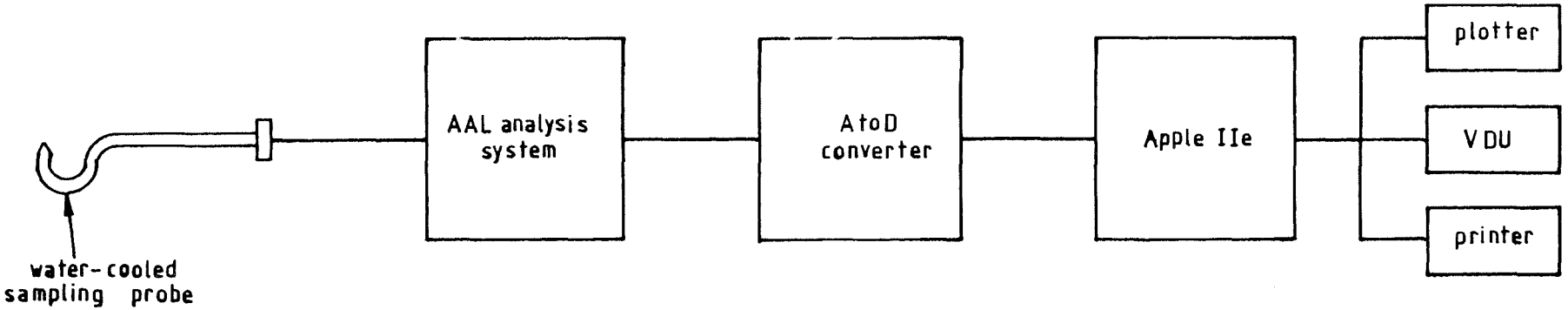

Fig (3.15) Layout of concentration measuring system

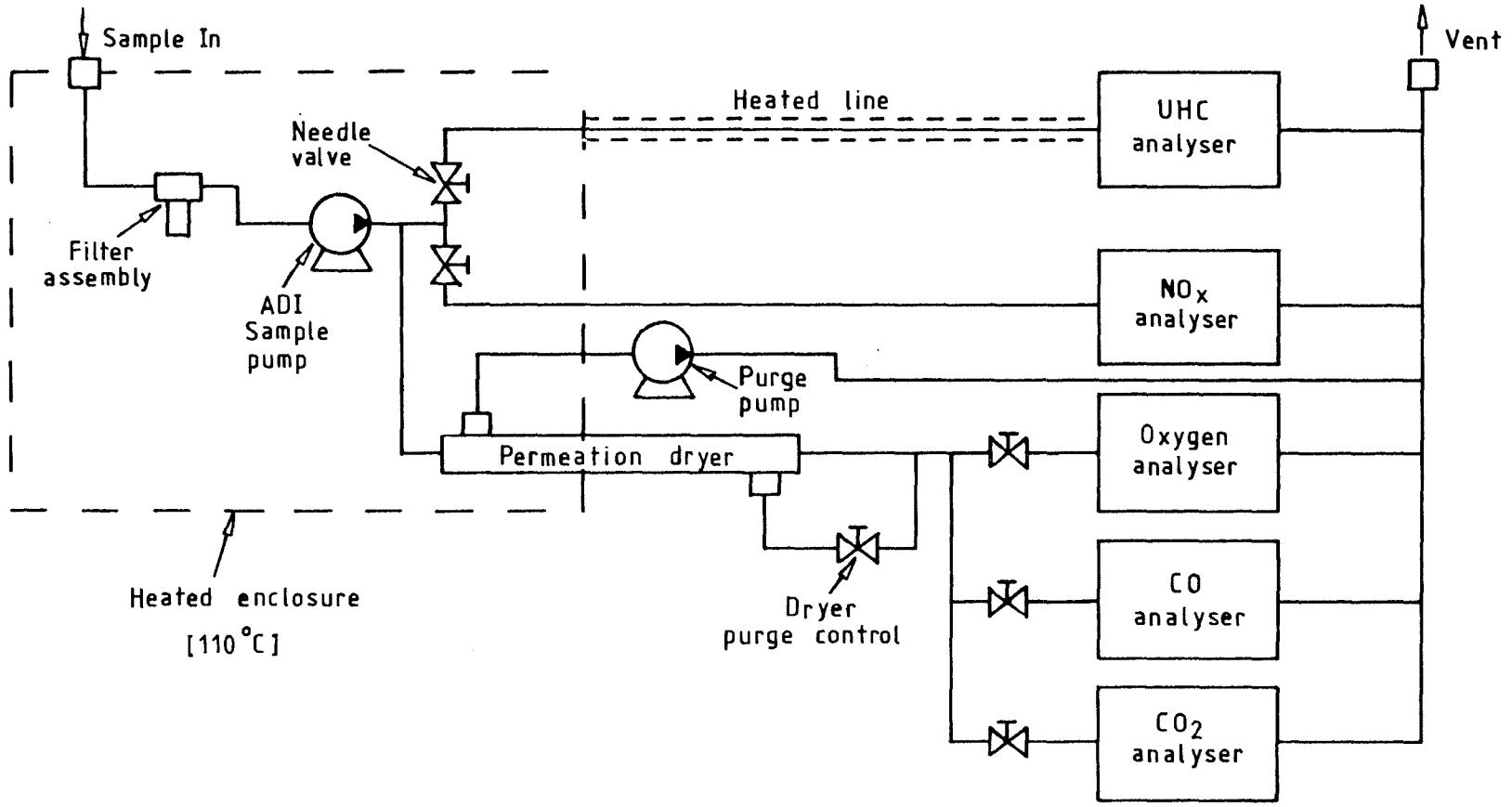

Fig (3.16) Details of sampling system

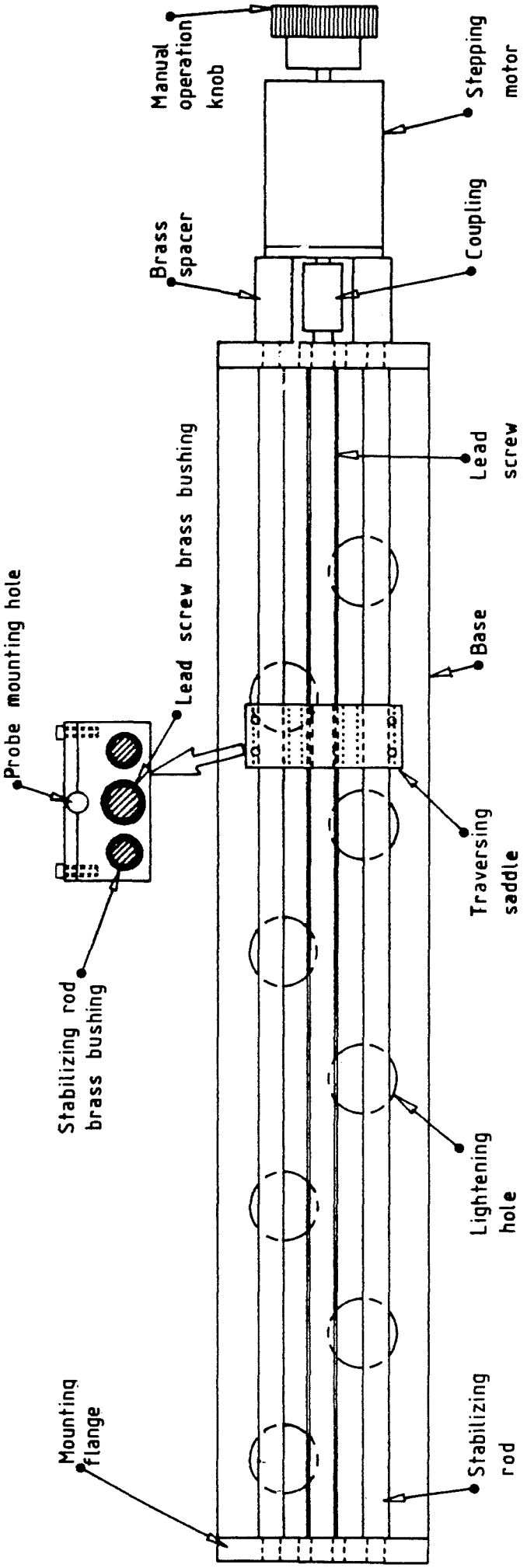

Fig (3.17) Details of traversing mechanism

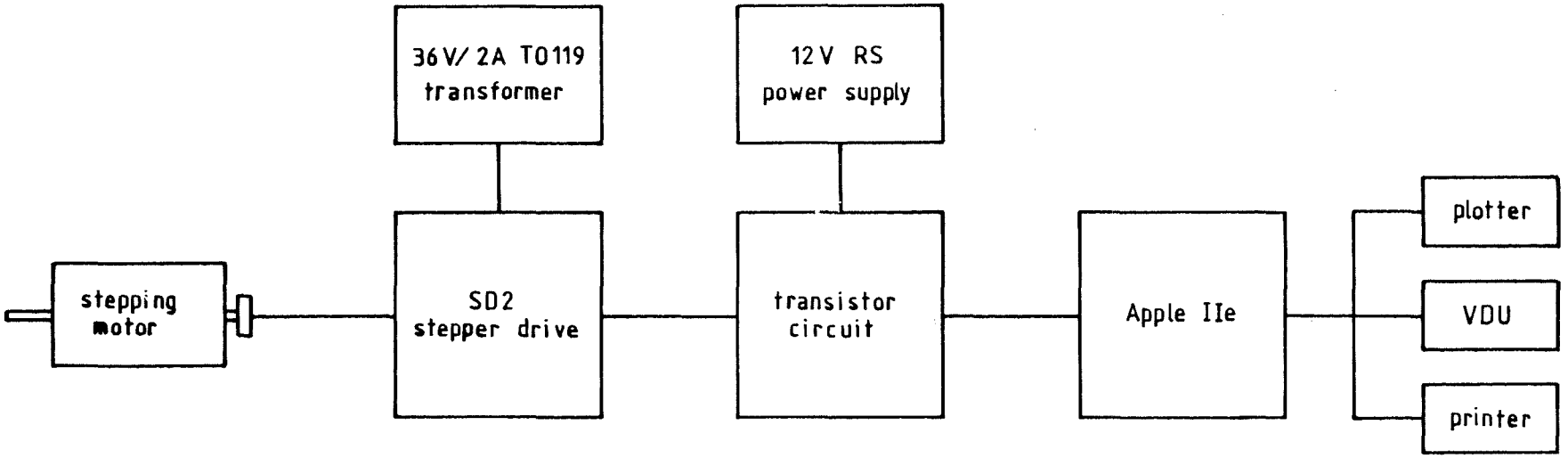

Fig (3.18) Details of automatic traversing mechanism

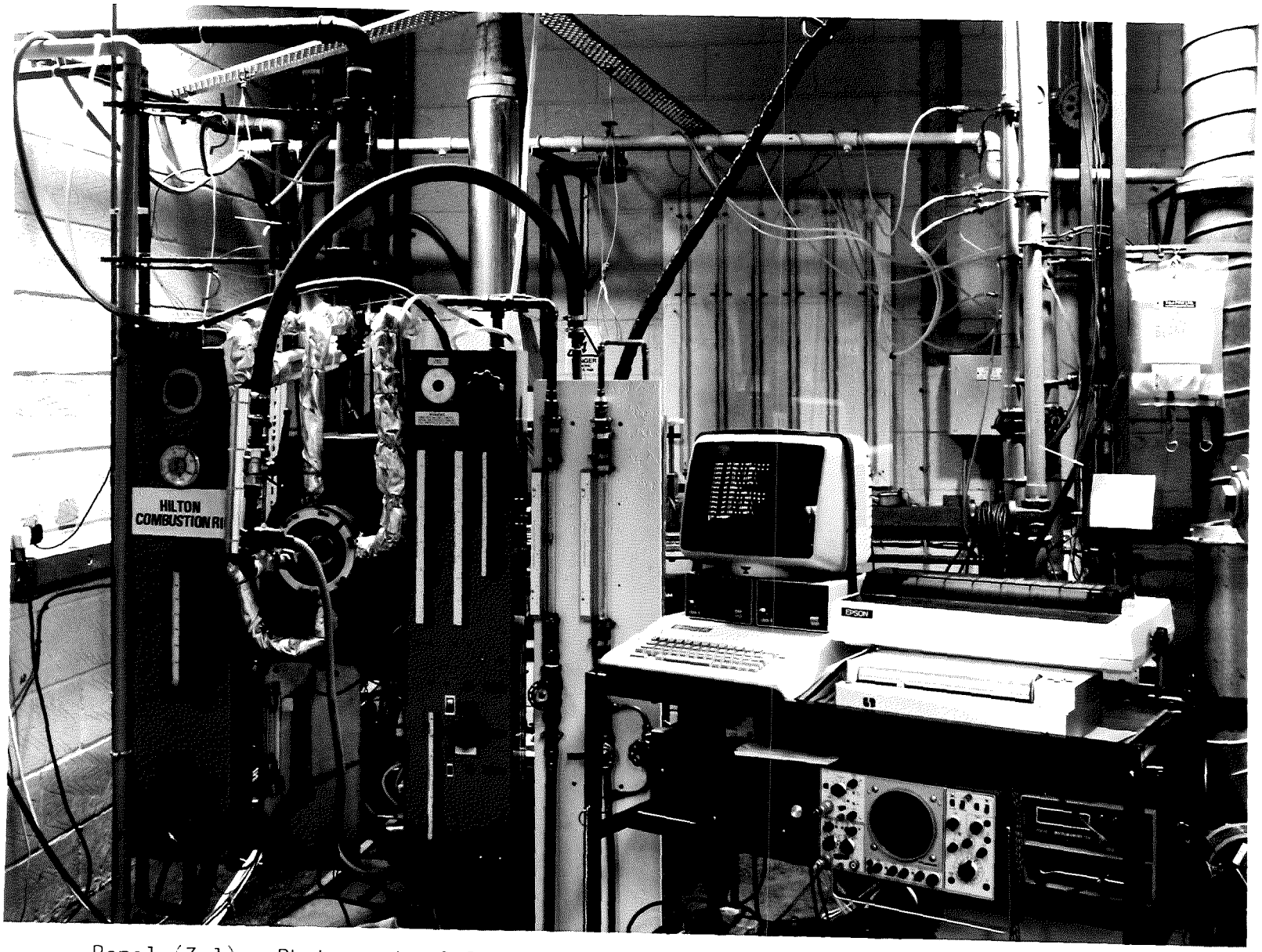

Panel (3.1) : Photograph of front section of furnace.

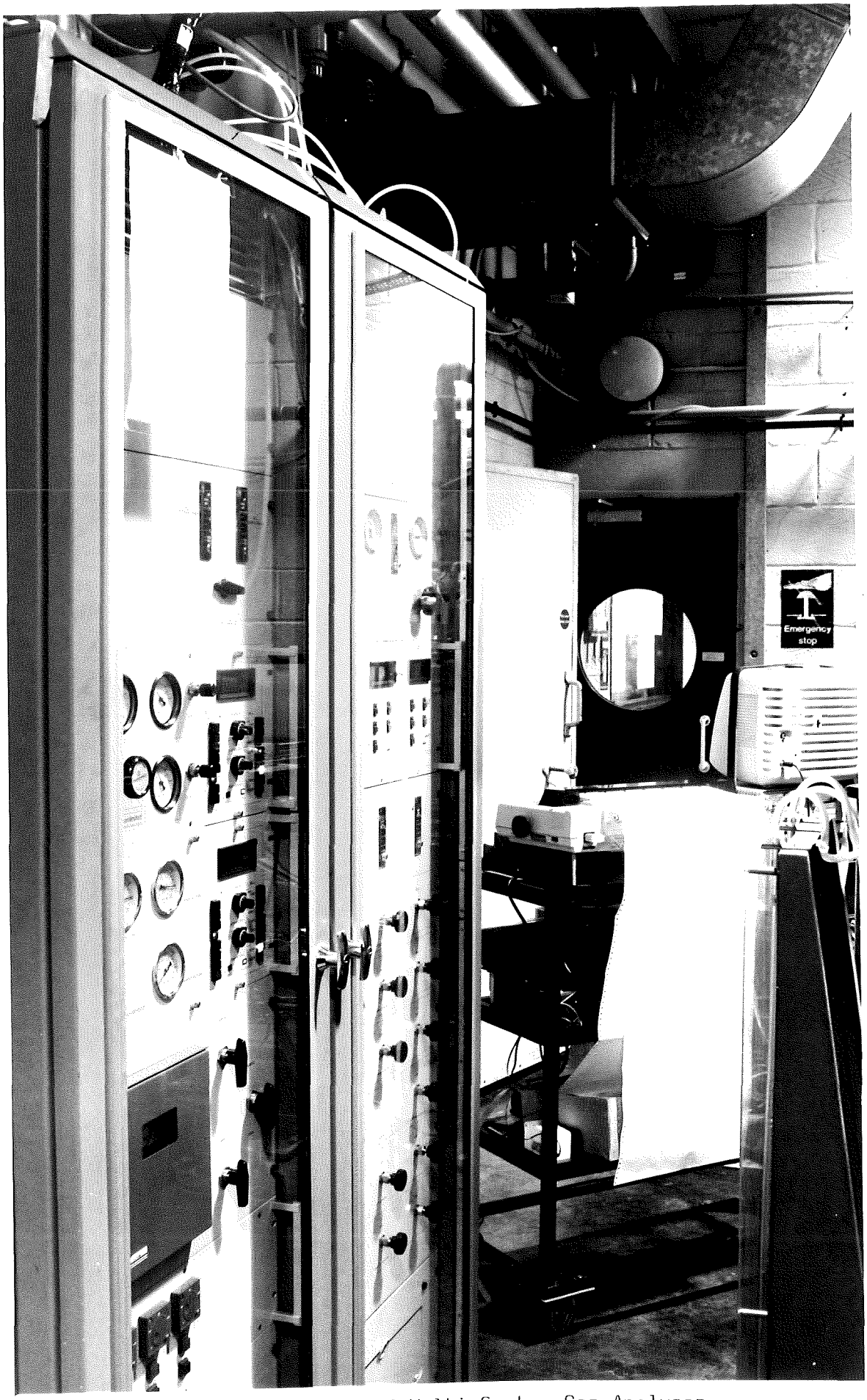

Panel (3.2) : Photograph of Multi-System Gas Analyser

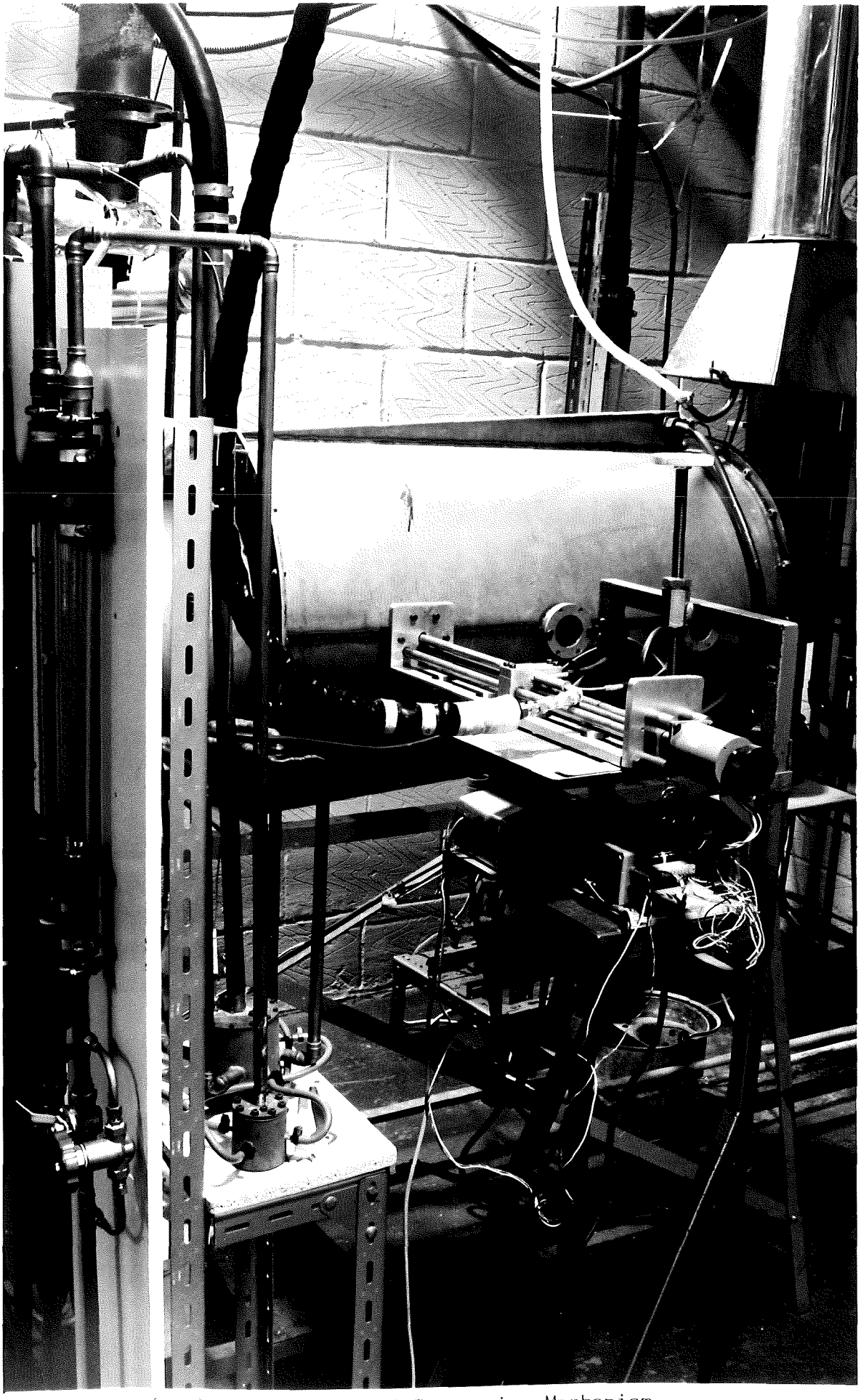

Panel (3.3) : Photograph of Traversing Mechanism.

CHAPTER 4

STABILITY LIMITS RESULTS

4.1 Introduction

This chapter deals with the stability limit measurements carried out on the experimental rig using both natural and low calorific value gases. Data were collected under quite a wide range of experimental conditions. Due to the limitations of the combustion air compressor, blow-off limits based on increases in the velocity of the secondary air at the mouth of the burner was not possible. Instead it was decided to keep the momentum at the burner exit, for each level of excess air, nearly constant throughout the experiment and to reduce the calorific value of the fuel by nitrogen dilution until the flame blew off.

In order to estimate the location of the flame inside the quarl, four Cr/Al thermocouples were buried on the internal surface of the quarl. They were located at distances of 50, 100, 150 and 200 mm from the burner outlet and were cemented at about 2 mm beneath the surface. These four thermocouples were monitored throughout the whole series of tests and in addition the temperature of the exhaust gas and cooling-water outlet were also recorded.

The rest of this chapter is divided into three sections. Section (4.2) gives an outline of the experimental conditions under which the stability limits data were collected. Section (4.3) deals with the presentation and discussion of the results in particular the effects of secondary air temperature, swirl number and excess air levels on them. Section (4.4) provides the closure to this chapter.

4.2 Experimental Conditions and Procedures

Stability limits data based on the blow-off of the main flame as a result of increasing the nitrogen content of the fuel were collected for a wide range of operating conditions. Five combustion air preheat temperatures, (38, 100, 200, 250 and 300°C), four swirl numbers (0, 0.418, 0.689 and 0.964) and three levels of excess air (10%, 20% and 30%) were investigated.

The furnace was started burning 3 kg/h of natural gas at the chosen swirl number, excess air level and secondary air preheat temperature. The cooling-water flow rate was adjusted to 364 kg/h and the two variacs trimmed to give the desired combustion air temperatures. About one hour was allowed to elapse for conditions inside the furnace to stabilize. The quarl, exhaust gas and cooling-water outlet temperatures were then noted.

The calorific value of the gas was then reduced by gradual dilution with oxygen-free nitrogen coupled with a reduction of natural gas flow rate, thus keeping the total mass flow rate of the fuel mixture constant at 3 kg/h. Again about 30 minutes were allowed to elapse for conditions in the furnace to stabilize. The quarl, exhaust gas and cooling-water outlet temperatures were taken again. A further reduction in the calorific value of the fuel was made and the same processes as described above were repeated. This was continued until the calorific value of the fuel supplied to the burner was too weak to sustain a flame thus resulting in a blow-off.

The furnace was restarted and the procedures described above repeated with a different excess air level. After the three excess air levels

were investigated, the secondary air temperature was changed and the stability limits data from their resulting flames taken. The combination of three excess air levels and five secondary air temperatures resulted in fifteen sets of blow-off data at one swirl number. By varying the swirl number a further fifteen sets of blow-off data were collected using the same excess air levels and secondary air preheat temperatures as before. In total, sixty sets of blow-off data together with their corresponding exhaust gas, cooling-water outlet and quarl temperatures were collected. The last was monitored at four different points (50, 100, 150 and 200 mm) along the inside surface from the burner exit.

4.3 Presentation and Discussion of Stability Limits Data

Blow-off data for all the conditions mentioned in section (4.2) are presented in Fig. (4.1) to (4.4). In all the stability curves shown, the absicca represents the percentage of nitrogen in the fuel mixture on a gravimetric basis. It should be noted here that the stability limit of a flame is represented by the maximum amount of nitrogen in the mixture that the burner could sustain prior to blow-off. Table (4.1) gives the various calorific values investigated with the corresponding mass of natural gas and oxygen-free nitrogen for each making a total mass flow rate of the fuel mixture 3 kg/h. For the above-mentioned figures, the secondary air temperature entering the furnace is represented on the ordinate.

The shaded dots on the curves represent conditions under which the flames maintained good stability and the open ones indicate blow-off.

The cross-shaded regions on the curves represent a form of safety band where combustion is undesirable except for investigative purposes. This area also indicates the onset of instability of the flame which is also accompanied by an increase in noise level at the burner mouth and sometimes a slight vibration of the whole furnace. The width of the cross-shade represents an estimate of the level of instability prior to blow-off: noise and vibration increased with level of instability.

Figures (4.1) (a), (b) and (c) represent the stability curves for 10, 20 and 30 percent excess air respectively. These data were obtained without any swirl being imparted to the secondary air; in other words with a swirl number of zero. Subsequent figures up to (4.4) show data collected at swirl numbers of 0.418, 0.689 and 0.964; again with (a), (b) and (c) indicating an excess air level of 10, 20 and 30 percent respectively. Although all the data collected during the tests on stability limits are accounted for in Figs. (4.1) to (4.4), a clearer presentation and comparison is obtained when the ordinate variables are changed as described in the next paragraph.

Figures (4.5) to (4.9) represent plots of swirl number against the percentage of nitrogen in the fuel mixture. Again (a), (b) and (c) denote 10, 20 and 30 percent excess air level. Each figure represents the stability data at a constant secondary air temperature, ranging from 38°C for the case of Fig. (4.5) to 300°C for Fig. (4.9).

The effects of excess air at fixed swirl numbers on the stability limit of the flames are shown on Fig. (4.10) to (4.13). Here (a), (b) and (c) denote secondary air temperatures of 38°C, 200°C and 300°C respectively. Similarly Fig. (4.14) to (4.18) show the effects of

excess air on the stability limit of the flames but this time at fixed secondary air temperature. In this case (a), (b) and (c) denote swirl number of 0, 0.689 and 0.964 respectively.

The values presented in Tables (4.2) and (4.3) give an indication of what is happening to the flame front, or more precisely the location of maximum temperature of the flame, inside the quarl. The calorific values of the fuel mixture quoted are that prior to blow-off. Table (4.2) represents data for swirl numbers of zero and 0.418 at excess air levels of 10, 20 and 30 percent over a range of secondary air temperatures from 38°C to 300°C. Similar informations are given in Table (4.3) but at swirl numbers of 0.689 and 0.964. The last two columns of the tables show the location of maximum temperature inside the quarl for cases when pure natural gas fuel was used under similar operating conditions.

The effects of secondary air preheat, without any swirl, on the stability limit of the flames are shown in Fig. (4.1). For the 10% excess air case very little improvement was obtained by preheating the air up to 250°C. At a secondary air preheat temperature of 300°C a stable flame was possible with a leaner fuel containing an extra 5 percent oxygen-free nitrogen in the mixture. The range over which the flame became unstable, as indicated by the width of the cross-shaded area, was wider at the lower preheat values. When operating with 20% excess air an increase in the stability limit was noticed after preheating the air to 200°C. Increasing the preheat value from 200°C to 300°C allowed combustion to proceed with an extra 10% nitrogen in the mixture. With 30% excess air the improvement in stability started with a preheat value of 100°C to the secondary air supply.

Comparing Figs. (4.1) (a), (b) and (c) indicate that without preheat (i.e. 38°C) the stability of the flames decreases with increase in excess air levels. Similar comparisons with a preheat value of 300°C to the combustion air show an increase in the stability of the flames with an increase in excess air level. At 10% excess air the flame blew off when the mixture contained 58% of nitrogen but with 30% excess air the flame could tolerate a mixture with 66% of nitrogen. The effects of preheating combustion air supplied to furnaces burning low calorific value gases have been demonstrated by Schreier (1981) and the results shown above are in good agreement with his findings. An improvement in the stability of the flames by increasing the excess air was also noticed by Schreier (1981) and Beltagui and Maccallum (1976).

Imparting a small amount of swirl to the secondary air does improve the stability limits over the whole range of preheating investigated, as shown in Fig. (4.2). This improvement is noticed over all three excess air levels. This stabilizing effect is more apparent when none or very little preheat (100°C) is used on the secondary air. For the 10% excess air case with no preheat, there is an increase of about 8 points in nitrogen content when compared with the zero swirl case. Moving across to 20% and 30% excess air cases do not show much improvement over the 10% case. But when they are compared with their corresponding conditions without swirl, improvements of 15 and nearly 20 points in the nitrogen content of the mixture were noticed respectively for the situation without any preheat. In fact comparing Figs. (4.2) (a), (b) and (c) show a slight decrease in the stability of the flames with an increase in the excess air level in particular at the higher preheat temperatures. This is perhaps due to the cooling effects of excess air on the flames as noticed by many other investigators.

Further increase in the swirl number up to 0.689 as shown in Fig. (4.3) does not produce a noticable improvement on the stability limit of the flames. There is a very slight improvement in the 10% excess air case without any preheat. A small reduction of about 3 points for the case with maximum preheat of 300°C and 30% excess air is noticed. Working at the maximum swirl number of 0.964 over the whole range of excess air does not show any benefits at all. There is very little to choose between the data obtained at a swirl number of 0.689 and that at 0.964. So it is evident that there is a limiting value both for swirl and secondary air preheat. This limiting effect on the swirl number has also been noticed by Beltagui and Maccallum (1976) and Leuckel and Fricker (1976). They pointed out that once a CRZ was well established in the flow, further increase in the swirl intensity did not produce any improvement in the flame.

Considering Figs. (4.1) to (4.4) it is very clear that an increase in the secondary air temperature on its own will improve the stability limit of the flames. This improvement is more pronounced for preheat temperatures of 200°C or above. The main effect of adding swirl to the combustion air is to improve the flame stability limits for conditions when only a small amount (100°C) or no preheating is available. This effect is further increased when higher excess air levels are supplied to the burner.

The effects of swirl on the stability limit of flames are best represented by Fig. (4.5) to (4.9). Comparison of Figs. (4.5) (a), (b) and (c) indicate clearly that the maximum benefit of swirl is obtained by increasing its value from zero to 0.418. Further increase in the swirl intensity made very little improvement on the stability limit of

the flames. It is also clearly demonstrated that the stability limit of the flames deteriorated quite rapidly with an increase in excess air level when no swirl was imparted to the combustion air. Once a small amount of swirl was used, there was a definite improvement in the stability. The above results are for cases when no secondary air preheat was used.

The effects of swirl and excess air at fixed secondary air temperatures are shown in Figs. (4.5) to (4.9). Considering the case with 100°C preheat, Fig. (4.6), using 10%, 20% and 30% excess air gave very similar stability patterns when compared to the same conditions without any preheating. With 30% excess air, Fig. (4.6) (c), a deterioration of the stability limit was evident when the swirl number was increased above 0.689. This deterioration was noticed earlier at 20% excess air when the preheating value was increased to 200°C, Fig. (4.7) (b). A slight increase in the stability limit was also noticed at zero swirl for the 30% excess air case. Fig. (4.8) represents stability limits with 250°C combustion air preheat. For the 10 and 30 percent excess air cases, deterioration in the stability limit of the flames was evident above a swirl intensity of 0.418. The 20% excess air case Fig. (4.8) (b) showed no change in the stability limit with an increase in swirl. With 300°C preheat, Fig. (4.9), all three excess air levels showed a decrease in the stability limits after the swirl number was increased above 0.418. It should again also be noted here that for the zero swirl situation there was an increase in the stability of the flames, as indicated by the amount of nitrogen in the fuel mixture, with an increase in excess air level.

Figures (4.10) to (4.13) show the effects of preheating at constant swirl; (a), (b) and (c) denote secondary air preheat temperatures of 38°C, 200°C and 300°C respectively. Fig. (4.10) (a) shows the very worst case under which the furnace could operate, no preheat and no swirl. The stability limit of the flames were sharply reduced with an increase in the excess air level. Operating at 10% excess air allowed combustion of a fuel mixture containing almost 55% of nitrogen by mass. This figures was reduced to about 44% and the onset of instability had started quite early for the 30% excess air case. With 200°C preheat, the stability limit of the flames decreased when the excess air was increased from 10 to 20%; further increase in the excess air level to 30% produced a recovery on the stability limits. This is a very peculiar situation and the only explanation must be based on the intermixing between the fuel and air jets. A clearer understanding of the situation will result after considering the inflame combustion measurements data. Using 300°C preheat, Fig. (4.10) (c), the flame stability is enhanced with an increase in excess air level; the onset of instability was also retarded at the same time.

With a swirl intensity of 0.418, Fig. (4.11), all three cases of preheat showed a decrease in the stability limits as the percentage excess air was increased, but all the mixtures could tolerate an extra 10% of nitrogen when compared with the no swirl situation of Fig. (4.10). Similar results are shown on Figs. (4.12) and (4.13) with swirl intensities of 0.689 and 0.964. The only differences noticed are in the 10% excess air cases showing a slight improvement on the stability due to the secondary air preheat. Comparing Fig. (4.11) (c) with (4.13) (c) show a slight deterioration on the stability limit of the

flames with an increase in swirl intensity over the three values of excess air investigated. Figures (4.14) to (4.18) show the effects of excess air on the stability of the flames at fixed secondary air temperatures. In these cases (a), (b) and (c) relate to a swirl intensity of 0, 0.689 and 0.964 respectively. Although some of these data are repeated, the format in which they are presented show more clearly how the stability limits are affected with increasing swirl intensity and constant secondary air temperature.

From the data presented so far, it is clear that a combination of both swirl and preheat contributed to the enhancement of the stability limit of the flames. This improvement was also dependent on the excess air level at which the furnace was operated. The three subsections that follow summarize the main effects of secondary air preheat, swirl intensity and excess air levels on the stability limit of the flames. Subsection (4.3.4) deals with the effects of the location of the maximum temperature inside the quarl on the stability limit of the flames.

4.3.1 Effects of Secondary Air Temperature

Preheating the secondary air with the absence of swirl is only beneficial if its temperature is above 250°C. However the full advantages of preheating are exploited if a small amount of swirl is imparted to the secondary air. It should also be noted that the only situation when the stability limits kept increasing over the range of excess air investigated was when the furnace was operated with zero swirl and a secondary air preheat temperature of 300°C. But alas this situation does not allow the weakest mixture to be used.

4.3.2 Effects of Swirl

Figures (4.14) to (4.18) show a definite improvement on the stability limit of the flames no matter what value of secondary air temperature was used. These improvements were very dependent on the percentage of excess air supplied to the furnace. Whenever a swirl intensity above 0.418 was used to stabilize a flame, its stability limit was reduced when the excess air level increased. This tended to back up the observations and suggestions of Fricker and Leuckel (1976). They pointed out that the main effect of swirl was to promote mixing of the fuel and air rather than to increase the reverse flow of hot burnt gases back into the burner quarl region. They also indicated that there was very little improvement on the flame stability once a minimum amount of swirl, sufficient to create an internal recirculation zone in the flow, was imparted to the combustion air. For the cases studied here it seems as if a swirl number of 0.689 was the limiting value for the system used. This value of 0.689 appears to be a bit low but the ratio of $L_{q/Dq}$ for the quarl used in the furnace was about 2 and studies made by Leuckel and Fricker (1976) showed that the higher the ratio of $L_{q/Dq}$, the better the stability of the flame. Perhaps this was why only a small amount of swirl was required to improve the stability limits in this study.

4.3.3 Effects of excess air

Referring to Figs. (4.10) to (4.18) it is clearly shown that increasing the percentage excess air supplied to the furnace caused a reduction in the stability limit of the flames in all but two cases. So the dilution effects of excess air are fairly evident based on the data presented. These two cases which actually show an increase in the stability limit of the flames occurred when preheated combustion air

temperatures of 250°C and 300°C were used in the absence of swirl. But as pointed out earlier, these two conditions did not give the most favourable stability limits; they were merely an improvement from the so-called worst case of no preheat and no swirl. Similar effects have been noticed by Schreier (1981) but his fuel mixture contained hydrogen which does improve the stability of flames. The improvement in stability limits may be due to the better mixing conditions obtained in the reaction zone when the burner momentum was increased under these operating conditions.

4.3.4 Effects of maximum temperature location inside the quarl

For swirl numbers of 0 and 0.418, Table (4.2), it is clearly evident that the flame front shifted further downstream along the quarl when the calorific value of the fuel was reduced. This was noticed over the whole range of excess air used despite the fact that an extra 4.5 kg/h of air flowed through the burner with every 10% increase in excess air level. Similar effects were noticed when the furnace was operated with a swirl number of 0.689. The above results show that the burner operation was fairly independent of momentum over the range of variables mentioned above. A simple explanation of this lift off may be the lack of heat release from the low calorific value gases required to keep the ignition front as close as possible to the burner mouth. It is unfortunate that there are no known measurements inside the quarl of a similar system elsewhere for comparative purposes.

Considering the maximum swirl number (0.964) case, Table (4.3), there seems to be very little difference between the natural and low calorific value gas cases. Perhaps more noticeable are the cases with 200°C secondary air preheat which tended to behave in a similar fashion to the

low swirl number situations. For the remaining preheat conditions it seems that the swirl was strong enough to keep the ignition front from moving further downstream with a change in calorific value of the gas. These results also prove that the flame was stabilized inside the quarl and this was not surprising as the quarl length tc diameter ratio was greater than two and the ratio between the length of the furnace to that of the quarl was only three.

4.4.4 Closure

It has been shown that in the absence of swirl, secondary air preheating was only beneficial to the stability of the flames if the air was heated to a temperature of 250°C or above. By imparting a small amount of swirl to the secondary air there was a substantial improvement on the flame stability. Using a swirl intensity above 0.418 caused a slight deterioration to the stability of the flames when the excess air level was increased. In general there was a definite improvement on the stability with swirl addition which was independent of the secondary air temperature. From the data presented, the dilution effects of excess air were fairly evident as will be shown later in the temperature and concentration profiles. The surface temperatures inside the quarl indicated a downstream shift in the location of the flame front when LCV gases were used in most of the cases investigated.

The data presented in this chapter are interesting in themselves. However, the main purpose of obtaining them was to indicate the conditions that were near blow-off so that inflame combustion measurements could be made at these points for further investigations of the stability mechanism. These investigations were based on inflame temperature, velocity and concentration measurements and are dealt with in the next chapter.

Considering 3 kg of Natural Gas & Nitrogen Mixture

C.V. MJ/kg	Mass of N.G. kg	Mass of N_2 kg	% N_2
53.13	3.000	0.000	0.0
45.00	2.541	0.459	15.3
40.00	2.259	0.741	24.7
38.00	2.145	0.855	28.5
35.00	1.976	1.024	34.1
33.00	1.863	1.137	37.9
30.00	1.694	1.306	43.5
29.00	1.637	1.363	45.4
28.00	1.581	1.419	47.3
27.00	1.524	1.476	49.2
26.00	1.468	1.532	51.1
25.00	1.412	1.588	52.9
24.00	1.355	1.645	54.8
23.00	1.299	1.701	56.7
22.00	1.242	1.758	58.6

Table (4.1) : Mass fractions of LCV Gases

CV of Fuel MJ/kg	Swirl No.	Excess Air %	Preheat (°C)	Max.Temp. Location Inside Quarl (mm) LCV Gas Flames (100)	(150)	Max.Temp. Location Inside Quarl (mm) Natural Gas Flames (100)	(150)
25.0	0	10	38		x		x
27.5	0	20	38		x	x	
31.0	0	30	38		x		x
27.5	0	10	100		x	x	
28.0	0	20	100		x	x	
29.0	0	30	100		x	x	
25.0	0	10	200		x	x	
26.0	0	20	200		x	x	
23.0	0	30	200		x	x	
25.0	0	10	250	x		x	
23.0	0	20	250		x	x	
21.0	0	30	250		x	x	
22.5	0	10	300		x	x	
21.0	0	20	300		x	x	
19.0	0	30	300		x	x	
20.0	0.418	10	38		x		x
20.0	0.418	20	38		x	x	
21.0	0.418	30	38		x	x	
19.0	0.418	10	100		x		x
19.0	0.418	20	100		x	x	
20.0	0.418	30	100		x	x	
18.0	0.418	10	200		x	x	
19.0	0.418	20	200		x	x	
19.0	0.418	30	200		x	x	
16.0	0.418	10	250		x	x	
17.0	0.418	20	250		x	x	
17.0	0.418	30	250		x	x	
15.0	0.418	10	300		x	x	
16.0	0.418	20	300		x	x	
17.0	0.418	30	300		x	x	

Table (4.2) : Quarl Temperature Measurements

CV of Fuel MJ/kg	Swirl No.	Excess Air %	Preheat (°C)	Max.Temp. Location Inside Quarl (mm) LCV Gas Flames (150)	(200)	Max.Temp. Location Inside Quarl (mm) Natural Gas Flames (100)	(150)
19.0	0.689	10	38	x		x	
20.0	0.689	20	38	x		x	
20.0	0.689	30	38	x			x
18.0	0.689	10	100	x		x	
19.0	0.689	20	100	x		x	
19.0	0.689	30	100	x		x	
17.0	0.689	10	200	x		x	
17.0	0.689	20	200	x		x	
18.0	0.689	30	200	x		x	
16.0	0.689	10	250	x		x	
17.0	0.689	20	250	x		x	
18.0	0.689	30	250	x		x	
16.5	0.689	10	300	x		x	
16.0	0.689	20	300	x		x	
17.0	0.689	30	300	x		x	
19.0	0.964	10	38	x			x
20.0	0.964	20	38	x			x
20.0	0.964	30	38		x		x
18.0	0.964	10	100	x			x
20.0	0.964	20	100	x			x
20.0	0.964	30	100		x		x
17.0	0.964	10	200		x		x
18.0	0.964	20	200		x		x
19.0	0.964	30	200		x		x
17.0	0.964	10	250	x		x	
17.0	0.964	20	250	x			x
19.0	0.964	30	250		x		x
16.0	0.964	10	300	x		x	
17.0	0.964	20	300	x		x	
19.0	0.964	30	300		x		x

Table (4.3) : Quarl Temperature Measurements

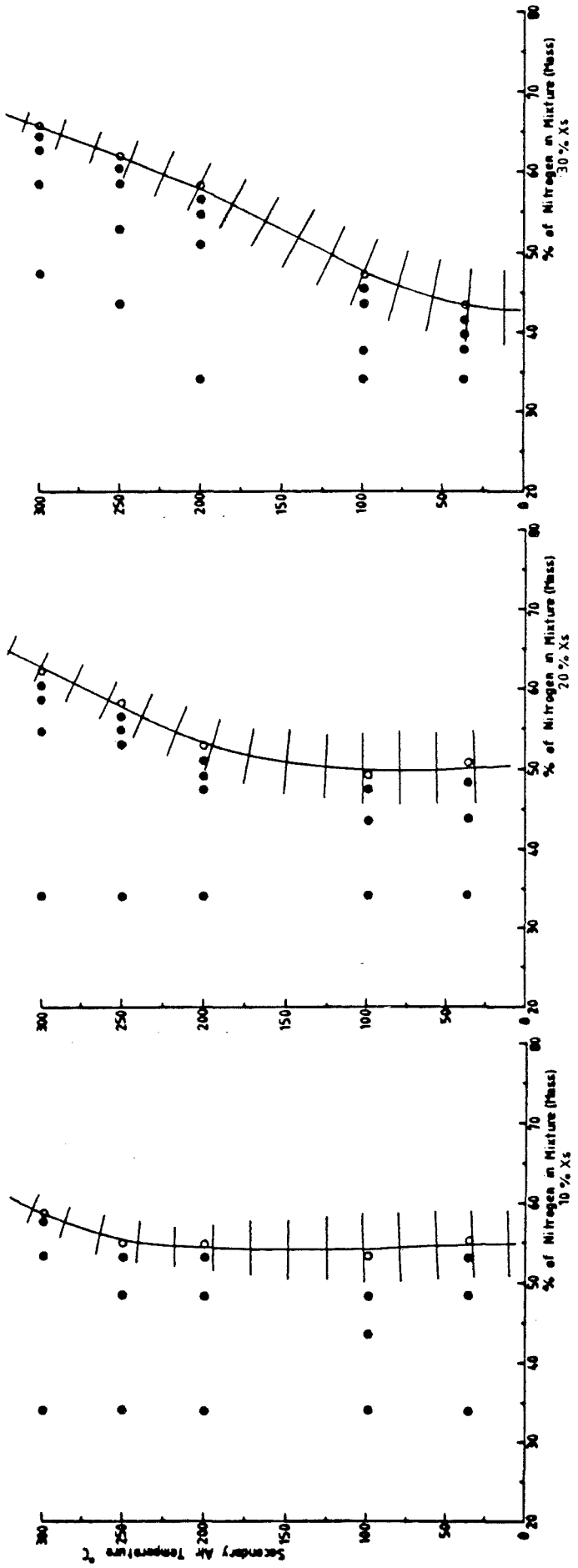

Fig.(4.1) Effects of secondary air temperature and excess air at zero swirl.

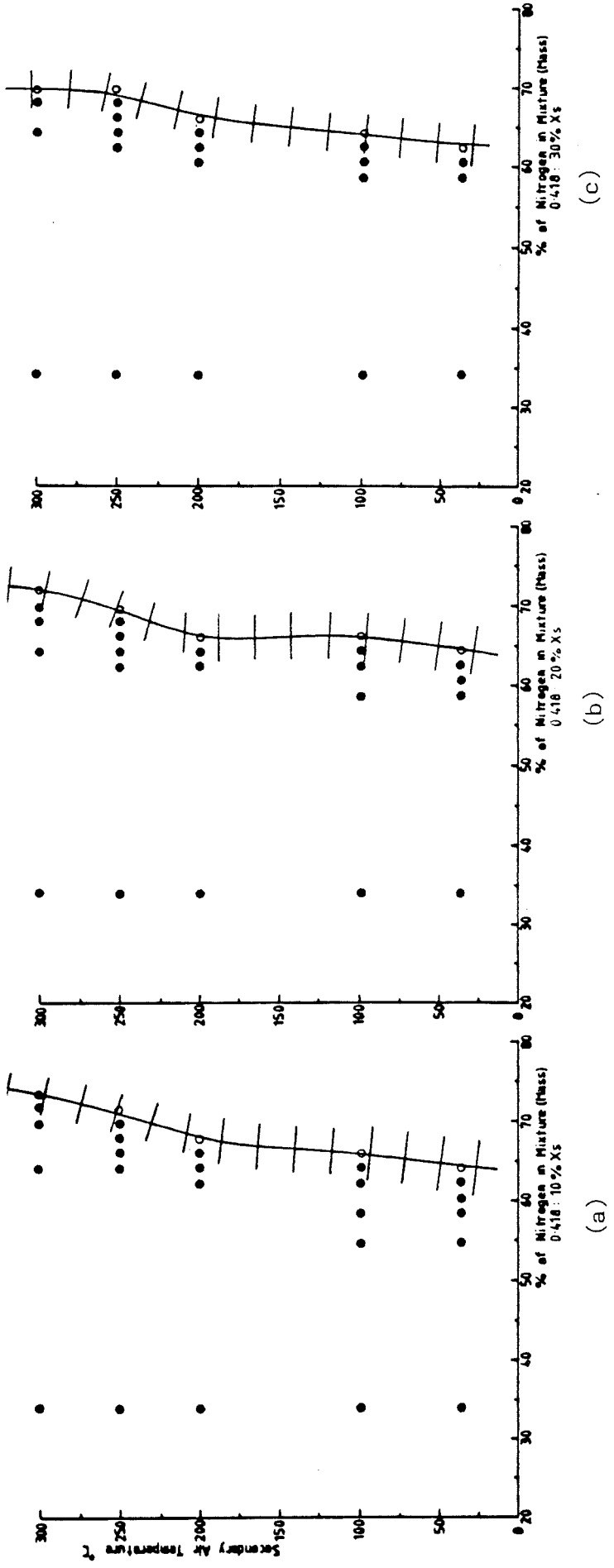

Fig.(4.2) Effects of secondary air temperature and excess air at a swirl number of 0.418.

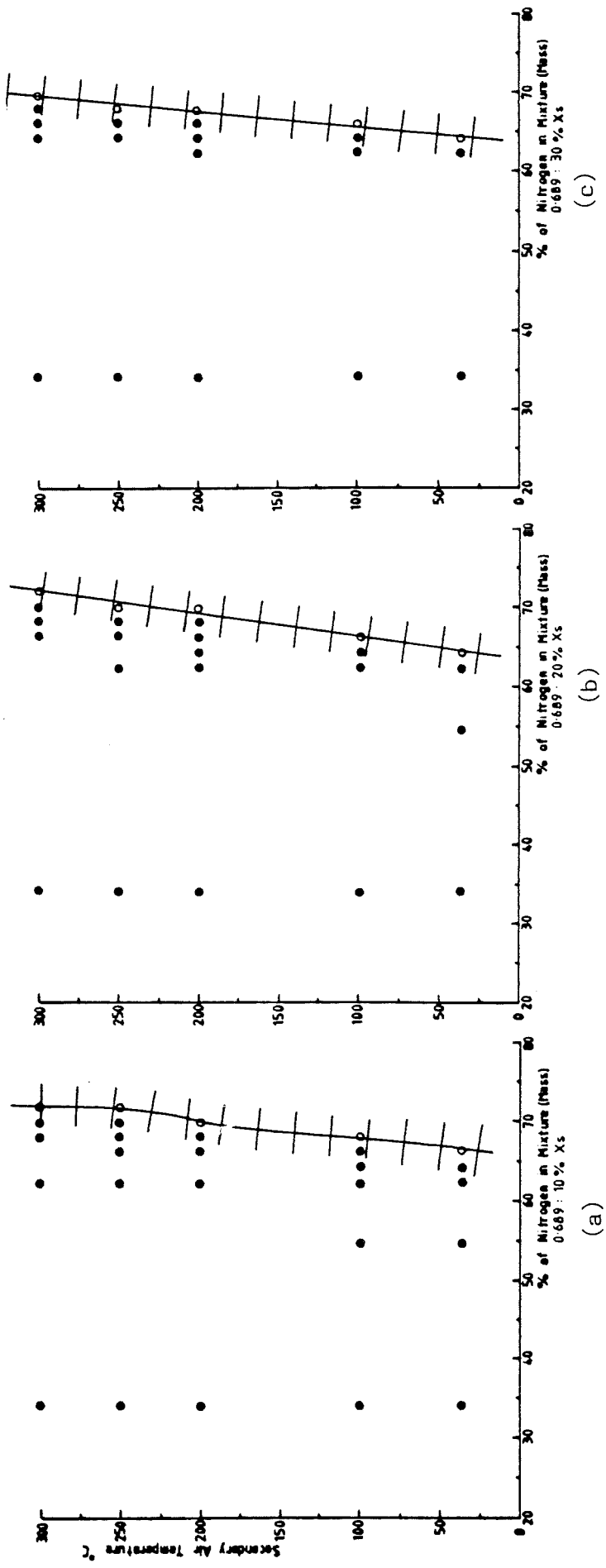

Fig.(4.3) Effects of Secondary air temperature and excess air at a swirl number of 0.689.

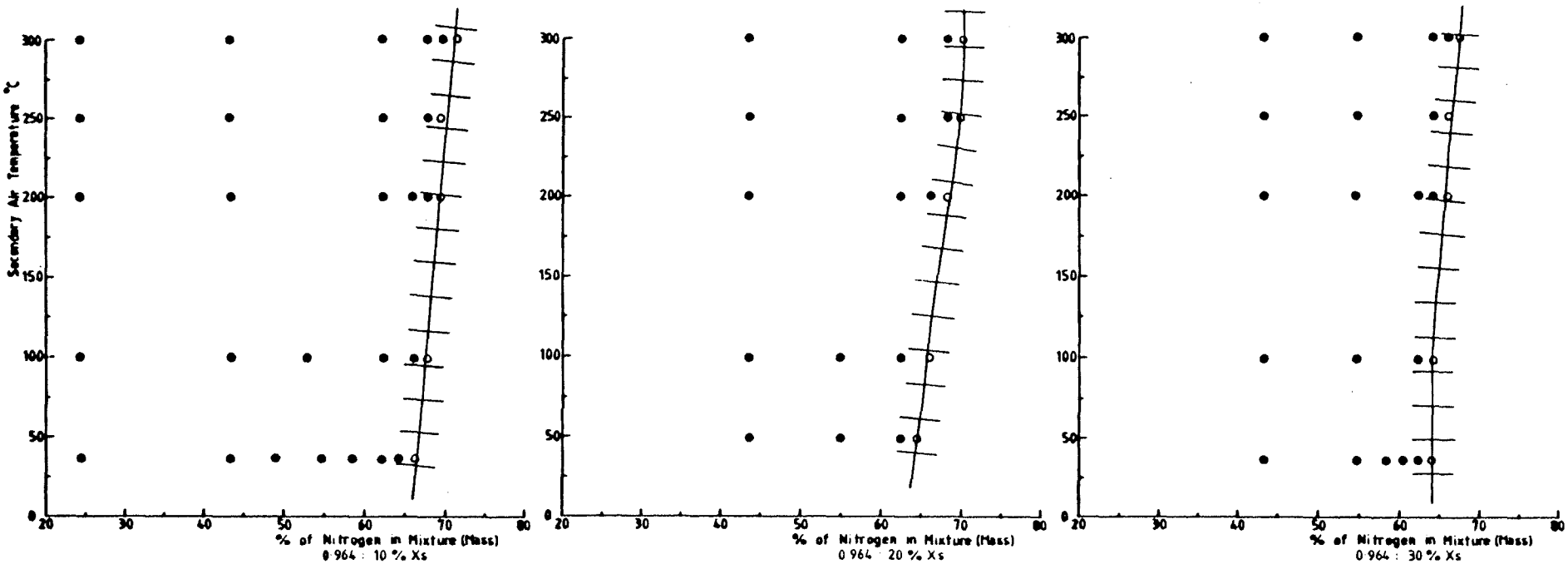

(a) (b) (c)

Fig.(4.4) Effects of Secondary air temperature and excess air at a swirl number of 0.964.

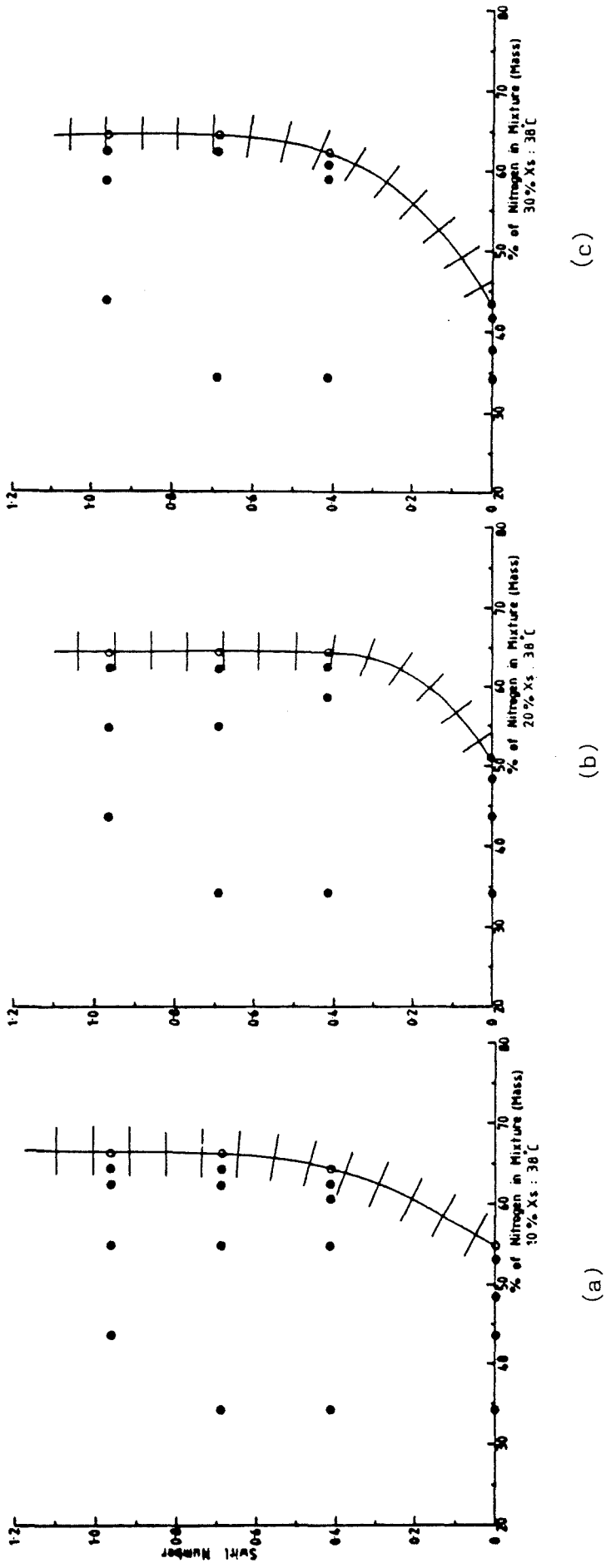

Fig.(4.5) Effects of swirl and excess air of a preheat temperature of 38°C.

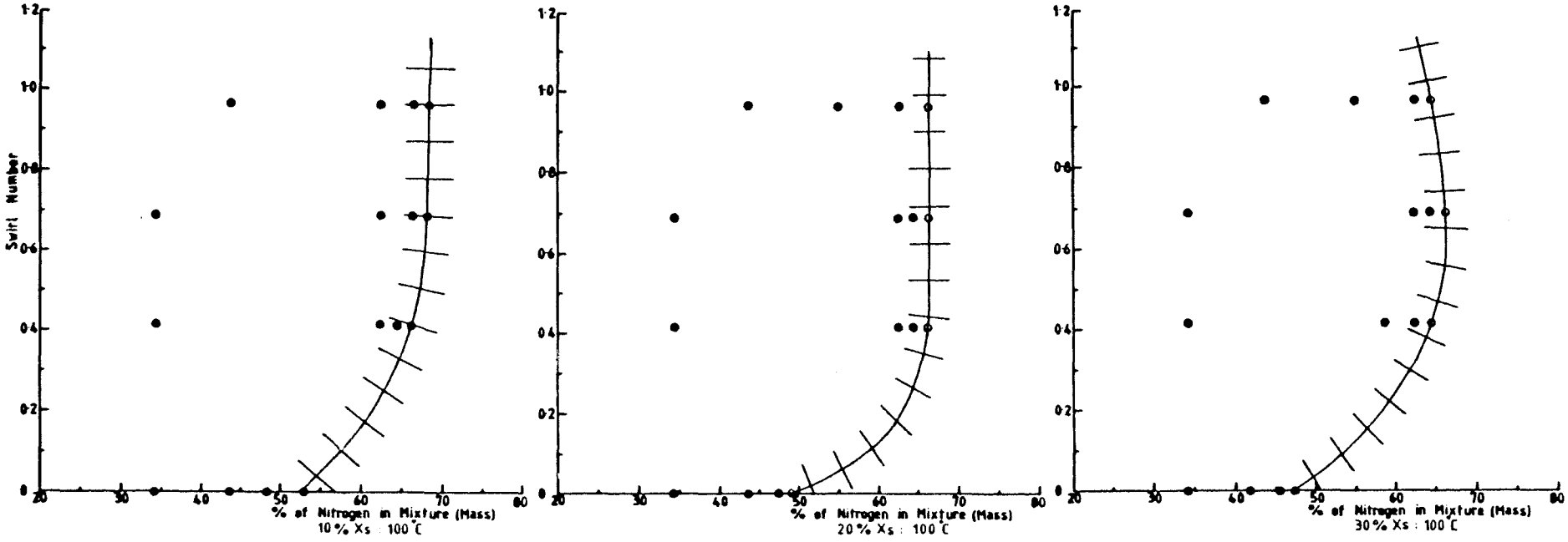

(a) (b) (c)

Fig.(4.6) Effects of swirl and excess air at a preheat temperature of 100°C.

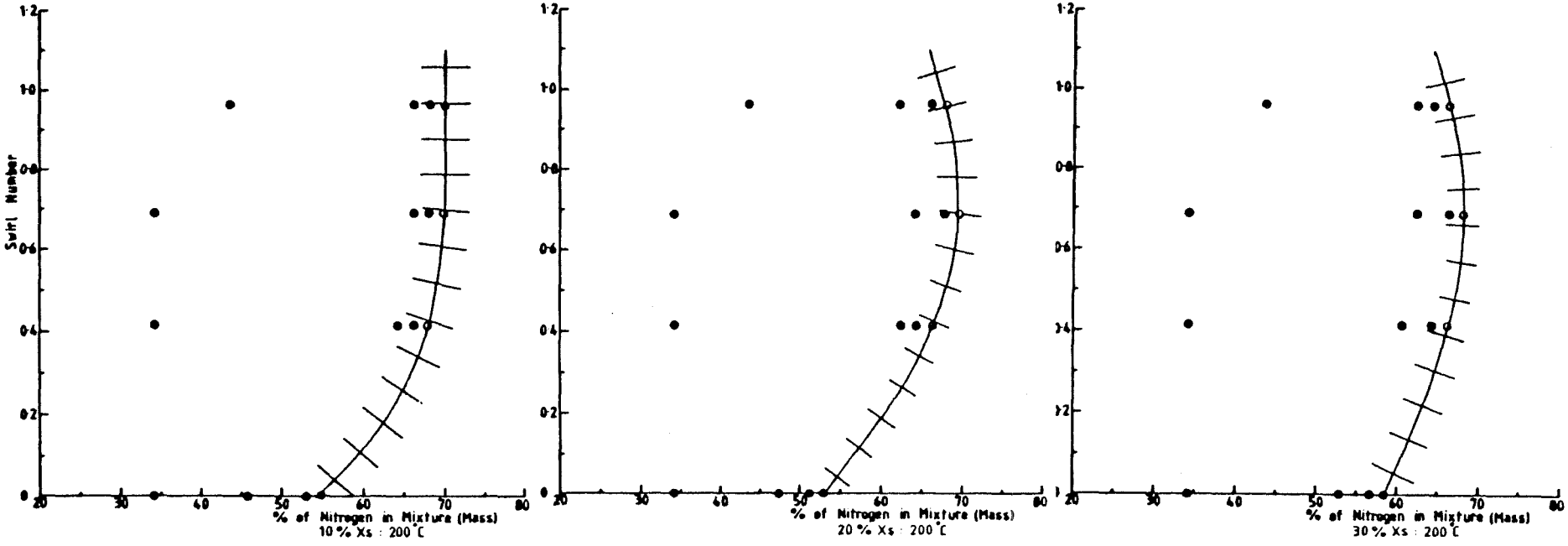

(a) (b) (c)

Fig.(4.7) Effects of swirl and excess air at a preheat temperature of 200^{o}C.

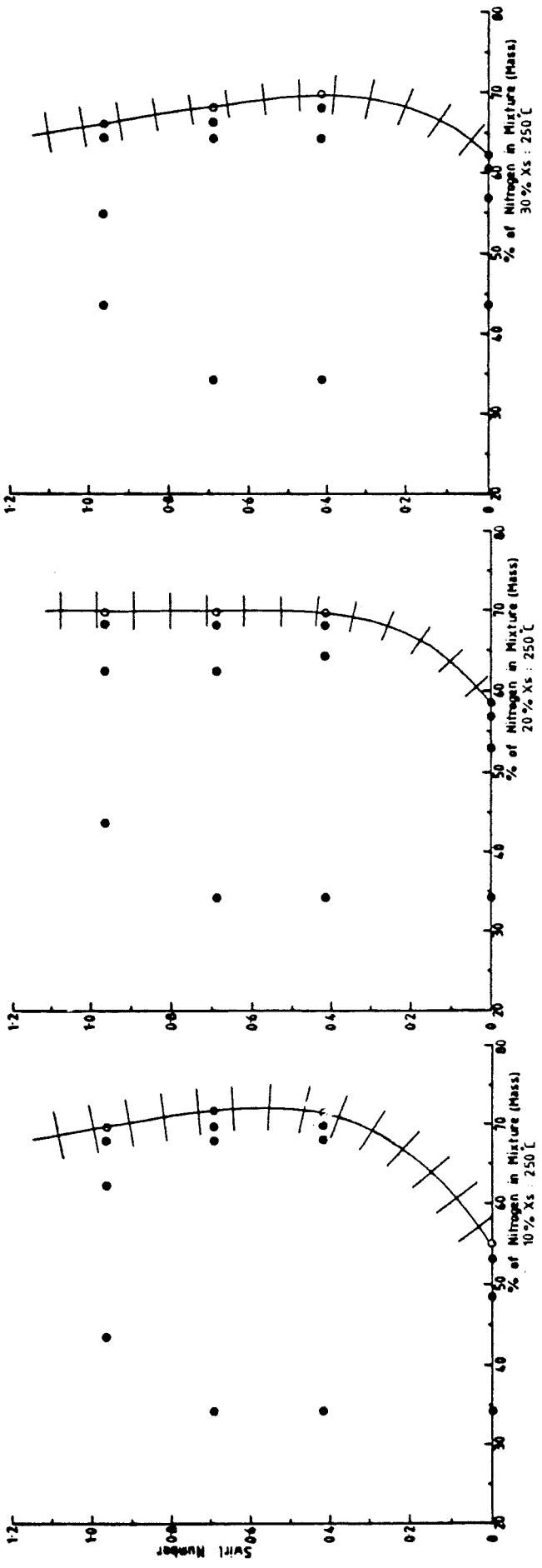

Fig.(4.8) Effects of swirl and excess air at a preheat temperature of 250°C.

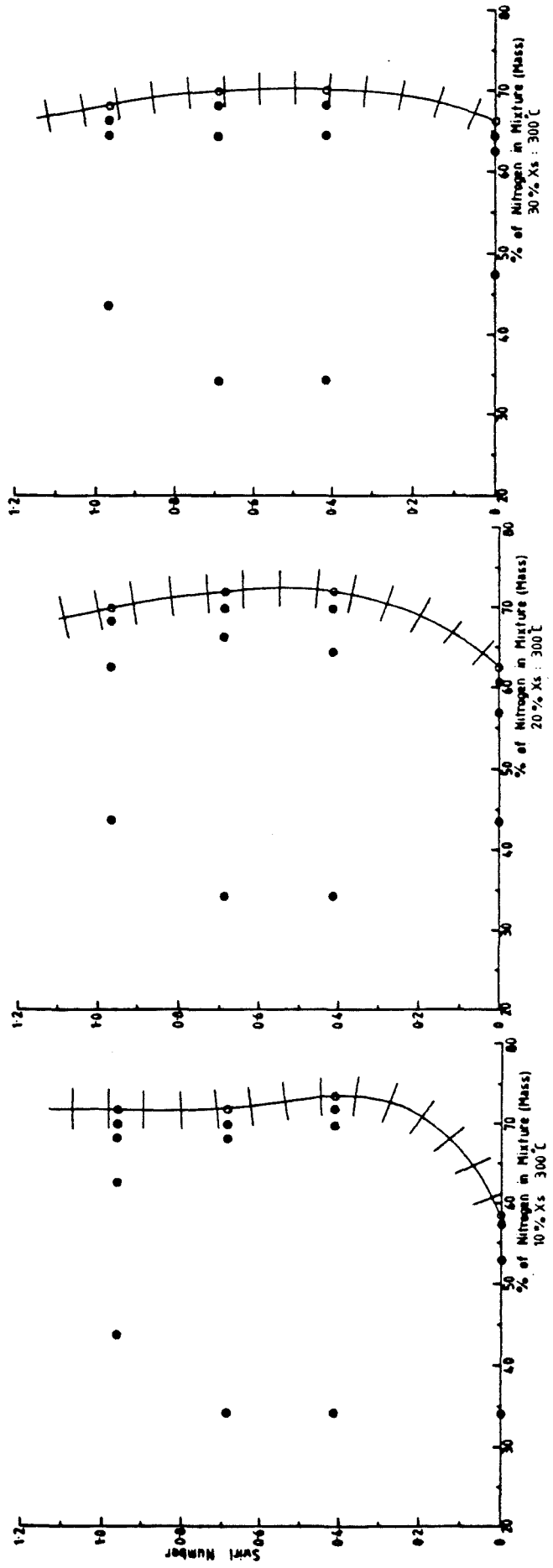

Fig.(4.9) Effects of swirl and excess air at a preheat temperature of 300°C.

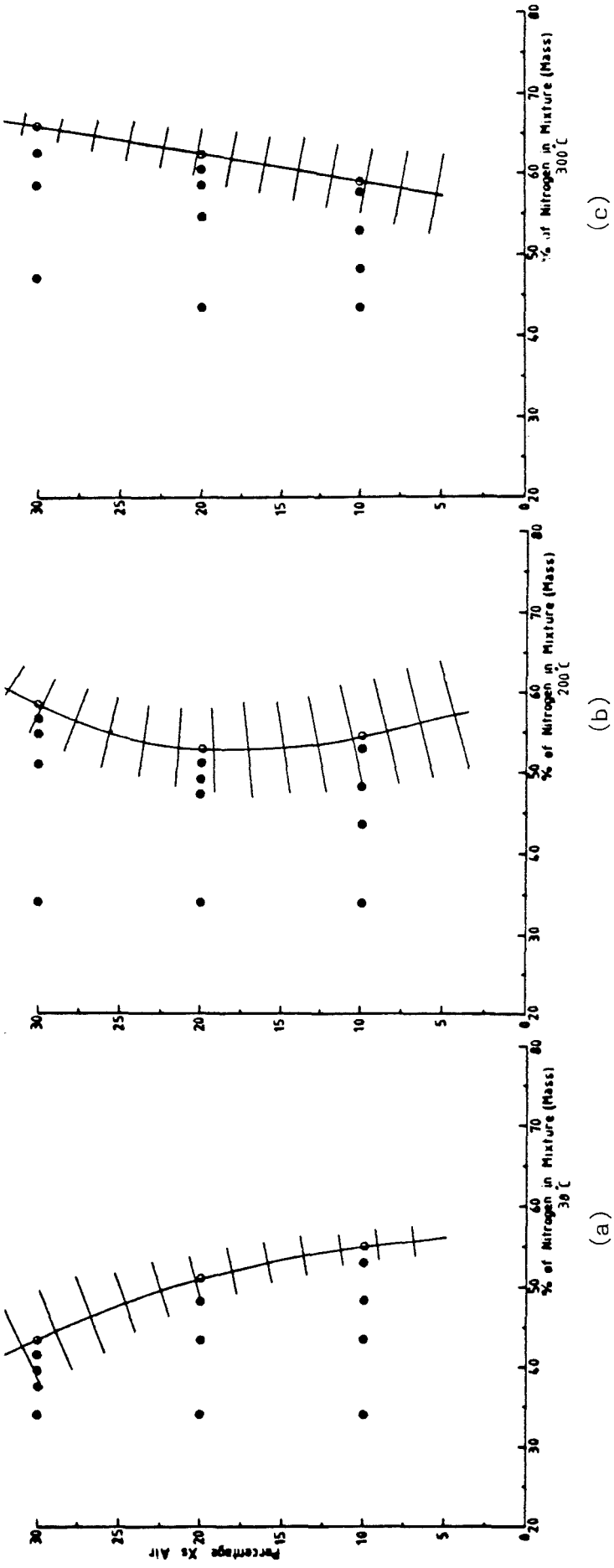

Fig.(4.10) Effects of excess air and preheat at zero swirl.

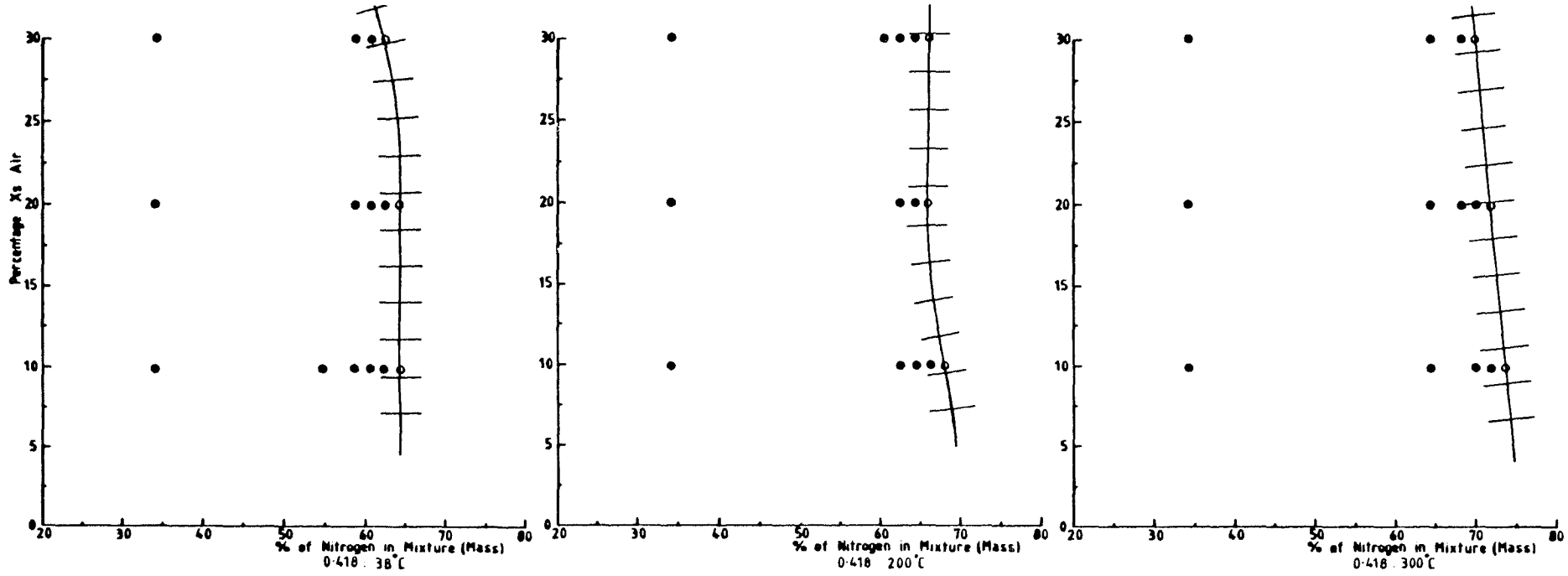

(a) (b) (c)

Fig.(4.11) Effects of excess air and preheat at a swirl number of 0.418.

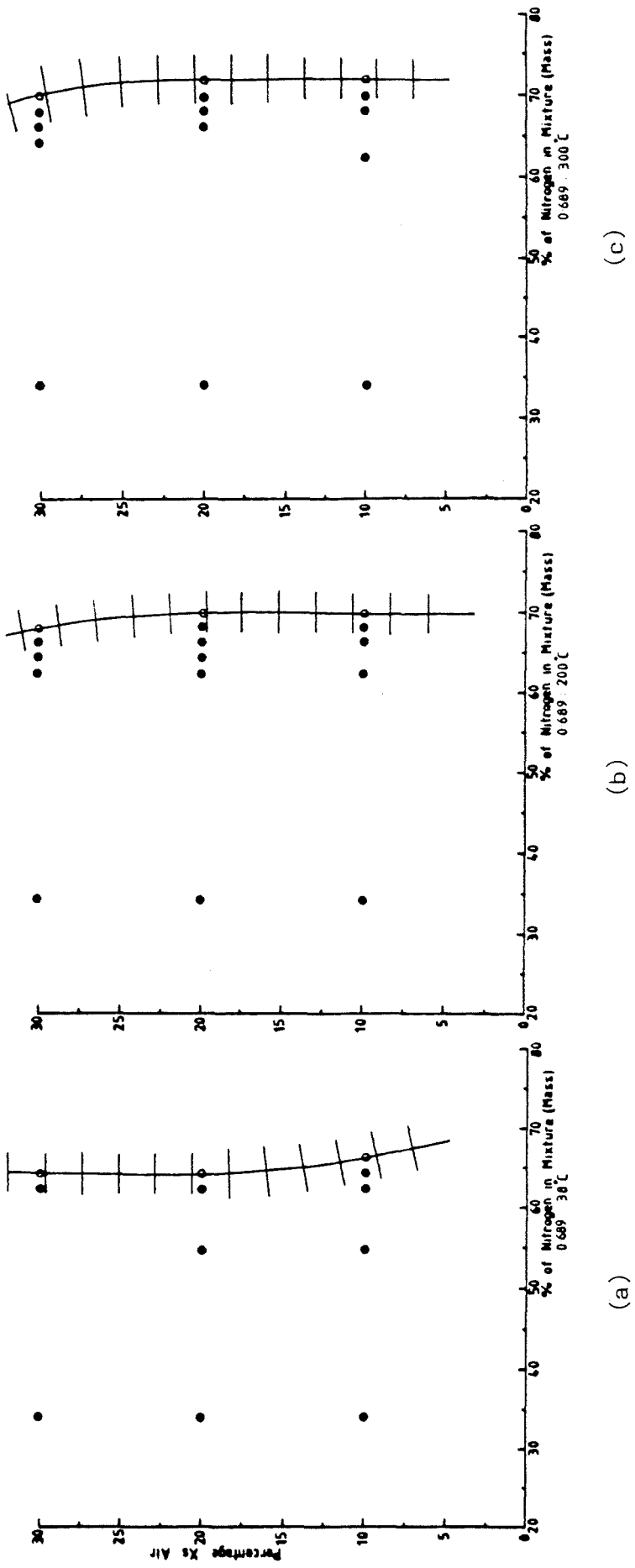

Fig.(4.12) Effects of excess air and preheat at a swirl number of 0.689.

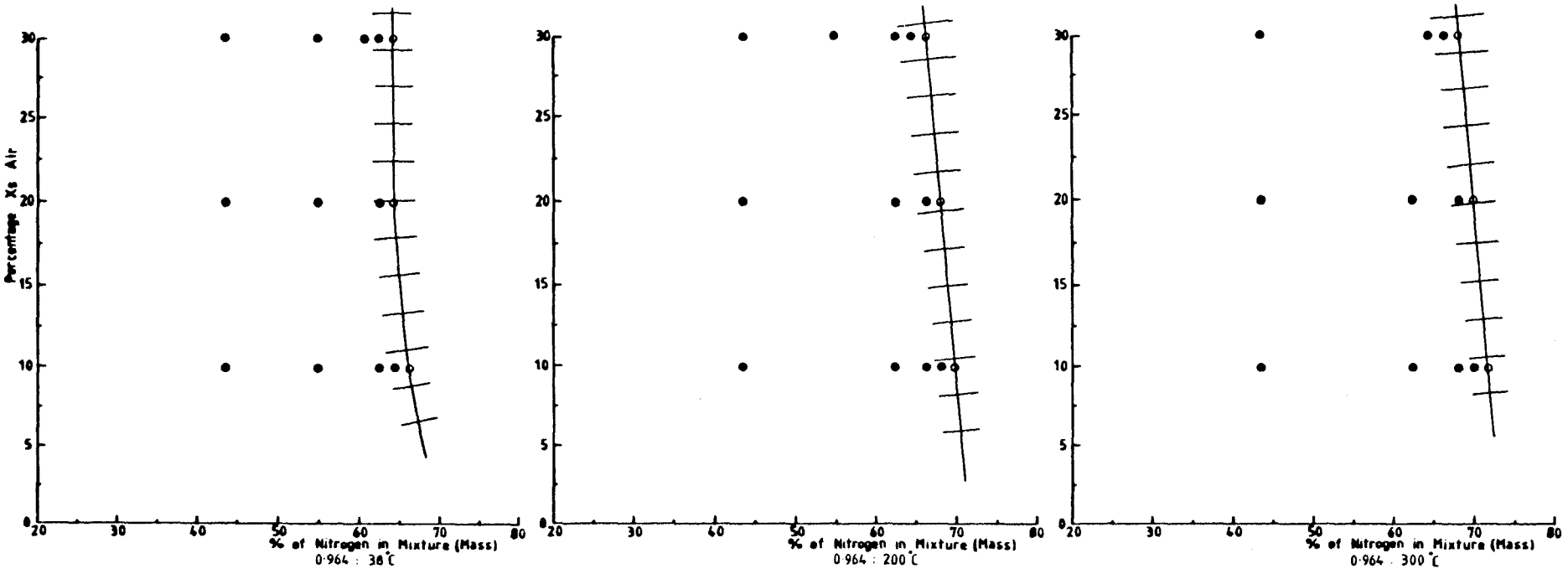

(a) (b) (c)

Fig.(4.13) Effects of excess air and preheat at a swirl number of 0.964.

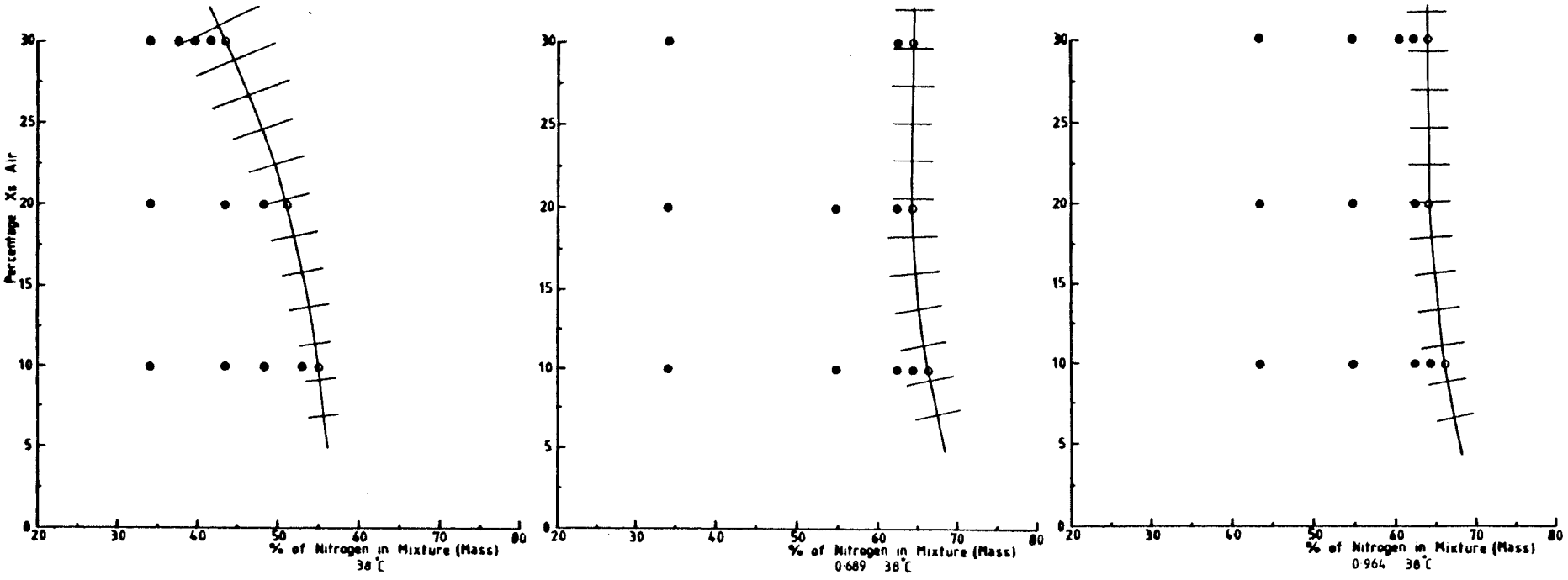

Fig.(4.14) Effects of excess air and swirl at a preheat temperature of $38^{O}C$.

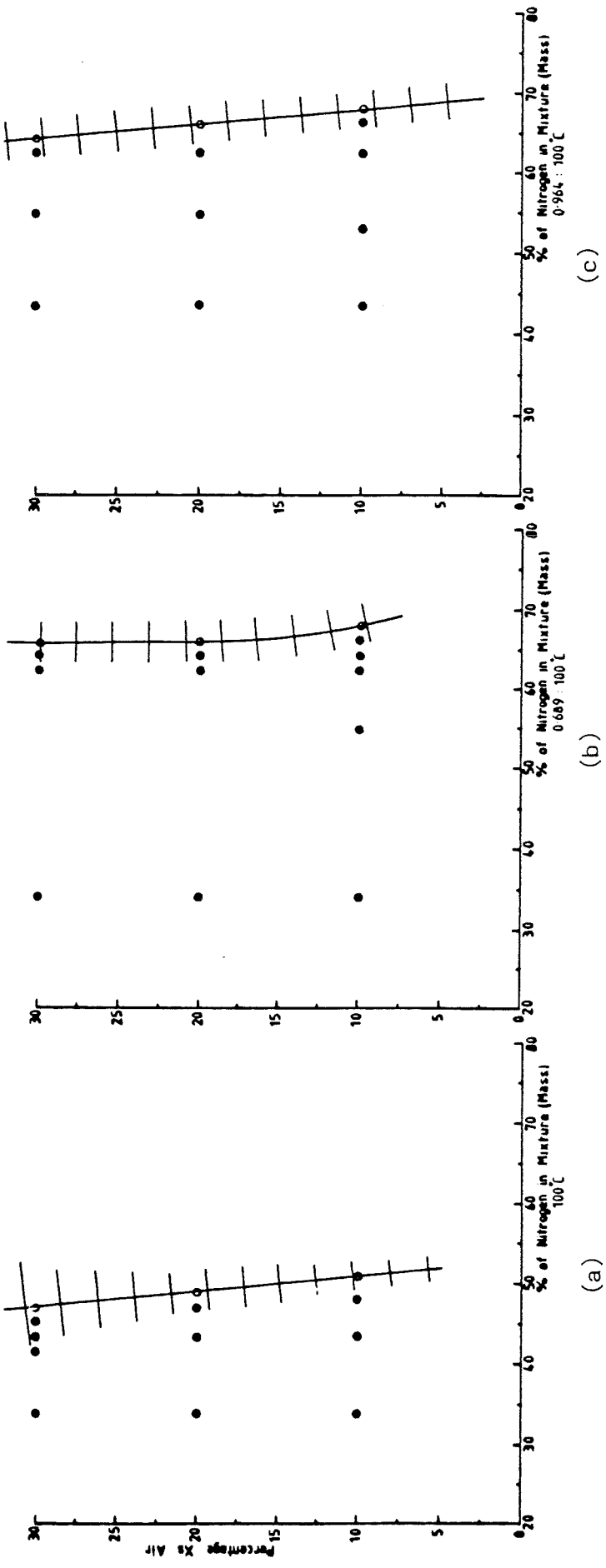

Fig.(4.15) Effects of excess air and swirl at a preheat temperature of 100°C.

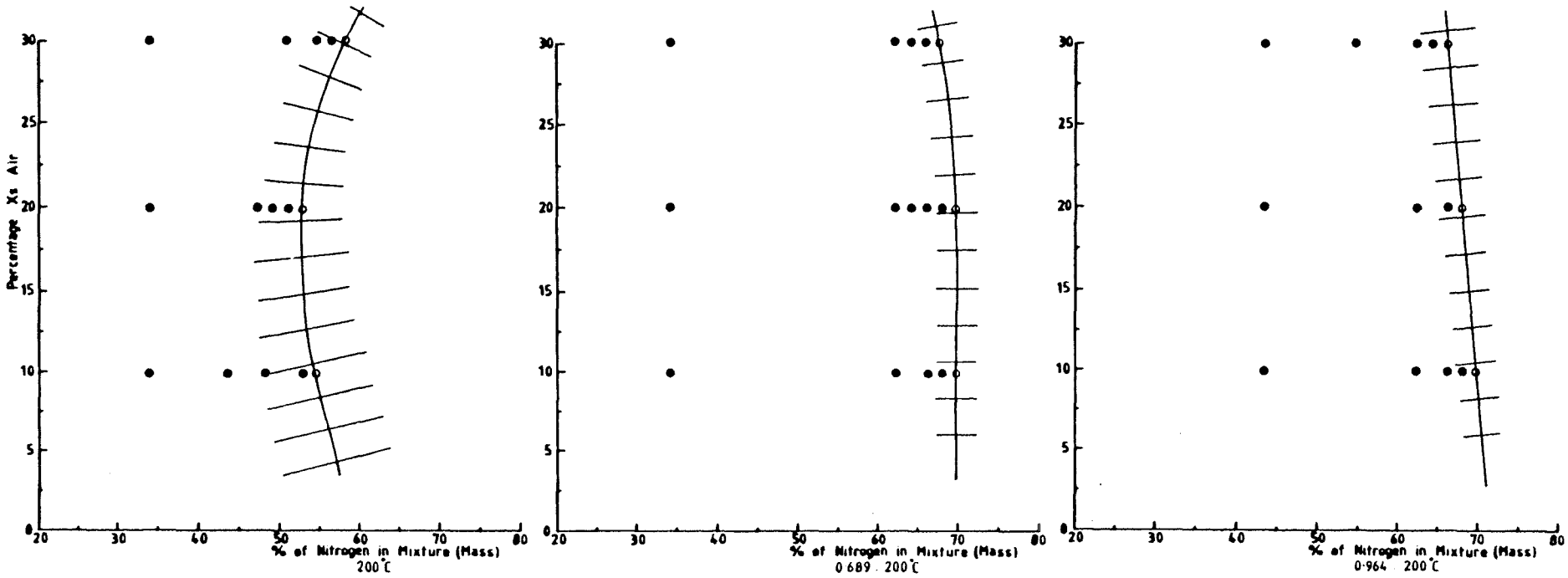

Fig.(4.16) Effects of excess air and swirl at a preheat temperature of 200°C.

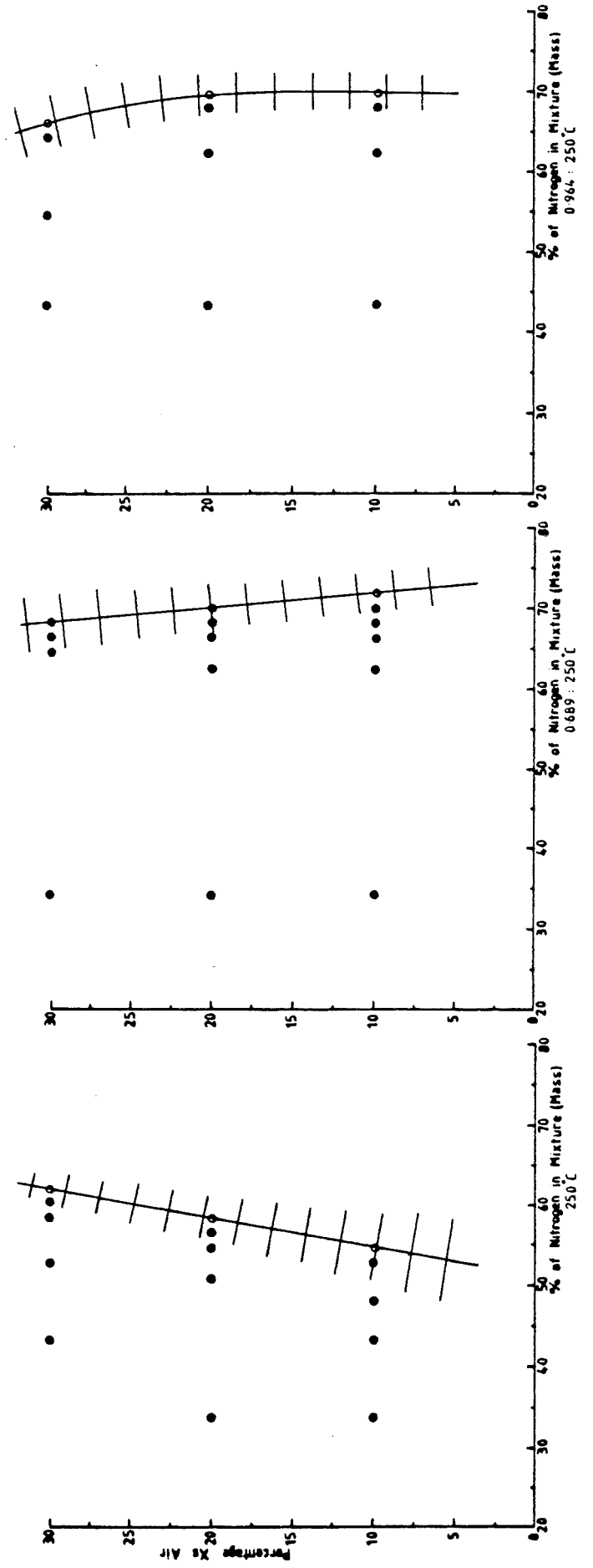

(a) (b) (c)

Fig. (4.17) Effects of excess air and swirl at a preheat temperature of 250°C.

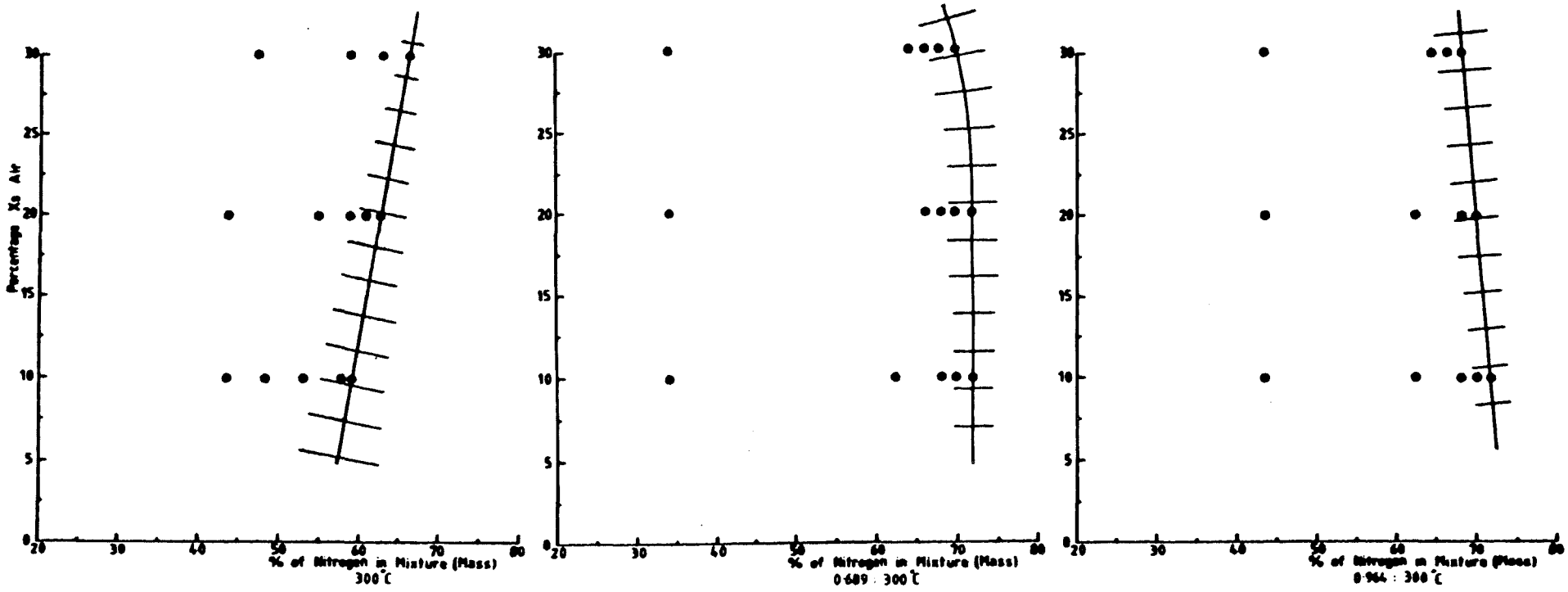

(a) (b) (c)

Fig.(4.18) Effects of excess air and swirl at a preheat temperature of 300^{o}C.

CHAPTER 5

INFLAME COMBUSTION MEASUREMENT RESULTS

5.1 Introduction

This chapter deals with the combustion measurements carried out in order to investigate flame conditions near the blow-off limits. Inflame temperature, velocity and concentration measurements were obtained to acquire a better understanding of the blow-off mechanism of confined turbulent diffusion flames. Due to the long measurement periods required to collect data for one operating condition, it was not possible to investigate all the blow-off situations reported in the previous chapter. To prevent blow-off while collecting inflame combustion data, the calorific value of the fuel used was set at 3 MJ/kg above its blow-off value for each operating condition investigated.

All the data were collected at the first port (X/D = 0.445) which was closest to the burner. Temperature measurements for near blow-off flames were made for three swirl numbers, three excess air levels and three secondary air preheat temperatures. Velocity and concentration measurements were also collected for two swirl numbers, three excess air levels and two secondary air preheat temperatures. For all the above operating conditions, corresponding data were collected with the furnace being fired on pure natural gas at a mass flow rate of 3 kg/h so that they could be used as reference. In addition, temperature, and concentration measurements were also made at the exhaust duct for all the different conditions investigated. These measurements were used to calculate the burnout rate in order to get an idea of the combustion efficiency of the system.

The rest of this chapter is divided in four sections. Section (5.2) outlines the experimental conditions and procedures under which the inflame combustion measurements were carried out. The different measuring techniques used are given in section (5.3) which is divided into three subsections, each one dealing with temperature, velocity and concentration in turn. The experimental results are presented in section (5.4) which is also divided in three subsections as above. Section (5.5) deals with the discussion of the experimental results, with seven subsections dealing with the effects of excess air, swirl and preheat. The burnout rate measurements are also given with the proposal of a stabilizing mechanism. The relationship between stability limits and combustion measurements is also discussed.

5.2 Experimental Conditions and Procedures

Inflame combustion measurements at various operating conditions were collected in the near-burner region (X/D = 0.445) and at the exhaust of the furnace. The calorific value of the fuel used was based on the stability limit measurements from the previous chapter. Temperature measurements were made for three excess air levels (10%, 20% and 30%), three swirl numbers (0, 0.689 and 0.964) and three secondary air preheat temperatures (38°C, 200°C and 300°C). Velocity and concentration measurements were collected for three excess air levels (10%, 20% and 30%), two swirl numbers (0 and 0.964) and two secondary air preheat temperatures (38°C and 300°C). Corresponding measurements were also carried out at the same operating conditions as described above but firing on pure natural gas instead. Additional concentration data for the low calorific value gases were collected over the three levels of

excess air investigated. In these cases, the preheat was set at 200°C and the swirl numbers were 0, 0.689 and 0.964.

The furnace was started with a firing rate of 3 kg/h burning natural gas. The excess air level, cooling-water flow rate and secondary air temperatures were set to the desired values. The appropriate measuring probe which was mounted on the traversing gear mechanism, was then connected to the measuring port of the furnace. The connecting leads and pipes were then taken to the dedicated measuring instruments and then finally to the microprocessor. A full hour was allowed to elapse for the furnace to reach a stable condition and this was done whenever the furnace was started from cold conditions. The mass flow rate of the nitrogen was then gradually increased while that of natural gas simultaneously decreased, until the predefined calorific value of the mixture was reached. The total mass of the fuel mixture was always kept at 3 kg/h for all the tests carried out. The furnace was allowed to run for a further 30 minutes for conditions to stabilize after which the furnace settings were given a final check to ensure that they were at the required values.

The microprocessor was then prompted to initiate the data collection procedure. Throughout the measurement period, the settings of the excess air levels, the secondary air temperature, the mass flow rates of natural gas and nitrogen, as appropriate, were monitored and adjusted to their correct values in case of deviation. At the end of data collection, the operating conditions were left unchanged for a repeated run or were changed to new settings for a different stability situation, depending upon what measurements were being carried out. For new

settings, the furnace was allowed to stabilize over a further 30 minutes period before data collection was commenced.

The procedures described above were repeated until all the excess air levels and secondary air temperatures had been investigated. The measurements were then repeated with a pure natural gas firing situation under the same operating conditions as their low calorific value counterpart. The swirl number was then changed to the value required and the whole data collection procedures were repeated as described above.

5.3 Measuring Techniques

As different probes were employed for the inflame measurement of temperature, velocity and concentration, a different measuring technique was required for each. This section which is divided into three parts deals with the particular measuring techniques required for the operation of each specific probe.

5.3.1 Temperature

Inflame temperature measurements were carried out using a 40 μm fine wire thermocouple probe. The probe was mounted on a saddle which was attached to the traversing mechanism for insertion into the furnace.

At the beginning of data collection, a subroutine in the temperature measurement program allowed the probe to traverse quickly up to the centre line and back to the starting position. This was done in order

to check if the fine thermocouple wire was able to stand the high velocity and temperature levels present inside the furnace close to the burner outlet for the particular operating condition investigated. It also set the probe at the correct starting point. Temperature data were then collected over a period of 50 seconds at each of the 23 locations between the centre line and furnace wall at regular intervals of 10 mm. In that 50 seconds period, 1000 different temperature readings were taken and the average value was stored in the microprocessor's memory. A further 20 seconds were given for conditions to settle down after each probe movement. Two runs were made for each operating condition and the average was used to plot the temperature profiles, see Table (A1) of Appendix (A).

5.3.2 Velocity

A five-hole pitot probe was used to measure the inflame velocity profile across the furnace. The probe was carefully aligned on the traversing mechanism such that the measuring head was located on the centre line and parallel to the axis of the furnace when the unit was bolted to the measuring port. The cooling water supply to the probe was adjusted and the five flexible tubes connecting the probe to the micromanometer secured. The same locations as traversed during the temperature measurements were used and the measuring period at each point took about 5 minutes. During this time the pressure readings were taken a total of 1500 times for each of the five pressure tappings on the probe head. These pressure readings were then computed into the average velocity, the conical and dihedral angles of the gas stream. The probe was then moved to the next measuring point by a subroutine in the velocity

program and a delay of 20 seconds was allowed before the resumption of data collection for conditions to stabilize after the probe movement. After the last measuring location, the probe was motored back to the starting point and the measurements were repeated for the same furnace operating conditions. A table listing the furnace operating conditions and the values of mean velocity, conical angle and dihedral angle at each of the measuring point for each run was then printed, see Table (A2) of Appendix (A).

5.3.3 Concentration

Inflame concentration measurements were made with the help of a water-cooled stainless steel sampling probe. Again the same sort of aligning precautions, as mentioned for the five-hole probe, were taken. The temperature of the cooling-water coming out of the probe was always kept very close to the boiling point by adjusting its flow rate throughout the measuring period. This was vital as cold spots at any point inside the probe could have caused the sample gas to condense. No attempt was made to sample the combustion gases isokinetically as Tine (1961) and Bilger (1977) pointed out the uncertainties associated with swirling turbulent flows with substantial recirculation. The measuring locations were the same as those used for the temperature and velocity cases. Each location was sampled for a duration of about 15 minutes with a 20 seconds interval inbetween measuring location to allow the flow to settle after the probe movement. A total of 2000 readings were taken for each species measured at each measuring location and the average were stored. The combustion gases were sampled for five different species, UHC, NO_x, O_2, CO and CO_2. Due to the long period involved in collecting a set of concentration data, only one run was

done for each operating condition. All the instruments used were calibrated and checked both before and after sampling was completed to ensure proper operation of the gas analyser. At the end of the run, the computer automatically printed out all the concentration measurements together with the furnace operating conditions, see Table (A3), Appendix (A).

5.4 Presentation of Experimental Results

This section deals with the presentation of the experimental results obtained for the inflame combustion measurements. Data for both L.C.V. and natural gas flames were collected for a number of different operating conditions and those of the L.C.V. gas cases were dependent on the stability limit measurements obtained in the previous chapter. Three subsections are used to present the results, each one dealing with temperature, velocity and concentration in turn.

5.4.1 Temperature Measurements

Figures (5.1) to (5.5) show the temperature profiles obtained for a range of operating conditions of the furnace. Figure (5.1(i)) shows the case when pure natural gas was fired with no swirl or preheat to the secondary air. The percentage excess air values are indicated by the symbols used as shown on the graph. Considering Fig.(5.1(i)), the values printed after the symbols represent the excess air level and the excess air factor respectively. The excess air factor is the inverse of the equivalence ratio. Figure (5.1(ii)) shows the temperature profiles under the same operating conditions as in Fig. (5.1(i)) but for

a low calorific value gas flame. The values after the symbol in this case represent the calorific value of the gas used, the equivalent excess air supplied and the excess air factor in turn. This is applicable to all the L.C.V. gas cases which, apart from Fig.(5.1), are presented on the (b) figures. The equivalent excess air (EEA) was based by considering the total mass of fuel used as natural gas; in other words it was the same mass flow rate of air used as in the pure natural gas situation for that particular level of excess air investigated. This was done to keep the momentum at the burner mouth constant for each excess air level considered. The real value of excess air supplied was represented by the excess air factor (EAF) in which only the amount of natural gas used in the fuel mixture was considered.

In Figs.(5.2) to (5.5), both the natural and L.C.V. gas flames data are represented on one graph. They were of course obtained for the same operating conditions which are given at the top of each graph. For example, Fig.(5.2(i)(a)) represents natural gas flames data without any swirl and with secondary air preheat of 200°C; the corresponding L.C.V. gas flames data are presented in Fig. (5.2(i)(b)).

5.4.2 Velocity Measurements

In addition to the mean velocity, the data collected also gave the conical and dihedral angles of the flow and a good description of the method is given in Appendix (A). The values of these angles are plotted above their corresponding mean velocity data such that not only the magnitude but also the direction of the flow inside the combustor can be obtained.

The mean velocity, conical and dihedral angles are plotted against the radial distance, with R=0 representing the centre line. All these measurements were taken at one axial location (X/D = 0.445) which was the closest port to the burner.

Figures (5.6) to (5.13) represent the velocity data collected and in all these cases (a), (b) and (c) denote 10%, 20% and 30% excess air supplied to the combustor based on a mass flow rate of 3 kg/h of natural gas being fired through the burner. Figure (5.6) represents data for pure natural gas flames without swirl and preheat to the secondary air while Fig.(5.7) shows L.C.V. gas flames data under similar operating conditions. The effects of preheating the secondary air to 300°C, again without any swirl, on the velocity data are shown in Fig.(5.8) with the corresponding L.C.V. data represented on Fig. (5.9). Figures (5.10) and (5.11) show the effects of swirl without any preheat on natural and L.C.V. gas flames respectively. Finally the effect of both swirl and secondary air preheat are represented in Figs.(5.12) and (5.13).

The data plotted show the values obtained for both runs, connected by an error bar. This gives an indication on the accuracy of the measurements and it also shows the difficulty of obtaining velocity data using a five-hole pitot probe. It is clear that the data obtained in the central reaction core are within the repeatability limits of the experiment. Those of the outer zone are somewhat suspect and it may be due to reverse flow which is difficult to detect using such a probe.

5.4.3 Concentration Measurements

Concentration data of five species UHC, NO_x, O_2, CO and CO_2 are presented in Figs. (5.14) to (5.25) for two swirl numbers (0 and 0.964), two secondary air preheat temperatures (38°C and 300°C) and the usual three excess air levels. In all these figures, (a) represent data for natural gas firing situation while (b) show the data collected for L.C.V. gas flames. The species concentration are plotted against the radial location inside the furnace with R=0 representing the centre line. Additional concentration data are presented in Appendix (B) for various operating conditions.

Figure (5.14) shows the case when the furnace was operated without any swirl or preheat on 10% excess air while the following two figures (5.15) and (5.16) are for the same conditions but with 20% and 30% excess air respectively. Similarly, Figs. (5.17) to (5.19) represent data for zero swirl and secondary air preheat temperature of 300°C. Figures (5.20) to (5.22) show concentration measurements for maximum swirl (0.964) situation without any preheat while Figs. (5.23) to (5.25) represent conditions with maximum swirl and maximum preheat to the secondary air (300°C). It should again be noted that for all the L.C.V. gas flames, the true excess air level is represented by the excess air factor (EAF). This excess air is based on the actual amount of natural gas present in the total mass of the fuel mixture the flow rate of which was kept at 3 kg/h for all the experiments.

5.5 Discussion of Experimental Results

The following three subsections concentrate on the effects of excess air, swirl and secondary air preheat on the temperature, velocity and concentration measurements taken for both natural and L.C.V. gas flames.

5.5.1 Effects of Excess Air

From the data collected it is clear that an increase in excess air level caused a decrease in the temperature level attained inside the combustor and this applied for all the natural gas firing situation regardless of whether swirl or preheat was used or not, (Figs. 5.1(i)) and all the (a) figures presented in Fig. (5.2) - (5.5)(i) and (ii). The cause was the resulting dilution effect, (Fricker and Leuckel (1976)). A similar comment cannot be made for the L.C.V. gas cases as the temperature level attained within the combustor depended strongly on the C.V. of the fuel used and also in particular on the EAF. There was very little difference in the velocity profiles for the zero swirl cases with or without preheat, Figs. (5.6) and (5.8). The sizes of the reaction core also remain the same with increase in excess air level and there was very little change in the flow direction. For the L.C.V. gas flames there is a decrease in both the reaction volume and the maximum flow velocities with increasing excess air. This situation prevailed regardless of the secondary air preheat temperature or the C.V. of the fuel used, (Figs. (5.7) and (5.9)). For swirling flows there was very little change in both the maximum velocity and the reaction volume, formed by the central recriculating core, when the excess air was increased. This applied to both natural and L.C.V. gas flames and was independent of the temperature of the secondary air supplied, (Figs. (5.10) to (5.13)).

Considering the concentration measurements, it is clear that for the natural gas firing situations without any swirl or preheat, an increase in excess air caused an increase in the oxygen level inside the furnace

as well as a reduction in CO_2 and NO_x, (Figs. (5.14)(a) to (5.16)(a)). The levels of CO and UHC were very low and the effect of increasing excess air on them was not significant. For the L.C.V. gas flames, the concentration of all the species were very dependent on the C.V. of the fuel used; but for cases where the same EAF were used, e.g. Fig.(5.15(b) and (5.16)(b), it is evident that an increase in excess air caused little change in the concentration of all the other species with the exceptions of UHC and CO which showed a decrease in value. A similar effect was noticed by Syred et al. (1977) on their waste gas combustor. With preheat, there was very little change in the level of NO_x concentration with increasing excess air for pure natural gas. Again there was an insignificant amount of UHC at all locations but the CO measurements were substantial in the core region of the flames and decreased in value as the excess air was increased, (Figs. (5.17)(a) to (5.19)(a)). There was also an increase in oxygen concentration and a decrease in the carbon dioxide value. For the L.C.V. gas cases, (Figs. (5.17)(b) to (5.19)(b)), there was a very small amount of NO_x formed at all excess air levels but the UHC and CO concentrations were significant. Substantial amount of O_2 and very little CO_2 were also present. This indicates inefficient combustion. Their concentration levels were dependent on the CV of the fuel used and in these cases close comparisons cannot be made as both the CV and the EAF were different for each excess air level.

For natural gas flames with swirling flows and without secondary air preheat, (Figs. (5.20)(a) to (5.22)(a)), an increase in excess air caused a decrease in NO_x and CO_2 concentrations, an increase in the O_2 level and insignificant changes in the very low concentrations of CO and UHC. For the corresponding L.C.V. gas flames, Fig. (5.20)(b) to

(5.22)(b), the CO and UHC levels were very high across the whole furnace and they showed an increase in concentration, for fuels having virtually the same CV, as the excess air level was increased. The concentrations of the other species were dependent on the EAF used but the trend seems to be the same as described for the natural gas flames situations.

The effects of excess air for both maximum swirl (0.964) and maximum preheat (300°C) conditions on the concentration measurements are shown in Fig. (5.23) to (5.25). For the natural gas flames, (Figs. (5.23(a) to (5.25)(a), there was a decrease in the NO_x and CO values and very little UHC in all three cases; as expected there was an increase in the O_2 concentration coupled with a decrease in the CO_2 level. In the L.C.V. gas flames, (Figs. (5.23)(b) to (5.25)(b)), the concentrations of NO_x, CO and UHC were low for the three excess air levels investigated when compared with similar flames under the other operating conditions as mentioned previously. Again the concentrations of CO_2 and O_2 were dependent on the fuel's CV and the EAF used.

5.5.2 Effects of Swirl

Beginning with the zero preheat situation, the effects of imparting swirl to the secondary air on the temperature profiles are shown in Figs. (5.1)(i) and (ii) and (5.5)(i). The most obvious effect was a reduction in the centre line maximum temperature, but the temperature levels in the outer recirculation zone, (R >140 mm), were increased from about 500°C to about 700°C for the natural gas flames and these were independent of the excess air level. Similar effects were noted for the L.C.V. gas flames but the temperature levels were dependent on the

EAF and the CV of the fuel used. When the secondary air was preheated, (Figs. (5.2)(ii) and (5.3)(ii)), the same effects as described above were demonstrated on the temperature profiles.

Comparing the velocity profiles for the zero preheat situations using natural gas, Figs. (5.6) and (5.10) show a large reduction of the mean velocity in the central core area. There were also substantial fluctuations as indicated by the long error bars on both the conical and dihedral angles. This was an indication of central core recirculation created by the swirl as demonstrated by other workers, e.g. Beltagui and Maccallum (1976), Chedaille et al. (1966) and Fricker and Leuckel (1976). Similar effects were noted on the velocity profiles of the L.C.V. gas flames, (Figs. (5.7) and (5.11)) and they were all independent of the excess air levels used. The same situation was observed when the secondary air was preheated to 300°C for both the natural gas flames, (Figs. (5.8) and (5.13)), and the L.C.V. gas flames, (Figs. (5.9) and (5.14)).

Figures (5.14) and (5.20) show the results of imparting swirl on the concentration measurements for flames without any preheat and for the same excess air level employed. For the natural gas flames, (Fig.(5.14)(a) and (5.20)(a)), the concentrations of all the species, with the exception of CO, were in the same range when compared for the two flows. With swirl, there was a decrease in the steepness of the CO_2, NO_x, CO and O_2 curves in the central core region indicating an increase in the flame thickness. The decrease in CO level coupled with a slight increase in the CO_2 values caused by the addition of swirl indicated more efficient initial mixing in the core region of the flame, (Lilley (1977)). The existence of this well-stirred recirculation zone

has been demonstrated by Fricker and Leuckel (1976) and Mathur and Maccallum (1967) for example, and they also showed a reduction in the reaction volumes as indicated by the corresponding velocity profiles, (Figs. (5.6)(a) and (5.10)(a)). For the L.C.V. gas flames under similar furnace settings, (Figs. (5.14)(b) and (5.20)(b)), the concentration of all the species showed flat profiles in the outer recirculation zone up to the furnace wall, (100 mm $<$ R $<$ 220 mm). This indicates the presence of only hot reaction products in these regions. Similar effects were noted for both the 20% and 30% excess air situations when swirl was imparted to the secondary air, (Figs. (5.15) and (5.21) and Figs.(5.16) and (5.22)).

Using preheated air, flatter concentration profiles were recorded for both natural and L.C.V. gas flames with the addition of swirl, (Figs. (5.17) and (5.23)). This effect was more pronounced in the L.C.V. gas flames particularly in the outer zone regions, (R $>$ 100 mm). Again the individual species concentration were dependent on the EAF and the CV of the fuel used. In cases when the EAF and CV were similar, it was still difficult to discern differences in concentration values in L.C.V. gas flames due to swirl. The UHC measurement was the most difficult as a small fluctuation in the natural gas supply resulted in a massive jump in its concentration level. Similar effects as described above were noticed for the 20% and 30% excess air cases with preheat, (Figs. (5.18) and (5.24) and Figs. (5.19) and (5.25)).

5.5.3 Effects of Preheating the Secondary Air

Preheating the secondary air supplied to the combustor caused a radial

shift in the location of maximum temperature for the natural gas firing situation without any swirl, (Figs. (5.1)(i), (5.2)(i)(a) and (5.3)(i)(a)). For the zero preheat case, (Fig.(5.1)(i)), the maximum temperature was located on the centre line; this was shifted to about R = 40 mm for 200°C preheat, (Fig.(5.2)(i)(a)) and to about R = 60 mm for a preheat of 300°C, (Fig.(5.3)(i)(a)). The value of this maximum temperature was approximately the same for all the three cases, i.e. about 1650°C for the 10% excess air. This indicated an elongation of the flame further substantiated by the corresponding velocity profiles as shown in Figs (5.6) and (5.8); this applied to all the three excess air level investigated. So there appeared to be an increase in flow velocities with increase in the temperature of the secondary air for the above mentioned conditions.

For the L.C.V. gas flames with zero swirl, the maximum temperature level was always located at R $\simeq$ 50 mm regardless of the temperature of the secondary air supplied or the CV of the fuel used, (Figs. (5.1)(ii), (5.2)(i)(b) and (5.3)(i)(b)). There was an increase in flow velocity with the introduction of preheat to the secondary air and this also applied for the 20% and 30% excess air situations, (Figs. (5.7) and (5.9)). With swirling flows, there was very little change on the temperature profiles resulting from preheating the secondary air for the natural gas flames, (Figs. (5.4)(i)(a) and (5.4)(ii)(a)). For the L.C.V. gas flames with the same CV input, e.g. Figs. (5.4)(i)(b) and (5.4)(ii)(b) for the 10% excess air case, there was a definite increase in the temperature level with the introduction of preheat. There did not appear to be much difference in the magnitude of the velocity inside the combustor with swirling flows, regardless of whether the air was

preheated or not and this applied for all three excess air levels investigated for both natural and L.C.V. gas flames, (Figs. (5.10) to (5.13)).

Comparing the concentration measurements for say the 20% exess air trial without swirl for the natural gas flames, (Figs. (5.15)(a) and (5.18)(a)), revealed a definite increase in the NO_x values with the addition of preheat. There was very little change in the CO, CO_2, O_2 and UHC levels. There was also an increase in the diameter of the central core as indicated by the shifting of the peaks and by the velocity profiles, (Figs. (5.6)(b) and (5.8)(b)), with the use of preheat. The L.C.V. gas flames measurements also showed the same tendency but cannot really be compared with each other as they had different CV and EAF, (Figs. (5.15)(b) and (5.18)(b)). With swirling flames, e.g. Figs. (5.22)(a) and (5.25)(a), at 30% excess air, there was again an increase in the NO_x concentration with all the other species remaining nearly unchanged when the secondary air supply was preheated. For the L.C.V. gas flames, (Figs. (5.22)(b) and (5.25)(b)), there was a large reduction in the UHC concentration with the addition of preheat. There was also a small decrease in the CO values but the other species remained nearly constant. Too much emphasis cannot be put on this last finding as the CV and EAF were not the same for the two cases, but a slight improvement in the combustion quality can be discerned. For the 10% and 20% excess air situations, very similar results were obtained.

5.5.4 Degrees of Burnout Measurements

In order to quantify the combustion efficiency of the system using both natural and L.C.V. gas flames, burnout rate values were calculated at

both the sampling point (X/D = 0.445) and the exhaust. The following expression proposed by Eickhoff and Leuckel (1984) was used to determine the rate of burnout.

$$b(x) = 1 - \left[2\pi \int_0^{\infty} \rho u \sum c_i h_i \, y dy / \dot{M}_o h_o\right]$$

where

h_i and h_o are the lower calorific values of the partially burnt or unburnt fuel components in the gas sample and that of the fuel mixture supplied.

c_i is the measured unburnt and partially burnt mass fraction

$\dot{M}_o$ is the mass flow rate of the fuel supplied

ρ and u are the local density and velocity respectively

and y is the radial distance from the centre of the furnace.

In this case, the unburnt component was CH_4 and the partially burnt one was CO which were both obtained from the inflame concentration measurements. Concentration and temperature measurements were also obtained, for the various operating conditions used, for both natural and L.C.V. gas flames at the exhaust to calculate the degree of burnout at the exit. The degree of burnout was calculated from the above equation by a microprocessor using the combustion data collected. The appropriate calculations are shown in Appendix (B). Table (5.1) show the burnout rate values obtained at X/D = 0.445 and the values at the exhaust are shown in Table (5.2).

From the results, it is clear that the overall burnout rates (exhaust) for the natural gas flames were higher than the L.C.V. gas ones. Perhaps the surprising results were for the conditions when L.C.V. gas was fired with maximum swirl but without preheat which gave burnout rates of 91.17%, 84.66% and 84.99% for 10%, 20% and 30% excess air in turn. It should also be noted that for no swirl and 300°C preheat situation, the L.C.V. gas results at the sampling port (X/D = 0.445) showed very poor burnout rate of 91.8%, 64.8% and 17.9% for 10%, 20% and 30% excess air. The low value of burnout at 30% excess air may be caused by flame lift-off. These values improved quite substantially to 99.44%, 97.77% and 92.75% by the time the flow reached the exhaust section. This proved that considerable reaction was still taking place along the length of the combustion chamber beyond the sampling port.

For the natural gas firing situations, the rates at which the combustion reactions proceeded were quite fast supporting the concept of premixed combustion, (Eickhoff et al. (1984)) while those for L.C.V. gases under certain operating conditions were fairly slow as shown when the burnout rates at X/D=0.445 are compared with those at the exhaust. One possible reason may be the amount of heat store in the quarl of the burner. As can be seen from Table (5.3), for natural gas firing cases the quarl temperature is very high all along its length for most of the operating conditions used. These same readings are fairly low for all the L.C.V. gas flames. So the initial release of energy within the quarl section is very important for good combustion efficiency to be achieved.

5.5.5 Stabilizing Mechanism

In order to understand what sort of mechanism was responsible for the flame blow-off, the combustion data were used on the extinction criterion described below. The blow-out criterion proposed here is similar to the one put forward by Broadwell, Dahm and Mungal (1984). It is all based on the extinction mechanism formulated by Peters and Williams (1982) and although strictly applicable only to turbulent free diffusion flames, it was nevertheless applied to the present confined turbulent flame data to determine if there was any agreement. It should therefore be noted that only the main reaction core portion is being treated here and the availability of velocity and temperature data for the different operating conditions are essential.

The proposal put forward by Broadwell, Dahm and Mungal suggests that blow-out will occur when the ratio of the local mixing time, t_d, to a characteristic chemical reaction time, t_c, is less than some critical value denoted by ξ. From work carried out by Dimotakis et al. (1983) and Dahm et al. (1984) it was suggested that

$$t_d \simeq (d/u)$$

where d and u are the local jet diameter and velocity respectively. This time scale is based on the large scale motions which control the mixing inside the furnace. The flame theories of Mallard and Le Chatelier and of Zeldovich, Frank-Kamenetskii and Semenov (from Glassman (1977)) showed that the flame speed is related to the diffusivity and a characteristic chemical time by the following expression

$$S \simeq (K/t_c)^{1/2}$$

where $K = k/\rho Cp$

k = thermal conductivity

Cp= specific heat at constant pressure

ρ = the local density

So, K/S^2 represents the characteristic chemical time t_c.

From the above expressions, the flame should blow-off when ε, as given by the equation below, reaches a critical value

$$\varepsilon = t_d/t_c.$$

The laminar flame speed S, for the fuel mixtures used was calculated from the following expression given by Chakravarty (1984) which was based on previous work done by Spalding (1956), Yumlu (1967, 1968) and Scholte and Vaags (1959)

$$S^2_{mix} = \{1 - \alpha_i\} \; S^2$$

where

$$\alpha_i = \frac{\text{mass of (additive + air) at a given mixture equivalence ratio}}{\text{mass of total mixture}}$$

and S is the laminar burning valocity of methane.

The above analysis was applied to the data collected in the furnace and the results are given in Table (5.4). Details of the calculations can be found in Appendix (B). It is clearly evident from these results that there is an excellent correlation between the data and the blow-off mechanism proposed. For most of the natural gas flames which were far from blow-off conditions, the ε values averaged 6.15. For the L.C.V.

gas flames which were very near to blow-off, the average value of $\mathcal{E}$ was 4.9. This compares very favourably with the value of 4.8 obtained by Broadwell, Dahm and Mungal (1984) on their turbulent diffusion flames. The value obtained using our data is a bit higher because the furnace was operated using fuel with a CV which was 3 MJ/kg above the values at which extinction occurred. Therefore it can be argued that the mechanism put forward by Peters and Williams can be considered as a feasible explanation for flame blow-off in confined turbulent flames provided only the central main reaction zone is considered using local measurements of temperature and velocity.

5.5.6 Relationship between Stability Limits and Combustion Measurements

Starting with the zero preheat and zero swirl trial, which gave the worst stability as shown in chapter 4, the temperature gradients in the region of 60 mm $<$ R $<$ 120 mm are quite steep, (Fig. (5.1)(ii)). This indicates the existence of a thin flame and high shear flow region which can result in the diffusional rate between the fine turbulence scales exceeding the reaction rate thus causing extinction. The corresponding velocity profiles, (Fig.(5.7)), also show quite high values of mean velocity in the core region, but the temperatures are also higher as shown in Fig. (5.1)(i), so the reaction rates were much faster than for the L.C.V. gas flames, thus preventing the diffusional rate from swamping the reaction rate which can cause extinction. The concentration measurements shown in Fig. (5.14)(b) to (5.16)(b) represent the conditions inside the furnace burning L.C.V. gas at the above mentioned conditions. There was an increase in the UHC and CO levels as the CV of the fuel was reduced and as conditions were very

close to the blow-off limits for all the three excess air levels, this can only mean that partial extinction is taking place. There is still plenty of oxygen present so the lack of oxidant cannot be the cause of this. The poor stability limits are reflected by the low EAF that were possible under these conditions. The values of ε given in Table (5.4) for these operating conditions provide good support for the above explanations.

Increasing the secondary air temperature allowed weaker fuel mixtures to be combusted, and these are reflected by the higher EAF used, (Fig.(5.2)(i)(b) and (5.3)(i)(b)). It is clear from these temperature profiles that there was a decrease in the steepness of the gradients with an increase in the secondary air preheat and this occurred for all the three excess air levels investigated. This indicates an increase in the flame thickness with preheat and comparison of the velocity profiles given in Figs. (5.8) and (5.9) show a decrease in the mean velocity but an increase in the central reaction core diameter when the CV of the fuel is reduced. Similar effects, as mentioned above are noted on the concentration measurements as the blow-off limits are approached. Therefore the same type of extinction mechanism was responsible for flames burning with preheated secondary air and this is substantiated by the values of ε shown in Table (5.4). So preheating the secondary air causes the flame thickness to increase thus permitting tolerance of a weaker fuel mixture than would be possible without any preheat.

The effects of using swirl without preheat on the stability of the flames are shown in Fig. (4.5) and it is evident that there was a definite improvement. Comparison of the temperature profiles,

(Fig.(5.5)(i)(b)), shows very similar effects, caused by the addition of preheat but the peak temperatures were lower. There was a large decrease in the core velocity, (Fig.(5.11)), when compared to the zero swirl situations. The increase in the concentration of UHC and CO was again noted with the decrease in CV of the fuel but there seems to have been a redistribution of the hot combustion products in the outer recirculation zone of the furnace and these are indicated by the flat profiles obtained. Increasing the excess air had very little effect on the above findings.

Using swirl together with preheat also resulted in good stability, (Fig.(4.9), especially at low swirl numbers. The temperature measurements showed very flat profiles for both natural and L.C.V. gas flames, (Figs. (5.2(ii) and (5.3)(ii)). The mean velocities were not very high especially in the core area and this applies for all the three excess air levels. The surprising fact is a sharp decrease in the UHC and CO concentrations under these conditions. This is translated into the good combustion efficiency values shown in Table (5.1). The reason is most probably the high temperature levels existing across the furnace under these operating conditions indicating good recirculation of the product of combustion thus maintaining good stability for the weaker fuel mixture used.

5.5.7 Closure

The combustion measurements were critically analysed for conditions which were close to blow-off. Burnout rates at the sampling port were generally high ($>95\%$) for natural gas but in some cases, for L.C.V. mixtures, were extremely low ($<20\%$) suggesting flame lift off; however

at the exhaust burnout was high in all cases showing that combustion was proceeding beyond the sampling port. A blow-off criterion based on the ratio of the mixing time to a chemical reaction one, denoted by ε, showed that for near-limit flames ε was consistantly close to 4.9; therefore flames with $\varepsilon > 4.9$ were stable. This establishes an important criterion for determination of stability in confined situations. The combustion measurements for the L.C.V. mixtures also showed the existence of thin flames for conditions without preheat and zero swirl. The thickness of the flame increases with swirl and preheat thus improving the stability limits. In most of the L.C.V. gas cases, high levels of CO and UHC were detected indicating that partial extinction was taking place prior to blow-off.

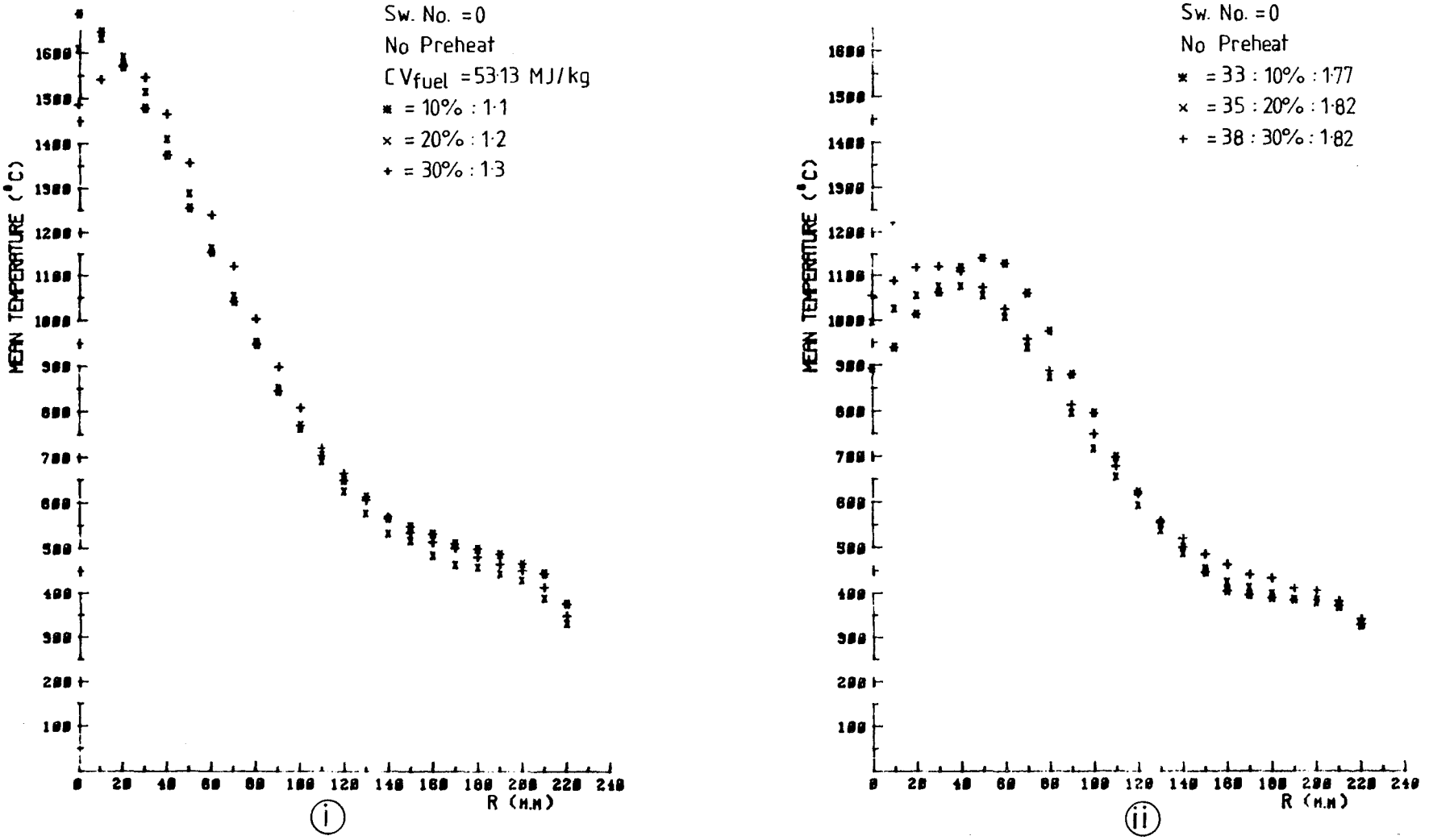

Fig.(5.1) Temperature Measurements

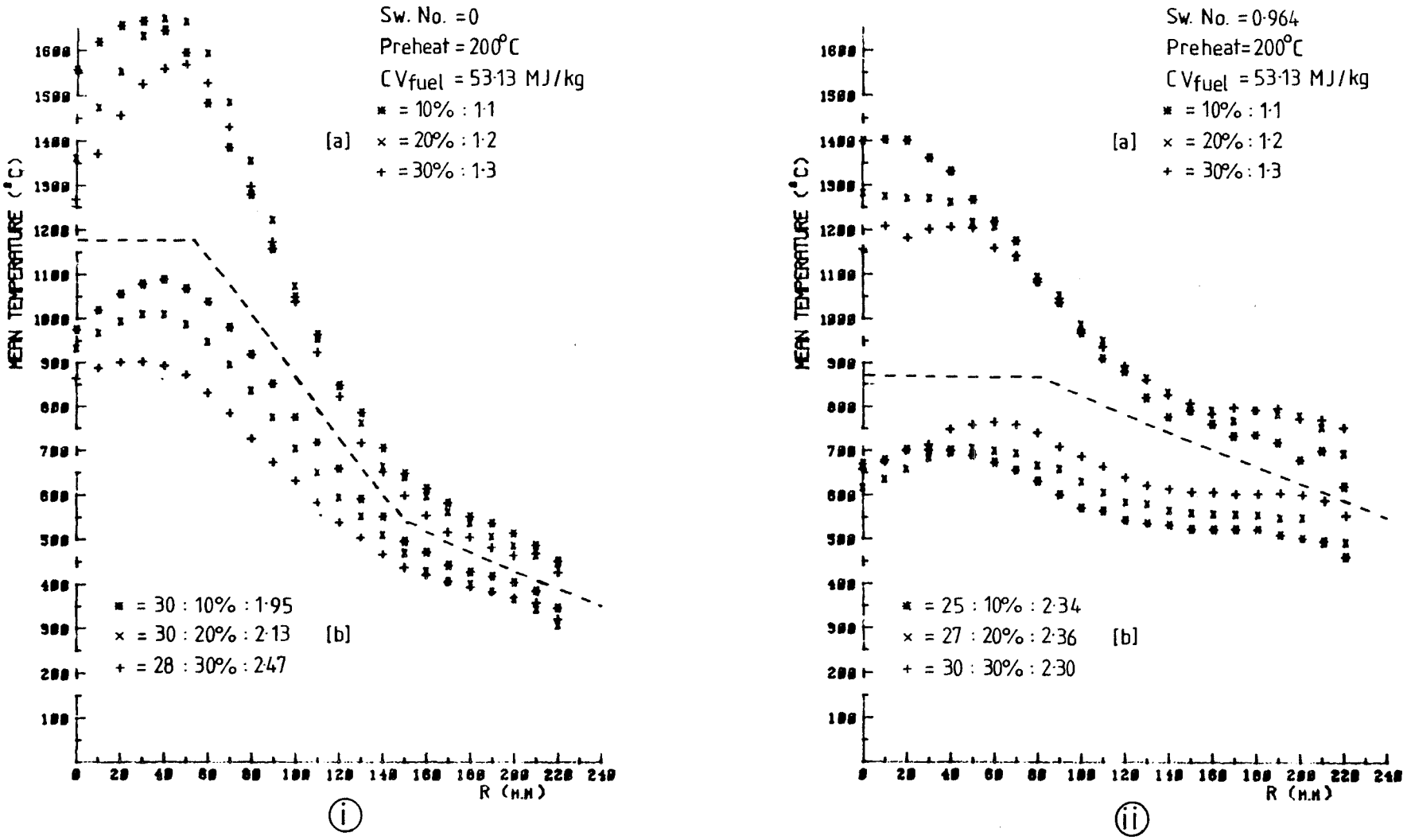

Fig.(5.2) Temperature Measurements

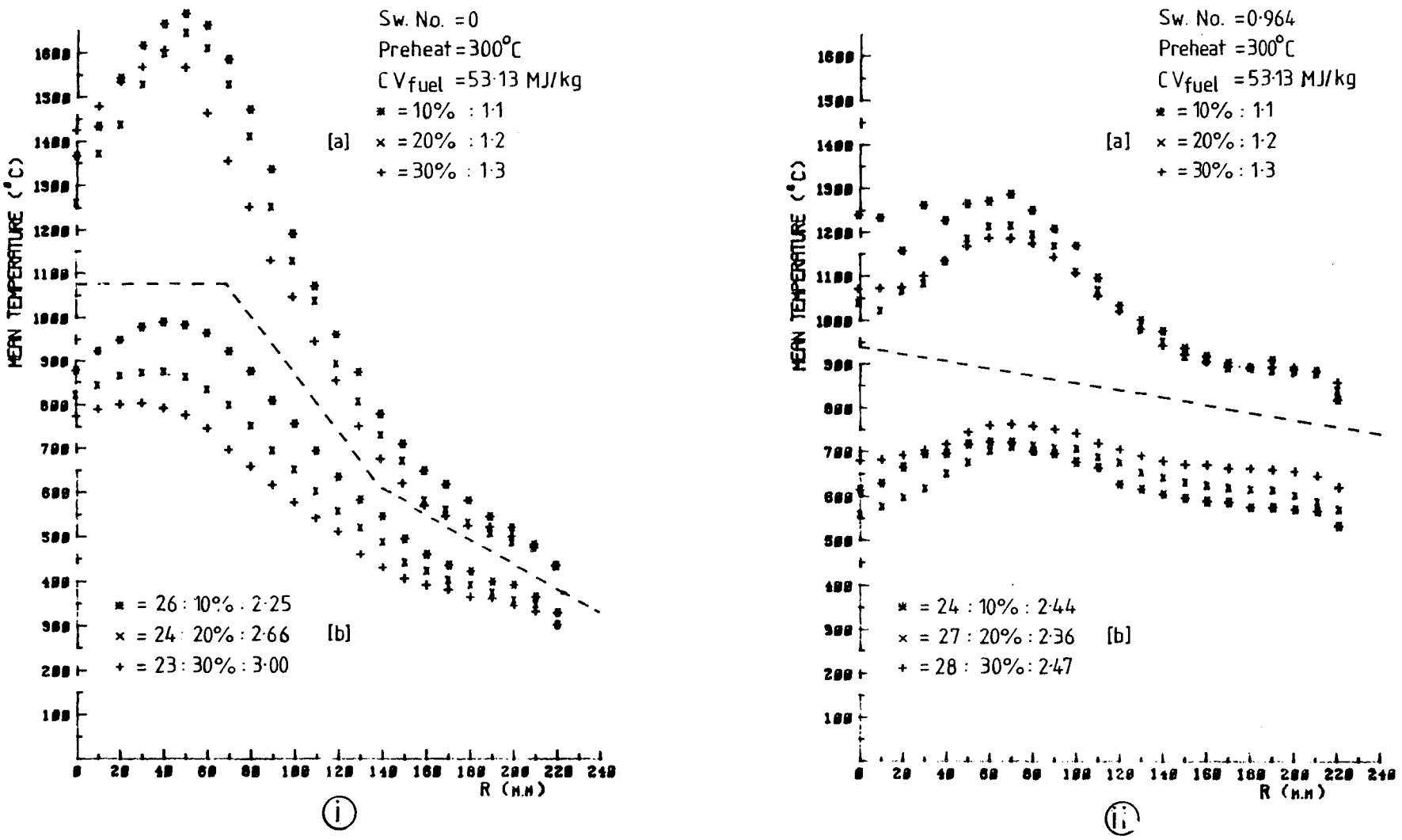

Fig.(5.3) Temperature Measurements

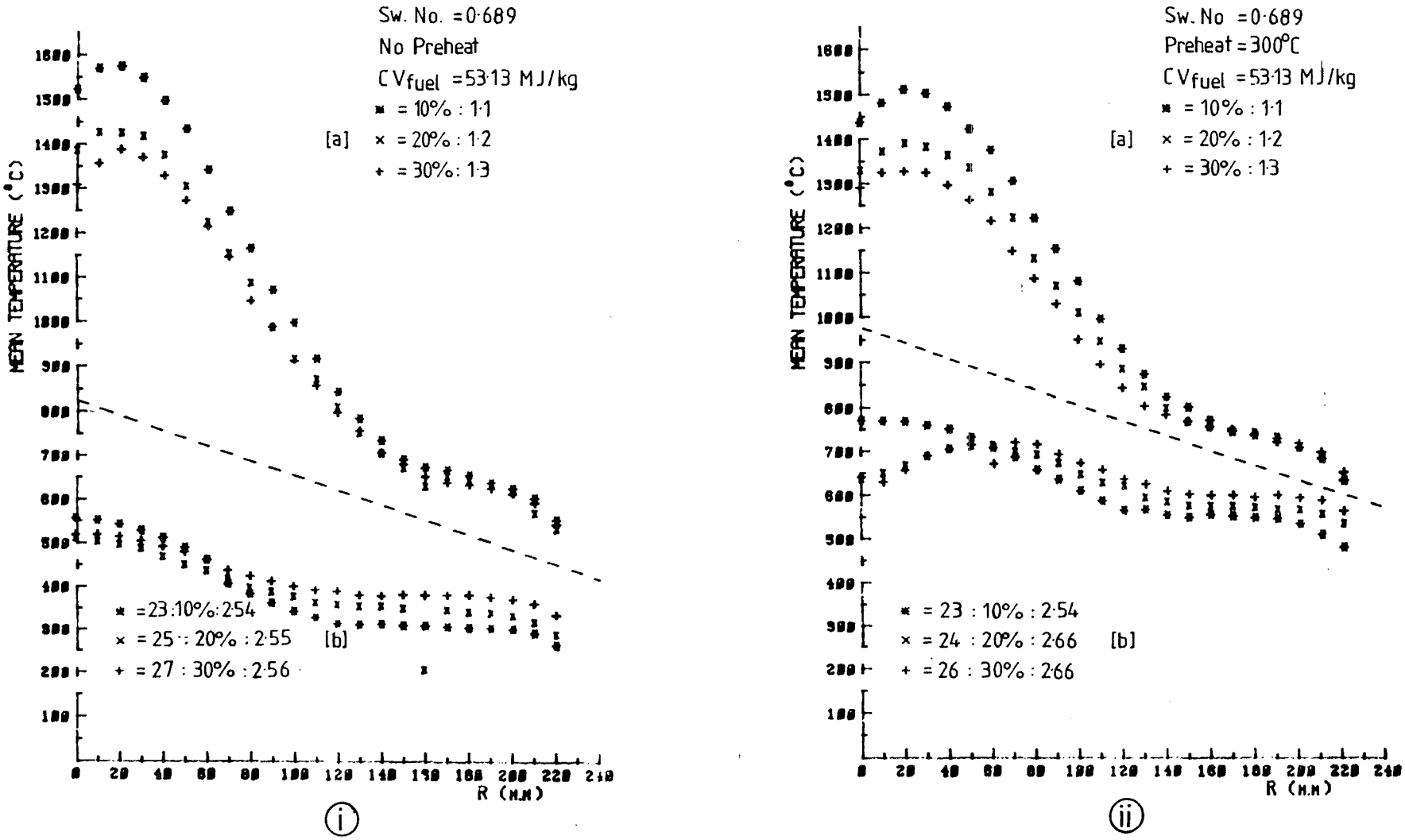

Fig.(5.4) Temperature Measurements

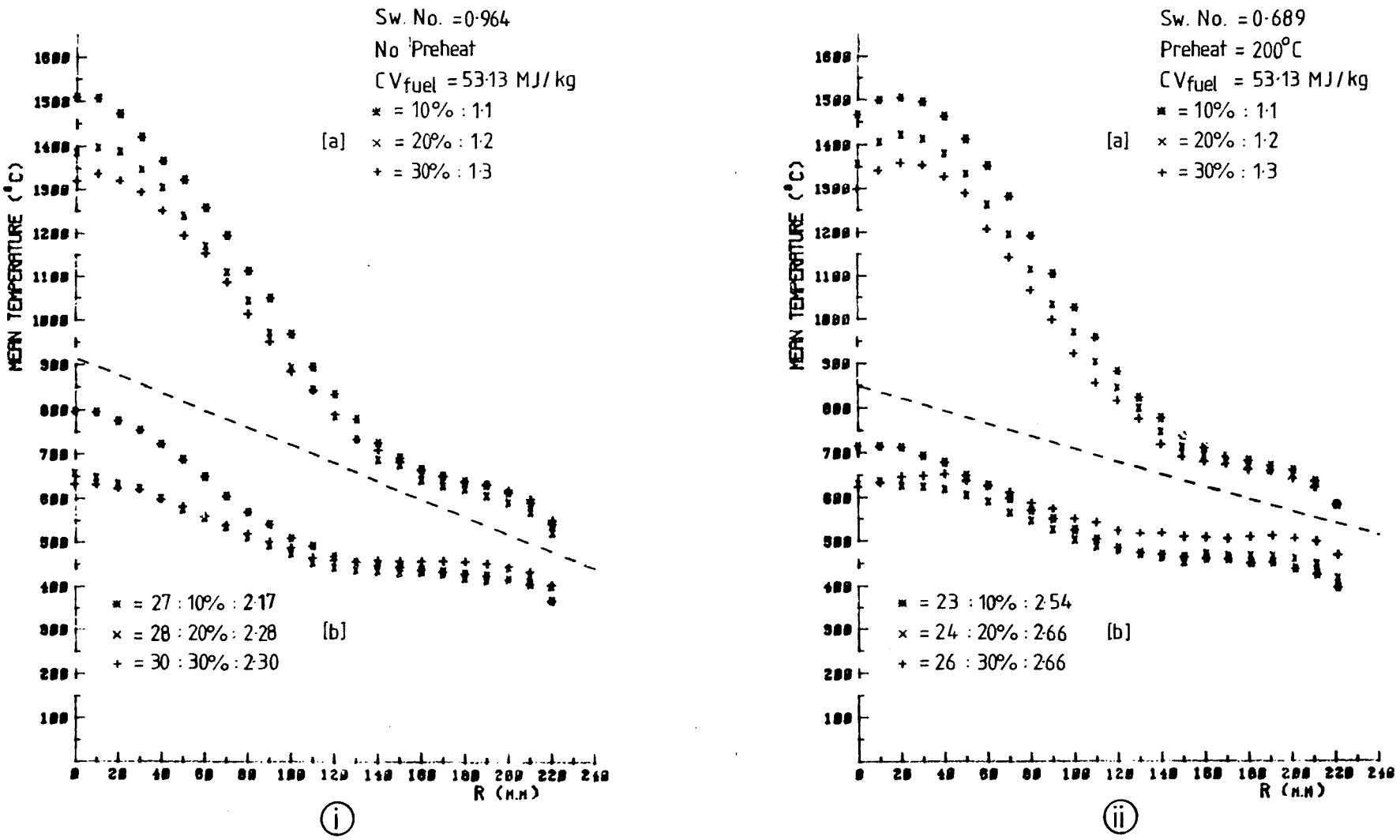

Fig.(5.5) Temperature Measurements

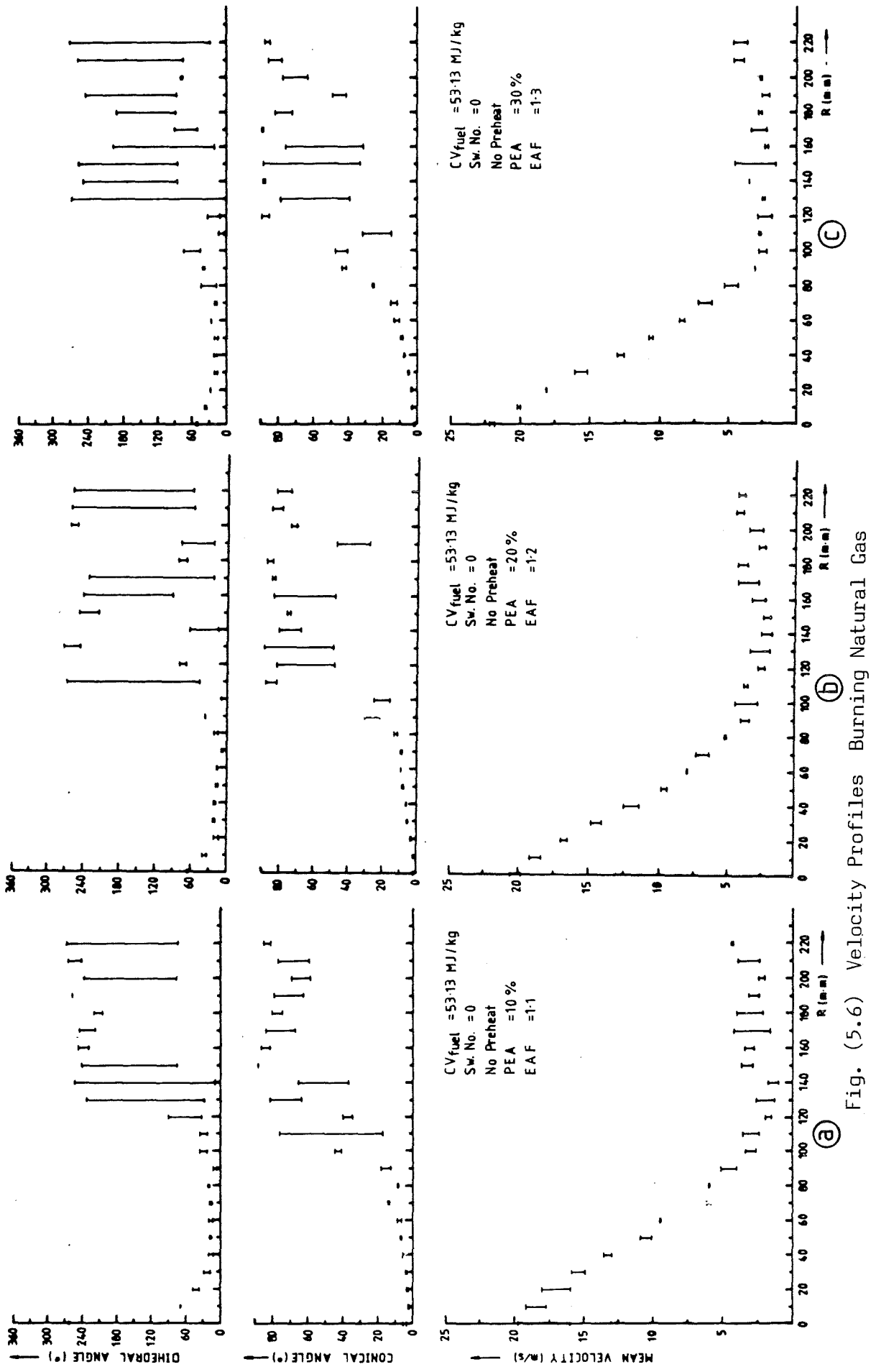

Fig. (5.6) Velocity Profiles Burning Natural Gas

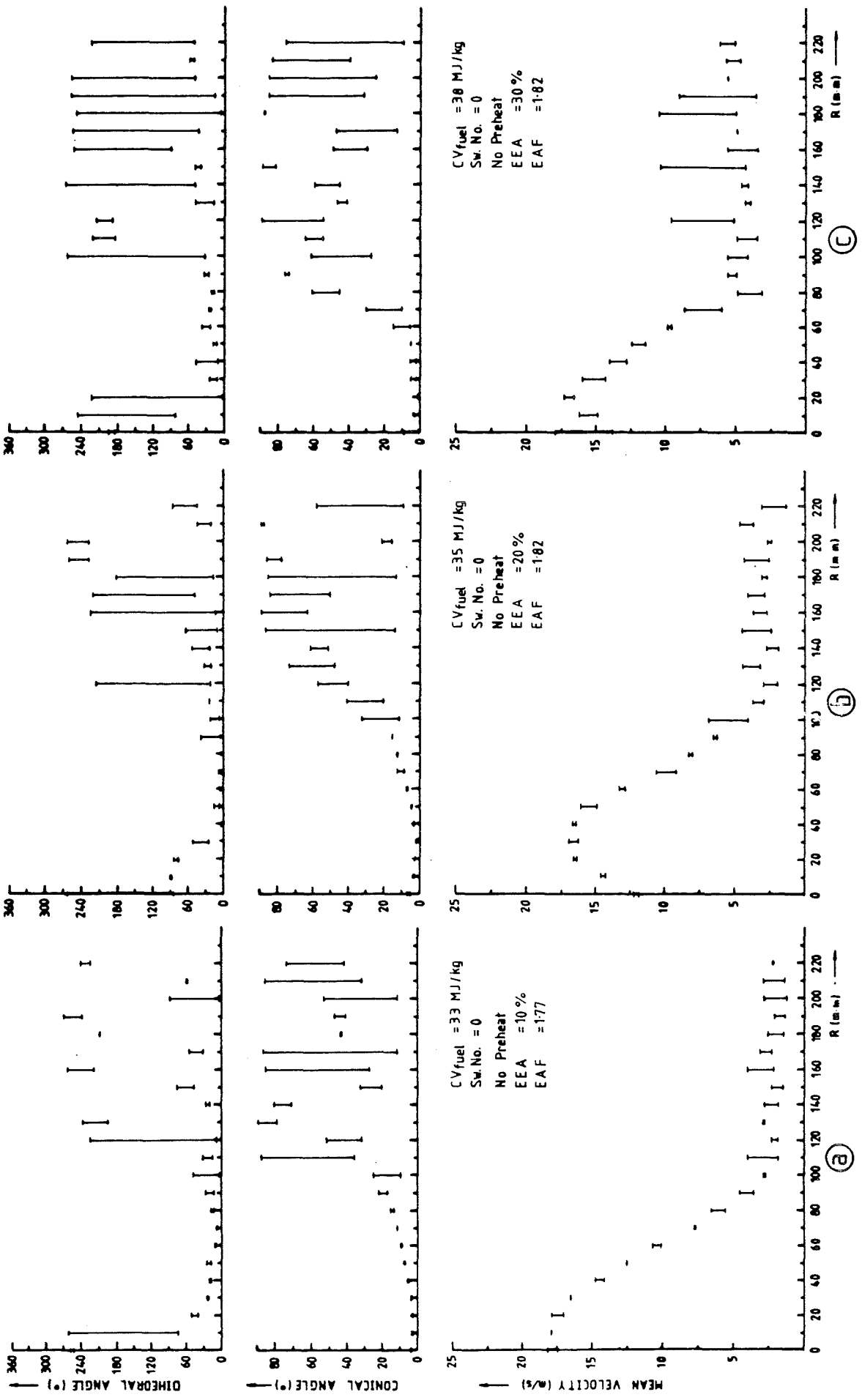

Fig.(5.7) Velocity Profiles Burning LVC Gas

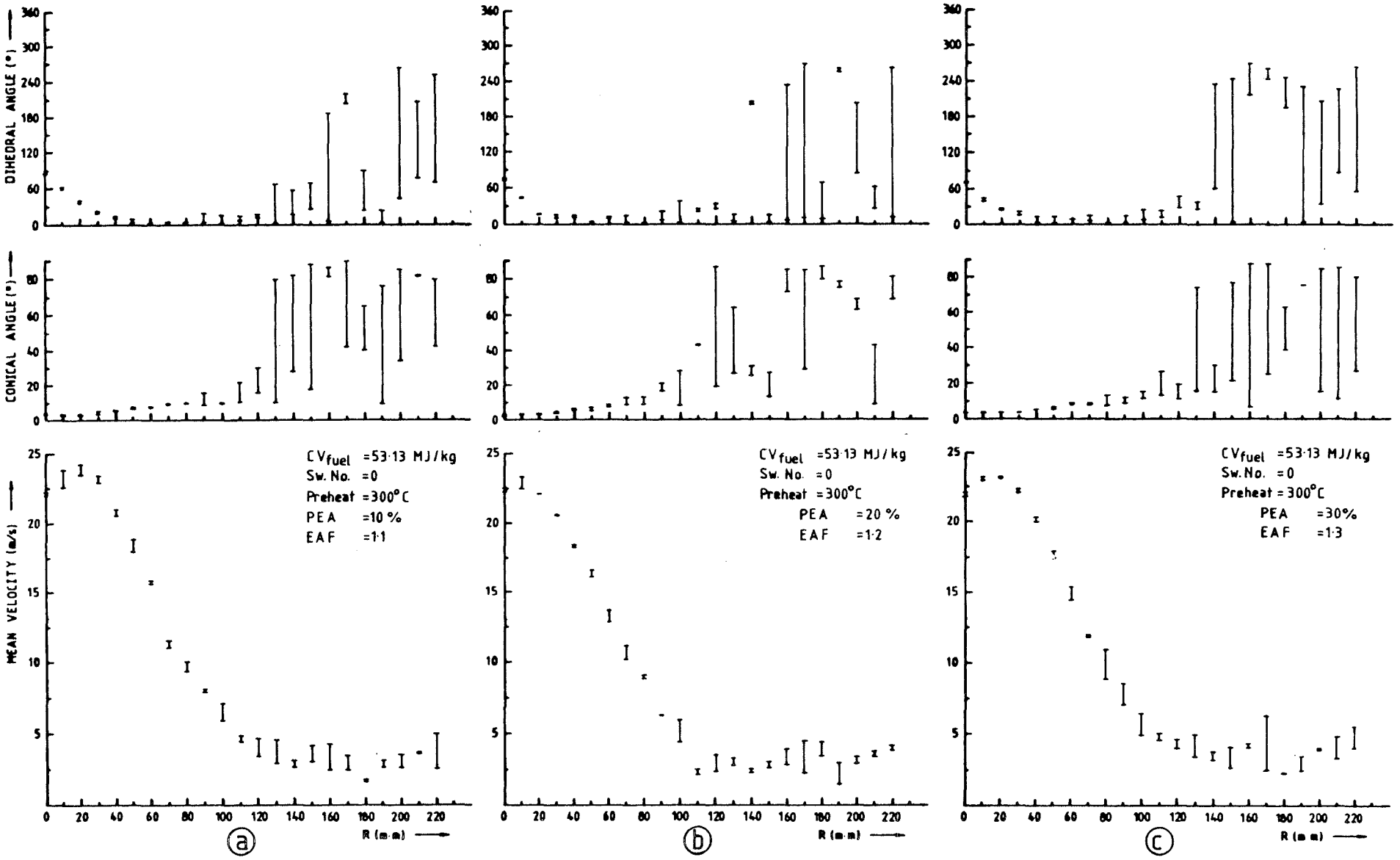

Fig.(5.8) Velocity Profiles Burning Natural Gas

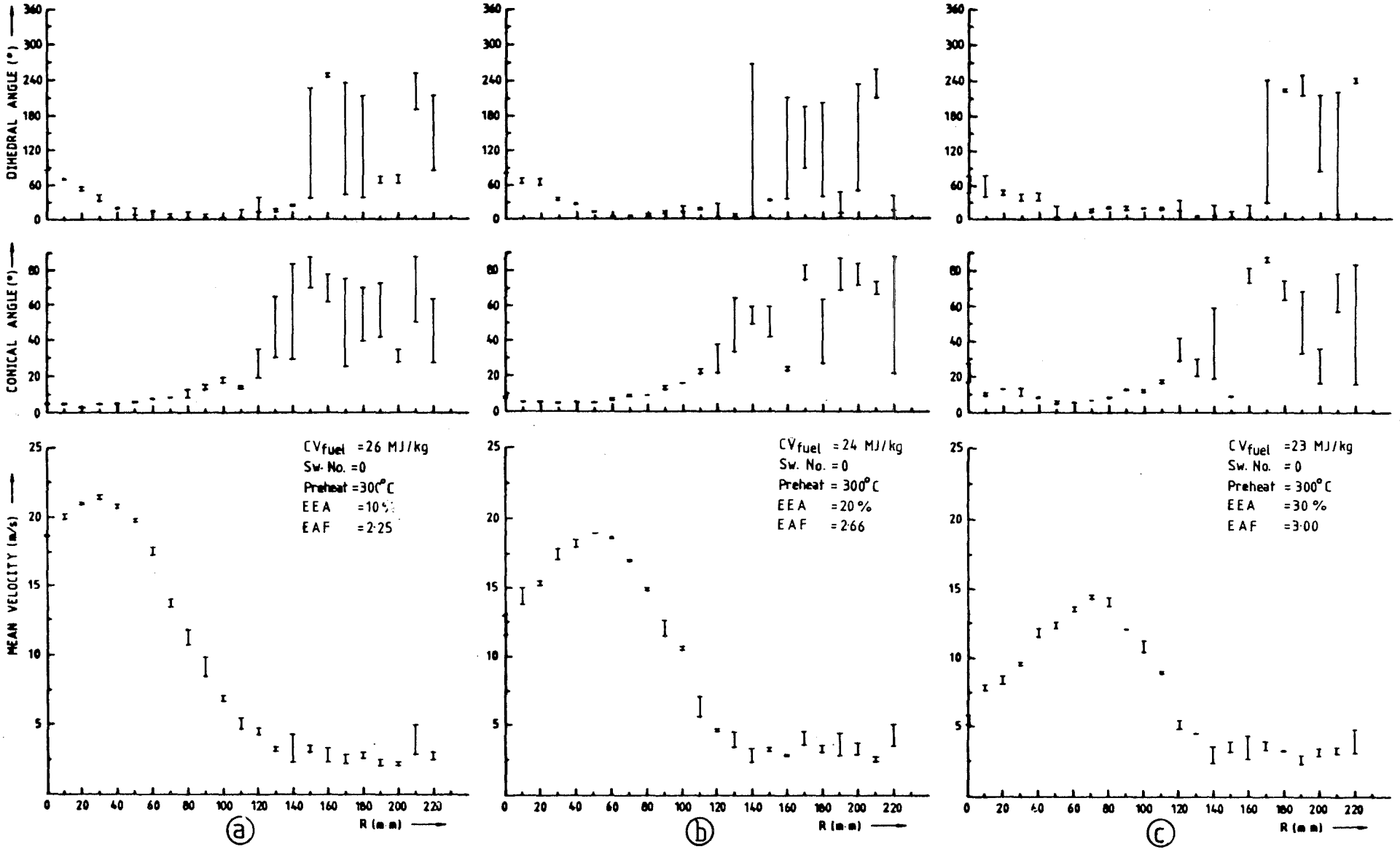

Fig.(5.9) Velocity Profiles Burning LCV Gas

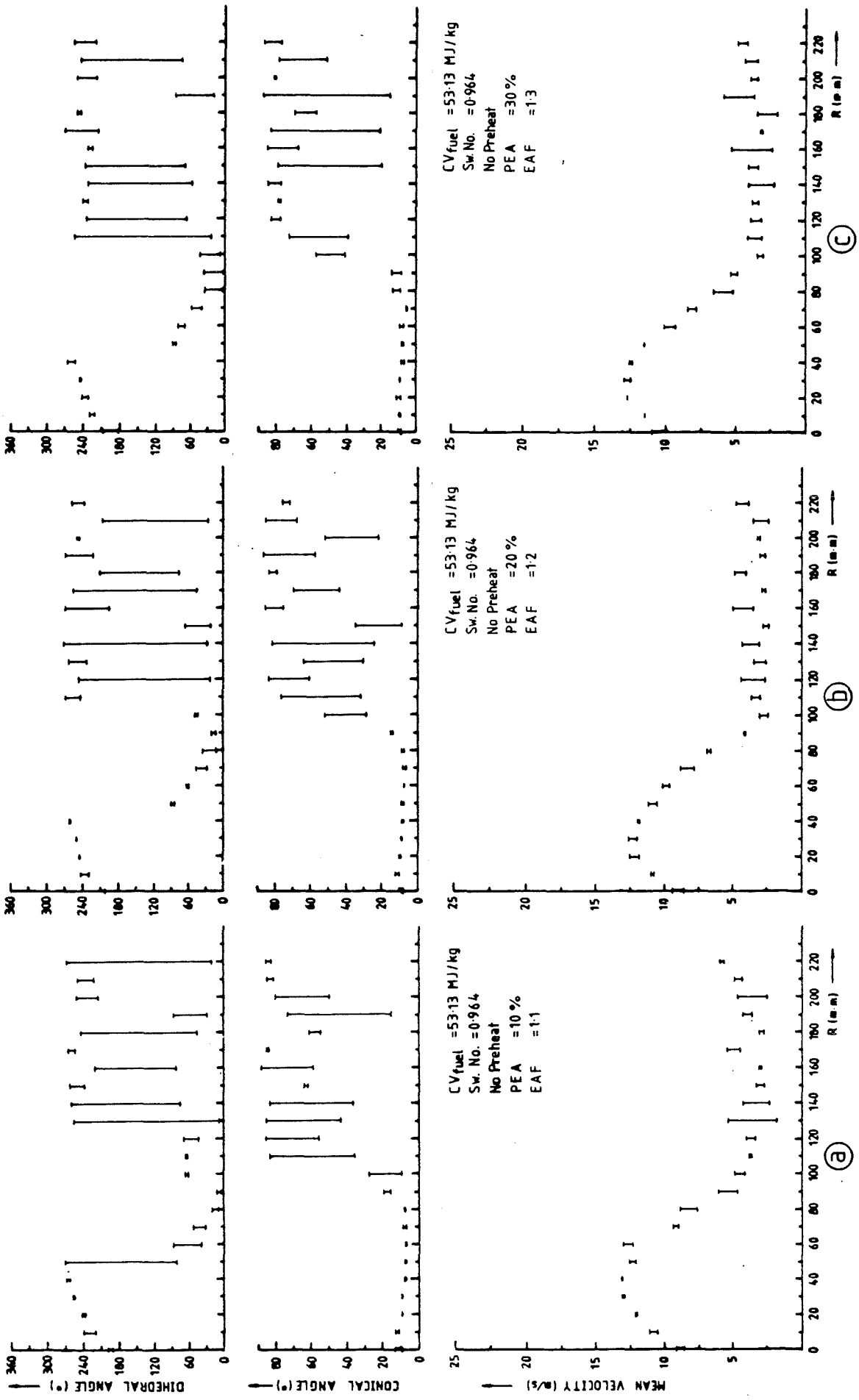

Fig.(5.10) Velocity Profiles Burning Natural Gas

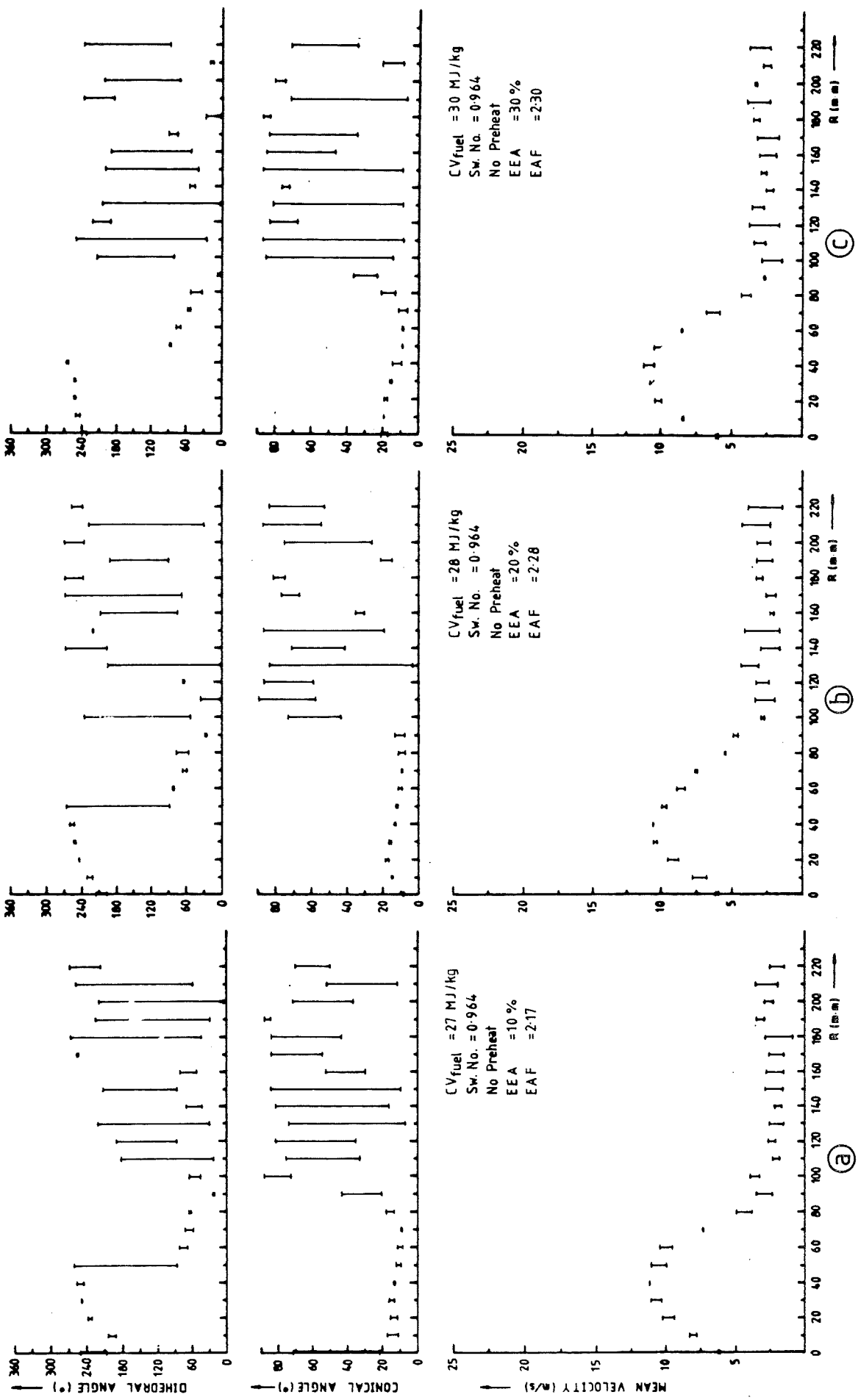

Fig.(5.11) Velocity Profiles Burning LCV Gas

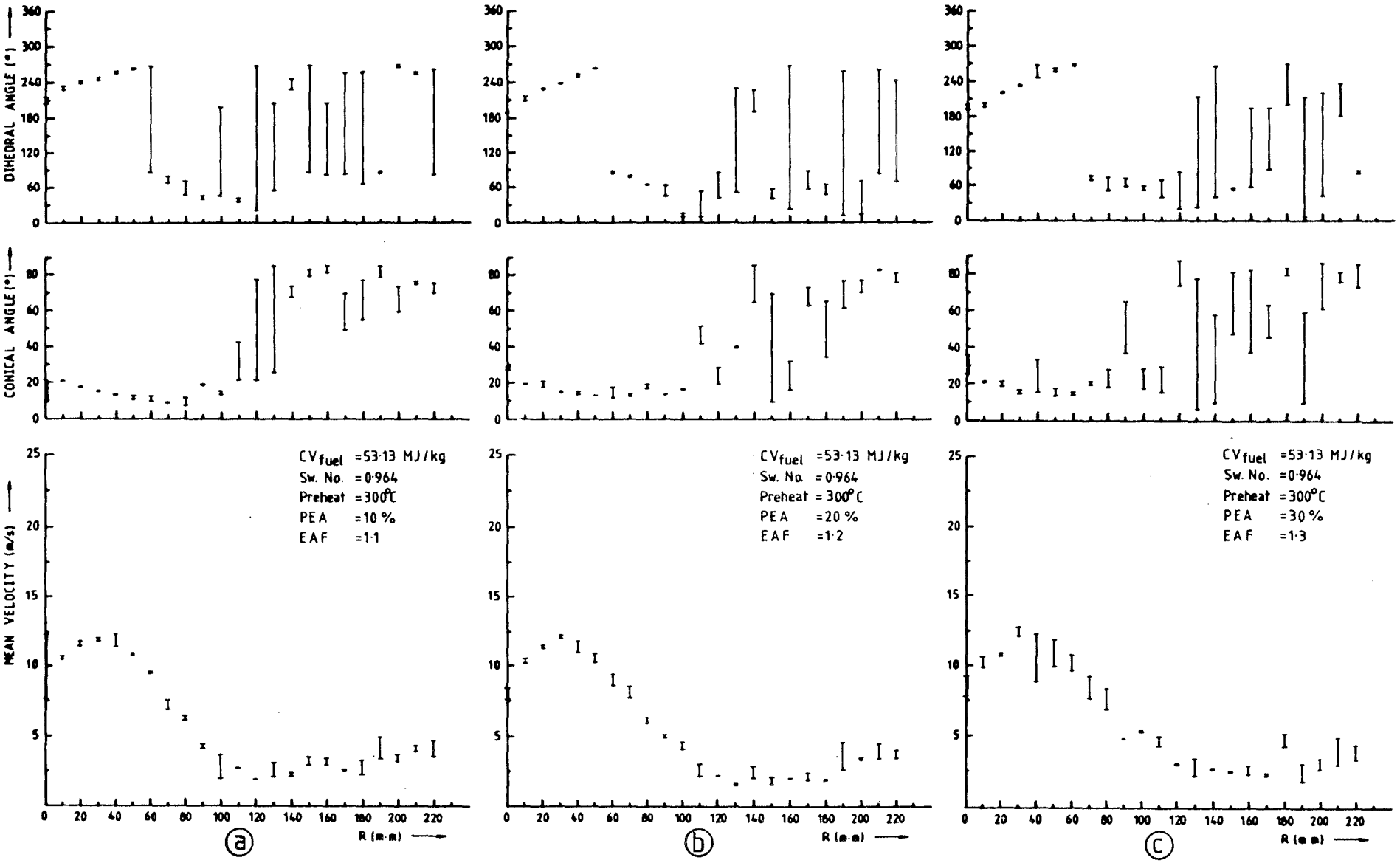

Fig.(5.12) Velocity Profiles Burning Natural Gas

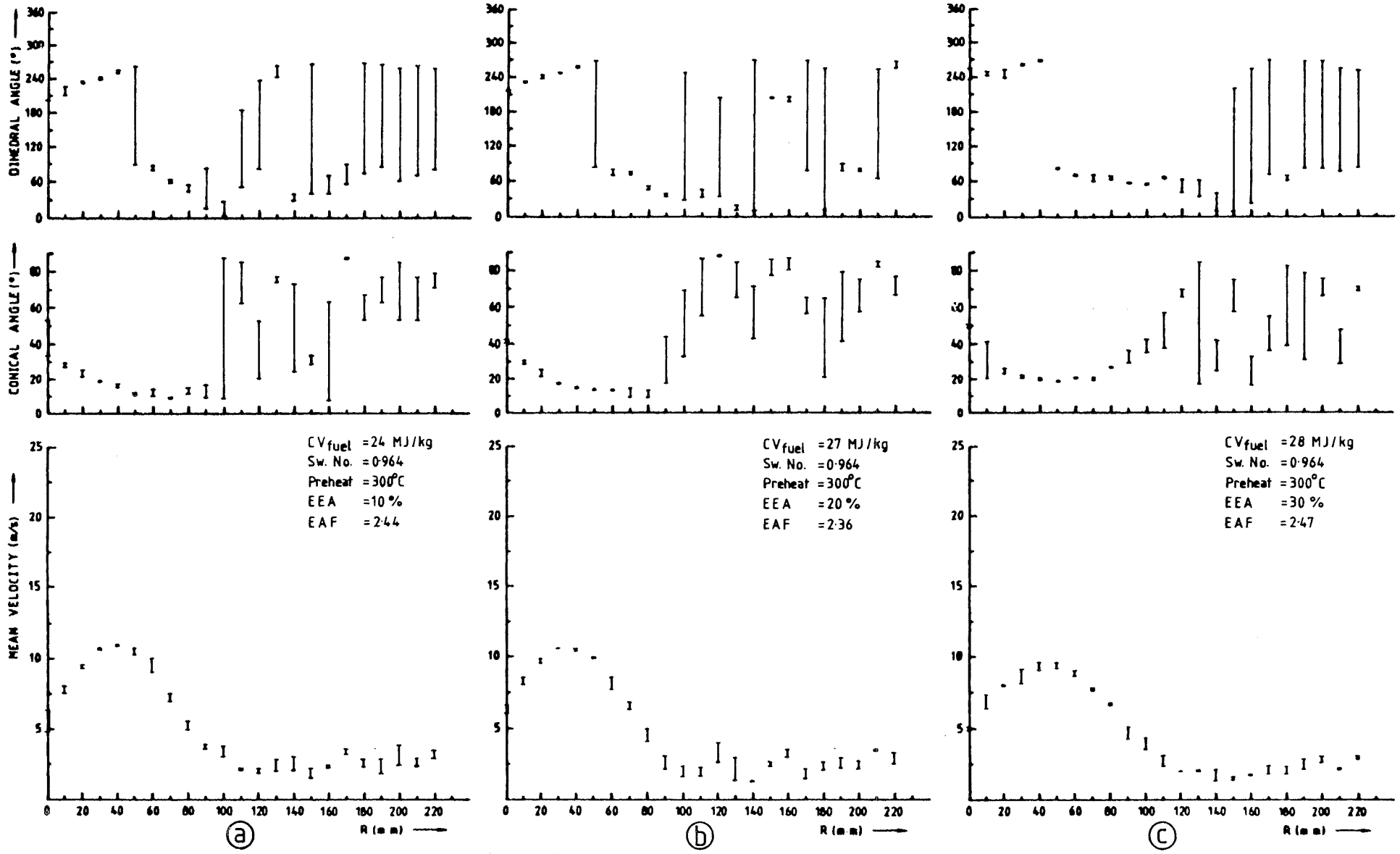

Fig.(5.13) Velocity Profiles Burning L.C.V. Gas

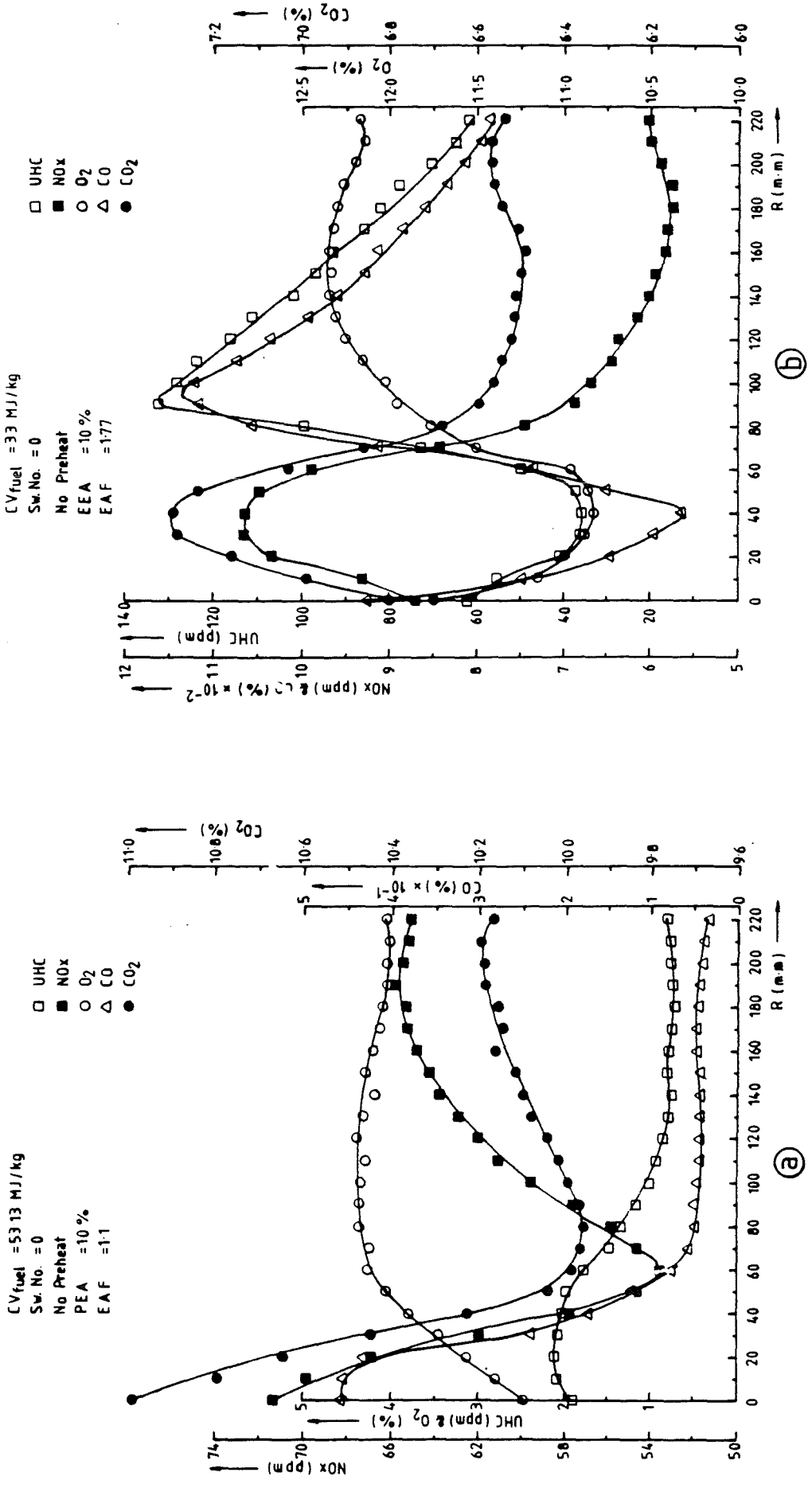

Fig.(5.14) Concentration Measurements

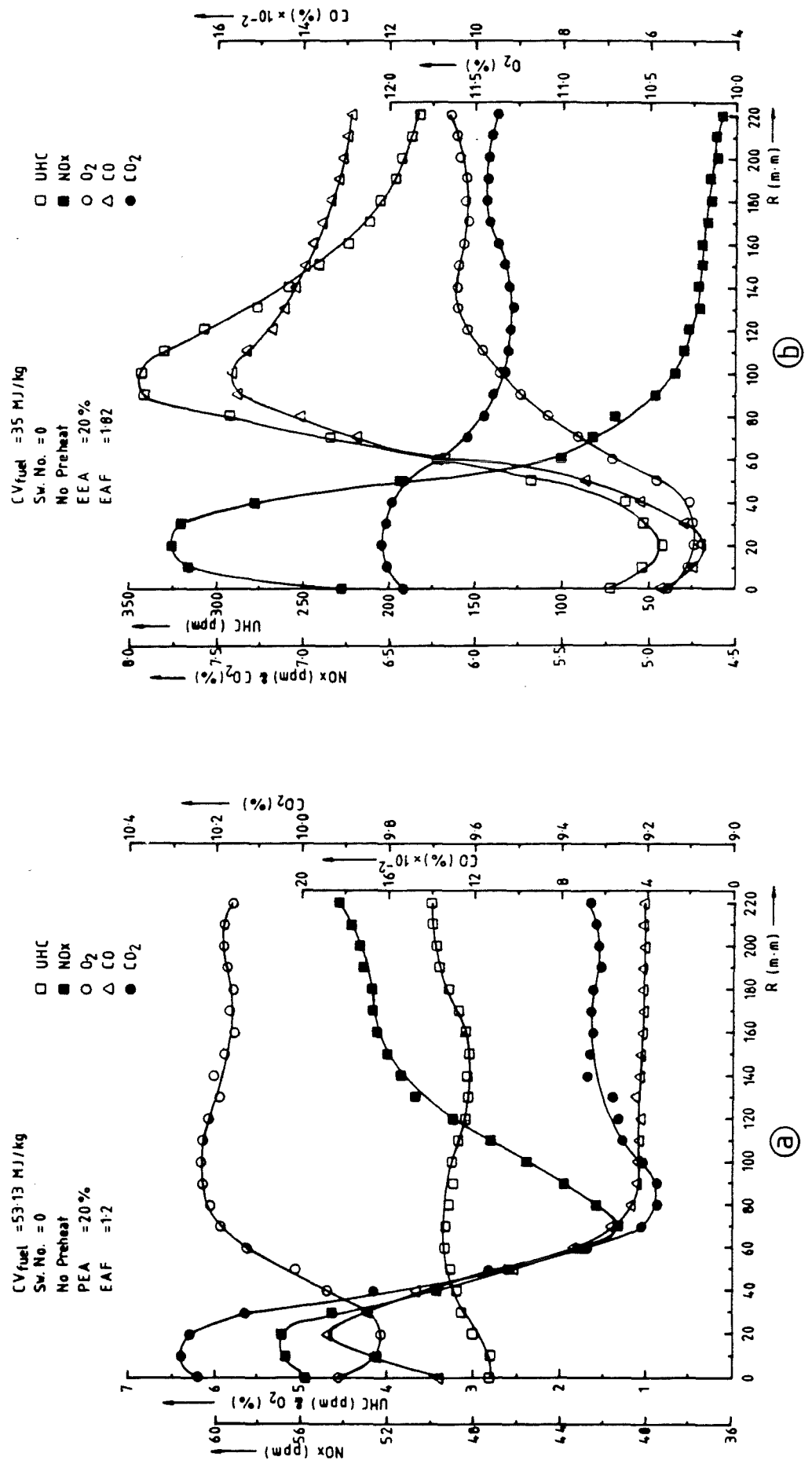

Fig.(5.15) Concentration Measurements

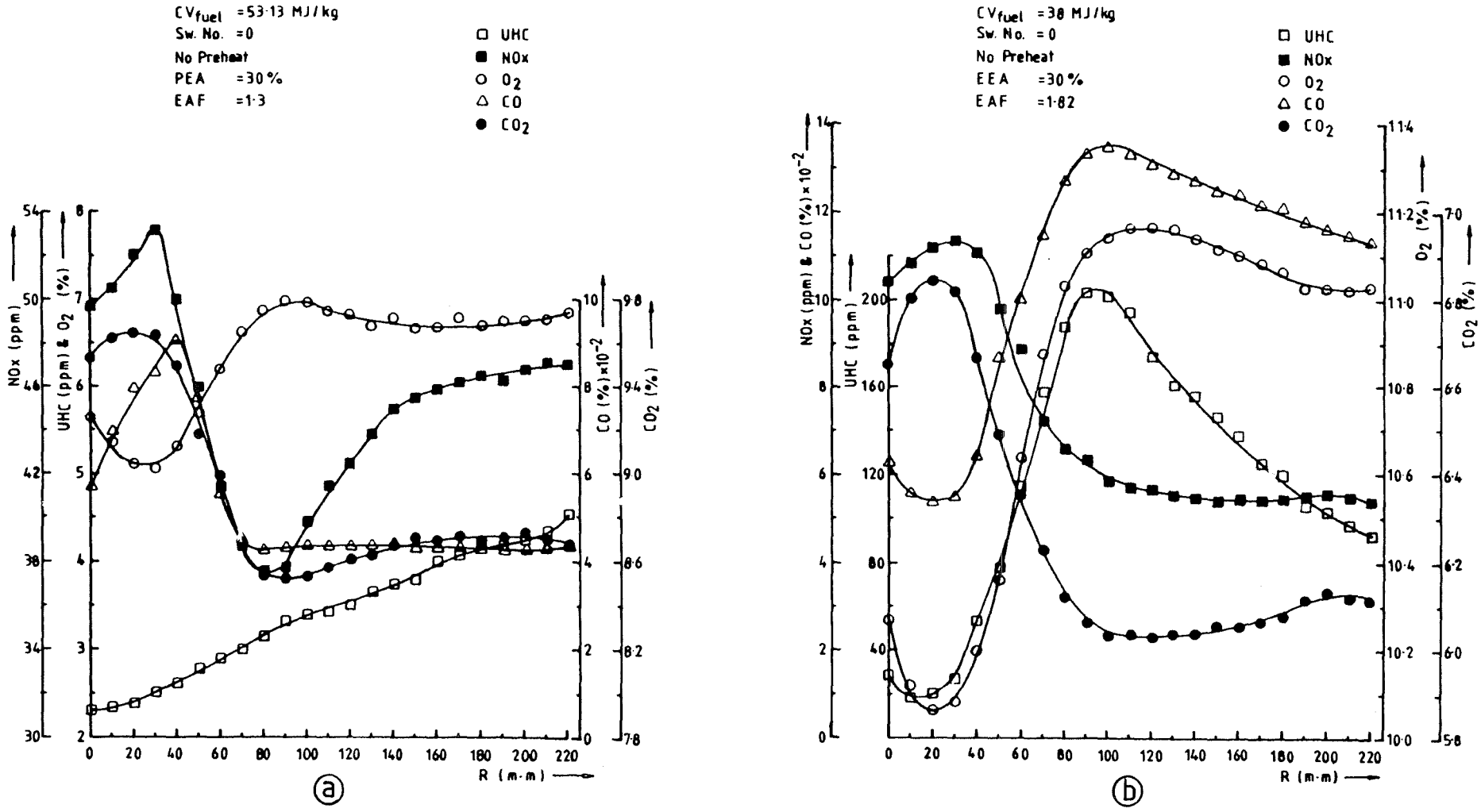

Fig.(5.16) Concentration Measurements

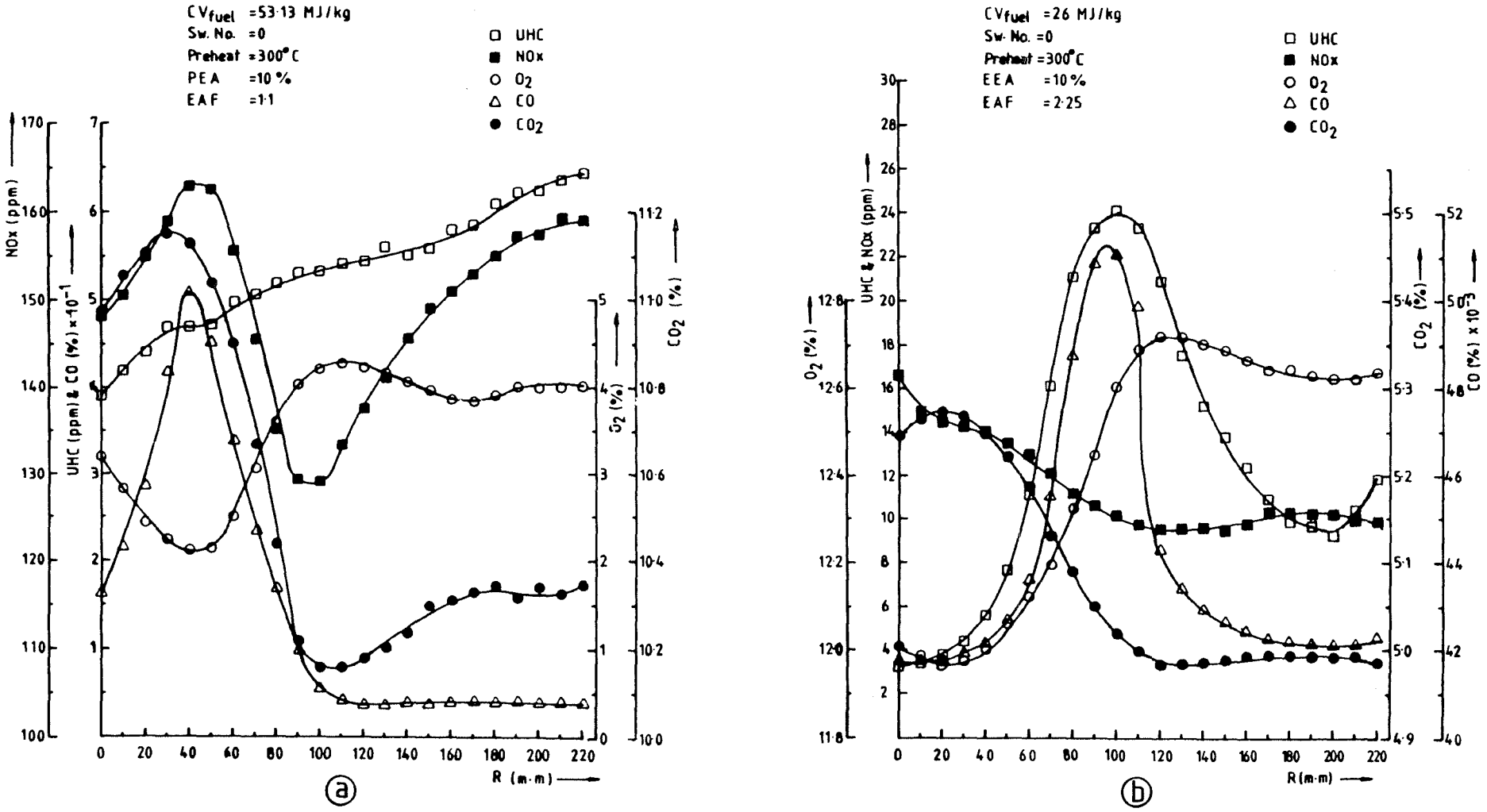

Fig.(5.17) Concentration Measurements

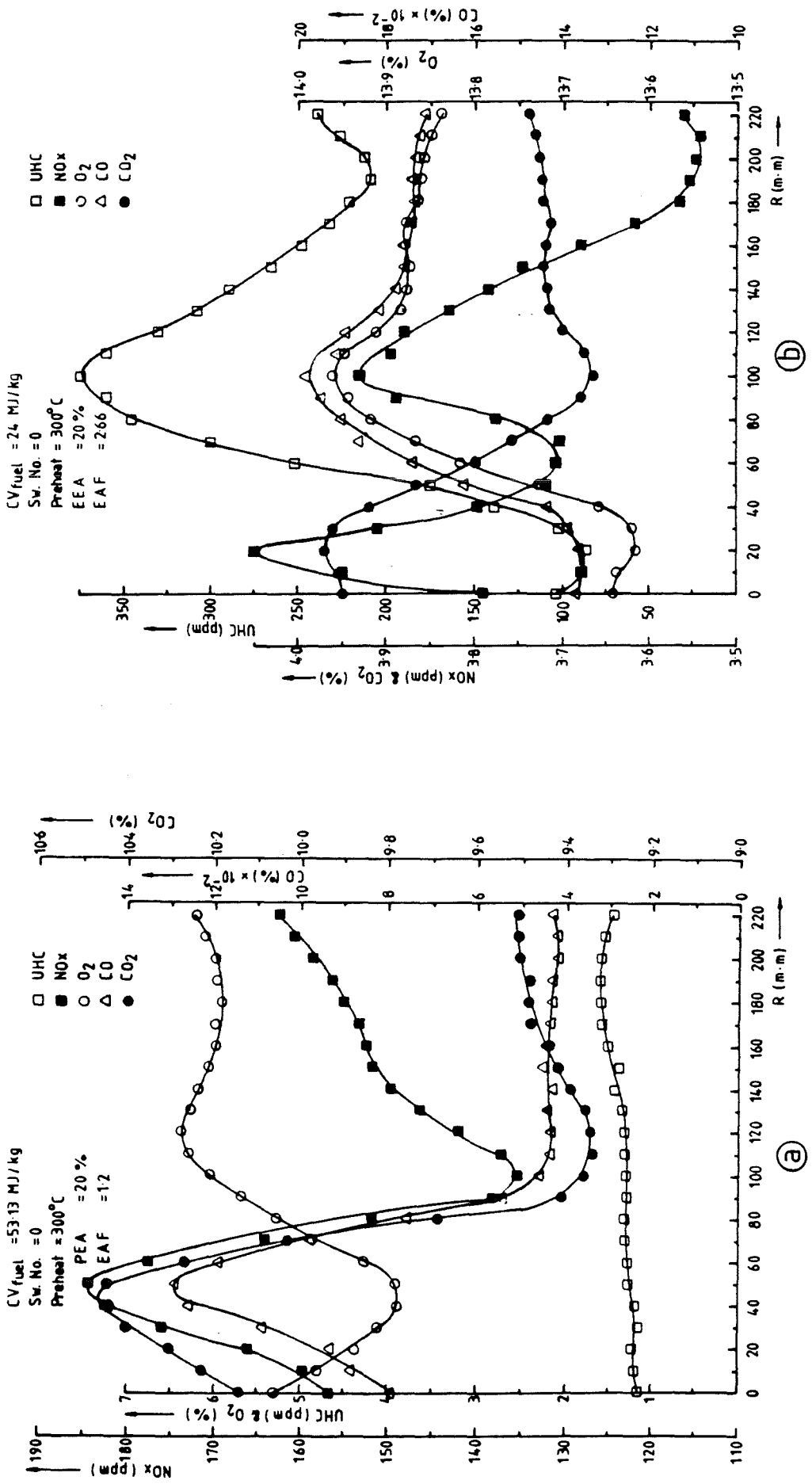

Fig.(5.18) Concentration Measurements

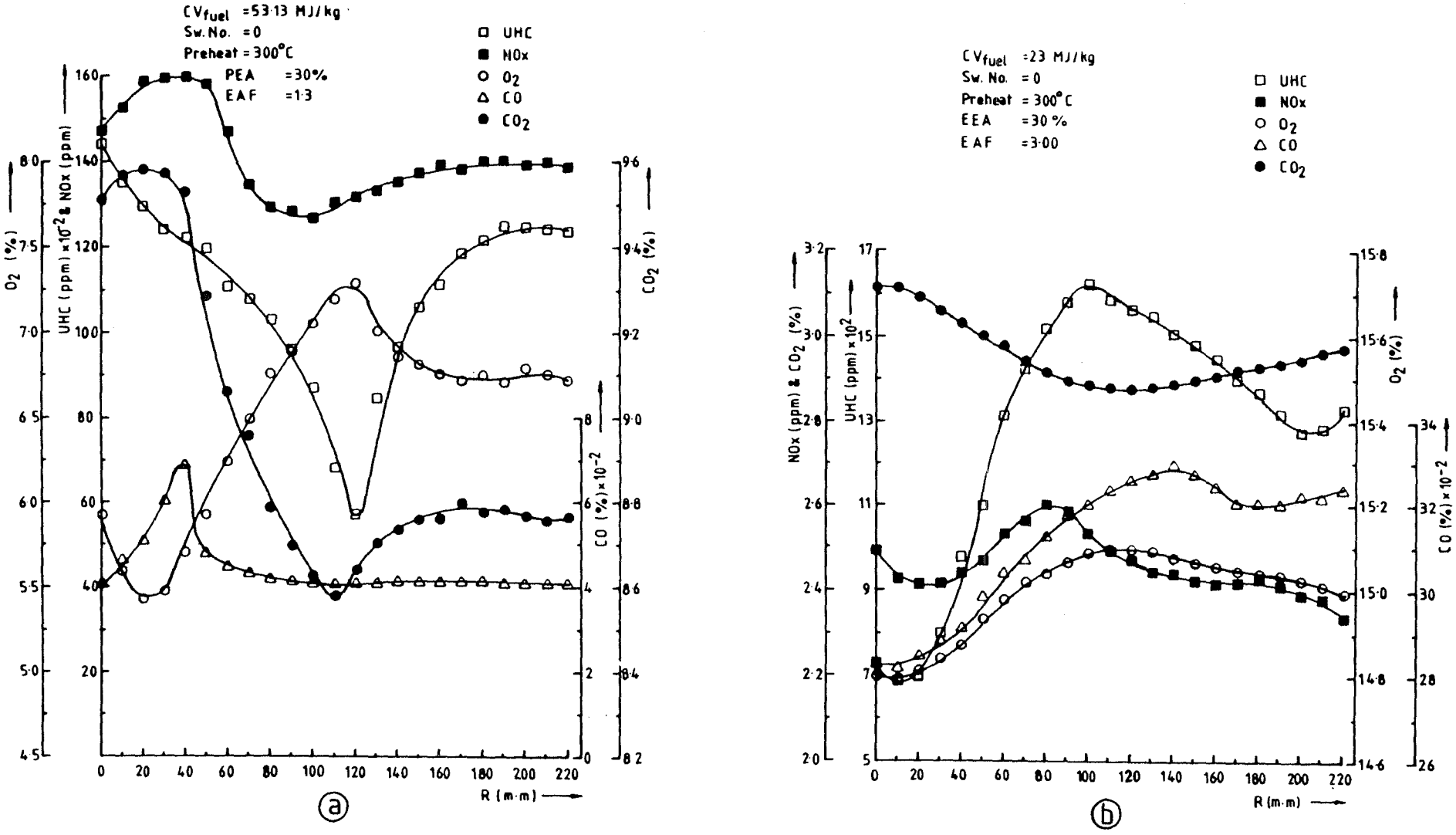

Fig.(5.19) Concentration Measurements

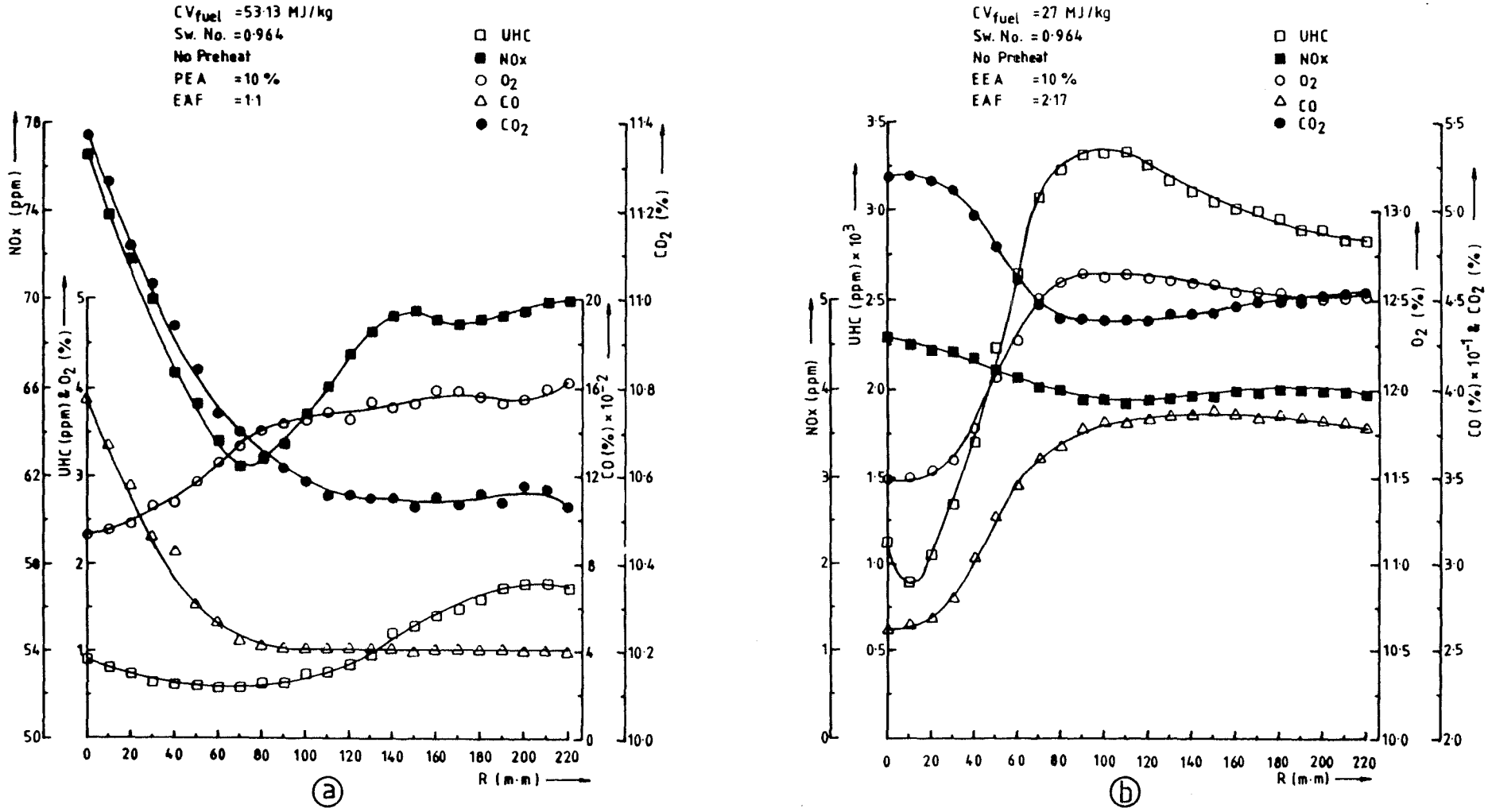

Fig.(5.20) Concentration Measurements

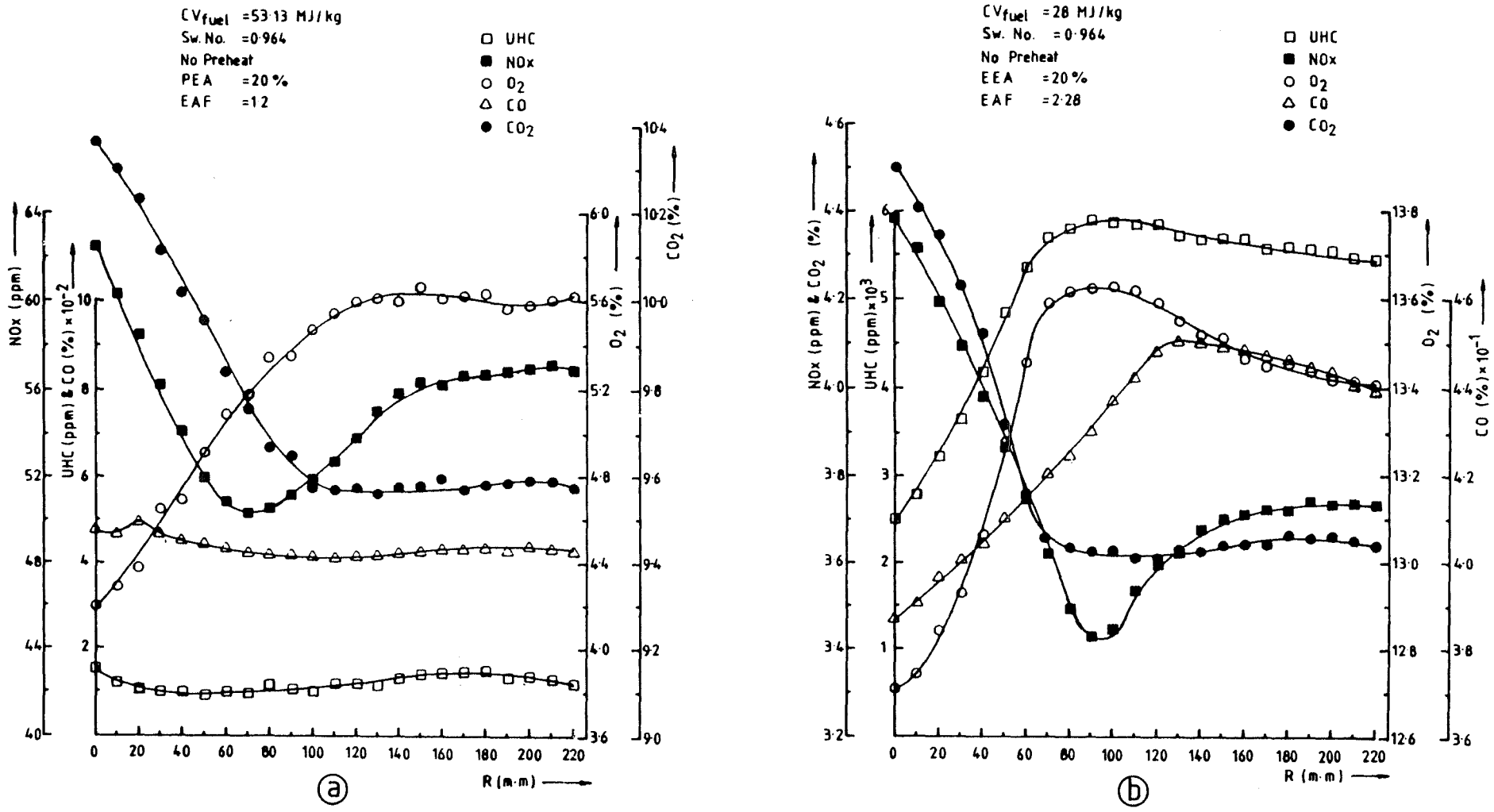

Fig.(5.21) Concentration Measurements

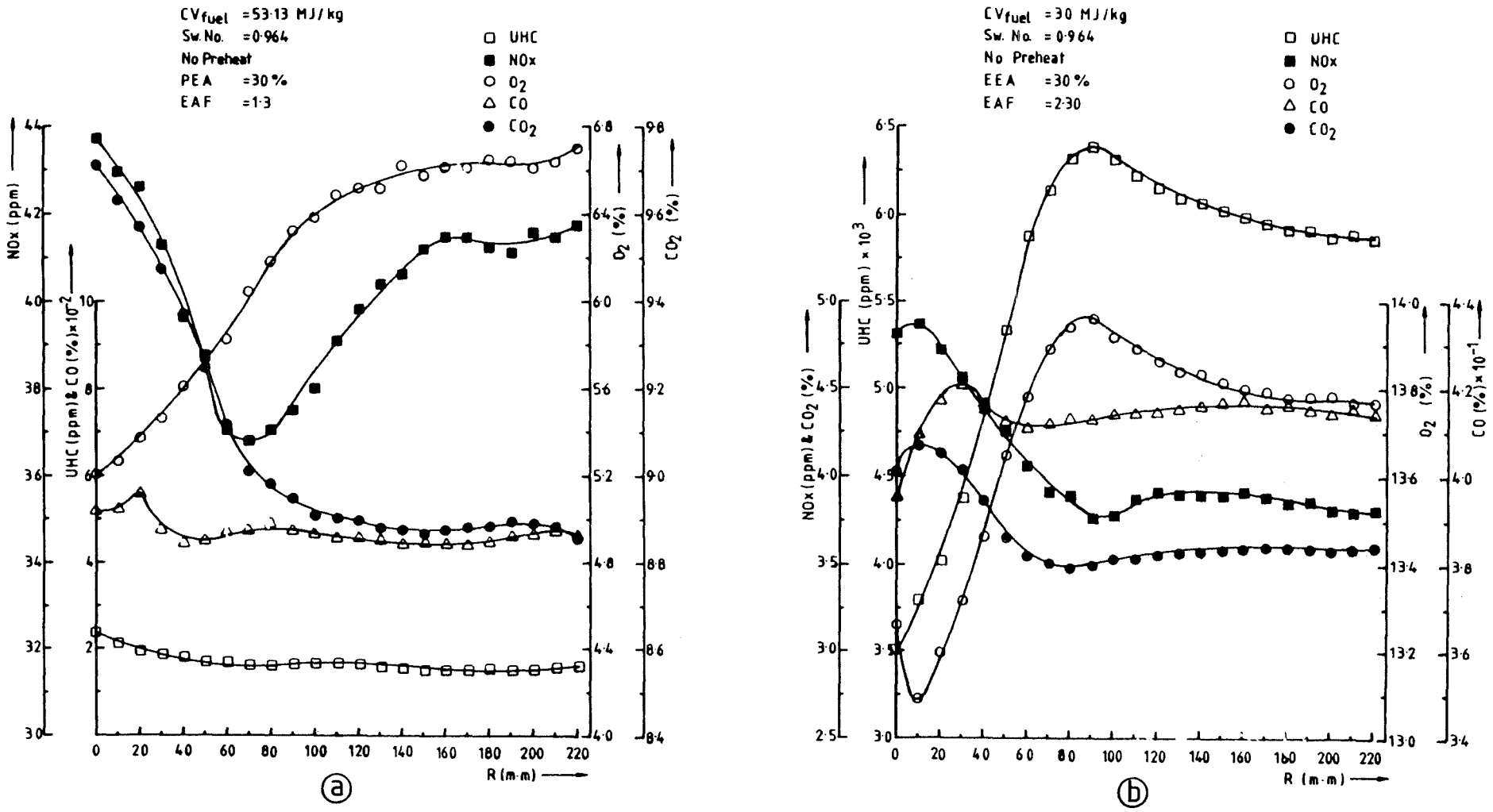

Fig.(5.22) Concentration Measurements

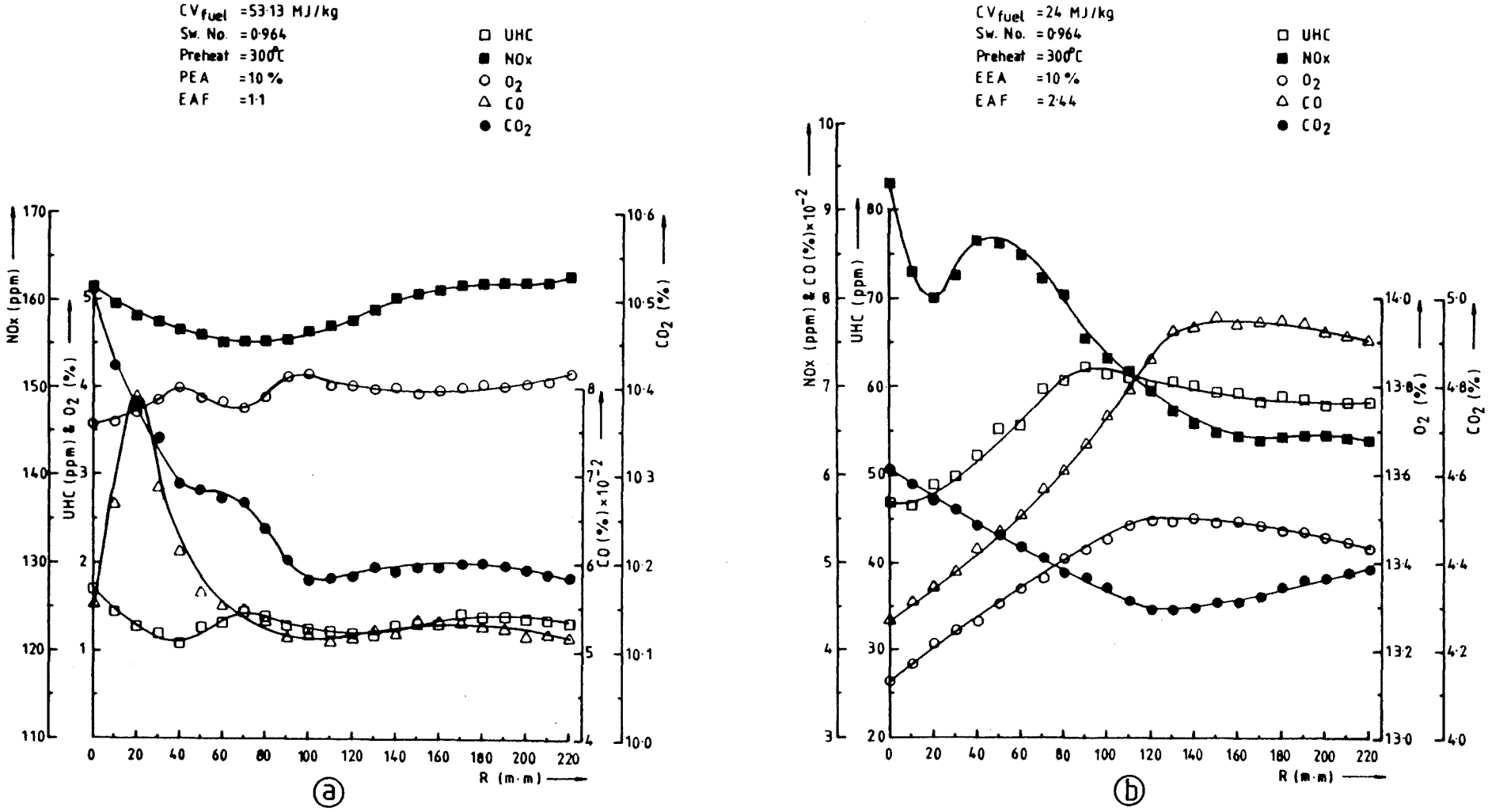

Fig.(5.23) Concentration Measurements

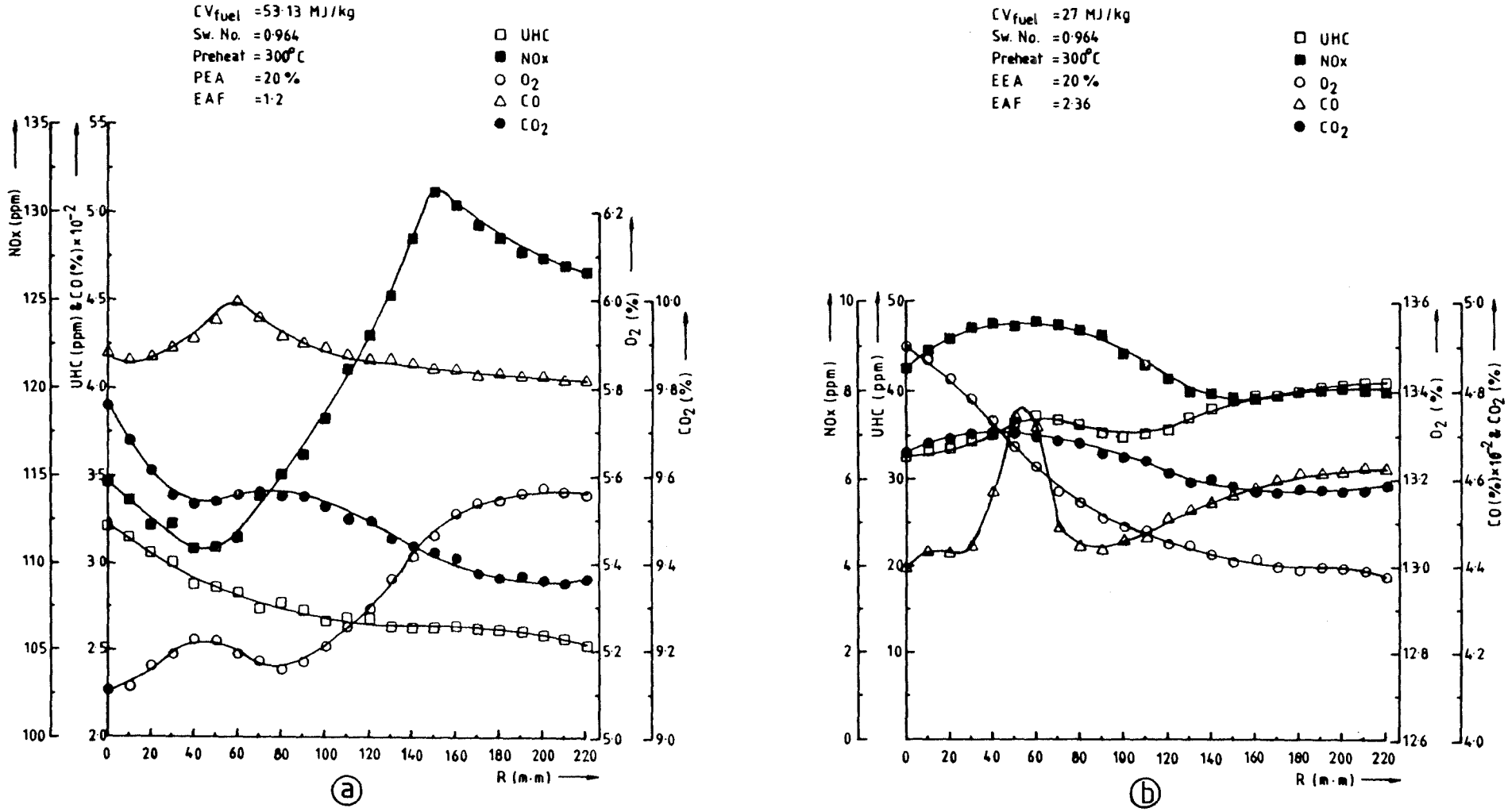

Fig.(5.24) Concentration Measurements

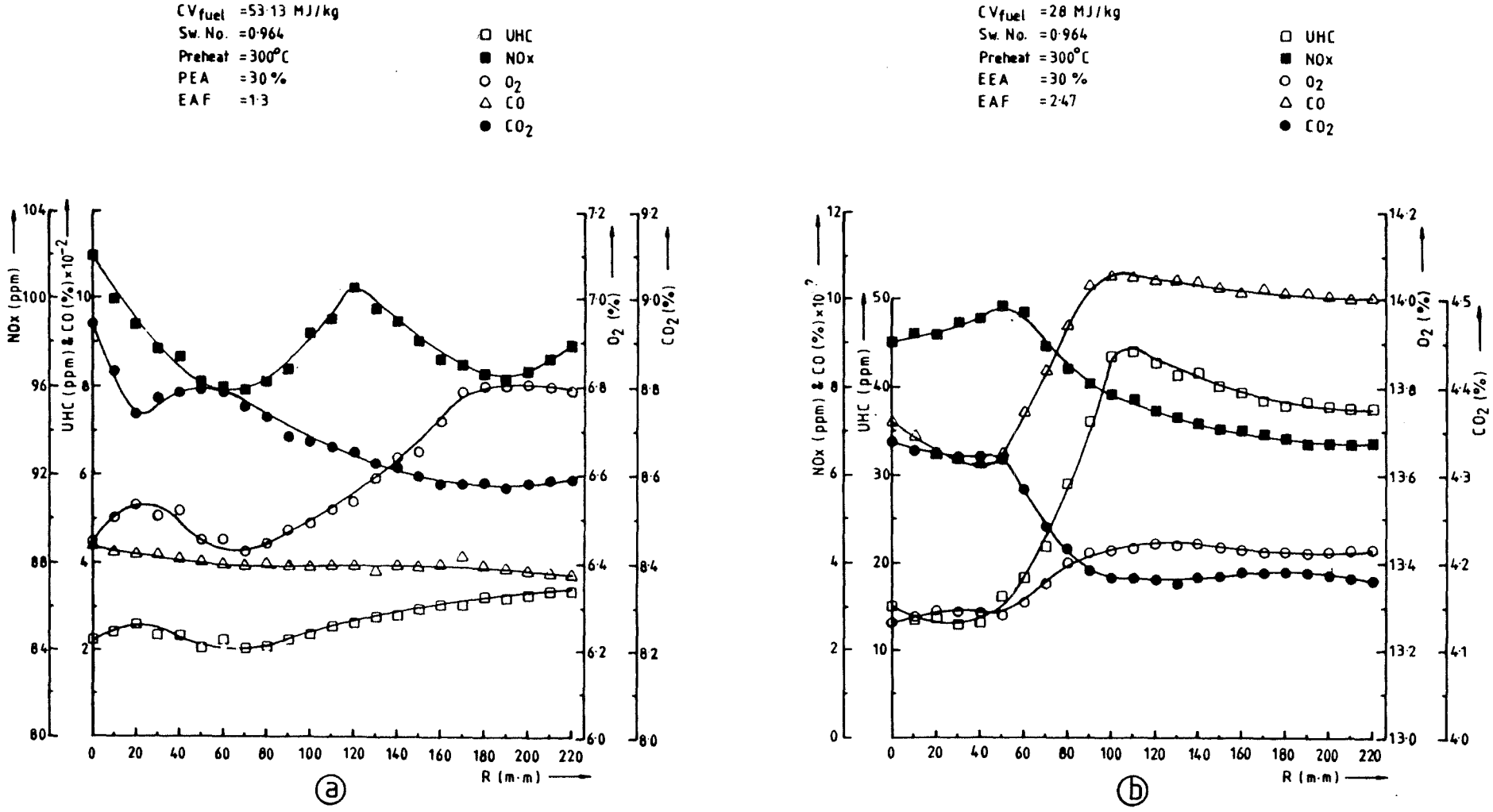

Fig.(5.25) Concentration Measurements

MJ/kg CV	SW	Preheat °C	Xs Air	b(x) %
53.13	0	38	10	96.2
"	"	"	20	96.6
"	"	"	30	97.4
33	"	"	10	91.3
35	"	"	20	81.7
38	"	"	30	81.6
53.13	"	300	10	92.1
"	"	"	20	96.4
"	"	"	30	97.1
26	"	"	10	91.8
24	"	"	20	64.8
23	"	"	30	17.9
53.13	0.964	38	10	98.6
"	"	"	20	99.1
"	"	"	30	99.2
27	"	"	10	53.0
28	"	"	20	27.7
30	"	"	30	24.5
53.13	"	300	10	99.2
"	"	"	20	99.0
"	"	"	30	99.1
24	"	"	10	96.0
27	"	"	20	95.8
28	"	"	30	95.1

Table (5.1) Burnout Rate at X/D = 0.445

The L.C.V. (i.e. CV $<$ 53.13 MJ/kg) used above are 3 MJ/kg above the blow-off values.

MJ/kg CV	SW	Preheat °C	Xs Air	b(x) %
53.13	0	38	10	99.82
"	"	"	20	99.76
"	"	"	30	99.76
33	"	"	10	99.45
35	"	"	20	98.91
38	"	"	30	98.74
53.13	"	300	10	99.81
"	"	"	20	99.83
"	"	"	30	99.69
26	"	"	10	99.44
24	"	"	20	97.77
23	"	"	30	92.75
53.13	0.964	38	10	99.85
"	"	"	20	99.83
"	"	"	30	99.83
27	"	"	10	91.17
28	"	"	20	84.66
30	"	"	30	84.99
53.13	"	300	10	99.86
"	"	"	20	99.84
"	"	"	30	99.83
24	"	"	10	99.25
27	"	"	20	99.56
28	"	"	30	99.09

Table (5.2) Burnout Rate at Exhaust

MJ/kg CV	SW	Preheat °C	Xs Air	Temp °C at 50 mm*	Temp °C at 150 mm*
53.13	0	38	10	432	616
"	"	"	20	392	547
"	"	"	30	356	532
33	"	"	10	200	480
35	"	"	20	197	474
38	"	"	30	223	509
53.13	"	300	10	570	655
"	"	"	20	577	694
"	"	"	30	557	692
26	"	"	10	374	611
24	"	"	20	342	540
23	"	"	30	326	502
53.13	0.964	38	10	331	526
"	"	"	20	277	765
"	"	"	30	185	1220
27	"	"	10	170	385
28	"	"	20	151	376
30	"	"	30	140	410
53.13	"	300	10	563	611
"	"	"	20	485	582
"	"	"	30	473	618
24	"	"	10	332	511
27	"	"	20	335	519
28	"	"	30	328	503

* Distance from burner outlet along inside quarl surfaces

Table (5.3) Internal Quarl Surface Temperature

MJ/kg CV	SW	Preheat °C	Xs Air	ε
53.13	0	38	10	5.95
"	"	"	20	5.91
"	"	"	30	5.89
33	"	"	10	4.89
35	"	"	20	4.91
38	"	"	30	4.81
53.13	"	300	10	6.06
"	"	"	20	6.03
"	"	"	30	6.25
26	"	"	10	4.87
24	"	"	20	4.96
23	"	"	30	4.95
53.13	0.964	38	10	6.10
"	"	"	20	6.20
"	"	"	30	6.23
27	"	"	10	4.95
28	"	"	20	4.81
30	"	"	30	4.94
53.13	"	300	10	6.29
"	"	"	20	6.32
"	"	"	30	6.52
24	"	"	10	4.91
27	"	"	20	4.83
28	"	"	30	4.82

Table (5.4) Blow-off Criterion

CHAPTER 6

SUMMARY AND CONCLUSIONS

6.1. Summary

The principal objective of this project was to investigate the stability limits of low calorific value gases under various furnace operating conditions. A Hilton Combustion unit was modified into a research test facility on which to carry out the experiments. A double-concentric pipe burner system, as commonly used in industrial practices, was utilized and facilities for providing swirl, preheat to the secondary air and the use of LCV fuels were incorporated in the system. Natural gas and nitrogen were metered separately and fed to a mixing chamber in order to obtain a homogeneous fuel mixture with the required calorific value. An ultraviolet flame scanner unit with its ancillary electronics were used to detect flame failure. A manual shut-off valve, a class 1 solenoid valve in the fuel line and an explosion vent were added to the modified furnace in order to reduce accident risks in the event of an explosion. An automatic data logging system using a motorized traversing gear controlled by a central microprocessor was developed and employed for the collection of combustion data. The temperature, velocity and concentration programs worked successfully and expedited data collection.

Stability limits measurements were obtained for three excess air levels, four swirl numbers and five secondary air preheat temperatures. These measurements were based on complete blow-off of the flame. The

stability limits measurements were presented and discussed in relation to the effects of the various operating conditions used. In order to obtain an understanding of the blow-off mechanism involved, combustion measurements were made in the near-burner region (X/D = 0.445). Due to time restrictions, conditions for only two swirl numbers, two secondary air preheat temperatures and three excess air levels were investigated. Inflame temperature, velocity and concentration data were collected for conditions which were close to the blow-off limits. Similar measurements were repeated for pure natural gas flames and the data were used as reference. A fine-wire (40 μm) thermocouple was used for the temperature measurements while a 5-hole pitot probe was utilized to obtain velocity data. A water-cooled stainless steel sampling probe was used to sample the combustion gases which were analysed on an Analysis Automation Analyser System which determined concentrations of UHC, NO_x, O_2, CO and CO_2.

The influences of swirl, secondary air preheat and excess air levels on the combustion measurements were presented and discussed. Combustion data were also collected at the exhaust section of the furnace. These data were used to calculate the degree of burnout in order to obtain the combustion efficiency of the system. The degrees of burnout under various operating conditions were also calculated for combustion data obtained at the sampling port, (X/D = 0.445). They were compared with the ones obtained at the exhaust section. In order to establish an extinction mechanism for the various operating conditions, the combustion data were used to calculate a blow-off criterion which was based on the theories proposed by Peters and Williams. Extinction was detected by the ultraviolet flame scanner which operated a warning light when the flame blew-off. The blow-off criterion was obtained from the

parameter ε which is the ratio of a characteristic mixing time (t_d) to a characteristic chemical reaction time (t_c). Finally the relationships between the stability limits measurements and the combustion data were discussed.

The remainder of this chapter is presented in two sections. Section (6.2) provides the main conclusions of this work and section (6.3) outlines the recommendations for future work.

6.2 Conclusions

Modifications to the experimental rig successfully allowed the use of swirl and preheat on the secondary air supply firing both natural and LCV gas. The safety systems incorporated in the furnace proved adequate and worked satisfactorily.

Data for the stability limits measurements have been presented in various formats which highlight the effects of swirl, secondary air preheat and excess air level independently.

Temperatures were measured on the internal surface of the quarl. The location of maximum temperature along the quarl was found to be independent of the level of excess air and secondary preheat when the swirl number was at or below 0.689. This applied to both natural and LCV gases. For the maximum swirl condition, (0.964), the maximum temperature locations fluctuated substantially when LCV gas mixtures were fired. With natural gas flames, the maximum temperature was located 50 mm upstream in the quarl when compared to LCV gas flames. This was almost independent of the excess air levels or secondary preheat temperatures used.

With regard to the flame stability preheating alone was beneficial only if the temperature of the air was above 250°C. Imparting swirl to the secondary air gave a definite improvement on the stability limits of the flames regardless to the secondary air temperature supplied. For conditions when the swirl number was above 0.418, a slight decrease in the flame stability was noted with increasing excess air levels. There was also very little improvement on the stability limits of the flames when swirl numbers above 0.689 were used. This value of 0.689 appears to be a limiting swirl number which provides adequate recirculation to promote maximum flame stability under various excess air levels and secondary air preheat temperatures.

The stability limits of the flames were severely reduced with increasing excess air levels and the absence of swirl when the temperature of the secondary air was below 250°C. However, with the introduction of a small amount of swirl and moderate preheat temperatures ($\simeq$ 200°C), considerable improvements on the stability of the flames were noted at all three excess air levels. The measurements also revealed that using the maximum swirl and preheat did not provide the best stability results. This indicates that furnaces using a low cost burner system to give moderate swirl ($\simeq$ 0.5) and the exhaust gases to preheat the secondary air ($\simeq$ 200°C) can achieve very satisfactory flame stability performances for a wide range of LCV gases. A possible explanation of this phenomenon is flame stretch resulting from the excessive torsional force caused by increasing the swirl number plus an increase in velocity at the burner mouth caused by preheating the combustion air to a higher temperature.

The combustion measurements showed that an increase in excess air level, for natural gas flames, caused a reduction in the temperature inside the furnace as would be expected from the dilution effect and this was found to be independent of swirl and preheat. For LCV gas flames the temperature levels were dependent on the calorific values of the fuel mixtures used.

The effects of increasing excess air for natural gas flames surprisingly showed very little change in the velocity profiles regardless of the swirl intensity or preheat temperatures. However, there was a noticable decrease in the core velocities with increasing excess air levels for the LCV flames with zero swirl. This was independent of the preheat temperatures of the secondary air. For swirling flows no substantial changes were noticed in the velocity profiles for all the various operating conditions investigated. It should be pointed out here that some of the above findings are contradictory and it may be that the velocity measurements at high temperatures using a five-hole pitot tube were subject to substantial errors.

Increasing the excess air levels caused a reduction in the concentration of UHC and CO for LCV flames using the same EAF, swirl and preheat. Very small amounts of NO_x were formed for all the LCV gas flames investigated due to the low flame temperatures associated with these cases.

Imparting swirl to the secondary air for the natural gas flames caused a decrease in the reaction core temperature, but the temperature levels in the outer recirculation zone increased; this applied for the various

operating conditions used. Similar effects were noted for the LCV gas flames but the value of the temperature levels were dependent on the EAF and the calorific value of the fuel used.

For natural gas flames with zero swirl, preheating caused a radial shift in the location of maximum temperature possibly indicating flame elongation. In contrast, maximum temperature levels of the LCV gas flames were located at a single radial position and were independent of the excess air levels or preheat.

The concentration measurements in the LCV gas flames showed a large increase in the UHC and CO levels for most of the operating conditions investigated when compared to their natural gas counterpart. This indicated that partial extinction was taking place prior to blow-off.

The degrees of burnout calculated at the sampling port were high for the natural gas flames under all operating conditions. For LCV gas flames, these values were quite low under certain operating conditions, possibly indicating partial flames lift-off or flame elongation beyond the sampling plane, but the overall combustion efficiency for these cases was reasonably high as shown by the burnout measurements obtained at the exhaust.

The blow-off criterion was based on the parameter ε obtained from the ratio of the characteristic mixing time (t_d) to the characteristic chemical reaction time (t_c). For flames close to the blow-off limits, the value of ε was consistently close to 4.9 compared with 6.2 for stable pure natural gas flames. The parameter ε was also found to be

independent of swirl number, preheat and excess air. From the results obtained, an important criterion for determination of stability in confined flames has been established thus supporting the extinction mechanism proposed by Peters and Williams.

6.3 Recommendations for future work

1. A better technique (LDA Anemometry) is desirable for velocity measurements under similar operating conditions to those investigated to provide more accurate data.

2. The combustion measurements performed should be extended to the remaining two sampling ports for complete mapping of the furnace. Axial measurements are also recommended.

3. Sampling ports should be added closer to the quarl exit: this would enable data to be collected within and flow visualisation techniques to be applied to the main reaction zone.

4. Various quarls with a range of half angles should be investigated and their influences on the stability limits assessed.

5. The influences of burner lip thickness and various ratios of burner pipe diameters should also be investigated with the objective of obtaining further improvements in flame stability.

6. Combustion measurements at intermediate operating conditions away from blow-off should also be carried out and the data used to reinforce the extinction mechanism investigated.

7. A natural gas booster and a more powerful air compressor should be fitted to the system to allow higher furnace loadings.

8. Combustion models should be developed for comparison with the data obtained in order to gain a more complete understanding of the processes occurring. This would then enable prediction under a wide range of operating conditions.

R E F E R E N C E S

1. Ahmad, N.T., Andrews, G.E., Kowkabi, M. and Sharif, S.F. (1984) "Centrifugal mixing forces in enclosed swirl flames'. 20th Symposium (Int.) on Combustion, pp.259-267.

2. Albright, L.J. and Alexander, L.G. (1956) 'Flow Characteristics, temperature and gas analysis' 6th Symposium (Int.) on Combustion, pp.464-472.

3. Andrews, G.E., Bradley, D. and Lwakabamba, S.B. (1975) 'Measurement of turbulent burning velocity for large turbulent Reynolds numbers'. 15th Symposium (Int.) on Combustion, pp.655-664.

4. Becker, H.A. (1975) 'Effects of concentration fluctuations in turbulent diffusion flames.' 15th Symposium (Int.) on Combustion, pp. 601-615.

5. Becker, H.A., Hottel, H.C. and Williams, G.C. (1963) 'Mixing and flow in ducted turbulent jets.' 9th Symposium (Int.) on Combustion, pp. 7-20.

6. Becker, H.A. Hottel, H.C. and Williams, G.L. (1967) 'The nozzle-fluid concentration field of the round turbulent, free jet.' Journal of fluid Mechanics, Vol.30, part 2, pp.285-303.

7. Becker, H.A., Hottel, H.C. and Williams, G.C. (1967)
'Concentration fluctuations in ducted turbulent jets.' 11th Symposium (Int.) on Combustion, pp. 791-798.

8. Becker. H.A., Liang, D. and Downey, C.I. (1981)
'Effect of burner orientation and ambient airflow on geometry of turbulent free diffusion flames.' 18th Symposium (Int.) on Combustion, pp.1061-1071.

9. Becker, H.A. and Yamazaki, S. (1978)
'Entrainment, momentum flux and temperature in vertical free turbulent diffusion flames.' Combustion and Flame : 33, pp.123-149.

10. Beér, J.M. (1972)
'Paper 1. Recent advances in the technology and furnace flames.' Journal of the Institute of Fuel, July 1972.

11. Beér, J.M. and Chigier, N.A. (1972)
'Combustion Aerodynamcis.' Applied Science Publishers Ltd.

12. Beltagui, S.A. and Maccallum, N.R.L. (1976)
'Aerodynamics of vane-swirled flames in furnaces.' Journal of the Institute of Fuel, December 1976.

13. Beltagui, S.A. and Maccallum, N.R.L. (1986)
'Stability limits of free swirling premixed flames. Part 1. Experimental correlation.' Journal of the Institute of Energy, September 1986.

14. Beltagui, S.A. and Maccallum, N.R.L. (1986)
'Stability limits of free swirling premixed flames. Part 2. Theoretical prediction.' Journal of the Institute of Energy, September 1986.

15. Beyler, C.L. and Gouldin, F.C. (1981)
'Flame structure in a swirl stabilized combustor inferred by radiant emission measurements.' 18th Symposium (Int.) on Combustion, pp.1011-1019.

16. Bilger, R.W. (1975)
'A note on Favre averaging in variable density flows.' Combustion Science and Technology, Vol. 11, pp. 215-217.

17. Bilger, R.W. (1976)
'Probe measurements in turbulent combustion.' A project SQUID workshop, Academic Press.

18. Bilger, R.W. (1980)
'Perturbation analysis of turbulent nonpremixed combustion.' Combustion Science and Technology, Vol.22, pp.251-261.

19. Bilger, R.W. & Beck, R.E. (1975)
'Further experiments on turbulent jet diffusion flames.' 15th Symposium (Int.) on Combustion, pp.541-552.

20. Birch, A.D., Brown, D.R., Dodson, M.G. and Thomas, J.R. (1978)
'The turbulent concentration field of a methane jet.'
Journal of Fluid Mechanics, Vol.88 III, pp.431-449

21. Bortz, S. (1983)
'Background and programme outline for the IFRF burner near field aerodynamics project.'
IFRF Doc. No. G14/a/2.

22. Bradley, D. and Entwistle, A.G. (1961)
'Determination of the emissivity, for total radiation, of small diameter platinum - 10% rhodium wires in the temperature range 600-1450°C.' British Journal of Applied Physics, Vol. 12, December 1961.

23. Bradley, D. and Matthews, K.J. (1968)
'Measurement of high gas temperatures with fine wire thermocouples.' Journal of Mechanical Engineering Science, Vol.10, No.4, April, 1968.

24. British Standard Institute (1984)
'Measurement of Fluid Flow in closed conduits.' BS 1042 : Section 1.4

25. Broadwell, J.E., Dahm, W.J.A. and Mungal, M.P. (1984)
'Blowout of turbulent diffusion flames.' 20th Symposium (Int.) on Combustion, pp.303-310.

26. Cernansky, N.P. and Sawyer, R.F. (1975)
'NO and NO_2 formation in a turbulent hydrocarbon/air diffusion flame.' 15th Symposium (Int.) on Combustion, pp. 1039-1050.

27. Chakravarty, A. (1984)
'The prediction of turbulent flame extinction.' Ph.D. thesis, University of London.

28. Chakravarty, A., Lockwood, F.C. and Sinicropi, G. (1984)
'The prediction of burner stability limit.'
Combustion Science and Technology, Vol. 42.

29. Chedaille, J., Leuckel, W. and Chesters, A.K. (1966)
'Aerodynamic studies carried out on turbulent jets by the IFRF.'
Journal of the Institute of Fuel, December, 1966.

30. Chigier, N.A. and Dvorak, K. (1975)
'Laser anemometer measurements in flames with swirl.' 15th Symposium (Int.) on Combustion, pp.573-586.

31. Claypole, T.C. and Syred, N.(1981)
'The effect of swirl burner aerodynamics on NO_x formation.'
18th Symposium (Int.) on Combustion, pp.81-89.

32. Dahm, W.J.A., Dimotakis, P.E. and Broadwell, J.E. (1984)
'Non-premixed Turbulent jet flames.'
AIAA Journal, 84-0369.

33. Davies, R.M. and Oeppen, B. (1972)
'Paper 2. Combustion and heat transfer in natural gas fired furnaces.' Journal of the Institute of Fuel, July 1972.

34. Dimotakis, P.E., Miake-Lye, R.C. and Papantoniou D.A. (1983)
Physical Fluids, 26 (11), 3185.

35. Dutton, B.C. and Souchard R.J. (1985)
'Gas interchangeability : prediction of incomplete combustion.' Journal of the Institute of Energy, December 1985.

36. Edmondson, H. and Heap, M.P. (1970)
'The correlation of burning velocity and blow-off data by the flame stretch concept.' Combustion and Flame : 15, pp.179-187.

37. Eickhoff, H., Lenze, B. and Leuckel, W. (1984)
'Experimental investigation on the stabilization mechanism of jet diffusion flames.' 20th Symposium (Int.) on Combustion, pp.311-318.

38. Elghobashi, S.E. and Pun, W.M. (1975)
'A theoretical and experimental study of turbulent diffusion flames in cylindrical furnaces.' 15th Symposium (Int.) on Combustion, pp. 1353-1365.

39. Fricker, N. and Leuckel, W. (1976)
'The characteristics of swirl-stabilized natural gas flames. Part.3 The effect of swirl and burner mouth geometry on flame stability.' Journal of the Institute of Fuel, September 1976.

40. Gaydon, A.G. and Wolfhard H.G. (1979)
'Flames. Their structure, radiation and temperature.'
4th Edition, John Wiley & Sons.

41. Glassman, I. (1977)
'Combustion.' Academic Press Inc. Ltd.

42. Godoy, S., Hirji, K., Lockwood, F.C and Miller, J. (1985)
'Stability limits of pulverised coal burners.'
Mech.Eng. Dept., Imperial College, Fluid Section Report FS/84/42.

43. Gokalp, I., Dumas, G.M.L. and Ben-Aim, R.I. (1981)
'Temperature field measurements in a premixed turbulent cool flame.' 18th Symposium (Int.) on Combustion. pp.969-976

44. Goodger, E.M. (1977)
'Combustion calculations, theory, worked examples and problems.'
The Macmillan Press Ltd.

45. Goulard, R. (1976)
'Combustion Measurements, modern techniques and instrumentation.'
Academic Press.

46. Günther, R. and Wittmer, V. (1981)
'The turbulent reaction field in a concentric diffusion flame.'
18th Symposium (Int.) on Combustion, pp.961-967.

47. Gupta, A.K., Syred, N. and Beér, J.M. (1975)
'Fluctuating temperature and pressure effects on the noise output of swirl burners.' 15th Symposium (Int.) on Combustion, pp.1367-1377.

48. Gupta, A.K., Swithenbank, J. and Beér, J.M. (1977)
'Modern diagnostics for the measurement of fluctuating quantities in flames.' Journal of the Institute of Fuel, December 1977.

49. Haniff, M.S. and Melvin, A. (1984)
'A condition for the lift-off of premixed flames - an asymptotic expansion approach.' Journal of the Institute of Energy, December 1984.

50. Hassan, M.M.A. (1983)
'A study of natural gas and pulverized coal diffusion flames.' Ph.D. thesis, University of London.

51. Hassan, M.M.A. Lockwood, F.C. and Moneib, H.A. (1980)
'Fluctuating temperature and mean concentration measurements in a vertical turbulent free jet diffusion flame.' Paper presented at the "Italian Flame Days", Milano, Vol.34, pp.357-372.

52. Hirji, K.A.A. (1986)
'Combustion measurements in pulverised coal flames.' Ph.D. thesis, University of London.

53. Hubbard, E.H. (1957)
'Effect of preheat combustion air.' Journal of the Institute of Fuel, Vol.30, pp.564-576.

54. Ishizuka, S. and Law, C.K. (1982)
'An experimental study on extinction and stability of stretched premixed flames.' 19th Symposium (Int.) on Combustion, pp.327-335.

55. Janicka, J. and Peters, N. (1982)
'Prediction of turbulent jet diffusion flame lift-off using a PDF transport equation.' 19th Symposium (Int.) on Combustion, pp.367-374.

56. Jarosinsk, J., Strehlow, R.A. and Azarbarzin, A. (1982)
'The mechanisms of lean limit extinguishment of an upward and downward propagating flame in a standard flammability tube.' 19th Symposium (Int.) on Combustion, pp.1549-1557.

57. Kalghatgi, G. (1981)
'Blow out stability of gaseous jet diffusion flames.' Part 1: In still air.' Combustion Science and Technology, Vol.30, pp.233-239.

58. Katsuki, M., Mizutani, Y. and Matsumoto, Y. (1987)
'An improved thermocouple technique for measurement of fluctuating temperaturess in flames.' Combustion and Flame : 67, pp.27-36.

59. Kent, J.H. and Bilger, R.W. (1973a)
'Turbulent diffusion flames.' 14th Symposium (Int.) on Combustion, pp.615-625

60. Kent, J.H. and Bilger, R.W. (1973b)
'Measurement techniques in turbulent diffusion flames.' 1st Australian Conference on Heat and Mass Transfer, Monash University, Melbourne, Australia, Sec. 4.4, pp 39-46.

61. Khalil, E.E. (1982)
'Modelling of furnaces and combustors.' Abacus Press.

62. Kotani, Y. and Takeno, T. (1982)
'An experimental study on stability and combustion characteristics of an excess enthalphy flame.' 19th Symposium (Int.) on Combustion, pp.1503-1509.

63. Lenze, B. (1982)
'The influence of recirculation and excess air on enclosed turbulent diffusion flames.' 19th Symposium (Int.) on Combustion, pp.565-572.

64. Leuckel, W. and Fricker, N. (1976)
'The characteristics of swirl-stabilized natural gas flames. Part 1: Different flame types and their relation to flow and mixing patterns.' Journal of the Institute of Fuel, June 1976.

65. Leventhal, L.A. and Saville, W. (1982)
'6502 Assembly language subroutines.' Osborne/McGraw-Hill, California.

66. Lilley, D.G. (1977)
'Swirl flow in combustion : a review.' AIAA Journal, Vol.15, pp.1063-1078.

67. Lockwood, F.C., El-Mahallawy, F.M. and Spalding, D.B. (1974)
'An experimental and theoretical investigation of turbulent mixing in a cylindrical furnace.' Combustion and Flame: 23, pp.283-293.

68. Lockwood, F.C. and Megahed, I.E.A. (1978)
'Extinction in turbulent reacting flows.' Combustion Science and Technology, Vol. 19, pp.77-80.

69. Lockwood, F.C. and Naguib, (A.S. (1976)
'Aspects of Combustion Modelling in Engineering Turbulent Diffusion Flames.' Journal of the Institute of Fuel, December 1976.

70. Lockwood, F.C. and Odidi, A.O.O. (1975)
'Measurement of mean and fluctuating temperature and of ion concentration in round free-jet turbulent diffusion and premixed flames.' 15th Symposium (Int.) on Combustion, pp.561-571.

71. Mathur, M.L. and Maccallum, N.R.L. (1967)
'Swirling air jets issuing from vane swirlers. Part 2. Enclosed jets.' Journal of the Institute of Fuel, Vol.40, pp.238-245.

72. Melvin, A. and Moss, J.B. (1975)
'Structure in methane-oxygen diffusion flames.' 15th Symposium (Int.) on Combustion, pp.625-636.

73. Menn, A. and Stotter, A. (1985)
'On combustion air/fuel ratio at variable ambient conditions.' Journal of the Institute of Energy, March 1985.

74. Merryman, E.L. and Levy, A. (1975)
'Nitrogen oxide formation in flames : the roles of NO_2 and fuel nitrogen.' 15th Symposium (Int.) on Combustion, pp.1073-1083.

75. Michel, J.B. and Payne, R. (1979)
'The use of blast furnace gas as a fuel in high temperature furnaces of the steel industry.' IFRF. Doc. No. F01/a/100.

76. Moneib, H.A. (1980)
'Experimental study of the fluctuating temperature in inert and reacting turbulent jets.' Ph.D. thesis, University of London.

77. Moss, J.B. (1980)
'Simultaneous measurements of concentration and velocity in an open premixed turbulent flame.' Combustion Science and Technology, Vol. 22, pp.119-129.

78. Najim, S.E., Styles, A.C. and Svred, N. (1981)
'Flame movement mechanisms and characteristics of gas fired cyclone combustors.' 18th Symposium (Int.) on Combustion, pp.1949-1957.

79. Negishi, N. (1982)
'Lean premixture combustion on a coaxial burner.' 19th Symposium (Int.) on Combustion, pp.441-447.

80. Nicholson, H.M. and Field, J.P. (1948)
'Some experimental techniques for the investigation of the mechanism of flame stabilization in the wakes of bluff bodies.' 3rd Symposium on Combustion, Flame and Explosion phenomena, pp.44-68.

81. Peters, N. (1983)
'Local quenching due to flame stretch and non-premixed turbulent combustion.' Combustion Science and Technology, Vol. 30.

82. Peters, N., Hocks, W. and Mohiuddin, G. (1981)
'Turbulent mean reaction rates in the limit of large activation energies.' Journal of Fluid Mechanics, Vol. 110, pp.411=432.

83. Peters, N. and Williams, F.A. (1982)
'Lift-off characteristics of turbulent jet diffusion flame.' AIAA Aerospace Science Members Meeting, Orlando, Florida.

84. Radhakrishnan, K., Heywood, J.B. and Tabaczynski, R.J. (1981)
'Premixed turbulent flame blow-off velocity correlation based on coherent structures in turbulent flows.' Combustion and Flame : 42, pp.19-33.

85. Rawe, R. and Kremer, H. (1981)
'Stability limits of natural gas diffusion flames with siwrl.' 18th Symposium (Int.) on Combustion, pp.667-677.

86. Rimai, L., Marko, K.A. and Klick, D. (1982)
'Optical study of a 2-Dimensional laminar flame : relation between tempeature and flow-velocity fields.' 19th Symposium (Int.) on Combustion, pp.259-265

87. Sadakata, M., Fujioka, Y. and Kunii, D. (1981)
'Effects of air preheating on emissions of NO, HCN and NH_3 from a two-stage combustion.' 18th Symposium (Int.) on Combustion, pp.65-72.

88. Sauba, R.N. (1984)
'Temperature and species concentration measurement studies in a vertically orientated coal/gas fired cylindrical furnace.' M.Phil./Ph.D. transfer report, Energy Centre, Middlesex Polytechnic.

89. Scholefield, D.A. and Garside, J.E. (1948)
'The structure and stability of diffusion flames.' 3rd Symposium on Combustion, Flame and Explosion phenomena, pp.102-110.

90. Scholte, T.G. and Vaags, P.B. (1959)
'The burning velocity of hydrogen air-mixtures and mixtures of some hydrocarbons with air.' Combustion and Flame: 3, pp.495-501.

91. Scholte, T.G. and Vaags, P.B. (1959)
'Burning velocities of mixtures of hydrogen, carbon monoxide and methane with air.' Combustion and Flame 3, pp.511-524.

92. Schreier, W. (1982)
'Technical aspects of lean gas utilization in iron and steel industry.' Progress report (July-Dec. 1981) IFRF, Doc. 3113/1982.

93. Schreier, W. (1983)
'Studies on Combustion of variable lean gases in iron and steel industry.' Proceedings of the IFRF 7th Members Conference, Session 1. Leeuwenhorst Congress Centre, Netherlands.

94. Sen, A.K. and Ludford, G.S.S. (1982
'Maximum flame temperature and burning rate of combustible mixtures.' 19th Symposium (Int.) on Combustion, pp.267-274.

95. Seshadri, K., Puri, I. and Peters, N. (1985)
'Experimental and theoretical investigation of partially premixed diffusion flames at extinction.' Combustion and Flame 61: pp.237-249

96. Shet, U.S.P., Sriramulu, V. and Gupta, M.C. (1981)
'A New approach to the correlation of turbulent burning velocity data.' 18th Symposium (Int.) on Combustion, pp.1073-1080

97. Sohrab, S.H. and Law, C.K. (1985)
'Influence of burner rim aerodynamics on polyhedral flames and flame stabilization.' Combustion and Flame 62: pp.243-254.

98. Spalding, D.B. (1956)
'A mixing rule for laminar flame speed.' Fuel, London, Vol. 35, pp.347-351.

99. Spalding, D.B. (1971)
'Combustion as applied to engineering.' Journal of the Institute of Fuel, April, 1971

100. Spalding, D.B. (1979)
'Combustion and Mass transfer.' Pergamon Press.

101. Stambuleanu, A. (1976)
'Flame combustion processes in industry.'
Abacus Press.

102. Starner, S.H. and Bilger, R.W. (1981)
'Measurement of scalar-velocity correlations in a turbulent diffusion flame.' 18th Symposium (Int.) on Combustion, pp.921-930.

103. Steward, F.R., Osuwan, S. and Picot, J.J.C. (1971)
'Heat-transfer measurements in a cylindrical test furnace.' 13th Symposium (Int.) on Combustion pp.651-660.

104. Strahle, W..C. (1982)
'Duality, dilatation, diffusion and dissipation in reacting turbulent flows.' 19th Symposium (Int.) on Combustion, pp.337-347.

105. Sunavala, P.D. (1961)
'Mixing and Combustion in coaxial streams. Part 1. Theories of recirculation.' Journal of Science and Industrial Research, Vol. 20B, pp.246-256.

106. Sunavala, P.D. (1962)
'Mixing and combustion in coaxial streams. Part 2. Simulation of heat, mas and momentum transfer.' Journal of Science and Industrial Research, Vol. 21B, pp.167-174.

107. Syred, N. and Beer, J.M. (1974)
'Combustion in swirling flows : a review.' Combustion and Flame 23 : pp.143-201.

108. Syred, N., Dahmen, K.R., Styles, A.C. and Najim, S.A. (1977)
'A review of combustion problems associated with low calorific value gases.' Journal of the Institute of Fuel, December. 1977.

109. Syred, N., Gupta, A.K. and Beer, J.M. (1975)
'Temperature and density gradient changes arising with the precessing vortex core and vortex breakdown in swirl burners.' 15th Symposium (Int.) on Combustion, pp.587-597.

110. Takagi, T., Ogasawara, M., Fujii, K. and Diazo, M. (1975)
'A study of nitric oxide formation in turbulent diffusion flames.' 15th Symposium (Int.) on Combustion, pp.1051-1059.

111. Taylor, A.M.K.P. and Whitelaw, J.H. (1980)
'Velocity and temperature measurements in a premixed flame within an axisymmetric combustor.' AGARD report from conference proceedings No.281.

112. Thring, M.W. and Newby, M.P. (1952)
'Combustion length of enclosed turbulent jet flames.' 4th Symposium (Int.) on Combustion, pp.789-796.

113. Tsuji, H. and Yamaoka, I. (1982)
'Structure and extinction of near-limit flames in a stagnation flow.' 19th Symposium (Int.) on Combustion, pp.1533-1540

114. Vanguikenborne, L. and Van tiggelen, A. (1966)
'The stabilization mechanism of lifted diffusion flames.' Combustion and Flame 10, pp.59-69.

115. Von Elbe, G. and Lewis, B. (1948)
'Theory of ignition, quenching and stabilization of flames of nonturbulent gas mixtures.' 3rd Symposium on Combustion, Flame and Explosion phenomena, pp.68-79.

116. Weinberg, F.G. (1975)
'Plenary lecture.' 15th Symposium (Int.) on Combustion, p.1.

117. Wohl, K., Kapp, N.M. and Gazley, C. (1948)
'The stability of open flames.' 3rd Symposium on Combustion, Flame and Explosion phenomena, pp.3-21.

118. Wu, H.L. and Fricker, N. (1976)
'The characteristics of swirl-stabilized natural gas flames. Part 2: The behaviour of swirling jet flames in a narrow cylindrical furnace.' Journal of the Institute of Fuel, September 1976.

119. Yanagi, T. (1977)
'Effects of probe sampling rates on sample composition.' Combustion and Flame 28, pp.33-44.

120. Yanagi, T. and Mimura, Y. (1981)
'Velocity-temperature correlation in premixed flame.' 18th Symposium (Int.) on Combustion, pp.1031-1039.

121. Yoshida, A. (1981)
'An experimental study of wrinkled laminar flame.' 18th Symposium (Int.) on Combustion, pp.931-939.

122. Yoshida, A. and Tsuji, H. (1982)
'Characteristic scale of wrinkles in turbulent premixed flames.' 19th Symposium (Int.) on Combustion, pp.403-411.

123. Yuasa, S. (1986)
'Effects of swirl on the stability of jet diffusion flames.' Combustion and Flame 66 : pp.181-192.

124. Yumlu, V.S. (1967)
'Prediction of burning velocities of carbon monoxide/hydrogen-air flames.' Combustion and Flame : 11, pp.190-194.

125. Yumlu, V.S. (1968)
'Effects of additives on the burning velocity of flames and their possible prediction by a mixing rule.' Combustion and Flame : 12, pp.14-18.

A P P E N D I X 'A'

DATE : 19-11-86

CONDITION NUMBER : 1

SWIRL NUMBER : .964

MASS FLOW RATE OF AIR : 52.38 kg/h

MASS FLOW RATE OF NATURAL GAS : 3 kg/h

MASS FLOW RATE OF NITROGEN : 0 kg/h

MASS FLOW RATE OF COOLING WATER : 364 kg/h

INLET TEMPERATURE OF COMBUSTION AIR : 38 Deg.Cen.

EXHAUST TEMPERATURE OF FLUE GASES : 537 Deg.Cen.

INLET TEMPERATURE OF COOLING WATER : 11 Deg.Cen.

OUTLET TEMPERATURE OF COOLING WATER : 73 Deg.Cen.

RADIAL LOCATION OF THERMOCOUPLE = R (m.m).

MEAN TEMPERATURE IN DEGREES CENTIGRADE.

	MEAN TEMPERATURE AT CONDITION 1		
R (m.m)	RUN1	RUN2	AVERAGE
0	1503	1512	1508
10	1506	1503	1505
20	1486	1454	1470
30	1441	1395	1418
40	1380	1347	1364
50	1321	1319	1320
60	1261	1251	1256
70	1192	1194	1193
80	1115	1107	1111
90	1053	1042	1048
100	962	970	966
110	892	894	893
120	836	828	832
130	782	772	777
140	736	712	724
150	695	686	691
160	669	660	665
170	648	651	650
180	638	641	640
190	632	630	631
200	615	612	614
210	595	585	590
220	539	546	543

Table (A1) : Sample of Temperature Readings

DATE : 17-6-86

STATION NUMBER : 1

SWIRL NUMBER : .964

MASS FLOW RATE OF AIR : 42.94 kg/h

MASS FLOW RATE OF NATURAL GAS : 0 kg/h

MASS FLOW RATE OF COOLING WATER : 1 kg/h

INLET TEMPERATURE OF COMBUSTION AIR : 1 Deg.Cen.

EXHAUST TEMPERATURE OF FLUE GASES : 1 Deg.Cen.

INLET TEMPERATURE OF COOLING WATER : 1 Deg.Cen.

OUTLET TEMPERATURE OF COOLING WATER : 1 Deg.Cen.

RADIAL LOCATION OF 5-HOLE PITOT PROBE = R (m.m).

MEAN VELOCITY IN m/s; ANGLES IN DEGREES.

Mean Velocity ,Conical Angle And Dihedral Angle at Station 1

R (m.m)	RUN1			RUN2			AVERAGE		
0	5.168	88.50	34.61	4.460	87.59	22.05	4.814	88.04	28.33
10	5.034	85.95	44.01	4.624	84.21	42.88	4.829	85.08	43.44
20	4.399	74.72	76.22	4.320	82.27	83.93	4.359	78.49	80.08
30	4.266	79.86	243.2	4.839	82.22	87.57	4.552	81.04	165.4
40	4.421	77.70	265.4	4.029	76.17	81.78	4.225	76.94	173.6
50	3.250	72.74	238.9	3.218	72.53	243.4	3.234	72.64	241.2
60	3.035	70.95	245.0	3.066	81.39	240.7	3.051	76.17	242.8
70	3.360	52.74	255.6	3.114	71.92	247.3	3.237	62.33	251.4
80	2.650	59.14	89.16	2.574	19.68	81.50	2.612	39.41	85.33
90	2.449	62.18	88.95	2.246	74.78	253.3	2.348	68.48	171.1
100	2.833	80.07	255.9	2.345	47.33	249.6	2.589	63.70	252.7
110	2.873	46.59	81.48	2.562	64.57	248.3	2.718	55.58	164.9
120	2.574	72.73	259.7	2.476	75.99	264.7	2.525	74.36	262.2
130	2.319	54.79	245.4	2.103	34.67	240.1	2.211	44.73	242.7
140	2.514	44.18	253.8	3.770	81.71	228.8	3.142	62.94	241.3
150	2.810	48.89	269.8	2.680	31.31	70.12	2.745	40.10	169.9
160	2.632	57.79	75.04	2.811	43.43	86.70	2.721	50.61	80.87
170	2.391	62.40	267.2	2.955	41.98	85.63	2.673	52.19	176.4
180	2.284	52.54	259.0	2.691	54.33	74.79	2.487	53.43	166.9
190	2.689	51.40	79.33	3.454	71.61	251.0	3.072	61.50	165.1
200	2.733	50.07	268.6	3.390	18.53	267.1	3.061	34.30	267.9
210	2.500	68.87	266.8	2.701	69.01	268.2	2.600	68.94	267.5
220	2.815	30.04	265.6	2.583	39.11	261.3	2.699	34.58	263.5

Table (A2) : Sample of Velocity Readings.

DATE : 18-2-87

RUN NUMBER : 2

SWIRL NUMBER : .964

MASS FLOW RATE OF AIR : 57.15 kg/h

MASS FLOW RATE OF NATURAL GAS : 1.525 kg/h

MASS FLOW RATE OF NITROGEN : 1.475 kg/h

MASS FLOW RATE OF COOLING WATER : 364 kg/h

INLET TEMPERATURE OF COMBUSTION AIR : 300 Deg.Cen.

EXHAUST TEMPERATURE OF FLUE GASES : 395 Deg.Cen.

INLET TEMPERATURE OF COOLING WATER : 4 Deg.Cen.

OUTLET TEMPERATURE OF COOLING WATER : 40 Deg.Cen.

RADIAL LOCATION OF SAMPLING PROBE = R (m.m).

CONCENTRATION OF UHC AND NOx IN p.p.m. REST IN % .

R	UHC	NOx	O2	CO	CO2
0	32.85	9.800	13.48	.0440	4.634
10	34.12	8.919	13.58	.0444	4.677
20	33.27	9 266	13.44	.0443	4.682
30	34.42	9.459	13.39	.0443	4.730
40	33.87	9.513	13.36	.0474	4.693
50	36.46	9.462	13.30	.0474	4.679
60	37.41	9.660	13.35	.0507	4.696
70	37.14	9.564	13.17	.0448	4.682
80	35.78	9.466	13.15	.0444	4.700
90	35.59	9.376	13.08	.0442	4.659
100	35.76	8.880	13.09	.0461	4.650
110	35.07	7.894	13.15	.0443	4.654
120	35.60	8.251	13.08	.0479	4.612
130	37.43	7.915	13.09	.0470	4.580
140	38.85	8.055	13.03	.0467	4.626
150	39.21	7.869	13.01	.0477	4.593
160	40.17	7.974	13.02	.0488	4.576
170	38.59	7.963	13.00	.0489	4.571
180	39.90	7.966	12.99	.0480	4.602
190	40.73	8.100	13.00	.0461	4.609
200	40.09	8.338	12.79	.0459	4.570
210	41.11	7.973	12.95	.0473	4.574
220	41.26	7.973	13.00	.0463	4.584

Table (A3) : Sample of Concentration Readings.

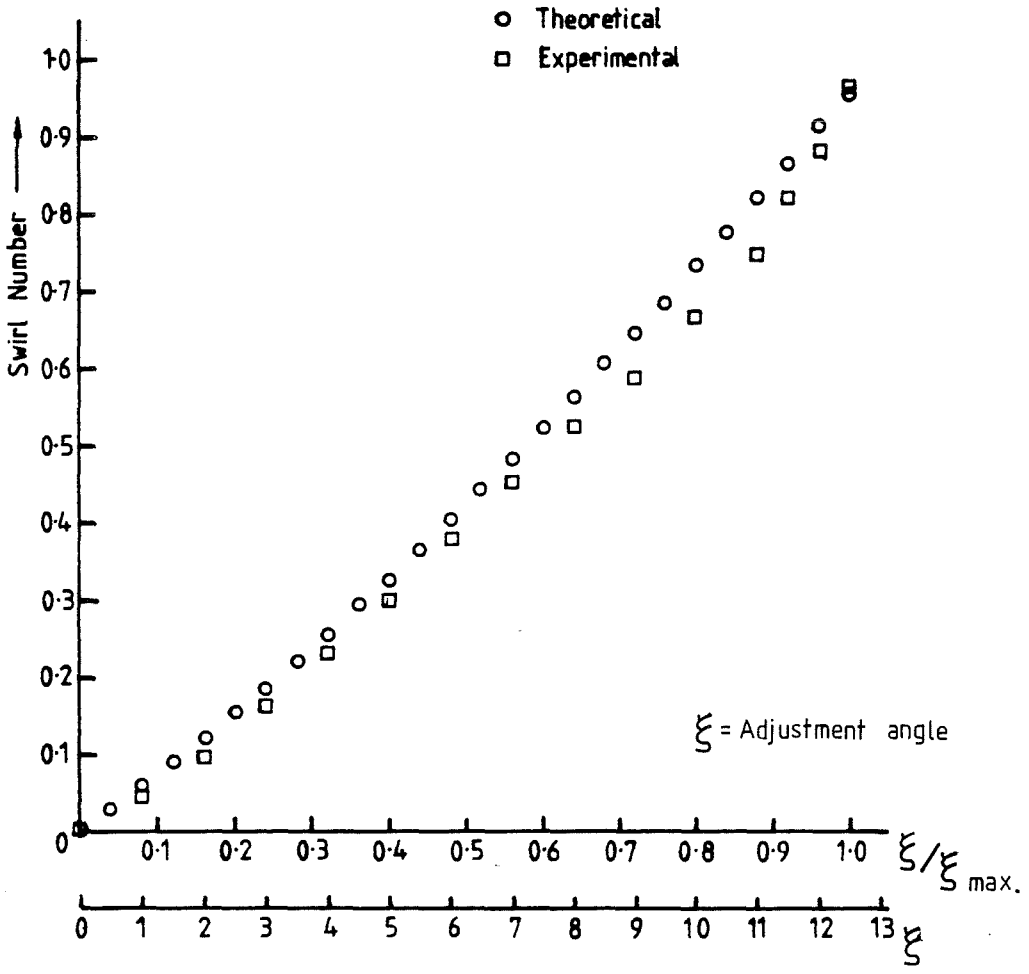

Swirl Generator Calibration

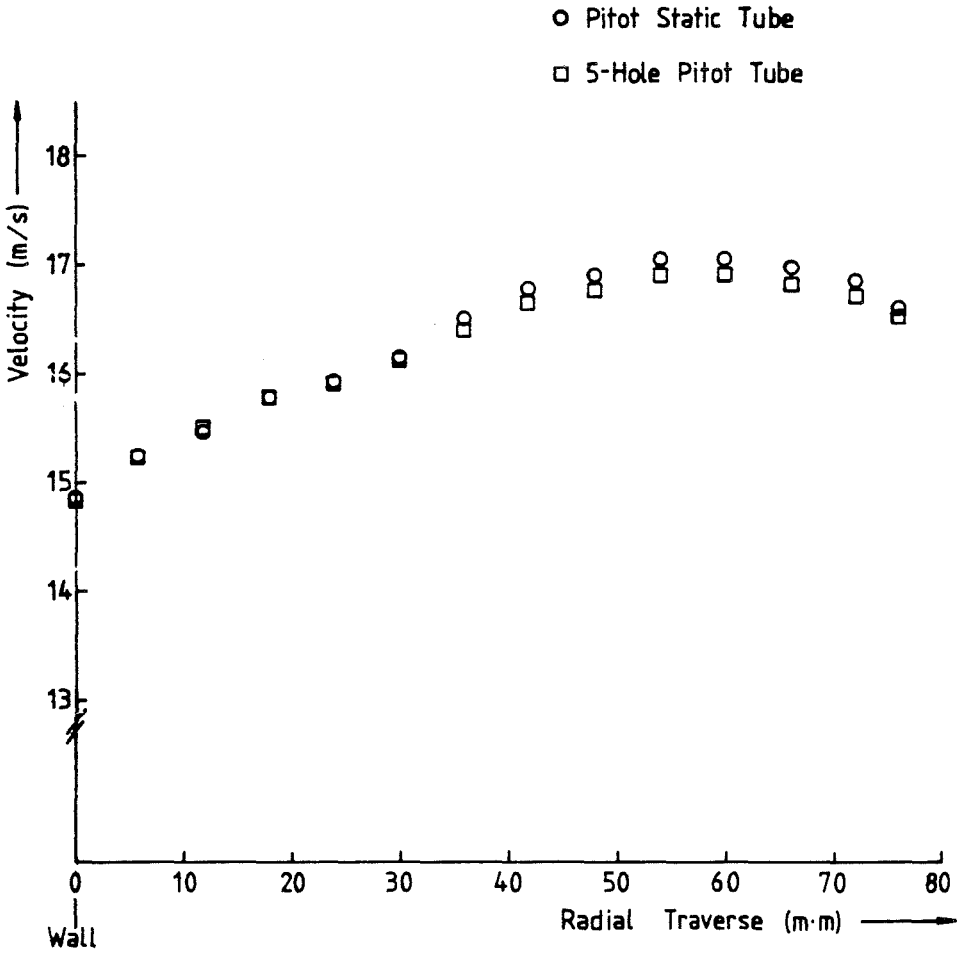

5-Hole Pitot Tube Calibration

Display mm H_2O	Voltmeter mV	Display mm H_2O	Voltmeter mV
100 % P		1 % P	
00.0	0.1	0.000	-1.000
05.0	124.3	0.050	125
10.0	249.0	0.100	250
15.0	374.0	0.150	375
20.0	500.1	0.200	500
25.0	624.5	0.250	625
30.0	749.0	0.300	750
35.0	874.0	0.350	875
40.0	999.5	0.400	1,000
60.0	1500	0.600	1,500
100.0	2500	1.000	2,500
150.0	3715	1.500	3,750
180.0	4490	1.800	4,500
199.9	5000	1.999	4,998

Table (A4) : Micromanometer Calibration

5-HOLE PITOT PROBE

PRINCIPLE OF OPERATION

1. If a spherical body is suspended in a stream of gas of known velocity, it is possible to calculate the velocity at any point on the sphere's surface from potential flow theory.

2. The tangentional velocity at an angle θn to the incident flow is

$$Vn = \frac{3}{2} \text{ Sin } \theta n.V \qquad \ldots (1)$$

(Theoretical Hydrodynamics - Milne, Thomson P489 Ch. 16-30)

Where V is the incident stream velocity.

3. The pressure Pn, at this point is given by

$$\frac{Pn}{\rho} + \frac{V^2n}{2} = \frac{Ps}{\rho} + \frac{V^2}{2} \qquad \ldots (2)$$

Where Ps is the free stream static pressure
ρ is the gas density

4. Thus solving for Pn and substituting Vn from equation (1)

$$Pn = Ps + \tfrac{1}{2} \rho V^2 \left(1 - \frac{9}{4} \text{Sin}^2\theta n\right)$$

$$= Ps + \tfrac{1}{2} \rho V^2 \, Kn \qquad \ldots (3)$$

Kn is known as the pressure recovery factor

5. If a sphere is constructed with 5 holes situated radially as shown in Fig. 1, the holes being the open ends of tube connections taken through the sphere mounting, and used to measure pressure, then this theory can be used to obtain a series of expressions relating gas velocity to the pressures and recovery factors of each hole.

$$P_0 = Ps + \tfrac{1}{2} K_0 \, \rho V^2 \quad \text{etc}$$

Thus $$P_0 - P_1 = \tfrac{1}{2} \rho V^2 (K_0 - K_1) \text{ etc} \qquad \ldots (4)$$

where the subscripts, 0, 1, 2, 3 and 4 refer to the hole positions on the pitot (Fig. 1).

6. Substituting for K_0, K, etc.

$$P_0 - P_1 = \frac{9}{8} \rho V^2 (\text{Sin}^2\theta_1 - \text{Sin}^2\theta_0) \text{ etc} \qquad \ldots (5)$$

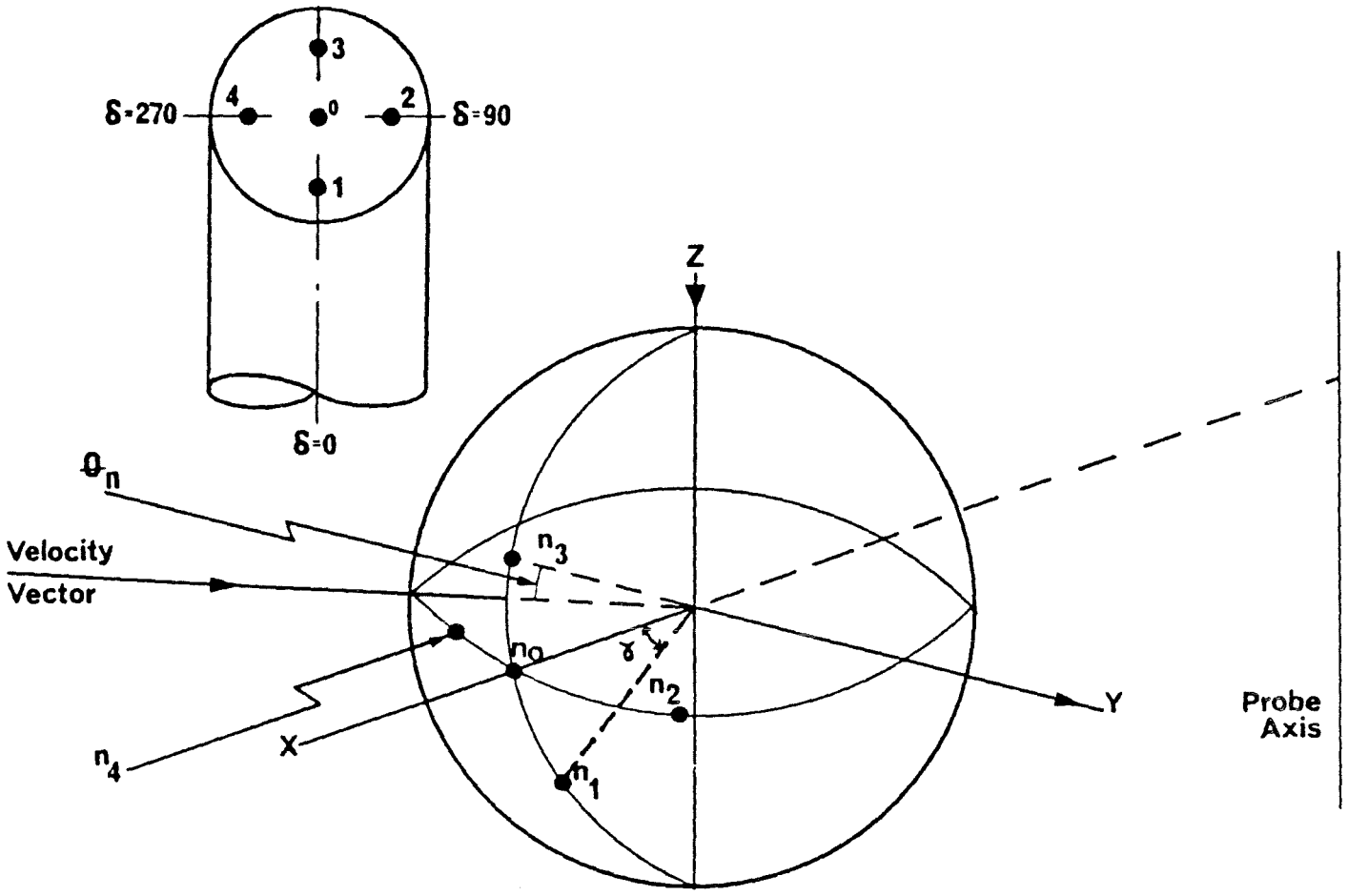

γ Conical angle at each of the holes n_1, n_2, n_3, n_4.

ϕ Conical angle formed by the velocity vector and the probe head axis

δ Dihedral angle between the flow plane and the meridian plan.

θ_n Angle between the velocity vector and the nth pressure hole.

Fig. 1 Definition of pitot angles

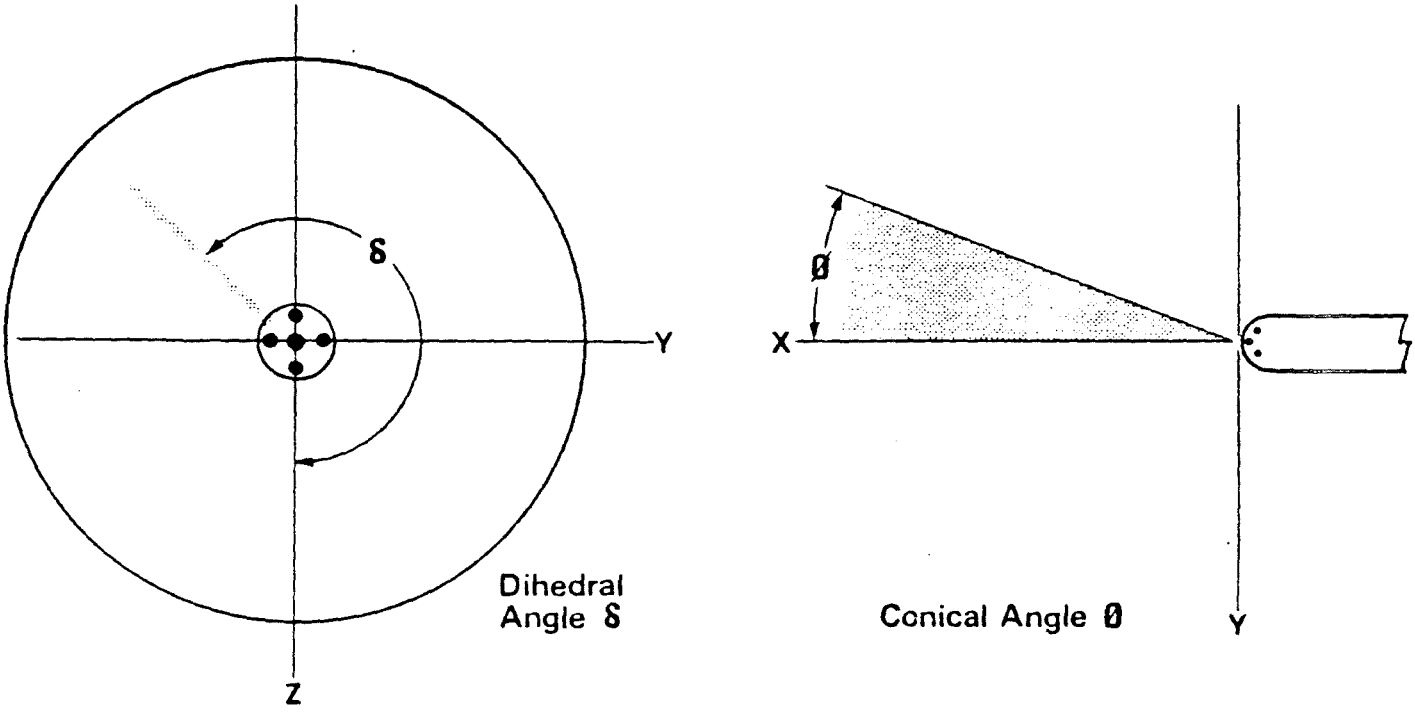

Fig. 2 Reference directions for angle determination

7. We now have a series of expressions relating pressures at the five holes to velocity and the angle θ between the velocity vector and the five holes.

8. From simple, but tedious, three dimensional geometry it is possible to express each of the angles θn in terms of the angles.

ϕ conical angle between the velocity vector and the probe axis.

δ dihedral angle between the flow plane and the meridian plane formed by holes, 1, O and 3.

γ the conical angle of each of the four holes, 1, 2, 3, 4.

See Figs. 1 and 2.

9. The results of this three dimensional analysis are

$$\begin{aligned}
\cos\theta_1 &= \cos\phi\cos\gamma + \sin\phi\sin\gamma\cos\delta \\
\cos\theta_2 &= \cos\phi\cos\gamma + \sin\phi\sin\gamma\sin\delta \\
\cos\theta_3 &= \cos\phi\cos\gamma - \sin\phi\sin\gamma\cos\delta \\
\cos\theta_4 &= \cos\phi\cos\gamma - \sin\phi\sin\gamma\sin\delta
\end{aligned} \qquad \ldots (6)$$

The problem is to isolate each of the angles ϕ, γ and δ and determine ϕ and δ (since γ is known from the pitot head geometry), and finally to calculate the velocity V and static pressure Ps from the pressures measured at the 5 holes.

10. Measurement of δ

By rearranging equations (6) we may write

$$\tan\delta = \frac{\cos^2\theta_2 - \cos^2\theta_4}{\cos^2\theta_1 - \cos^2\theta_3}$$

and since $\cos^2\theta = 1 - \sin^2\theta$

$$\tan\delta = \frac{\sin^2\theta_4 - \sin^2\theta_2}{\sin^2\theta_3 - \sin^2\theta_1}$$

and from equation 5 we find that

$$\tan\delta = \frac{P_2 - P_4}{P_1 - P_3} \qquad \ldots (7)$$

11. To determine which quadrant δ is in when $o<\delta<\frac{\pi}{2}$ $\tan\delta>o$

$\therefore \frac{P_2 - P_4}{P_1 - P_3} > o$ and from Fig. 3 $\theta_1<\theta_3$ and therefore $P_1 - P_3 > o$

since $P_1 - P_3 = \frac{9}{8} \rho V^2 (\sin^2\theta_3 - \sin^2\theta_1)$

when $\frac{\pi}{2}<\delta<\pi$ $\tan\delta<o$ $\therefore \frac{P_2 - P_4}{P_1 - P_3} < o$

and $\theta_1>\theta_3$ $\therefore P_1 - P_3 < o$

when $\pi<\delta<\frac{3\pi}{2}$ $\tan\delta>o$ $\therefore \frac{P_2 - P_4}{P_1 - P_3} > o$

and $\theta_1>\theta_3$ $\therefore P_1 - P_3 < o$

when $\frac{3\pi}{2}<\delta<2\pi$ $\tan\delta<o$ $\therefore \frac{P_2 - P_4}{P_1 - P_3} < o$

and $\theta_1<\theta_3$ $\therefore P_1 - P_3 > o$

12. The angle ϕ and consequently Velocity V and static pressure Ps are more difficult to isolate.

13. Work done at International Flame Research Foundation showed that by defining three new factors $K\phi$, KV and Kp a close approximation to the values ϕ, V and Ps could readily be obtained from measurement of pressures at the five holes.

14. The factors are defined in terms of the differential pressures as follows:-

$$K\phi = \left(1 - \frac{P_T}{2PR}\right)^{\frac{1}{2}} \qquad \ldots (8)$$

where $P_T = \sum_{n=1}^{4} (P_o - P_n)$

and $P_R = \left[\sum_{n=1}^{4} (P_o - P_n)^2\right]^{\frac{1}{2}}$

$$K_V = \frac{\frac{1}{2}\rho V^2}{P_R} \qquad \ldots (9)$$

$$K_p = \frac{2}{\rho V^2} (P_o - P_n) \qquad (10)$$

Each of these three factors are very weak functions of the angle δ and can be assumed to be independent of δ with only a small error.

15. By drawing up calibration curves of

$K\emptyset$ v $\emptyset$	Graph A	at the rear of this manual
KV v $\emptyset$	Graph B	
and Kp v $\emptyset$	Graph C	

The angle $\emptyset$ can be readily found by calculating $K\emptyset$ from equation 8 and using the graph A.

Velocity V is found by using the value of $\emptyset$ already calculated, obtaining K_v from graph B, and substituting in equation 9.

Static Pressure Ps is found from Graph C using K_p for the same value of $\emptyset$ and substituting this in equation 10.

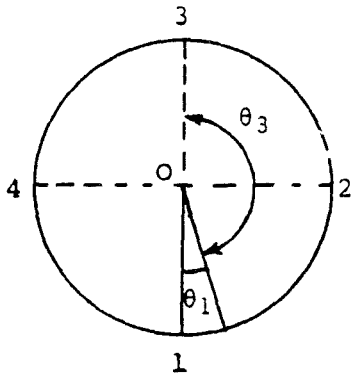

Fig. 3 Angle between the velocity vector and the pressure hole.

Calibration Curve for LAND 5-hole Pitot GRAPH A

TYPE PTOREIDS INSTRUMENT NO 82362

ANGLE FACTOR, $K_\phi = [1 - P_T]^{\frac{1}{2}}$ RELATED TO CONICAL ANGLE, ϕ DEGREES

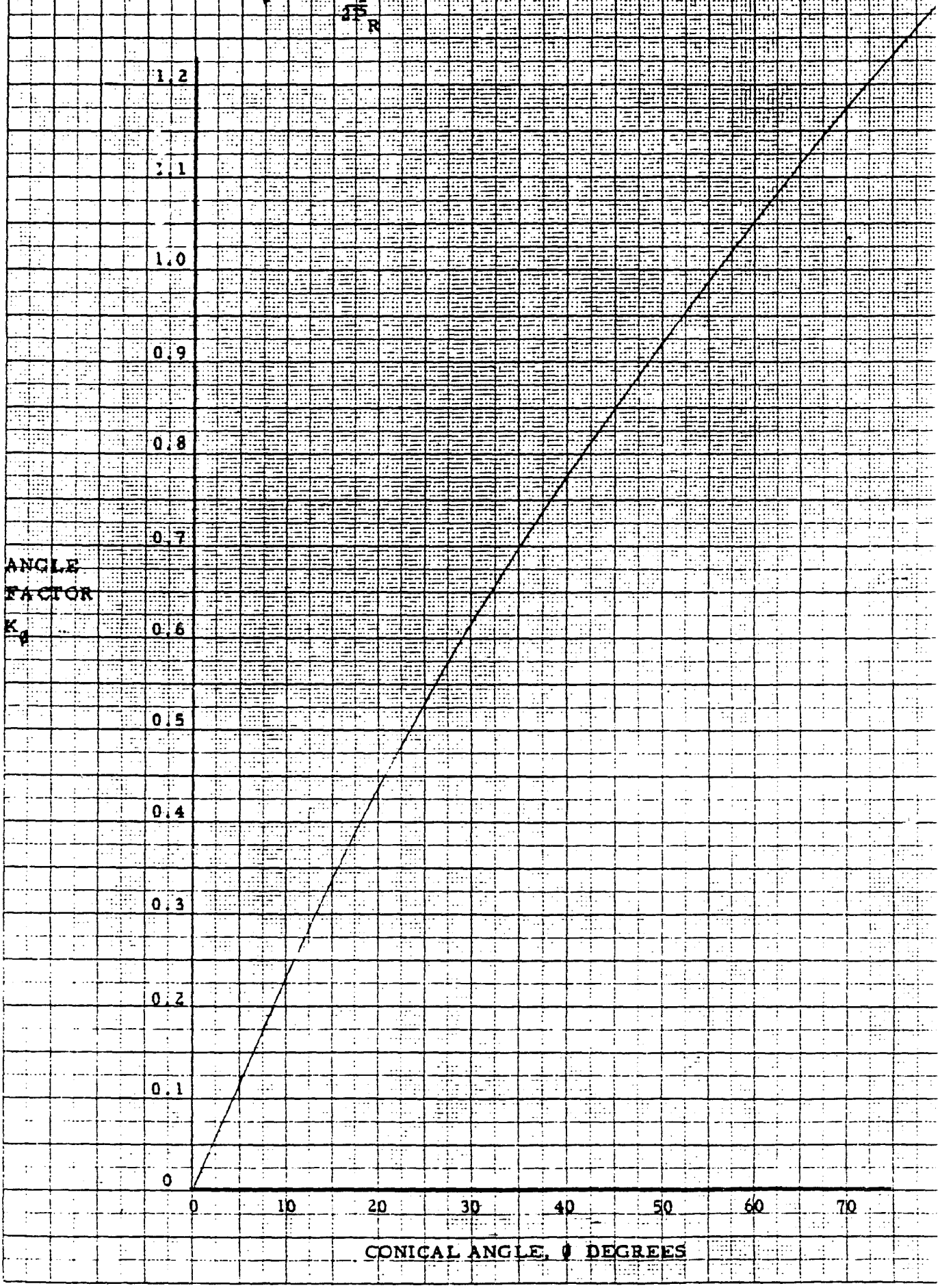

Calibration Curve for LAND 5-hole Pitot GRAPH B

PTOR6100 INSTRUMENT NO 823602

VELOCITY FACTOR, $K_V = \frac{[P_o - P_{atm}]}{P_R}$ = ϕ RELATED TO CONICAL ANGLE, θ DEGREES

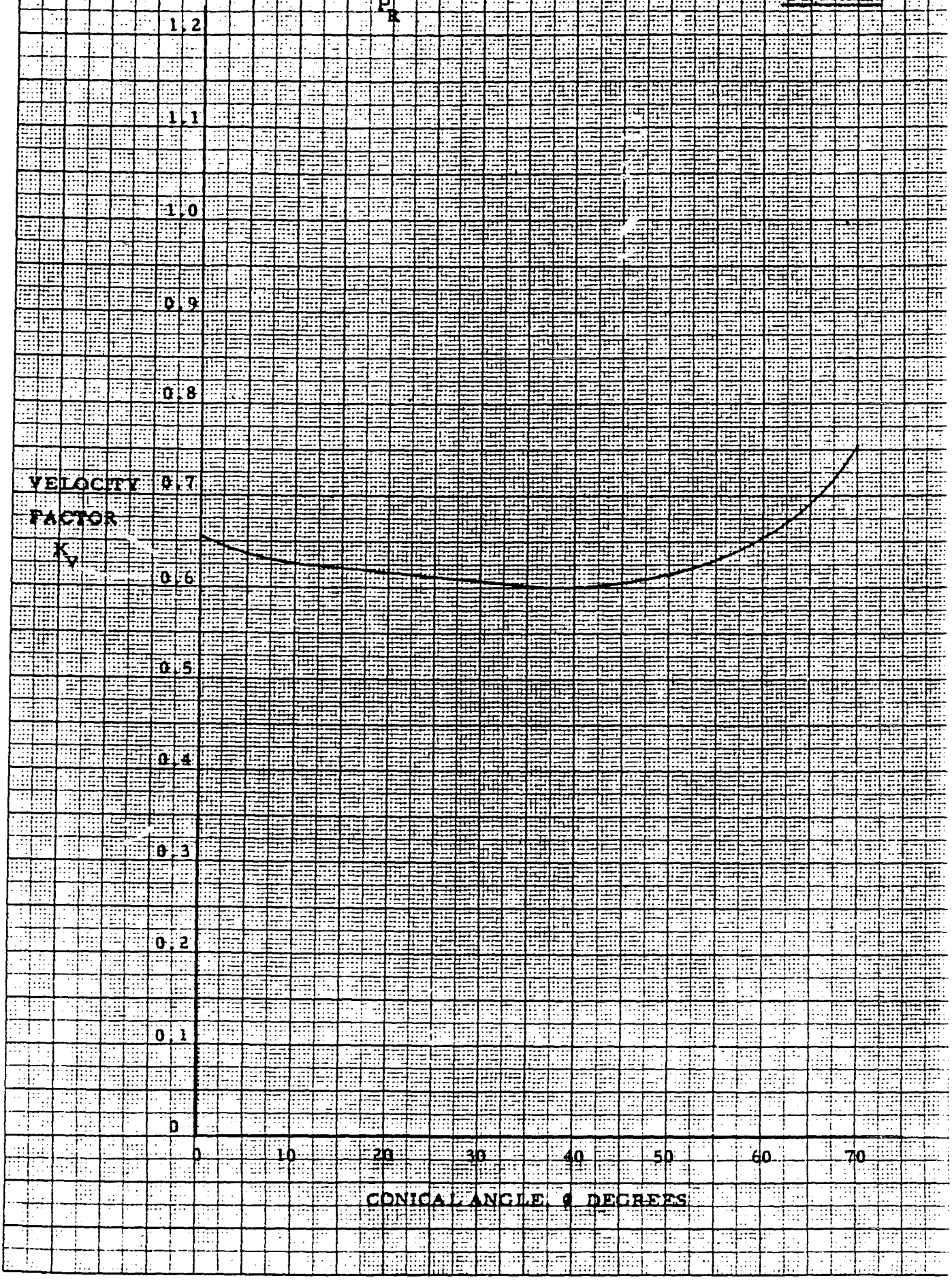

Calibration Curve for LAND 5-hole Pitot GRAPH C

TYPE PTORE10W INSTRUMENT NO 823602

PRESSURE FACTOR, $K_P = \frac{(P_o - P_{atm})_{\phi=\delta}}{(P_o - P_{atm})_{\phi=0}}$ RELATED TO CONICAL ANGLE, ϕ DEGREES

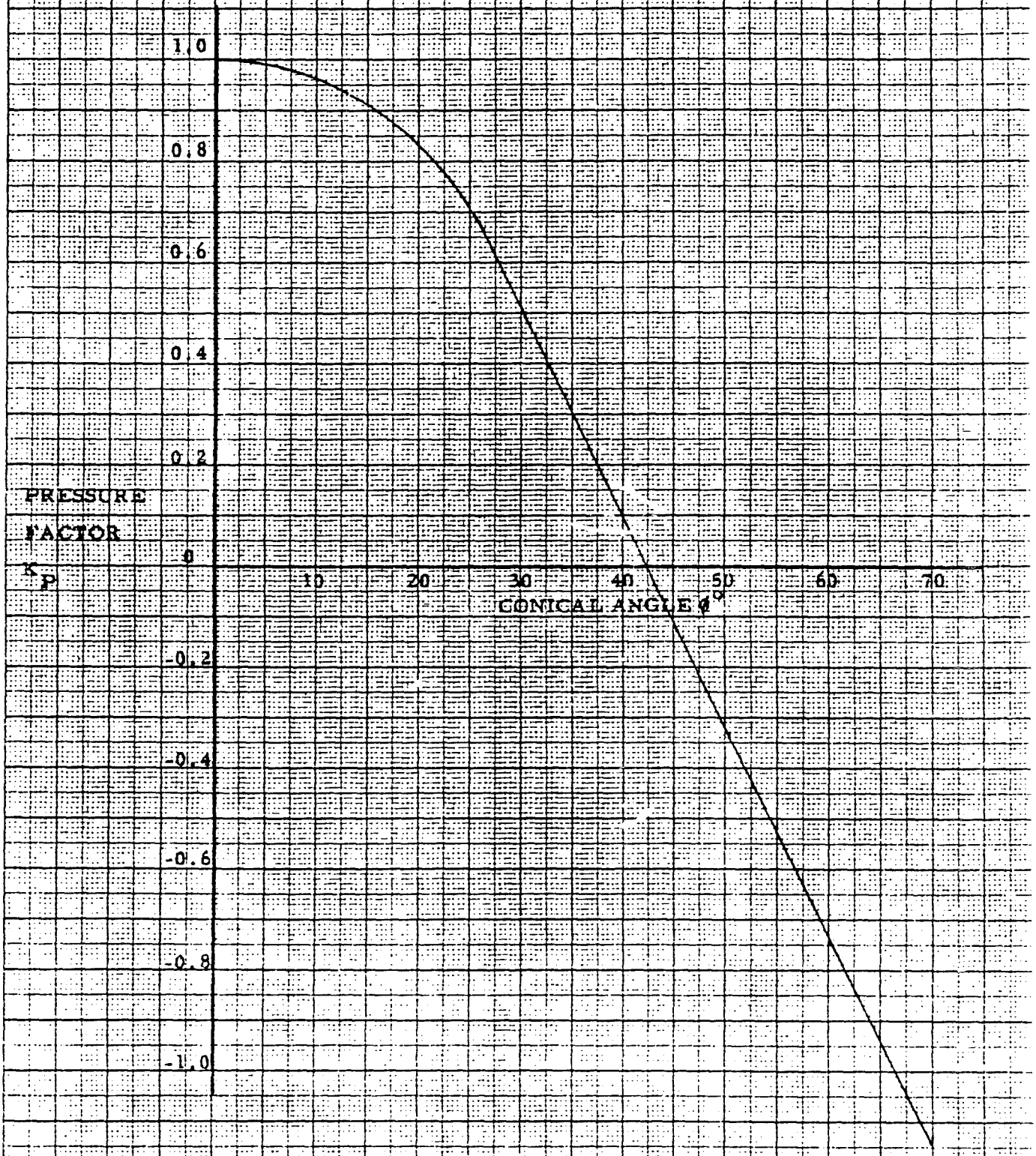

A P P E N D I X 'B'

BURNOUT RATE CALCULATIONS.

Consider a thin annulus of gas in the furnace at temperature T and thickness dy. Suppose the velocity of the gas is u m/s.

Volume of gas going through annulus per unit time = $2\pi y dy u$

Mass ,, ,, ,, ,, ,, ,, ,, ,, = $2\pi y dy u \rho$

where ρ is the density of combustion gases at temperature T.

Mass of CO going through annulus / unit time = $2\pi y dy u \rho c_i$

where c_i is the mass fraction of CO in the gas at temperature T.

Heat content of unburnt CO / unit time = $2\pi y dy u \rho h c_i$

where h is the calorific value of CO.

Total heat content of CO / unit time = $\int_0^R 2\pi y u \rho h c_i dy$

Burnout rate = 1 - (residual heat content / initial heat content)

$$= 1 - ((2\pi \int_0^R u \rho h c_i y dy) / (M_o h_o))$$

where M_o = mass flow rate of fuel.

h_o = CV of fuel.

Calculation of mass fraction (c_i).

Assume typical gas analysis as follows.

Species	Vol.%(wet)	Vol.%(dry)	Mol. Wt.
CO	x_1'	x_1	M_1
CO_2	x_2'	x_2	M_2
O_2	x_3'	x_3	M_3
N_2	x_4'	x_4	M_4
CH_4	x_5'	x_5	M_5
H_2O	x_6'		M_6

Measured CO on a dry basis is given by:-

$$x_1 \; / \; (x_1+x_2+x_3+x_4+x_5) \; x \; 100\%$$

Actual CO = Measured CO x $(x_1+x_2+x_3+x_4+x_5) \; / \; (x_1+x_2+x_3+x_4+x_5+x_6)$

Assume $x_6 = 2x_2$ as $2H_2O$ is formed for each CO_2.

Actual CO = Measured CO x $(x_1+x_2+x_3+x_4+x_5) \; / \; (x_1+3x_2+x_3+x_4+x_5)$

$$CH_4 + (0.79p \; N_2 + 0.21p \; O_2)$$

$$\longrightarrow CO_2 + 2H_2O + 0.79p \; N_2 + (0.21p - 2) \; O_2$$

On a dry basis we get

$$\longrightarrow CO_2 + 0.79p \; N_2 + (0.21p - 2) \; O_2$$

Vol. fraction of O_2 (dry basis) $= (0.21p - 2) / (p - 1) = (x_3 / 100)$

$$p = (200 - x_3) / (21 - x_3)$$

Vol. fraction of N_2 (dry basis) $= (0.79p) / (p - 1)$

$$= 0.79 \; x \; ((200 - x_3)/(21 - x_3)) \; / \; ((200 - x_3)/(21 - x_3) - 1)$$

$$0.79 \; x \; (200 - x_3) \; / \; 179 = x_4 \; / \; 100$$

$$x_4 = 79 \; x \; (200 - x_3) \; / \; 179$$

$$x_3 + x_4 = ((200 \; x \; 79) + 100 \; x_3) \; / \; 179$$

$$\text{Actual CO} = \text{Meas. CO} \; x \left[\frac{(x_1+x_2+ \frac{200 \; x \; 79}{179} + \frac{100}{179} \; x_3+x_5)}{(x_1+3x_2+ \frac{200 \; x \; 79}{179} + \frac{100}{179} \; x_3+x_5)} \right]$$

Let $\left[\quad \right]$ = wetness factor.

From typical gas analysis, total mass of comb. gases M is given by

$$(M_1x_1' + M_2x_2' + M_3x_3' + M_4x_4' + M_5x_5' + M_6x_6') \; / \; 100$$

and mass fraction of species i $= (M_ix_i') \; / \; (M_1x_1' + M_2x_2' + \ldots + M_6x_6')$

$$= (M_ix_i') \; / \; (M \; x \; 100)$$

$$\therefore M = \frac{\left(M_1x_1 + (M_2 + 2M_6)x_2 + M_3x_3 + M_4 \frac{79}{179} (200 - x_3) + M_5x_5 \right) \times \left[\quad \right]}{100}$$

$$= \beta \times (\text{wetness factor}) / 100$$

Mass fraction of species i = $M_ix_i \times (\text{wetness factor}) / \beta \times (\text{wetness factor})$

$$= M_ix_i / \beta$$

Now $M_1 = 28$

$M_2 = 44$

$M_3 = 32$

$M_4 = 28$

$M_5 = 16$

$M_6 = 18$

For example, mass fraction of CO =

$$28x_1 / (28x_1 + 80x_2 + 32x_3 + 12.36(200 - x_3) + 16x_5)$$

$$= 28x_1 / (28x_1 + 80x_2 + 44.36x_3 + 16x_5 + 2472)$$

Mass fraction of component i (c_i) =

$$M_ix_i / (28x_1 + 80x_2 + 44.36x_3 + 16x_5 + 2472)$$

The following is an example to find the values of ε for conditions given below.

Considering pure natural gas case without swirl and preheat using 10 % excess air.

$$\varepsilon = t_d / t_c$$

$$t_d = d / u \quad \& \quad t_c = K / S^2$$

$$K = k / \rho Cp$$

*From velocity data, taking average value at $R_j / 3$ (see footnote p.211)

$d = 240$ mm $= 0.24$ m

$u = 13.5$ m/s

$t_d = 0.24 / 13.5 = 0.0178$ s

Again taking average temperature at R / 3

$T_{average} = 1375\ ^{o}C \simeq 1650$ K

From gas encyclopedia + interpolation

$k = 22.90 \times 10^{-5}$ Cal.cm^{-1} s^{-1} K^{-1}

$= 0.0959$ J/msK

$\rho = 0.2079$ kg/m^3

$Cp = 0.2422$ kCal.kg^{-1} K^{-1}

$= 1014$ J/kgK

$K = 0.0959 / 0.2079 \times 1014 = 0.000455$ m^2/s

From Kalghatgi, S = 0.39 m/s for methane

$t_c = 0.000455 / (0.39)^2 = 0.00299$ s

So $= t_d / t_c = 0.0178 / 0.00299 = 5.9457$

For LCV gas without swirl and preheat at 10% excess air

From velocity data we get

$d = 180$ mm $= 0.18$ m

$u = 10$ m/s

$t_d = 0.18 / 10 = 0.0180$ s

From temperature data

$T_{average} = 1125\ ^{o}C \simeq 1400\ K$

$k = 20.97 \times 10^{-5}\ Cal.cm^{-1}\ s^{-1}\ K^{-1}$

$= 0.0878\ J/msK$

$\rho = 0.2487\ kg/m^{3}$

$Cp = 1014\ J/kgK$

$K = 0.0878 / 0.2487 \times 1014 = 0.000348\ m^{2}/s$

From Chakravarty (1984)

$S_m^2 = (1 - \alpha_i) S^2$

$\alpha_i = 1.1366 / 3 = 0.3789$

$S_m^2 = (1 - 0.3789) (0.39)^2$

$= 0.0945$

$S_m = \sqrt{0.0945} = 0.3074\ m/s$

S_m is the flame speed of the fuel mixture.

$t_c = 0.000348 / (0.3074)^2 = 0.0037$

$\therefore \varepsilon = 0.0124 / 0.0037 = 4.89$

* The actual velocity data used were the averaged values obtained by Simpson's Rule subroutine on the microprocessor. The average value at $R_j/3$ is sjust an estimated value based on simple jet theory.

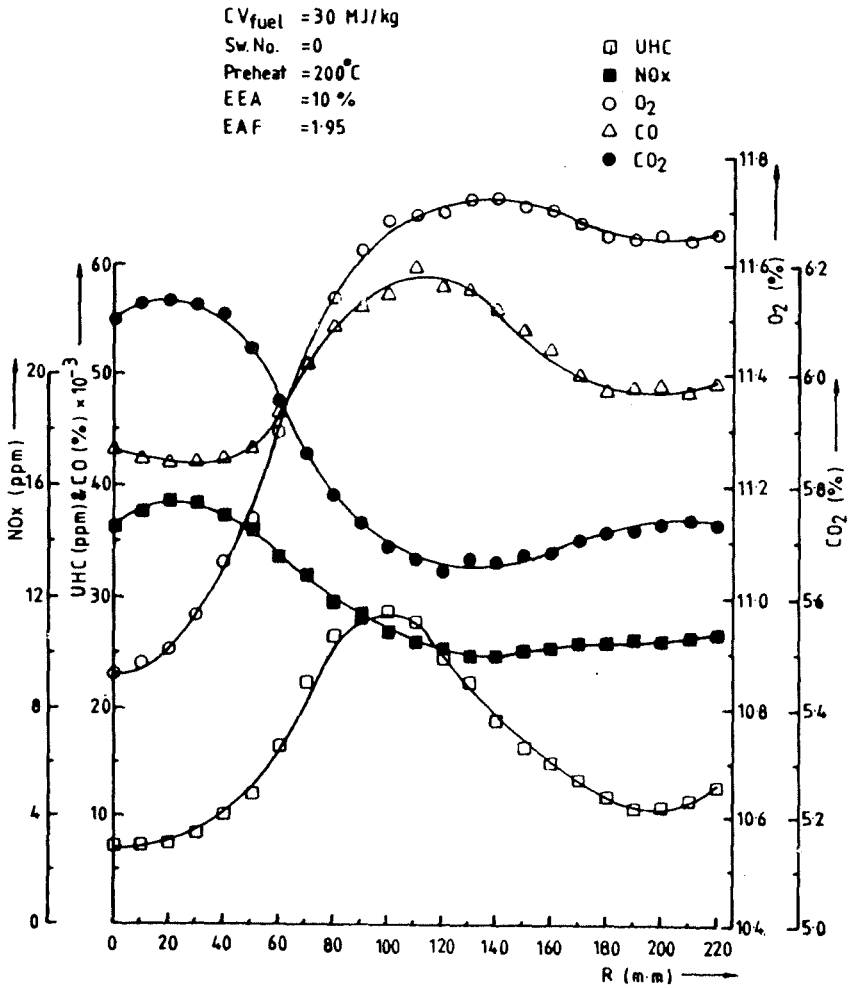

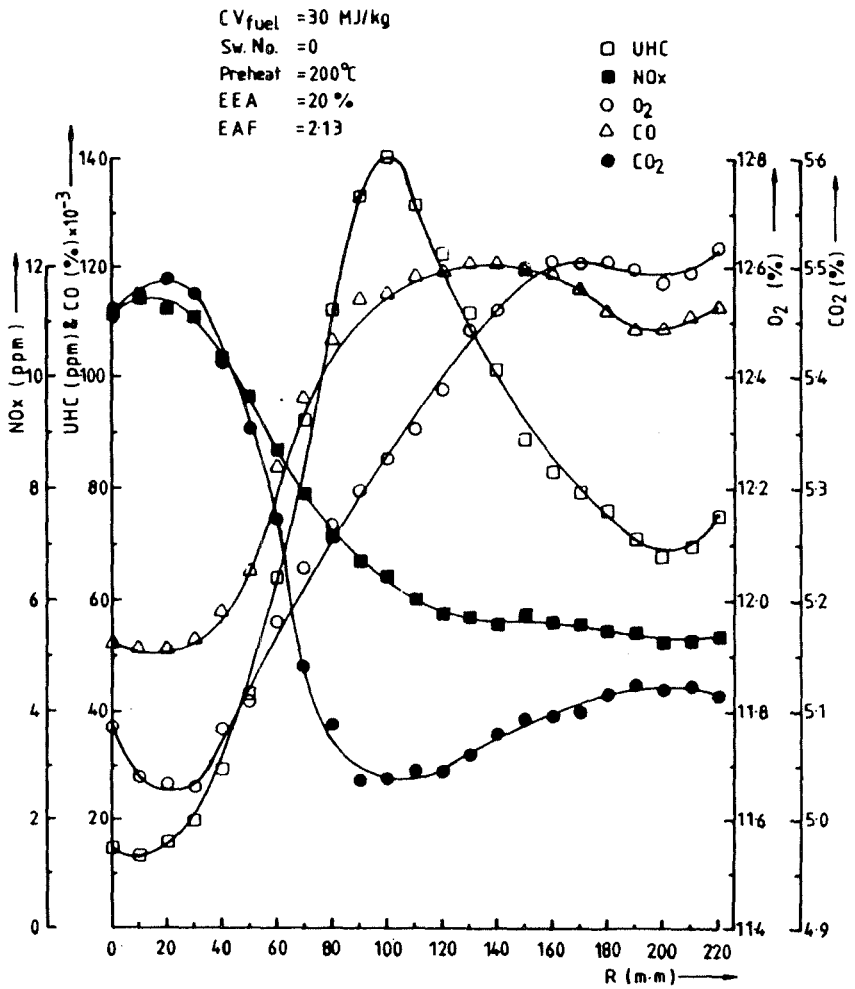

Additional Concentration Measurements

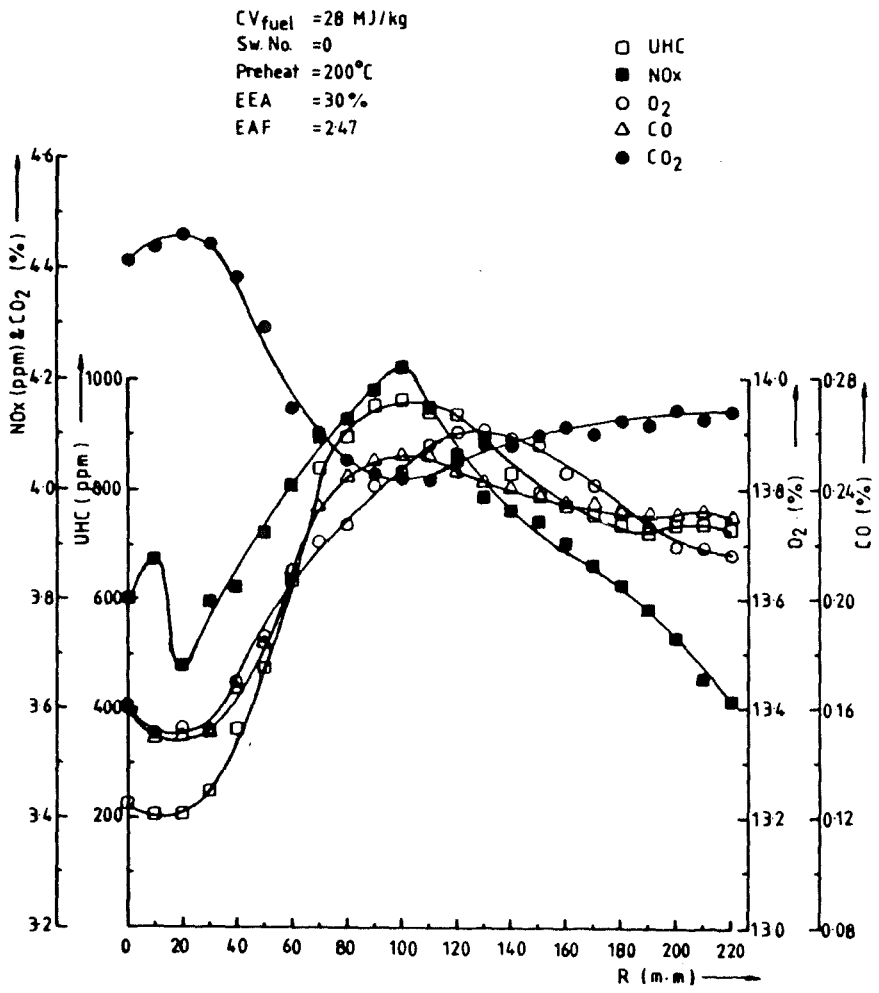

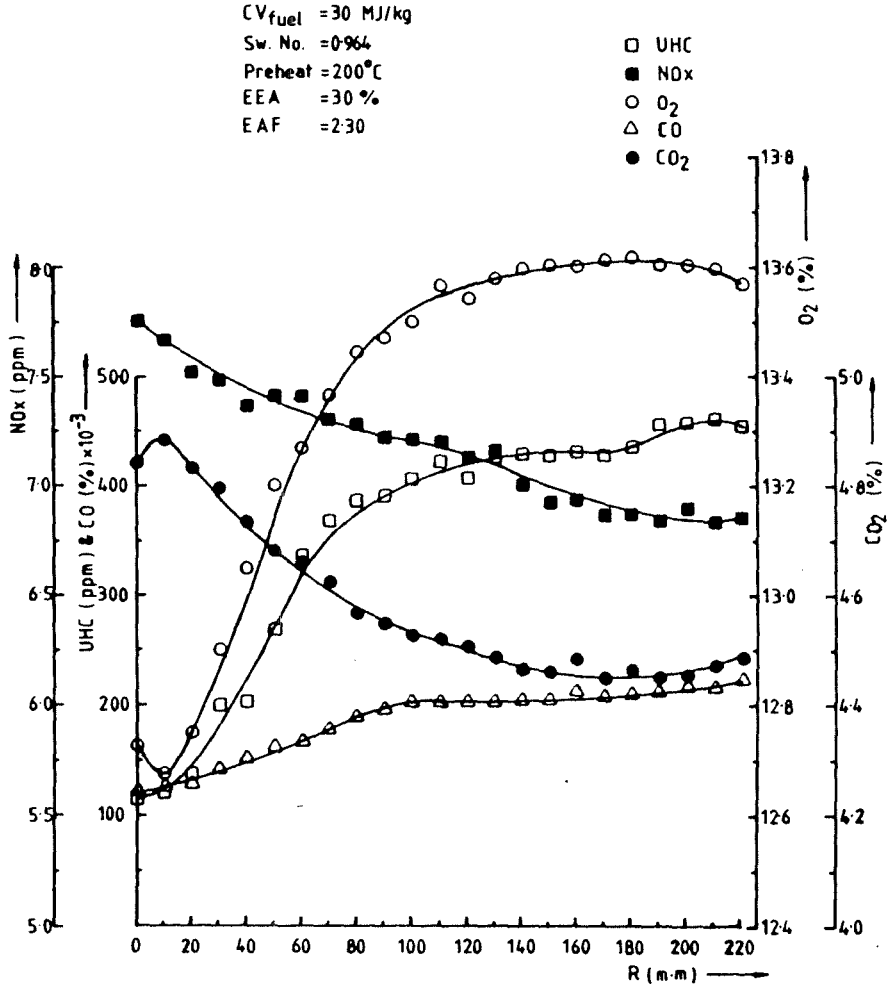

Additional Concentration Measurements

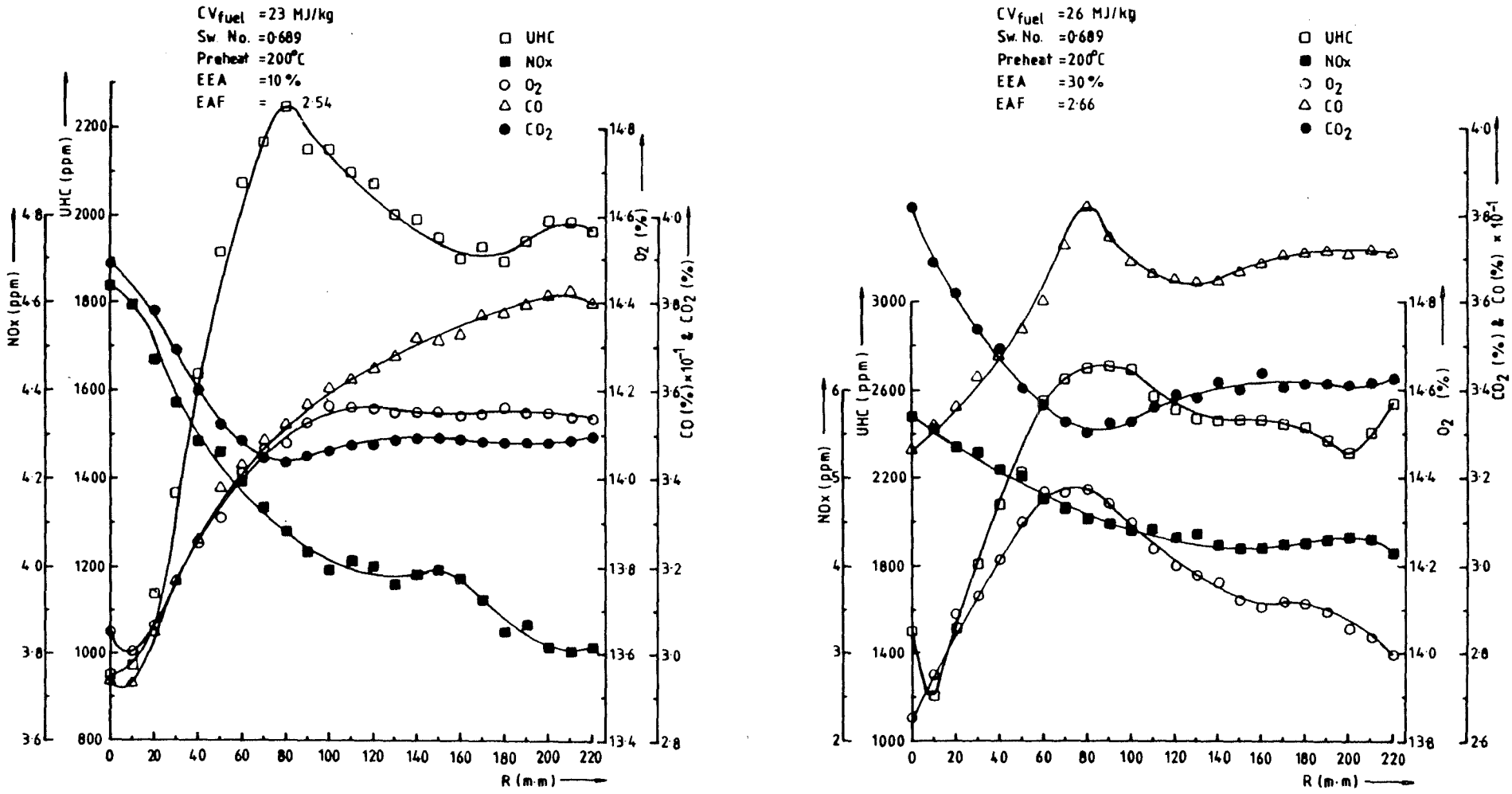

Additional Concentration Measurements

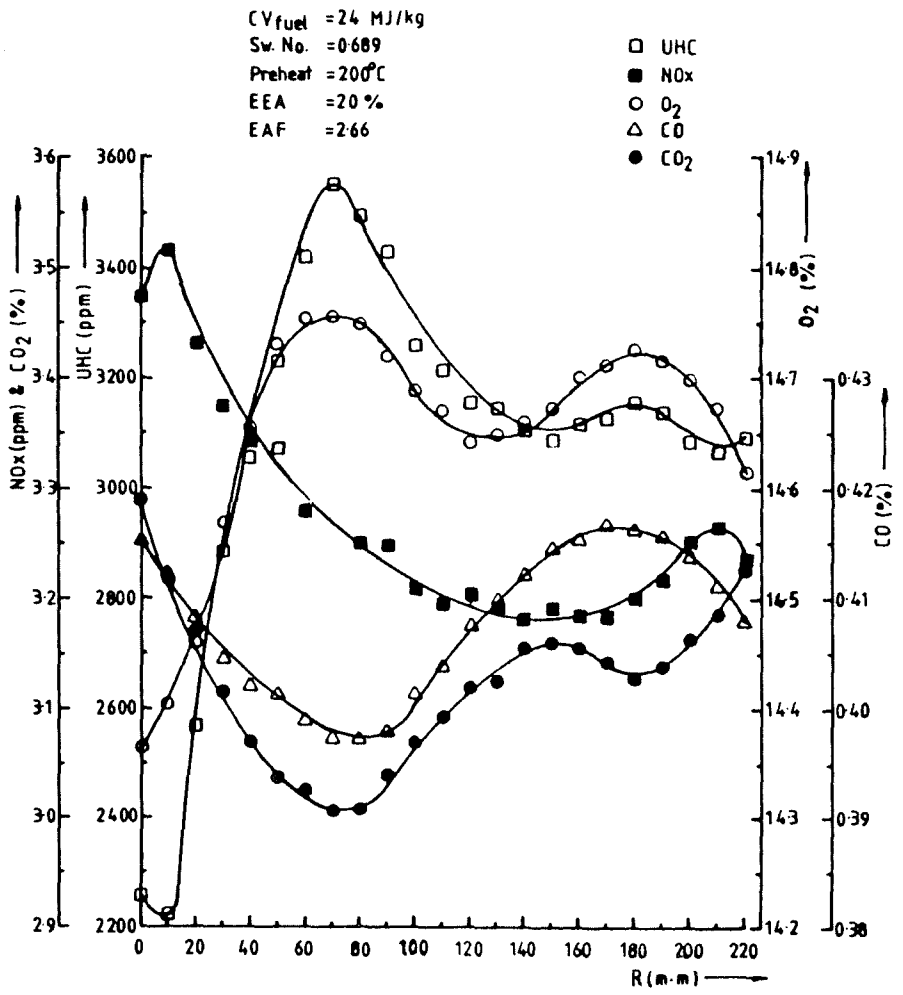

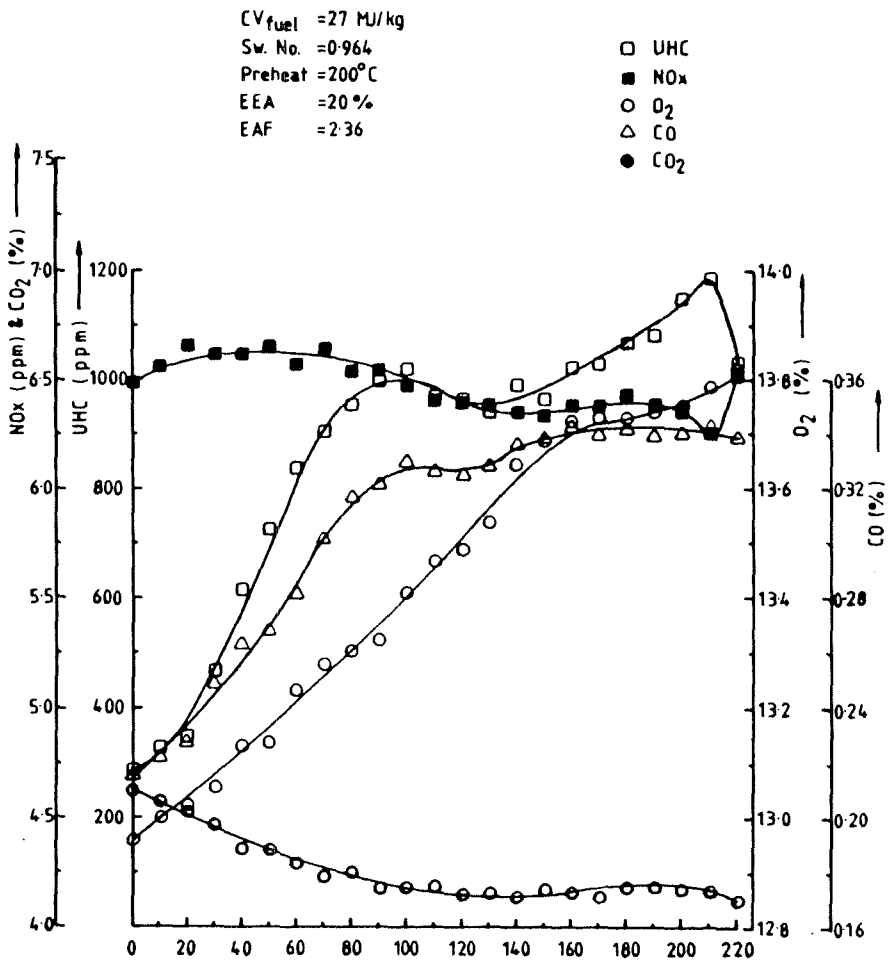

Additional Concentration Measurements

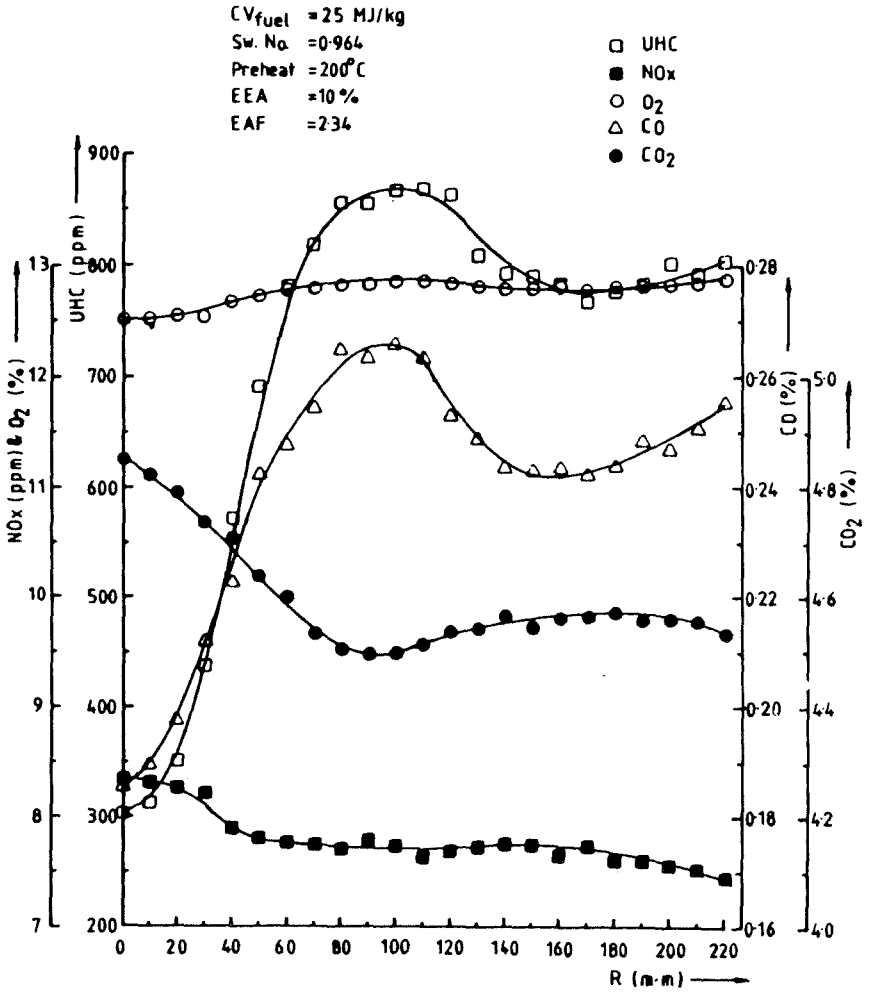

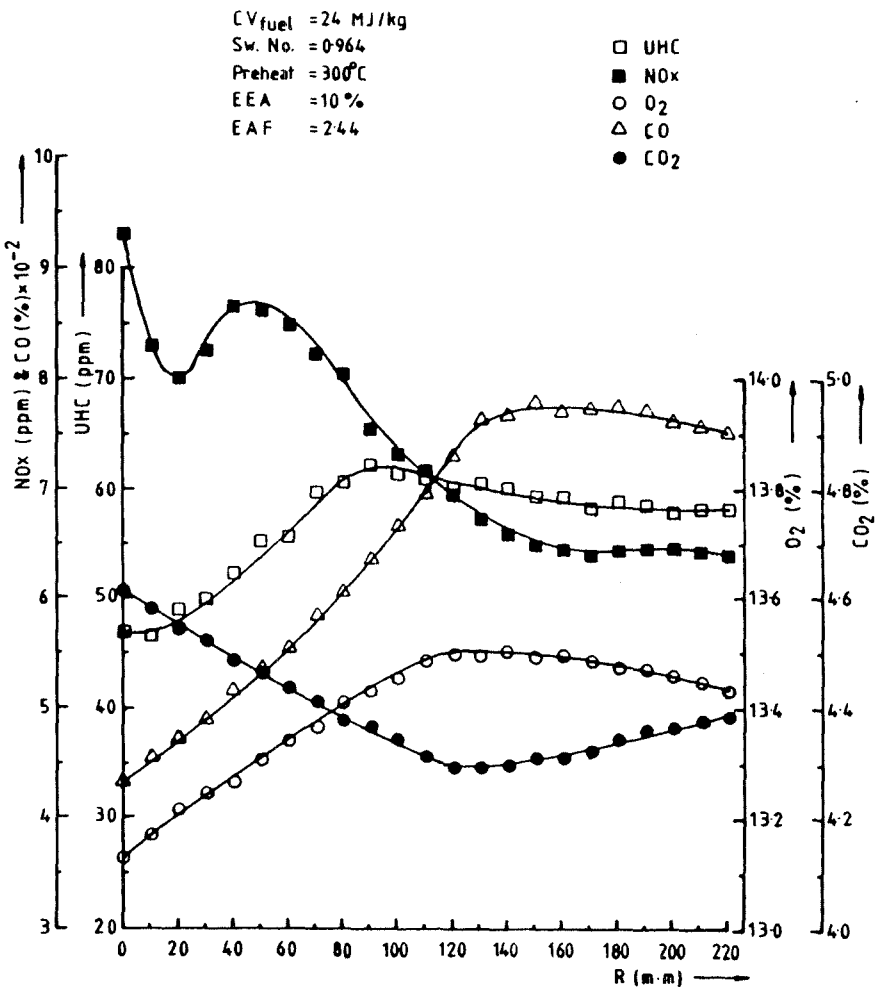

Additional Concentration Measurements